TPF 5(230): Evaluation of Plant Produced RAP Mixtures in the Northeast

Phase I Interim Report

Jo Sias Daniel, Ph.D., P.E.
Professor
Department of Civil Engineering
University of New Hampshire, Durham, NH 03824
Tel: (603) 862-3277; Email: jo.daniel@unh.edu

Tom Bennert
Research Professor
Center for Advanced Infrastructure and Transportation (CAIT)
Rutgers University, 100 Brett Road, Piscataway, NJ 08854
Tel: (609) 213-3312; Email: bennert@rci.rutgers.edu

Y. Richard Kim, Ph.D., P.E., F.ASCE
Distinguished University Professor
Department of Civil, Construction and Environmental Engineering
North Carolina State University, Raleigh, NC 27695-7908
Tel: (919) 515-7758; Fax: (919) 515-7908; Email: kim@ncsu.edu

Walaa Mogawer
Professor
Department of Civil and Environmental Engineering
Director, Highway Sustainability Research Center
University of Massachusetts Dartmouth
151 Martine Street, Fall River, MA 02723
Tel: (508) 910 -9824; Fax: (508) 999 -9120; Email: wmogawer@umassd.edu

Ashton Congalton
David Mensching
Mohammdreza Sabouri
Graduate Research Assistants

Michael Elwardany
Former Graduate Research Assistants

March 2014

Table of Contents

List of Figures

List of Tables

EXECUTIVE SUMMARY

This report summarizes findings from Phase I of a study that is funded through the Transportation Pooled Fund (TPF) Project 5(230): Evaluation of Plant Produced RAP Mixtures in the Northeast. Phase I of the project included testing on 18 plant-produced mixtures from New Hampshire, New York, and Vermont that contained reclaimed asphalt pavement (RAP) contents of 0% to 40% by total weight of mixture. The objectives of this research project were to: (1) evaluate the performance in terms of low temperature cracking, fatigue cracking, and moisture sensitivity of plant produced RAP mixtures in the laboratory and field; (2) establish guidelines on when it is necessary to bump binder grades with RAP mixtures; and (3) provide further understanding of the blending that occurs between RAP and virgin binder in plant-produced mixtures. Extensive material characterization was performed on specimens that were compacted at the plant and specimens that were fabricated from reheated mixture in the laboratory. The performance grade and |G*| master curves of tank binders and binder extracted and recovered from the mixtures were determined. Mixture testing included dynamic modulus, uniaxial fatigue, beam fatigue, overlay tester, thermal stress restrained specimen test, low temperature creep and indirect tensile strength, hamburg wheel tracking device, tensile strength ratio, and workability. Where possible, mixture testing was conducted on plant compacted and reheated specimens for comparison.

In general, the addition of RAP resulted in an increase in stiffness of the materials. The magnitude of the impact of higher RAP percentages varied with each set of mixtures and the test used to evaluate stiffness. Fatigue performance also varied depending on the test; crack initiation tests (uniaxial and beam fatigue) showed that many of the RAP mixtures performed similarly or better than the comparison virgin mixtures while the overlay tester (crack propagation) showed clear drops in performance at higher RAP contents. Low temperature testing showed trends similar to those observed with the stiffness measurements with warmer cracking temperatures observed with increases in RAP content. Workability decreased and rutting resistance increased with RAP content.

The impact of dropping the virgin binder PG grade to compensate for higher levels of RAP had varied results based on the mixtures evaluated. The extracted binder results show that the softer virgin binder grade improves both the high and low PG grades, but the magnitude of improvement varies with RAP content and mixture. A full PG grade improvement was not observed for any case. The mixture testing showed that the impact of using a softer virgin binder grade varies from mix to mix and for different mixture properties. It appears to help improve some properties, has negligible effect on others, and may make others worse.

The changes in measured properties appear to also be a function of the specimen preparation method (no reheating vs reheated in the lab), mix design variables that include the stiffness of the RAP and asphalt content, and production parameters such as mixing/discharge temperatures and silo storage times. In some cases the influence of these factors outweighs the impact of RAP level or PG grade of the virgin binder in the mixtures.

CHAPTER 1 INTRODUCTION

1.1 Background

Production of HMA mixtures with higher percentages of RAP is gaining more attention as a way to save money and more efficiently utilize existing resources. Many state agencies and contractors are very comfortable using RAP percentages up to 20% by total weight of mixture. However, questions about low temperature and fatigue performance and the need to bump binder grades limit the amount of HMA that is produced with greater than 15-20% RAP in many areas of the northeast US. Possible increased moisture susceptibility is also an issue in some regions. In the winter of 2009, the New Hampshire Department of Transportation (NHDOT) and Pike Industries, Inc. (PII) collaborated to perform an evaluation of extracted binder properties for various batch plant produced HMA mixtures containing 0-25% RAP. The results of that study were published in the Transportation Research Record in 2010 and were also presented at the 2009 North Eastern States Materials Engineers' Association (NESMEA) meeting. The general conclusion was that binder bumping was not necessary at the 20% RAP level for the mixtures evaluated.

The purpose of this pooled fund study is to expand on the initial work by PII and NHDOT by including higher RAP percentages, drum and batch plants, and mixture testing. The previous study was limited to testing of recovered binder properties which represent the fully blended condition between the RAP and virgin binder. Testing of plant-produced mixtures allows for evaluation of blending and the impact of higher RAP percentages on material properties and performance with respect to low temperature and fatigue cracking as well as moisture susceptibility of the mixtures containing RAP.

This project will add to the body of knowledge and types of RAP mixtures that have been evaluated in other research projects across the country. Ultimately, the industry needs to understand how RAP interacts with the virgin materials in a mixture so that the proper techniques and procedures can be developed and used to design and construct RAP mixtures that have equal or better performance than virgin mixtures.

1.2 Objectives and Scope of Interim Report

The overall objectives of this research project are to:

1. evaluate the performance in terms of low temperature cracking, fatigue cracking, and moisture sensitivity of plant produced RAP mixtures in the laboratory and field
2. establish guidelines on when it is necessary to bump binder grades with RAP mixtures
3. provide further understanding of the blending that occurs between RAP and virgin binder in plant-produced mixtures

Phase I of the project was conducted on mixtures that were produced in the 2010 construction season with the primary variables being the percentage of RAP in the mixture

and the virgin binder PG grade. Table 1-1 below presents a summary of the 18 mixtures that were evaluated as part of Phase I of the project. This interim report presents the results of the testing conducted on these Phase I mixtures.

Table 1-1 Phase I mixtures

Plant	NMAS (mm)	Virgin PG Grade	RAP Content (%) by total wt. of mix			
			0	20	30	40
Callanan NY (drum)	12.5	64-22	x	x	x	x
		58-28	-	-	x	x
Pike VT (batch)	9.5	58-28	x	x	x	x
		52-34	x	x	x	x
Pike NH (drum)	12.5	64-28	x	x	x	x

Testing and Analysis of Asphalt Binders and Mixtures

Binder Testing

Binders from the various RAP mixtures were extracted and recovered. Testing was done to determine the PG grading, including the critical cracking temperature determination, and partial binder master curve of the fully blended material. Testing was also done on the virgin binder and the recovered RAP binder.

Initial extractions and recoveries were performed by Pike Industries, Inc. The test results on these recovered binders did not follow expected trends for some of the mixtures, and it was discovered that different recovered binder specimen preparation procedures are used by Pike Industries and the two research labs. This was likely the reason for the unexpected results and in May 2013, the research team decided to perform new extractions and recoveries and re-test these binders. The new extractions and recoveries were performed by Rutgers University. This interim report includes the new binder results for all 18 mixtures.

Mixture Testing

Plant produced mixtures were sampled and then compacted at the plant to fabricate test specimens. Mix was also be reheated in the laboratory following an established procedure to fabricate additional laboratory test specimens and to allow for the comparison of plant mixed, plant compacted (PMPC) and plant mixed, laboratory compacted (PMLC) properties. Mixture testing included dynamic modulus, fatigue, low temperature creep compliance and strength, AASHTO T283, and the Hamburg Wheel Tracking Device (HWTD). The fatigue testing included push-pull testing following a draft AASHTO protocol being developed by North Carolina State University (NCSU) through Federal Highway Agency (FHWA) and the Mixture and Construction Expert Task Group (ETG). The failure criteria for RAP mixtures using the NCSU method were refined as part of this project. The overlay tester was conducted to provide additional information on the mixtures. Beam fatigue tests were also conducted on a subset of mixtures that had available

materials. The Thermal Stress Restrained Specimen Test (TSRST) was performed on the mixtures to evaluate low temperature cracking. Mixture testing allowed for the evaluation of the fatigue and low temperature properties and blending of the RAP mixtures. The HWTD following AASHTO T32404 'Standard Method of Test for Hamburg Wheel-Tracking Testing of Compacted Hot-Mix Asphalt (HMA) was used to evaluate the adhesion and moisture properties of the various mixtures. Additionally, the UMass Dartmouth workability device was used to test the effect of higher percentages of RAP on the workability of the mixtures.

The report is organized to present a description of the testing performed in Chapter 2, followed by individual chapters for each set of mixtures in Phase I. Chapter 6 presents a summary of all of the mixtures tested and Chapter 7 discusses the work being performed in Phase II and Phase III of the project as well as other future research needs.

1.3 Research Team

This project was conducted by the University of New Hampshire, Rutgers University, University of Massachusetts at Dartmouth, and North Carolina State University. Dr. Jo Sias Daniel at UNH is serving as the Principal Investigator and overseeing the research, performing data analysis, preparing reports, and presenting the findings. UNH has performed the T283 testing, Indirect Tensile creep and strength tests and the S-VECD fatigue testing on mixtures. Dr. Tom Bennert at Rutgers served as a co-PI and was responsible for the dynamic modulus, overlay tester, beam fatigue testing, extraction and recovery of the binders and binder testing, and analysis of the data and assisted in report preparation. Dr. Walaa Mogawer at UMass Dartmouth served as a co-PI and was responsible for a portion of the original binder testing, the TSRST, Hamburg, and workability testing and analysis of the data and assisted in report preparation. Dr. Richard Kim at North Carolina State University served as a co-PI on this project and was responsible for refining the S-VECD fatigue failure criteria for RAP mixtures.

1.4 Participating States and Technical Committee

The New Hampshire Department of Transportation is the lead agency for this project. Additional states that are participating in this study include: Maryland, New York, New Jersey, Pennsylvania, Rhode Island and Virginia. The Federal Highway Agency has also contributed funds to this project. The technical committee consists of representatives of each participating agency, as shown in Table 1-2.

Table 1-2 Technical committee members

Name	**Agency**
Nelson Gibson	FHWA
Denis Boisvert	NH DOT
Matt Courser	NH DOT
Zoeb Zavery	NYS DOT
Russell Thielke	NYS DOT
Eileen Sheehy	NJ DOT
Stacey Diefenderfer	VA DOT
Bob Voelkel	MD SHA
Timothy L. Ramirez	PA DOT
Jiang (John) Liang	RI DOT

CHAPTER 2 TEST DESCRIPTIONS

The laboratory testing conducted during the study comprised of asphalt mixture and liquid binder testing. The asphalt mixture testing was conducted on test specimens prepared at the asphalt plant (PMPC), as well as on loose mix brought back to the laboratory and reheated prior to sample fabrication (PMLC). The asphalt binder testing was conducted on both tank stored and asphalt binder extracted and recovered using solvent extraction procedures.

2.1 Binder Tests

The asphalt binder testing was conducted on two sets of liquid asphalt binders. The first set asphalt binders was sampled from the storage tank at the asphalt binder plant (called tank) and brought back to the laboratory for testing. All tank sampled asphalt binders were performance graded for Original, Rolling Thin Film Oven (RTFO), and Pressure Aging Vessel (PAV) aged conditions.

The second set of asphalt binders were extracted and recovered from sampled loose mix from the asphalt plant. The asphalt binder from the loose mix was extracted and recovered in accordance with AASHTO T164, *Procedure for Asphalt Extraction and Recovery Process* and ASTM D5404, *Recovery of Asphalt from Solution from Solution Using the Rotatory Evaporator*, using tri-chlorethylene (TCE) as the extracting solvent (Figure 2-1). After the recovery process, the asphalt binder was tested for the respective high temperature PG grade, in accordance with AASHTO M320, *Standard Specification for Performance-Graded Asphalt Binder*. The low temperature cracking properties of the asphalt binders were also evaluated in accordance with AASHTO R49, *Determination of Low-Temperature Performance Grade (PG) of Asphalt Binders.* The recovered asphalt binder was treated as an RTFO-aged asphalt binder, assuming that the aging that occurred at the asphalt plant was equivalent to what occurs during RTFO aging.

During the extraction and recovery process, the asphalt binder content was determined in accordance with AASHTO T164, *Procedure for Asphalt Extraction and Recovery Process.* The results are shown in Table 2-1. For most asphalt mixtures produced, a reduction in the solvent extraction measured asphalt content was found when compared to the design asphalt content. The differences were found to be larger for the VT mixtures than with the NY and NH mixtures. On average, the measured asphalt content of the VT mixtures were 0.38% lower than the design asphalt content. The NY and NH projects showed a better comparison, 0.10% and 0.04% lower, respectively. However, as can be seen in the table, there is variability within each project on a mix per mix basis.

Table 2-1 Asphalt content determination by solvent extraction (AASHTO T164)

Mix Type	% RAP	Asphalt Content from Solvent Extraction (%)	Design Asphalt Content (%)	Difference (Extraction - Design)
Callanan, NY PG58-28	30	4.96	5.20	-0.24
	40	4.93	5.20	-0.27
Callanan, NY PG64-22	0	5.04	5.20	-0.16
	20	5.15	5.20	-0.05
	30	5.46	5.20	0.26
	40	5.05	5.20	-0.15
Pike, VT PG52-34	0	6.29	6.70	-0.41
	20	6.18	6.80	-0.62
	30	6.17	6.60	-0.43
	40	6.32	6.60	-0.28
Pike, VT PG64-28	0	6.58	6.50	0.08
	20	6.27	6.70	-0.43
	30	6.13	6.60	-0.47
	40	6.12	6.60	-0.48
Pike, NH PG64-28	0	5.84	5.70	0.14
	20	5.46	5.70	-0.24
	30	5.31	5.70	-0.39
	40	6.02	5.70	0.32

2.1.1 *PG Grading*

The asphalt binders were performance graded (PG) in accordance with AASHTO M320, *Standard Specification for Performance-Graded Asphalt Binder*. A master table with all of the PG information is shown as Table 2-2. As would be expected, both the high temperature and low temperature PG grades of the recovered asphalt binders increased with the increase in RAP content. Using the data from all three field projects, it was determined that the high temperature PG increases 1.8ºC for every 10% of RAP used. Meanwhile, the low temperature PG grade also increased, but at a rate of 1.2ºC for every 10% RAP used.

Figure 2-1 Rotatory evaporator system at Rutgers University for asphalt binder recovery

Table 2-2 Summary of asphalt binder performance grading

Production Location	Base PG Grade Binder	Tank or Extracted with RAP Content	Continuous PG Grade (°C)				PG Grade (°C), AASHTO R29 & M320	Critical Cracking Temperature (°C), AASHTO R49	Extracted/Recovered Asphalt Content (%)
			High Temp (RTFO)	Low Temp		Intermediate Temp (PAV)			
				Stiffness	m-slope				
Callanan (NY)	58-28	Tank 7/30/10	60.3	-30.8	-31.7	17.2	58-28	-27	N.A.
		Tank 9/7/10	61	-34.6	-36.7	18.5	58-34	-30.2	N.A.
		Extracted - 30% RAP	72.1	-27.6	-26.5	21.7	70-22	-26.1	4.96
		Extracted - 40% RAP	81.7	-26.3	-22	22.9	76-22	-20.6	4.93
	64-22	Tank 7/30/10	67.3	-26.1	-26	22.1	64-22	-25.2	N.A.
		Tank 9/7/10	67	-26.3	-25.5	21.9	64-22	-23.1	N.A.
		Extracted - 0% RAP	75.5	-26.3	-22.2	24.7	70-22	-22.2	5.04
		Extracted - 20% RAP	78.3	-25.3	-21.8	25.3	76-16	-22.1	5.15
		Extracted - 30% RAP	78.4	-25.3	-19.9	26.4	76-16	-21.1	5.46
		Extracted - 40% RAP	80.9	-24.2	-17.6	27.2	76-16	-19.3	5.05
Pike (Portsmouth, NH)	64-28	Tank	66.3	-29.7	-29.5	19.9	64-28	-28	N.A.
		Extracted - 0% RAP	71.8	-29.5	-28.4	19.5	70-28	-25.7	6.29
		Extracted - 20% RAP	76.7	-28.9	-24.1	21.4	76-22	-25.9	6.18
		Extracted - 30% RAP	78.1	-28.2	-26.5	22.6	76-22	-27.6	6.17
		Extracted - 40% RAP	79.8	-27.9	-23.7	22.8	76-22	-25.7	6.32
Pike (Williston, VT)	52-34	Tank	56.3	-36.8	-32.5	12.1	52-28	-34.2	N.A.
		Extracted - 0% RAP	65.4	-36.9	-28.3	10.9	64-28	-33.3	6.58
		Extracted - 20% RAP	68.3	-35.3	-28.1	12.5	64-28	-31.9	6.27
		Extracted - 30% RAP	71.4	-34.8	-26.3	12.8	70-22	-32.7	6.13
		Extracted - 40% RAP	68.6	-33.4	-21	14.1	64-16	-28.4	6.12
	64-28	Tank	64.4	-31.7	-30.2	16.6	64-28	-30.6	N.A.
		Extracted - 0% RAP	67.4	-30.8	-28.1	17.7	64-28	-26.9	5.84
		Extracted - 20% RAP	69.6	-30.4	-27	18.9	64-22	-27.2	5.46
		Extracted - 30% RAP	74.7	-30	-23	19.9	70-22	-25.2	5.31
		Extracted - 40% RAP	78	-30.4	-24.9	18	76-22	-26.5	6.02

2.1.2 *Critical Cracking Temperature*

The low temperature critical cracking temperature was determined using the TSAR™ software developed by Abatech Consulting Engineers and conforming to AASHTO R49, *Determination of Low-Temperature Performance Grade (PG) of Asphalt Binders.* The analysis procedure utilizes the test data from the Bending Beam Rheometer (BBR) and Direct Tension Test (DTT). The BBR data is used to compute the thermal stress in the pavement using user-specified cooling rates and other material parameters, such as coefficient of linear expansion. The plot of thermal stress vs. temperature is then developed. Also plotted on the graph is the DTT failure stress vs. temperature. The location at which these two graphs intersect (BBR thermal stress and DTT failure stress) is noted as the low temperature critical cracking temperature. An example of this is shown in Figure 2-2.

The low temperature critical cracking temperature determined using AASHTO R49 and the low temperature binder grade, as determined using AASHTO R29, were plotted against one another and shown in Figure 2-3. The results show relatively good agreement between the NY (PG 58-28 and PG 64-22 binders) and the NH (PG 64-28 asphalt binder) mixtures. However, the agreement is not as good for the VT mixtures, which contained both a PG 64-28 and PG 52-34 binder. In reviewing the data, it appears that the PG 52-34 asphalt binder from the VT mixtures resulted in the poorest agreement among the two different test methods.

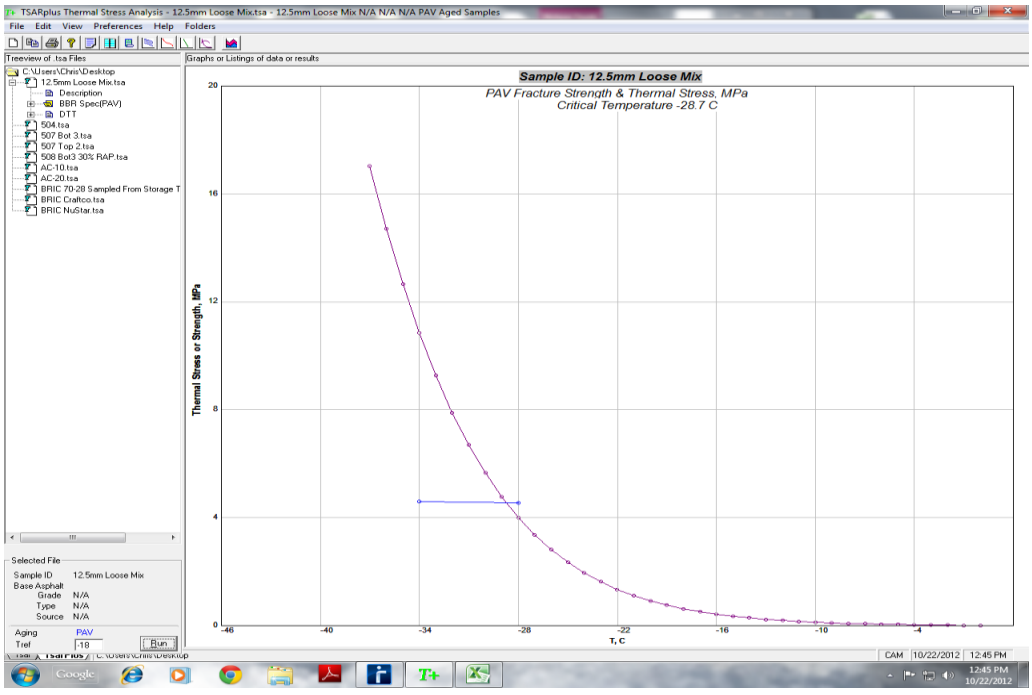

Figure 2-2 Screenshot from TSAR™ program calculating low temperature critical cracking temperature in accordance with AASHTO R49

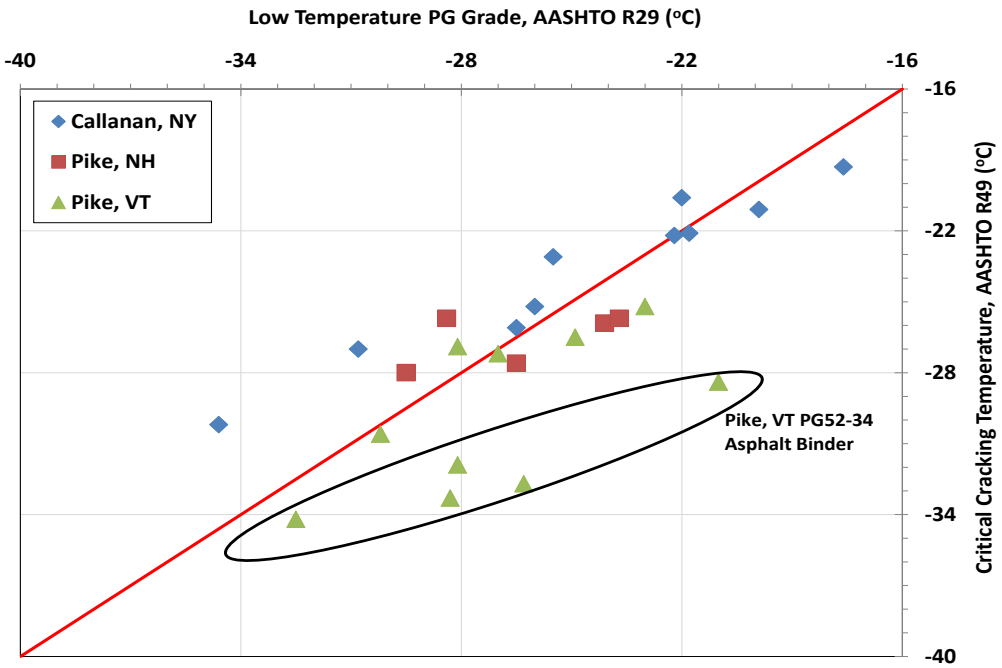

Figure 2-3 Low temperature PG grade comparison – AASHTO R29 vs. AASHTO R49

AASHTO R49 recommends the analysis to be conducted using a cooling rate of 1°C/hr with a starting temperature of 0°C. However, these parameters are generalized and may not actually represent true field conditions. In fact, most surface temperature measurements indicate two distinct cooling rates with their own respective starting temperature, as shown in Figure 2-4.

Figure 2-4 shows the two cooling rates and respective starting times for a surface temperature profile in Augusta, Maine. The upper part of the curve has a cooling rate of -2.8°C/hr with a starting temperature of 5.5°C. Meanwhile, the lower part of the curve indicates a cooling rate of -0.51°C/hr with a starting temperature of -3.8°C. This indicates that a cooling event having two separate cooling rates/starting temperatures that may affect the low temperature critical cracking temperature differently.

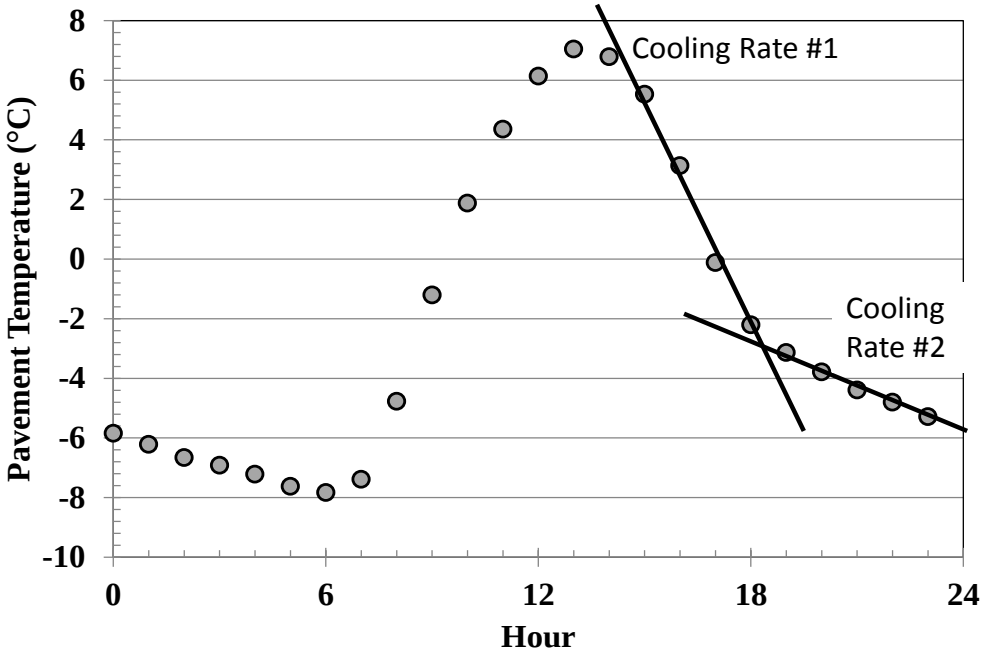

Figure 2-4 Field cooling rate at pavement surface (Augusta, Maine)

The analysis methodology described in AASHTO R49 allows for the determination of the low temperature critical cracking temperature at a multitude of cooling rate and starting temperature combinations, as long as there is enough test data to allow for the BBR thermal stress curve and DTT fracture stress curves to intersect. A parametric study of different starting temperatures and cooling rates was conducted for each mixture. The cooling rate was found to be the more significant factor with respect to low temperature critical cracking temperatures.

2.1.3 Master Stiffness Curves (G*)

The master stiffness curves of the respective extracted/recovered asphalt binder were also determined for these materials. The asphalt binder master curves are constructed by collecting the dynamic complex modulus (G*) and phase angle (δ) over a wide range of temperatures and loading frequencies. The master curve is then generated using the time-temperature superposition principle. A reference temperature, often 25ºC, is commonly used for which all of test data is shifted with respect to (Christensen and Anderson, 1992). For this study, the master curves were constructed using the RHEA software (Abatech, 2011).

In this study, the 4 mm geometry configuration (Figure 2-11) was used to measure the G* and δ of the extracted/recovered asphalt binder for some of the mixtures (Sui et al, 2010). The advantage of using the 4 mm geometry is that a much smaller amount of material is required for testing over the range of required temperatures. Typically, data from the BBR is necessary to provide the low temperature mechanical information needed to construct the master curve. However, the 4 mm geometry eliminates this need.

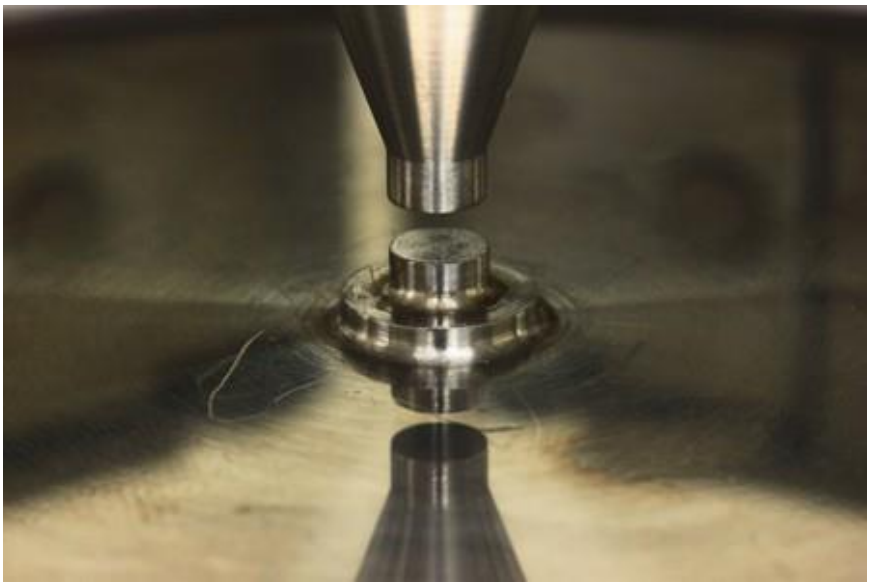

Figure 2-5 4 mm geometry for the dynamic shear rheometer

The form or shape of the G* master curve provides an indication of the "aging" characteristics of the asphalt binder. Figure 2-6 and Figure 2-7 show G* master curves for a PG 64-22 and PG 76-22 asphalt binder, respectively, that had undergone various levels of laboratory aging; RTFO, 20, 40, and 60 hours in the PAV. The constructed master curves shown in Figure 2-6 and Figure 2-7 clearly indicate that as the level of aging increases, the shape of the master curves become flatter and the magnitude of the shear modulus stiffer.

The same phenomena was originally noted by Christensen and Anderson (2002), who developed a model (Christensen-Anderson Model) that described shape parameters to define the master curves. Rheological Index (R) and Crossover Frequency (ω_o), are shape parameters within the model used to described the general slope and inflection point of the G* master curve (Figure 2-8). Therefore, as an asphalt binder undergoes different levels of aging, or rejuvenating, the shape parameters should change. Figure 2-9 shows how the Rheological Index and Crossover Frequency changes due to increased aging using the G* data shown in Figure 2-6 and Figure 2-7. As the respective asphalt binder ages, the shape parameters move from the upper left quadrant of the R – ω_o Space to the lower right quadrant. Therefore, by utilizing this methodology, one should be able to determine whether or not an asphalt binder has undergone a degree of aging, although an exact magnitude would not be able to be determined.

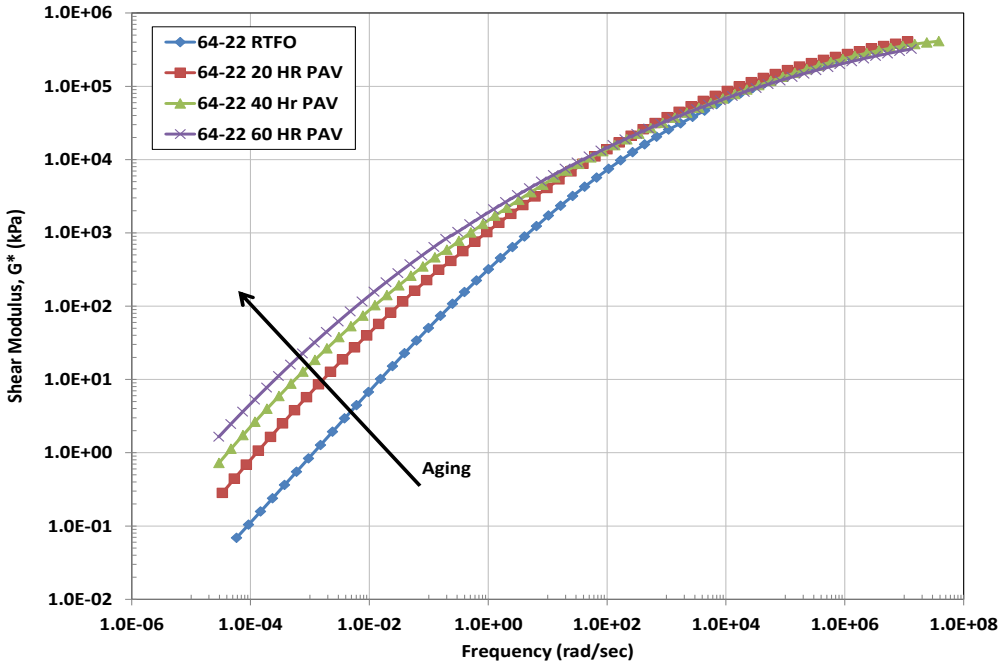

Figure 2-6 Shear modulus (G*) master curves for PG 64-22 asphalt binder

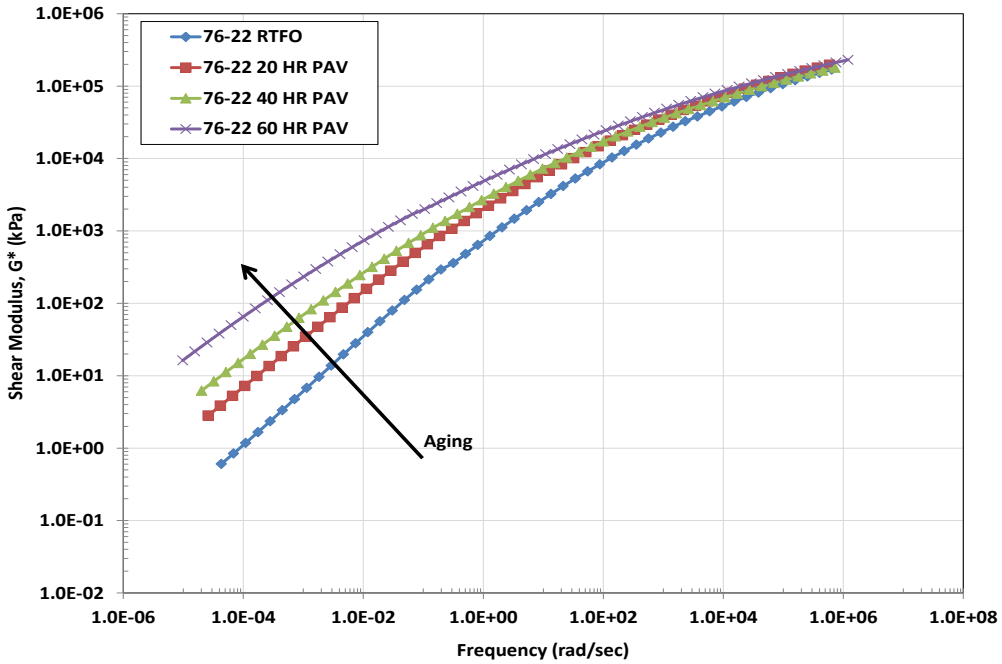

Figure 2-7 Shear modulus (G*) master curves for PG 64-22 asphalt binder

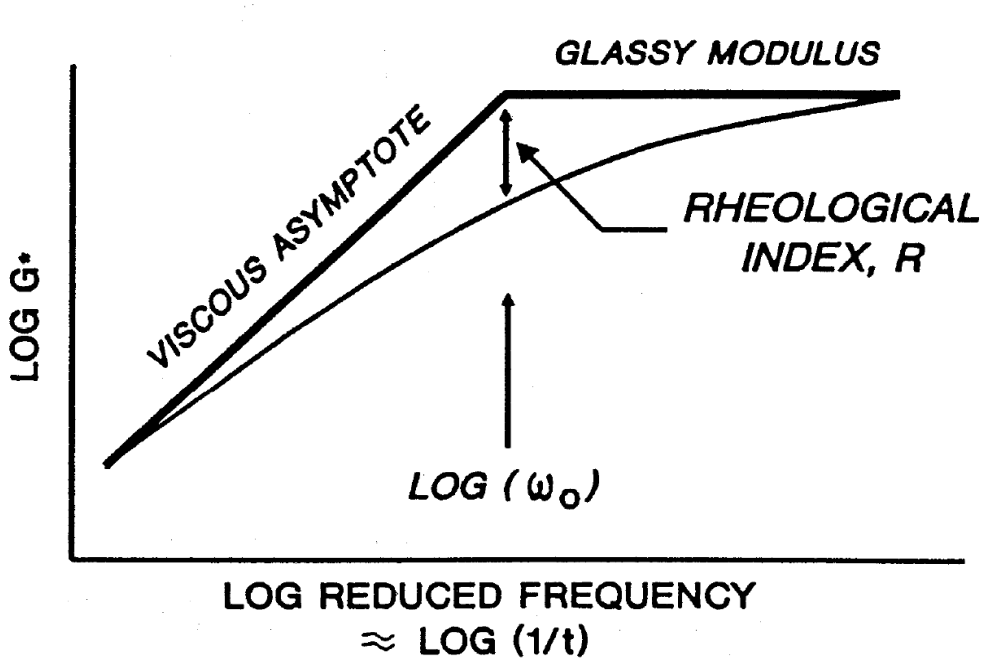

Figure 2-8 Christensen-Anderson model shape parameters

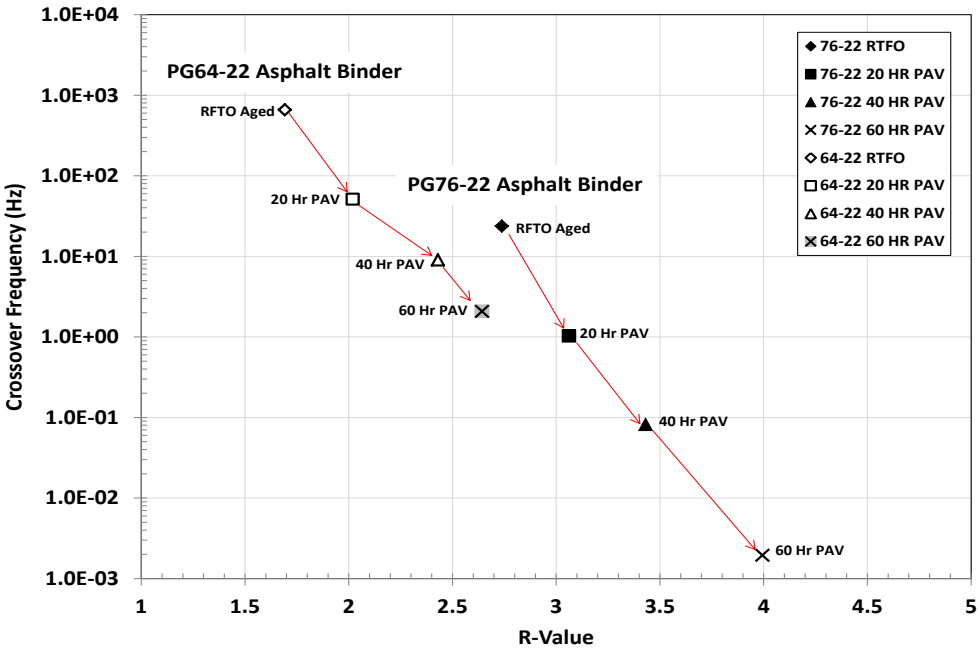

Figure 2-9 Christensen-Anderson model shape parameter changes due to different levels of aging

Along with a general trend of aging, the master curve analysis can also be utilized to evaluate the non-load associated cracking potential based on the work by Glover et al, (2005), Anderson et al. (2011), and Rowe (2011). Based on the original work of Glover et

al (2005), Rowe proposed to evaluate the following parameter, using master curve analysis, at a temperature of 15°C and loading frequency of 0.005 rad/sec.

$$\frac{G^*(\cos\delta)^2}{sin\delta} \qquad 2.1$$

When expressed in this manner, the proposed limiting value in Figure 5 is 9E-04 MPa at 0.005 rad/sec becomes $G^*(\cos\delta)^2/(\sin\delta) < 180$ kPa. The master curve information can then be expressed within Black Space (G* vs phase angle). Rowe's Black Space provides a means of assessing an asphalt binder and pre-screening it to determine if it is susceptible to cracking, using the same principles initially proposed by Glover et al. (2005).

Utilizing the same PG 64-22 and PG 76-22 asphalt binder samples shown earlier, Figure 2-10 shows that when plotted in Rowe's Black Space, as the degree of aging increases, the asphalt binders move from the lower right (passing) side of the proposed criteria to the upper left side (Failing) side of the proposed criteria. The migration of test results is intuitive as one would expect asphalt binders to be more susceptible to cracking as the degree of aging increases.

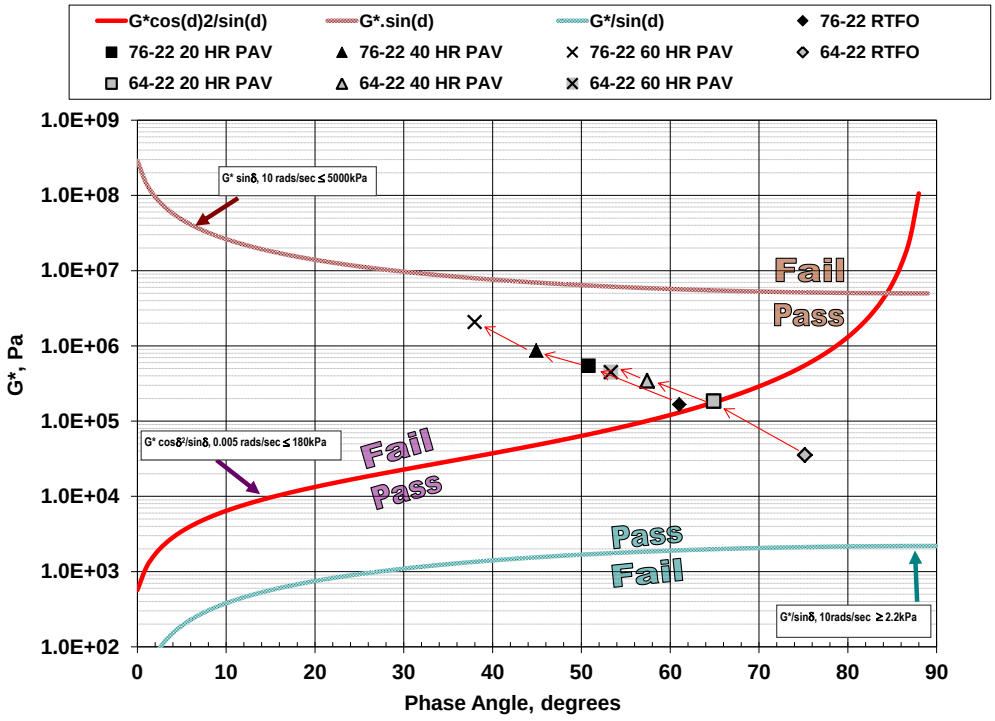

Figure 2-10 Rowe's (2011) black space analysis for non-load associated cracking potential

2.2 Mixture Tests

2.2.1 *Dynamic Modulus*

The AMPT (Asphalt Mixture Performance Tester) machine was used for the dynamic modulus testing in this study. The temperature control systems in the AMPT can achieve the required testing temperatures, ranging from 4°C to 54°C. In order to save time, specimen temperature conditioning was conducted in a support chamber outside the AMPT, and then the specimens were moved to the AMPT chamber. A temperature study was conducted to determine the temperatures at which the supporting temperature chamber and AMPT chamber should be set in order to achieve the target test temperatures for the shortest conditioning time. Table 2-3 summarizes the results of the temperature study for the dynamic modulus testing. The temperatures shown in Table 2-3 are the optimal temperatures determined from the lengthy temperature study. According to these results, the dynamic modulus test can start 30 minutes after the specimen is set in the AMPT chamber.

Table 2-3 AMPT temperature study results for dynamic modulus testing

Target Temperature, °C	Environmental Chamber Setting, °C	AMPT Setting, °C	Waiting Time, min.
4	2	2.5	30
19.5	19	19	30
40	40	40	30
54	56	55	30

Dynamic modulus testing was performed in load-controlled mode in axial compression following the protocol given in AASHTO TP 79. Tests were completed for all mixtures at 4°C, 20°C, 40°C, and 54°C and at frequencies of 25, 10, 5, 1, 0.5, and 0.1 Hz. Load levels were determined by a trial and error process so that the resulting strain amplitudes were between 50 and 75 microstrains. The testing order was from low to high temperatures and from high to low frequencies in order to minimize damage to the specimens. The complex modulus values were obtained from the final six cycles of each loading series, i.e., when the material reached the steady state. The dynamic modulus (|E*|) values were fitted for the coefficients of the sigmoidal function and time-temperature shift factors by optimizing the dynamic modulus mastercurve. After determining the shift factors, the dynamic modulus was converted to the relaxation modulus, E(t), of the Prony series form to obtain a constitutive relationship between strain and stress in the time domain. Finally, a power term, alpha (α), used in viscoelastic continuum damage (VECD) theory, was calculated from the maximum log-log slope, m, of the relaxation modulus and time using the relationship, $\alpha = 1 + 1/m$.

2.2.2 *Fatigue*

2.2.2.1 Simplified Viscoelastic Continuum Damage (S-VECD)

Simplified VECD (S-VECD) model is a mode-of-loading independent, mechanistic model that allows the prediction of fatigue cracking performance under various stress/strain amplitudes at different temperatures from only a few tests. The S-VECD model is composed of two material properties, that is, the damage characteristic curve that defines how fatigue damage evolves in a mixture and the energy-based failure criterion.

The S-VECD test method employs the controlled-crosshead direct tension cyclic test on 100 mm diameter, 130 mm tall cylindrical specimens cut and cored from 150 mm diameter, 178 mm tall gyratory specimens. Details of the test method can be found in AASHTO TP 107 *Determining the Damage Characteristic Curve of Asphalt Concrete from Direct Tension Cyclic Fatigue Tests*. Since the S-VECD test ends with the complete failure of the specimen, the properties measured from this test reflect the fatigue cracking resistance of asphalt mixture in both crack initiation and propagation stages.

The S-VECD testing was conducted using both the AMPT machine as well as a MTS 810 closed loop servo-hydraulic machine in this study. A temperature study similar to that conducted for dynamic modulus testing also was conducted for S-VECD fatigue testing; Table 2-4 shows the results. According to these results, cyclic testing can begin 60 minutes after the specimen is set in the AMPT chamber. The waiting time for cyclic testing is longer than in dynamic modulus testing because it takes more time to set up the specimen in the AMPT chamber for cyclic testing (end plates need to be screwed to the AMPT).

Table 2-4 AMPT temperature study results for S-VECD Fatigue testing

Target Temperature, °C	Environmental Chamber Setting, °C	AMPT Setting, °C	Waiting Time, min.
13	8	11.5	60
20	18	19	60
27	27	26.5	60

The remaining fatigue tests were conducted using the MTS 810 machine. This machine is capable of applying loads up to 20 kips, from 0.01 Hz to 25 Hz. The temperature control systems in the MTS can achieve the required testing temperatures, ranging from -10°C to 54°C. An asphalt concrete dummy specimen with a temperature probe placed in the middle of the specimen was placed inside the chamber in order to monitor the actual temperature of the specimen during testing.

The data acquisition system used for both the AMPT and MTS machine also is fully computer-controlled and is capable of measuring and recording data from several channels simultaneously. Six channels were used for this testing: four for the vertical linear variable differential transducers (LVDTs), one for the load cell, and one for the actuator. The data

acquisition programs were prepared using LabView software for data collection and analysis.

Vertical deformations were measured using four loose-core, CD-type LVDTs at 90° radial intervals with a gauge length of 70 mm. Targets were glued to the specimen face, and the LVDTs were mounted to the targets to measure the deformation in the middle part of the specimen. For consistency in the measurements, a gluing device was used to maintain consistent spacing between the LVDT targets. Figure 2-11 shows the test specimens with the LVDTs mounted on their sides. DEVCON® steel putty was used to glue the steel end plates and targets for the LVDTs that were used for testing the specimens.

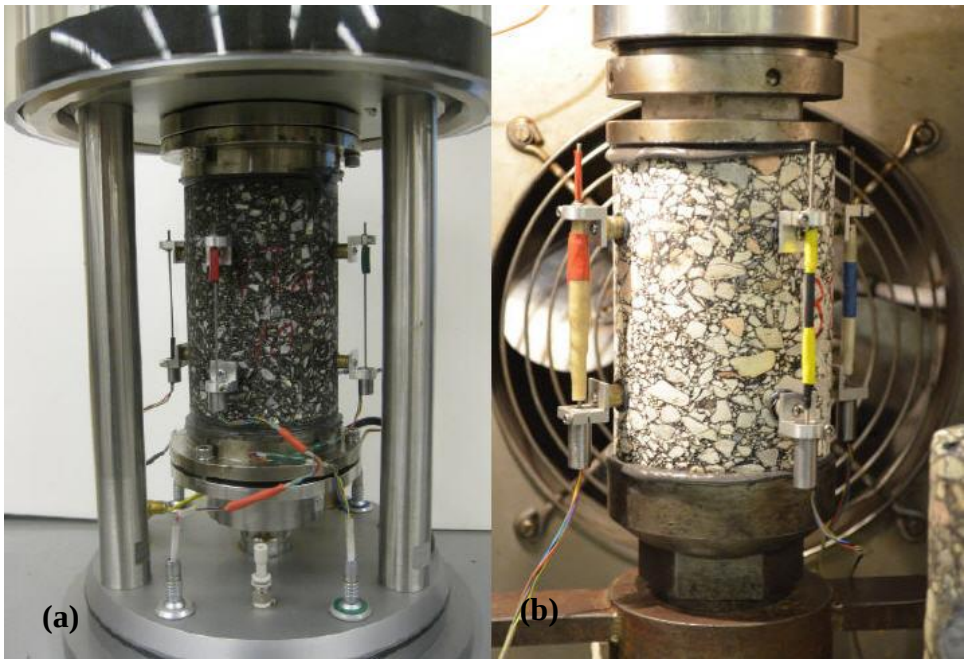

Figure 2-11 LVDT mounting and spacing: (a) AMPT and (b) MTS 810

Cyclic testing was conducted in three modes: crosshead-controlled (CX), stress-controlled (CS), and on-specimen strain-controlled (COS). Because the S-VECD fatigue performance characterization proved to be mode of loading-independent, characteristic curves could be derived from each of the aforementioned test modes. However, because COS testing is difficult to run and CS testing can damage equipment if improperly performed, the CX cyclic test was used for fatigue performance characterization in most of the cases.

Fingerprint dynamic modulus tests were conducted by determining the dynamic modulus ratio (DMR) to check the variability of the test specimens before running the direct tension cyclic tests. A DMR in the range of 0.9 to 1.1 guarantees that the linear viscoelastic properties obtained from the dynamic modulus tests can be used properly in the S-VECD analysis.

For the CX tests, the machine actuator's displacement was programmed to reach a constant peak level at each loading cycle. The actual on-specimen strain levels were significantly lower than the programmed ones due to machine compliance. The viscoelastic damage

characteristics were determined and used in developing the S-VECD model by conducting CX tests on the VT PG 64-28 mixtures at three temperatures of 7°C, 13°C, and 20°C and 10 Hz and on the NH PG 64-28 mixtures at 13°C and 10 Hz.

The CS test is similar to the CX test, but in this case the machine is programmed in such a way that the load reaches a constant peak and valley at each loading cycle. This test was performed on the VT PG 64-28 20% RAP lab fabricated mixture at 13°C and 10 Hz.

In the COS test, which is a true controlled strain test, the machine is programmed such that it maintains a constant on-specimen strain. Figure 2-12 shows the extensometers that were used in performing the COS tests. The tests were performed on the VT PG 64-28 0% RAP lab fabricated and VT PG 64-28 20% RAP lab fabricated mixtures at 13°C and 10 Hz.

Figure 2-12 The extensometers used for COS testing

All cyclic tests were performed at four to six different amplitudes to cover a range (from 1,000 to 100,000) of numbers of cycles to failure (N_f). Once the fatigue tests are conducted, the damage characteristic curves are developed by calculating the secant pseudo stiffness (S) and the damage parameter (S) at each cycle of loading. These values are cross-plotted to form the damage characteristic curve. An example of characteristic curves from fatigue tests conducted a different strain amplitudes is shown in Figure 2-13 for a VT mix. For all the mixtures, the exponential form shown in Equation 2.2 was used to fit the C versus S characteristic curves.

$$C(S) = e^{aS^b} \qquad 2.2$$

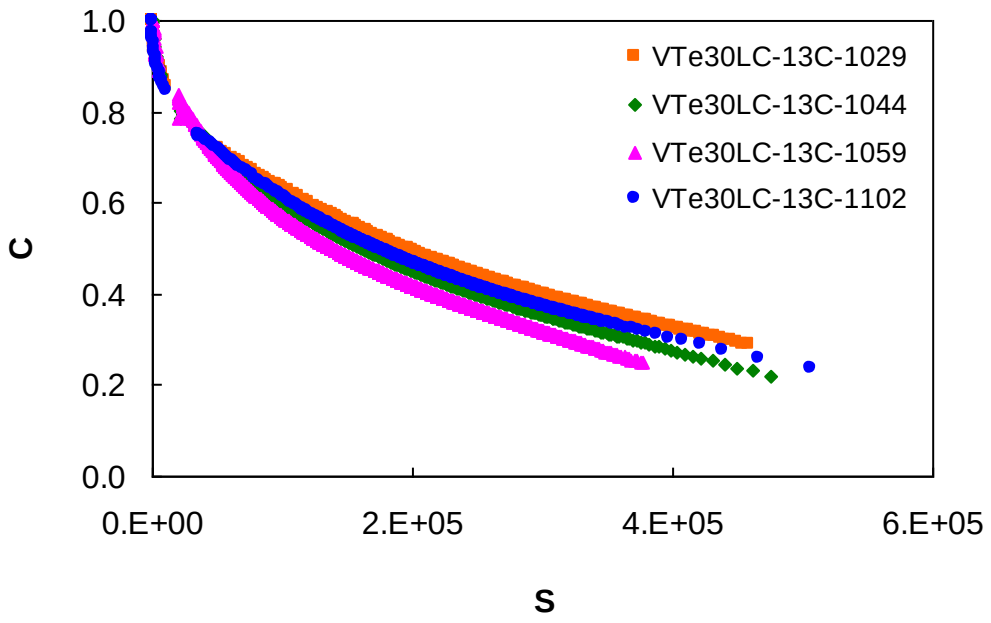

Figure 2-13 Individual results for CX testing for VT PG 64-28 30% RAP mixture at 13°C

The S-VECD fatigue failure criterion, called the G^R method, involves the released pseudo strain energy. This released pseudo strain energy concept focuses on the dissipated energy that is related to energy release due to damage evolution only and is fully compatible and predictable using the S-VECD model. G^R method development details are discussed in detail in Appendix A. Because the G^R characterizes the overall rate of damage accumulation during fatigue testing, it is reasonable to hypothesize that a correlation must exist between the G^R and the final fatigue life (N_f), because the faster the damage accumulates, the quicker the material should fail. A characteristic relationship, which is found to exist in both recycled asphalt pavement (RAP) and non-RAP mixtures, can be derived between the rate of change of the averaged released pseudo strain energy during fatigue testing (G^R) and the final fatigue life (N_f). Figure 2-14 shows this relationship for the VT PG 64-28 30% RAP mixture as an example.

The G^R failure criterion combines the advantages of the VECD model and this characteristic relationship, which both originate from fundamental mixture properties. This method is able to predict the fatigue life of asphalt concrete mixtures across different modes of loading, temperatures, and strain amplitudes within a typical range of sample-to-sample variability that is observed in fatigue testing. Using the derived relationship and the S-VECD model, the fatigue life of asphalt concrete under different modes of loading and at different temperatures and strain amplitudes can be predicted from dynamic modulus tests and CX cyclic direct tension tests at three to four strain amplitudes.

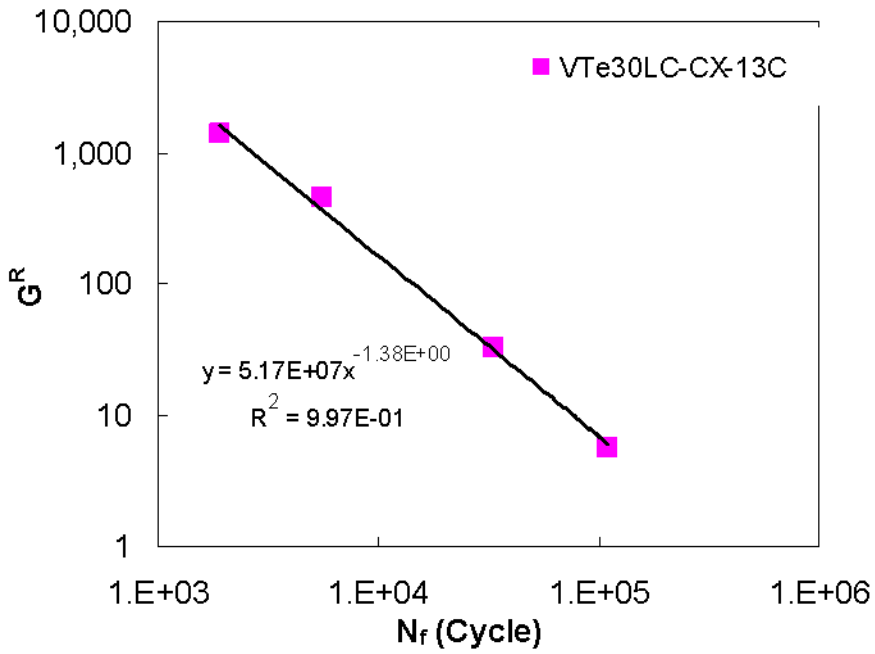

Figure 2-14 Relationship between GR and Nf for VT PG 64-28 30% RAP mixture at 13°C

2.2.2.2 Beam Fatigue

Flexural fatigue testing was conducted using the Flexural Beam Fatigue test procedure outlined in AASHTO T321, *Determining the Fatigue Life of Compacted Hot-Mix Asphalt (HMA) Subjected to Repeated Flexural Bending* (Figure 2-15). The applied tensile strain levels used for the fatigue evaluation were; 300, 500, 600, 700 and 900 micro-strains. However, the number of tensile strains used during the testing was sometimes reduced when the amount of loose mix available for testing was limited. AASHTO T321 is a test procedure to evaluate the crack initiation properties of the asphalt mixture. Therefore, "fatigue life" during this test is defined as the time at which crack initiation has begun.

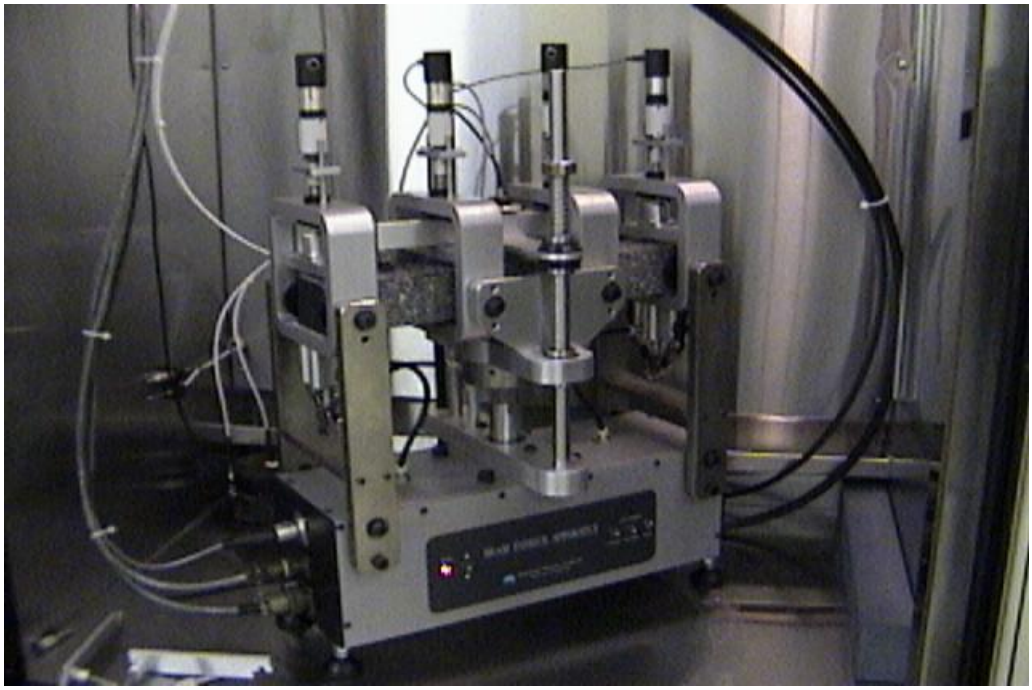

Figure 2-15 Flexural beam fatigue test apparatus

Samples used for the Flexural Beam Fatigue test were compacted using a vibratory compactor designed to compact brick samples of 400 mm in length, 150 mm in width, and 100 mm in height. After the specimen compaction was complete, the samples were trimmed to within the recommended dimensions and tolerances specified under AASHTO T321. The test conditions utilized were those recommended by AASHTO T321 and were as follows:

- Test temperature = 15^{o}C;
- Sinusoidal waveform;
- Strain-controlled mode of loading; and
- Loading frequency = 10 Hz

Due to limitations in material quantities, only one replicate per strain level was conducted.

2.2.2.3 Overlay Tester

The Overlay Tester, described by Zhou and Scullion (2005), has shown to provide an excellent correlation to field cracking for both composite pavements (Zhou and Scullion, 2005; Bennert et al., 2009) as well as flexible pavements (Zhou et al., 2007; Bennert and Maher, 2013). The Overlay Tester evaluates the asphalt mixture's ability to resist or retard crack propagation. Sample preparation and test parameters used in this study followed that of TxDOT Tex-248-F testing specifications. These include:

- 25°C (77°F) test temperature;
- Opening width of 0.025 inches;
- Cycle time of 10 seconds (5 seconds loading, 5 seconds unloading); and
- Specimen failure defined as 93% reduction in Initial Load

Five replicate specimens were tested for each mixture. The low and high values were discarded and the remaining three were used to calculate the average value and standard deviation.

Figure 2-16 shows a photo of the Overlay Tester used in this study.

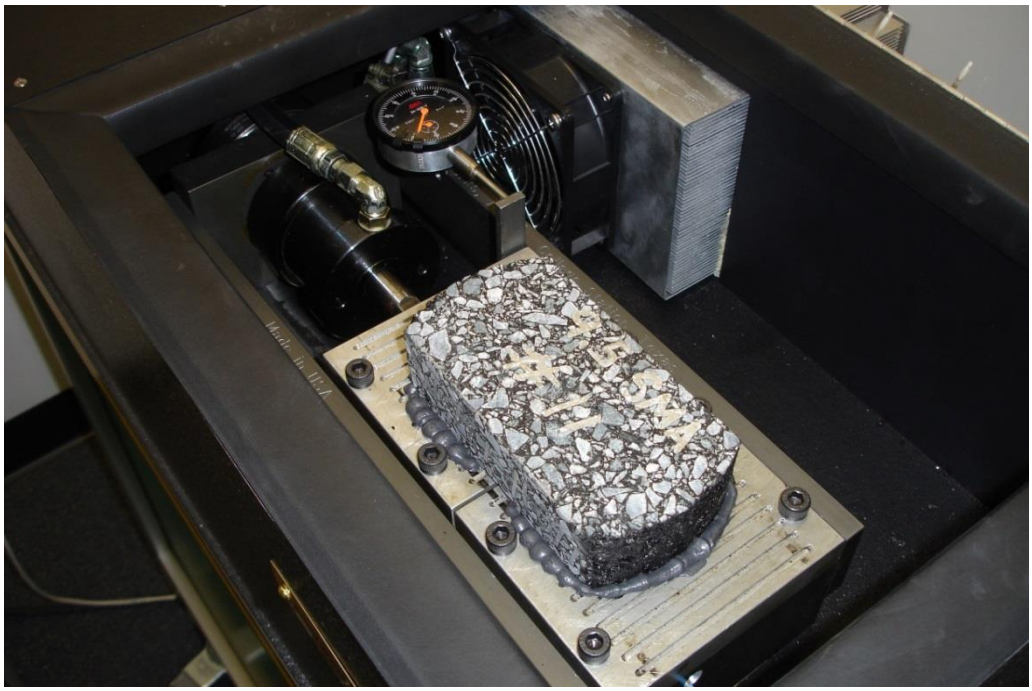

Figure 2-16 Overlay tester with a mounted test specimen

2.2.3 *Low Temperature*

2.2.3.1 Thermal Stress Restrained Specimen Test

In order to assess the low temperature cracking of the mixtures, each mixture was tested in the Thermal Stress Restrained Specimen Test (TSRST) device in accordance with AASHTO TP10-93. In the TSRST test, the asphalt specimen is cooled at a constant rate (-10°C/hour) while its original length is held constant by the TSRST device. As the specimen gets colder it is restrained from contracting, resulting in the accumulation of thermal stresses. Eventually the thermal stresses exceed the tensile strength of the specimen resulting in specimen fracture (crack). The temperature at which this fracture occurs is recorded and noted as the low cracking temperature of the mixture.

A minimum of three replicate gyratory specimens 185 mm (7.3 in) tall by 150 mm (5.9 in) in diameter were fabricated for each mixture. TSRST specimens were then cored and cut to a final height of 160 mm tall (6.3 in) by 54 mm (2.1 in) in diameter. The air voids of the final cut specimens were 6±1%.

2.2.3.2 Low Temperature Indirect Tensile Creep and Strength

Low temperature creep compliance and strength tests were conducted following AASHTO standard method of test for "Determining the Creep Compliance and Strength of Hot-Mix Asphalt (HMA) Using the Indirect Tensile Test Device" (AASHTO, T322-03). The indirect tensile test (IDT) at low temperatures was developed at Pennsylvania State University as part of the Strategic Highway Research Program (SHRP) A-005 research contract. The Pavement Community has been using the elastic solution for IDT testing that (Hondros, 1959) derived using the plane stress assumption. Then a dimensionless correction factor (C_{cmpl}) introduced by (Roque & Buttlar, 1992) was added to the elastic solution in order to account for the bulging of specimens that affects horizontal and vertical measurements. This phenomenon was observed during a finite element study of cylindrical specimen loaded on its diameter. The specification (AASHTO, T322-03) used the elastic solution corrected with the (C_{cmpl}) correction factor, shown in equation 2.3.

$$D(t) = \frac{\Delta X_{tm,t} \times D_{avg} \times b_{avg}}{P_{avg} \times GL} \times C_{cmpl} \quad 2.3$$

Where,

$D(t)$ = Creep compliance (1/Pa)
$\Delta X_{tm,t}$ = Computed trimmed mean of the six horizontal deformation arrays (m)
D_{avg} = average diameter of the three replicate specimens (m)
b_{avg} = average thickness of the three replicate specimens (m)
P_{avg} = average creep load of the three replicate specimens (N)
GL = gage length (m)
C_{cmpl} = dimensionless correction factor

Later, (Kim, Daniel, & Wen) introduced viscoelastic solution for the IDT creep test using the theory of linear viscoelasticity, shown in equation 2.4.

$$D(t) = -\frac{d}{p}\left[c\,U(t) + eV(t)\right] \quad 2.4$$

Where,

$D(t)$ = Creep compliance (1/KPa)
d = Specimen thickness (m)
p = Applied load (KN)
$U(t)$ = Horizontal deformation (m)
$V(t)$ = Vertical deformation (m)

c and e = Coefficients related to specimen diameter and gauge length (Dimensionless)

For this study, c = 0.611 and e = 1.685 for specimen with 150 mm diameter and 50.8 mm gauge length.

Specimens were tested using a closed-loop servo-hydraulic system manufactured by Instron Inc. shown in Figure 2-17. Testing experience showed that specimens tested at 0°C or lower generally behave linearly for testing durations up to 1000 sec, if creep loads are kept low enough. Loading magnitudes were picked by trial and error to limit horizontal tensile strains to 300 microstrains or less to safely ensure linear behavior, and greater than 50 microstrains to keep signal to noise ratio low enough. Actual loading duration was 100 sec.

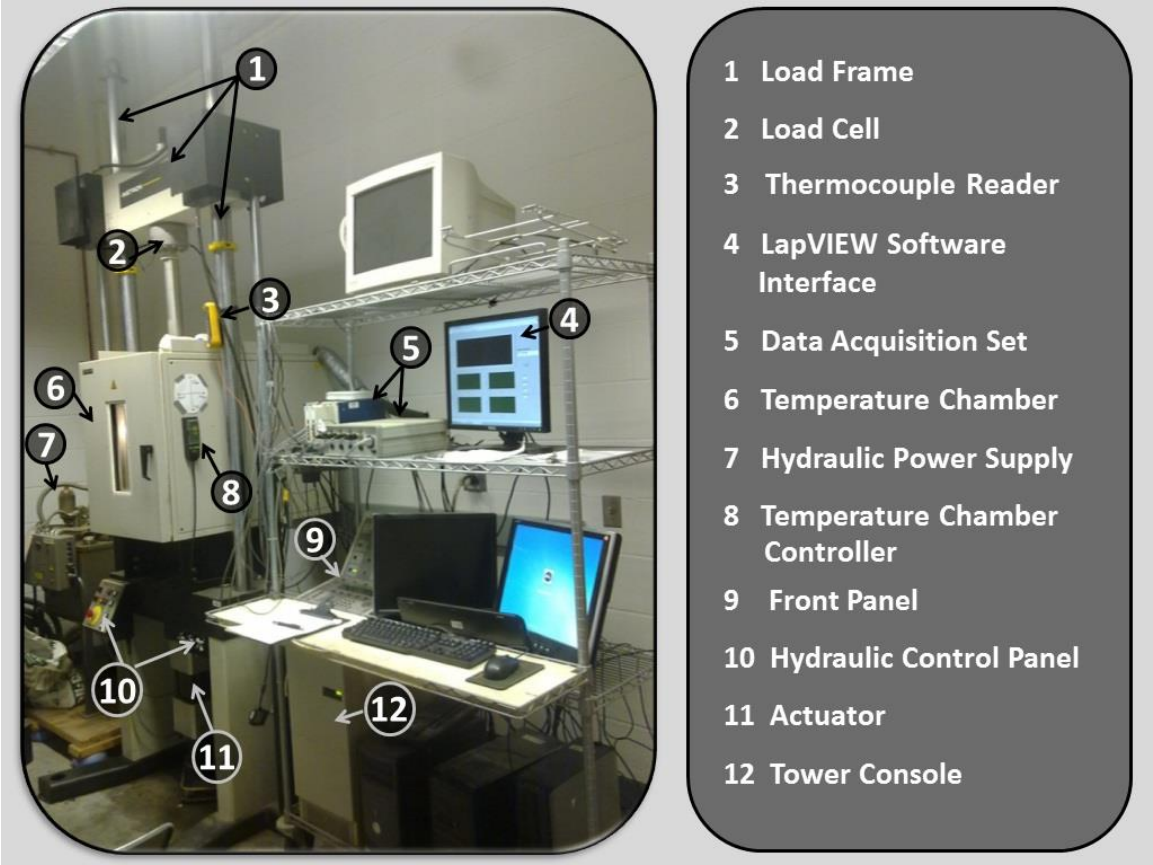

Figure 2-17 A closed-loop servo-hydraulic system manufactured by Instron Inc.

A dummy specimen with an embedded thermocouple was used to ensure that specimens reach the target testing temperature ±0.2°C. Taking in consideration that the specimen was never kept at 0°C or less for over 24 hours to avoid the effects of low-temperature physical hardening, a phenomenon observed by (Bahia, 1991). Specimens' thicknesses were measured following ASTM standards "Thickness or Height of Compacted Bituminous Paving Mixture Specimens" (ASTM, D3549).

Low temperature creep testing data analysis was done by calculating stresses and strains and fitting them to a generalized power law function to filter raw data from associated noise using a Matlab code. After this step, low temperature creep compliance was calculated using method described in (AASHTO, T322-03), (Christensen, 1998), and (Buttlar & Roque, 1994)

Strength testing was conducted following (AASHTO, T322-03) standards, with the one difference that only load versus time was recorded during testing.

The average tensile strength at -10C was selected to represent the undamaged tensile strength of the asphalt mixture at all temperatures as recommended by (Hiltunen & Roque, 1994). Asphalt mixture strength increases with decreasing temperature until a certain temperature where strength begins to decrease; this temperature varies from one mixture to another. The decrease in strength at very low temperatures is likely a result of stresses

induced by differential contraction between aggregate and binder which may cause internal damage and lower mixture strength. As the peak strength in Hiltunen & Roque's work always occurred at a temperature lower than -10ºC, strength measured at -10C may be considered as a conservative evaluation of undamaged tensile strength of mixtures at low temperatures.

Critical cracking temperature analysis for the mixtures was conducted using the LTSTRESS spreadsheet developed by Don Christensen. The creep compliance master curve is used to compute the thermal stress in the pavement using user-specified starting temperatures and cooling rates. The plot of thermal stress vs. temperature is then developed. The location at which the thermal stress curve meets the strength measured at -10ºC is defined as the low temperature critical cracking temperature. The standard starting temperature and cooling rate used for this analysis are 10ºC and 5.6ºC/hr, respectively.

2.2.4 *Moisture*

2.2.4.1 Hamburg Wheel Tracking Device (HWTD)

Testing was conducted in accordance with AASHTO T324 "Hamburg Wheel-Track Testing of Compacted Hot-Mix Asphalt (HMA)". The test is utilized to determine the susceptibility of the mixture to failure due to weakness in the aggregate structure, inadequate binder stiffness, or moisture damage. In this test, the mixture is submerged in heated water (typically 40-50ºC) and subjected to repeated loading from a 705 N steel wheel. As the steel wheel loads the specimen, the corresponding rut depth of the specimen is recorded. The rut depth versus numbers of passes of the wheel is plotted to determine the Stripping Inflection Point (SIP) as shown in Figure 2-18. The SIP gives an indication of when the test specimen begins to exhibit stripping (moisture damage).

Gyratory specimens for this study were fabricated using the SGC to an air void level of 7.0±2.0% as required by AASHTO T324. Testing in the HWTD was conducted at a test temperature of 50ºC (122ºF). The specimens were tested at a rate of 52 passes per minute after a soak time of 30 minutes at the test temperature. Testing terminated at 20,000 wheel passes or until visible stripping was noted.

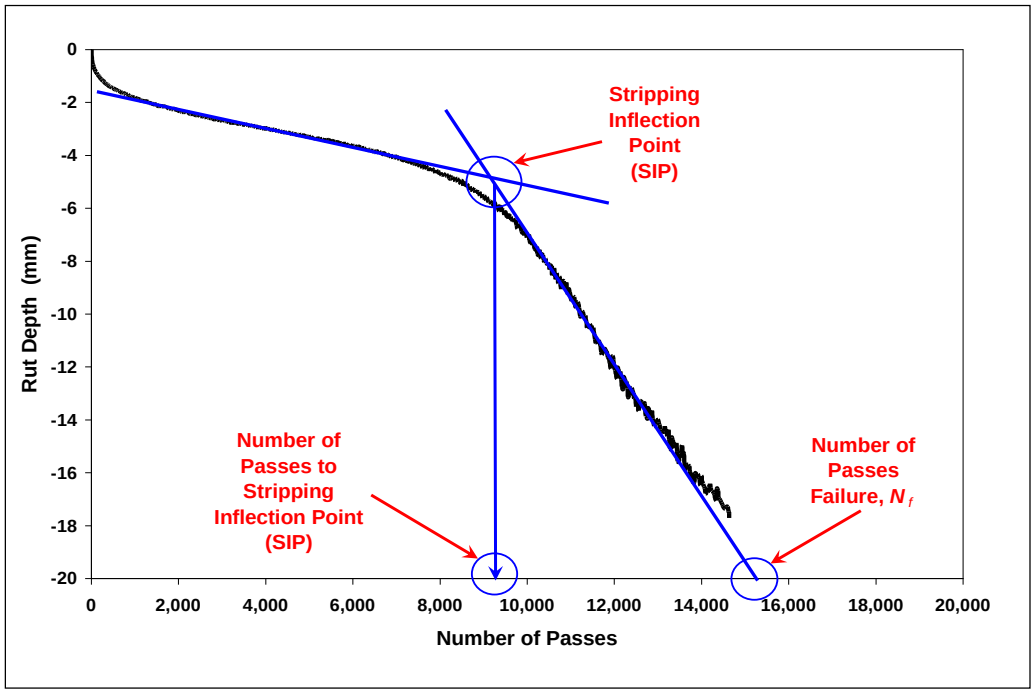

Figure 2-18 Determination of HWTD stripping inflection point (SIP)

2.2.4.2 Tensile Strength Ratio (TSR)

Mixture resistance to moisture induced damage was also evaluated using the modified Lottman test following AASHTO standard method of test for "Resistance of compacted Asphalt Mixtures to Moisture-Induced Damage" (AASHTO, T283-03). Six specimens were compacted to 7±0.5 % air void content. Specimen dimensions were 150mm in diameter by 95 ± 5 mm thick. These specimens were divided in to two sets of three specimens each, a control (unconditioned) set and a set subjected to conditioning of one freeze-thaw cycle following (AASHTO, T283-03). Specimens were assigned in each of the two sets in order to minimize the difference between the average air void content of each set. The ratio between average strength of the conditioned set to the average strength of the control set, also known as tensile strength ratio (TSR) was computed. A minimum TSR of 0.7 is usually specified. (NCAT, 1996)

Tensile Strength Ratio calculation:

$$S_t = \frac{2\,P}{\pi\,t\,D} \quad (2.5)$$

Where,

S_t = tensile strength, psi
P = maximum load, lbs.
t = specimen thickness, in.
D = specimen diameter, in

And,

$$\text{Tensile Strength Ratio } (TSR) = \frac{S_2}{S_1} \quad (2.6)$$

Where,

S_1 = average tensile strength of the control set.
S_2 = average tensile strength of the conditioned set.

2.2.5 *Workability Device*

Workability of each of the plant produced mixtures was evaluated because of potential concerns at higher RAP contents. These evaluations were conducted using a HMA workability device developed by the University of Massachusetts Dartmouth Highway Sustainability Research Center (HSRC). This device (Figure 2-19) is known as the Asphalt Workability Device (AWD) and has been used previously to evaluate high percentage RAP mixtures as well as mixtures incorporating WMA additives (Austerman et al., 2009). The AWD operates on torque measurement principles that have been previously established (Gudimettla et al., 2003); mixtures exhibiting lower torque at the same temperature are considered more workable.

The AWD rotates the loose HMA mixture at a constant speed (15 rpm for this study) and separately records the resultant torque exerted on a pug mill style paddle shaft embedded into the mixture (Figure 2-20). Concurrently the surface and internal temperatures of the mixture are recorded. As the mixture cools in ambient conditions, the torque exerted on the shaft increases thereby giving an indication of the workability of the mixture at different temperatures.

Figure 2-19 University of Massachusetts HSRC – asphalt workability device (AWD)

Figure 2-20 Asphalt workability device (AWD) pug mill style paddle

AWD test specimens were fabricated from loose plant produced mixture. Each loose mixture was reheated using the formal reheating procedure developed for this study. For each mixture, approximately 15kg of loose mixtures were introduced into the AWD at a temperature of 315°F (157°C) and testing commenced. The workability test and data collection continued until the mixture reached a temperature of 225°F (107°C). The AWD test commencement and termination temperatures were selected based on previous studies in order to ensure that the workability (torque) versus temperature relationship was captured.

For each mixture, based on the raw toque versus temperature data collected from the AWD, a best fit model in the form of an exponential line was fit to the data. These models were then utilized to develop a model curve plotted over the actual temperature range in which the torque data was collected. Note that mixtures exhibiting lower torque values at a given temperature are considered more workable.

CHAPTER 3 NEW HAMPSHIRE MIXTURES

3.1 Mixture Design Information

The New Hampshire mixtures were produced from a 2008 Gencor Ultra drum plant with 400 tons per hour capacity owned by Pike Industries and located in Portsmouth, New Hampshire (NH). Mixing times were determined to be approximately 40 seconds. The general mixture design information for the NH mixtures is shown in Table 3-1 and Table 3-2. The mixtures produced had a nominal maximum aggregate size of 12.5 mm with an optimum asphalt content of 5.7%. The RAP used in the NH mixtures has a continuous PG grade of 85.5-13.2. Based on the percent of binder in the mixtures determined from extraction and recovery, the virgin and 40% RAP mixtures contained more than the optimum amount of asphalt. The 20% and 30% RAP mixtures had lower binder content relative to the optimum. The gradations for the 20% and 30% RAP were similar to the virgin mixture. The percent passing the #100 and #200 sieves were lower in the 40% RAP mixture in comparison to the other RAP and virgin mixtures.

3.2 Plant Production Information

The plant production information for the NH mixtures is shown in Table 3-3. The asphalt mixtures were produced between 315 to 335^{o}F. The virgin mixture was produced at 330^{o}F and the RAP mixtures were produced between 310-315^{o}F. All mixtures were stored in the silo prior to discharging into the delivery trucks. However, the 40% RAP mixture was stored in the silo for a much longer time (6 hrs.) relative to the 20% and 30% RAP mixtures (1.0 and 1.25 hrs. respectively).

3.3 Binder Testing

3.3.1 *PG Grading*

The asphalt binder was sampled from the storage tanks, as well as extracted and recovered from the mixtures. The results of the PG grading are shown in Table 3-4, as well as Figure 3-1 and Figure 3-2. The test results indicate that as the RAP content increases, the PG grade gets warmer at both the low and high PG temperatures. The results also show that the low temperature PG grade of the extracted and recovered RAP mixtures are dictated by the m-slope, which is a function of the relaxation properties of the asphalt binder.

Table 3-1 Mix design information – all NH mixtures

Mix	PG Grade	NMAS (mm)	Design Asphalt Content (%)	% RAP	RAP Binder Content (%)	VMA	VFA	Extracted/ Recovered Asphalt Content (%)	% Binder Replacement
NH PG 64-28 0 % RAP	64-28	12.5	5.7	0	--	14.9	74.8	5.84	0.00
NH PG 64-28 20 % RAP	64-28	12.5	5.7	20	4.79	14.4	79.9	5.46	15.50
NH PG 64-28 30 % RAP	64-28	12.5	5.7	30	4.79	14.5	81.3	5.31	23.29
NH PG 64-28 40 % RAP	64-28	12.5	5.7	40	4.79	14.5	82.1	6.02	30.32

Table 3-2 Mixture gradations - all NH mixtures

Mix	**PG**	**Mixture Gradation**								
		12.5	**9.5**	**#4**	**#8**	**#16**	**#30**	**#50**	**#100**	**#200**
NH PG 64-28 0 % RAP	64-28	98.6	85.8	58.3	42.5	32.0	24.7	15.5	7.2	3.58
NH PG 64-28 20 % RAP	64-28	98.7	86.5	57.5	42.4	33.0	25.5	15.8	7.0	3.60
NH PG 64-28 30 % RAP	64-28	98.7	86.5	56.2	41.9	34.0	25.8	16.0	6.9	3.62
NH PG 64-28 40 % RAP	64-28	98.7	86.4	55.5	41.2	33.0	24.8	15.0	6.1	2.65

Table 3-3 Plant production information - all NH mixtures

Mix	**PG Grade**	**Plant Type**	**Aggregate Temp. (ºC/ºF)**	**Discharge Temp. (ºC/ºF)**	**Compaction Temp. (ºC/ºF)**	**Silo Storage time (hrs)**
NH PG 64-28 0% RAP	64-28	Drum	n/a	165.6/330	148.9/300	n/a
NH PG 64-28 20% RAP	64-28	Drum	n/a	157.2/315	154.4/310	1.0
NH PG 64-28 30% RAP	64-28	Drum	n/a	168.3/335	157.2/315	1.25
NH PG 64-28 40% RAP	64-28	Drum	n/a	168.3/335	157.2/315	6.0

Table 3-4 Summary of asphalt binder performance grading for NH mixtures

Production Location	Base PG Grade Binder	Tank or Extracted with RAP Content	Continuous PG Grade (°C)				PG Grade (°C), AASHTO R29 & M320	Critical Cracking Temperature (°C), AASHTO R49
			High Temp (RTFO)	Low Temp		Intermediate Temp (PAV)		
				Stiffness (MPa)	m-slope			
Pike (Portsmouth, NH)	64-28	Tank	66.3	-29.7	-29.5	19.9	64-28	-28
		Extracted - 0% RAP	71.8	-29.5	-28.4	19.5	70-28	-25.7
		Extracted - 20% RAP	76.7	-28.9	-24.1	21.4	76-22	-25.9
		Extracted - 30% RAP	78.1	-28.2	-26.5	22.6	76-22	-27.6
		Extracted - 40% RAP	79.8	-27.9	-23.7	22.8	76-22	-25.7

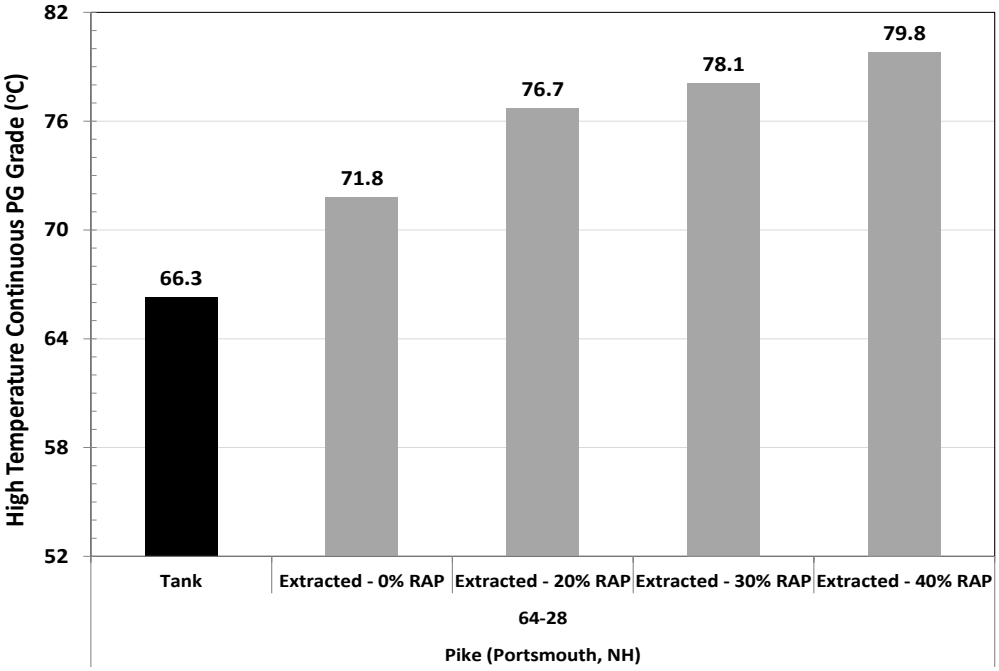

Figure 3-1 High temperature PG grade (Portsmouth, NH)

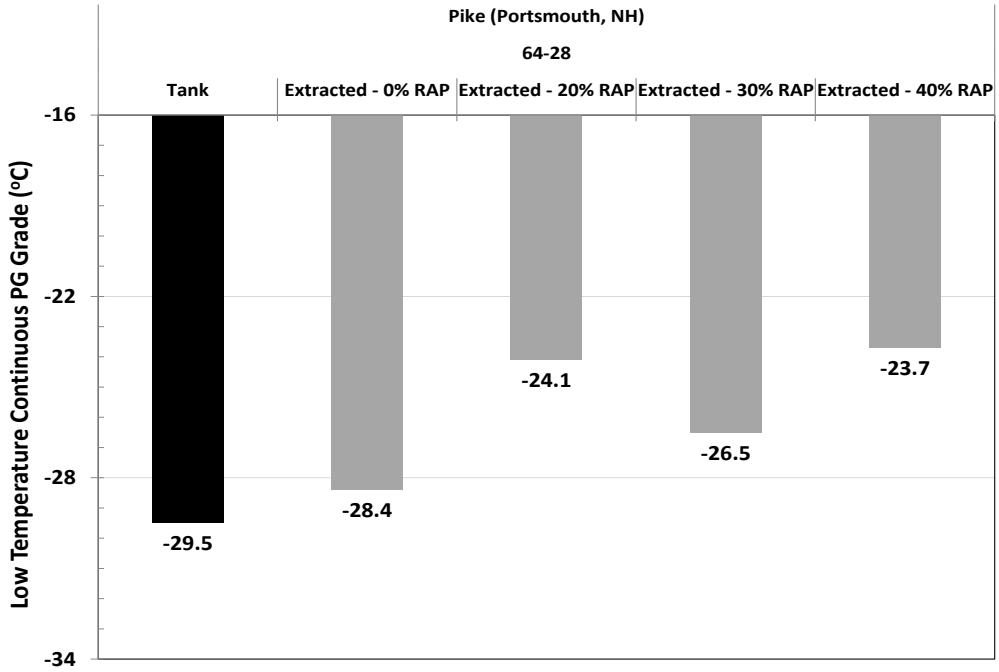

Figure 3-2 Low temperature PG grade (Portsmouth, NH)

3.3.2 *Critical Cracking Temperature (CCT)*

The low temperature critical cracking temperature was measured in accordance with AASHTO R49. The material test properties were used to evaluate different starting temperatures and cooling rates that could occur in the Northeast. It should be noted that the Critical Cracking Temperature (CCT) shown earlier in Table 3-4 is for the standard

starting temperature and cooling rate recommended in AASHTO R49 for reporting purposes.

The results of the CCT analysis are shown in Table 3-5 through Table 3-8. The tables indicated that starting temperature has little influence on the CCT of the asphalt binder. Meanwhile, the cooling rate is shown to have a significant impact on the CCT. The CCT changes almost a full PG grade when increasing the cooling rate from 1°C/hr to 10°C/hr. Generally, at the different cooling rates, the 20% and 30% RAP mixtures had a colder CCT relative to the virgin mixture. However, the 40% RAP mixture had a warmer CCT relative to the virgin mixture. This might be attributed to the actual degree of blending between the fresh and aged binders that is occurring in the different mixtures.

Table 3-5 Cooling rate vs. starting temperature – Pike, NH PG 64-28 & 0% RAP

64-28 0% RAP Portsmouth NH				
TCMODEL Critical Cracking Temperature (°C)				
Starting Temp of Cooling Event	Cooling Rate C/hr 1	Cooling Rate C/hr 2	Cooling Rate C/hr 5.6	Cooling Rate C/hr 10
10C	-25.6	-24.0	-21.5	-20.1
5C	-25.6	-24.1	-21.6	-20.2
0C	-25.7	-24.1	-21.7	-20.3
-5C	-25.8	-24.2	-21.9	-20.5

Table 3-6 Cooling rate vs. starting temperature – Pike, NH PG 64-28 & 20% RAP

64-28 20% RAP Portsmouth NH				
TCMODEL Critical Cracking Temperature (°C)				
Starting Temp of Cooling Event	Cooling Rate C/hr 1	Cooling Rate C/hr 2	Cooling Rate C/hr 5.6	Cooling Rate C/hr 10
10C	-25.7	-24.3	-22.0	-20.7
5C	-25.8	-24.3	-22.1	-20.8
0C	-25.9	-24.4	-22.3	-21.0
-5C	-26.0	-24.6	-22.5	-21.4

Table 3-7 Cooling rate vs. starting temperature – Pike, NH PG 64-28 & 30% RAP

64-28 30% RAP Portsmouth NH				
TCMODEL Critical Cracking Temperature (°C)				
Starting Temp of Cooling Event	Cooling Rate C/hr 1	Cooling Rate C/hr 2	Cooling Rate C/hr 5.6	Cooling Rate C/hr 10
10C	-27.6	-26.0	-23.5	-22.1
5C	-27.6	-26.0	-23.5	-22.1
0C	-27.6	-26.1	-23.6	-22.2
-5C	-27.7	-26.2	-23.8	-22.5

Table 3-8 Cooling rate vs. starting temperature – Pike, NH PG64-28 & 40% RAP

64-28 40% RAP Portsmouth NH				
TCMODEL Critical Cracking Temperature (°C)				
Starting Temp of Cooling Event	Cooling Rate C/hr 1	Cooling Rate C/hr 2	Cooling Rate C/hr 5.6	Cooling Rate C/hr 10
10C	-25.5	-23.4	-20.5	-19.0
5C	-25.6	-23.5	-20.6	-19.2
0C	-25.7	-23.7	-20.8	-19.4
-5C	-25.9	-24.0	-21.2	-19.8

3.3.3 *Asphalt Binder Master Curves*

The asphalt binder master curves, constructed using the asphalt binder extracted and recovered from the plant-compacted specimens, are shown in Figure 3-6. The master curves show that the stiffness of the asphalt binders converge at the lower temperatures (higher frequencies) but begin to separate at the higher temperatures (lower frequencies). The master curves do show that as the RAP content increases, the stiffness of the extracted/recovered asphalt binder also increases. Figure 3-4 shows the Rheological Index (R) – Crossover Frequency (ω_o) Space; the test results indicate that as RAP content increases, the asphalt binder behavior is that of a progressively aging asphalt binder. The extracted and recovered asphalt binders were also evaluated using Rowe's Black Space analysis in Figure 3-5. The test results indicate that asphalt mixtures containing more than 20% RAP would be "prone" to cracking, with the 20% RAP mixture falling on the border of the Pass/Fail criteria.

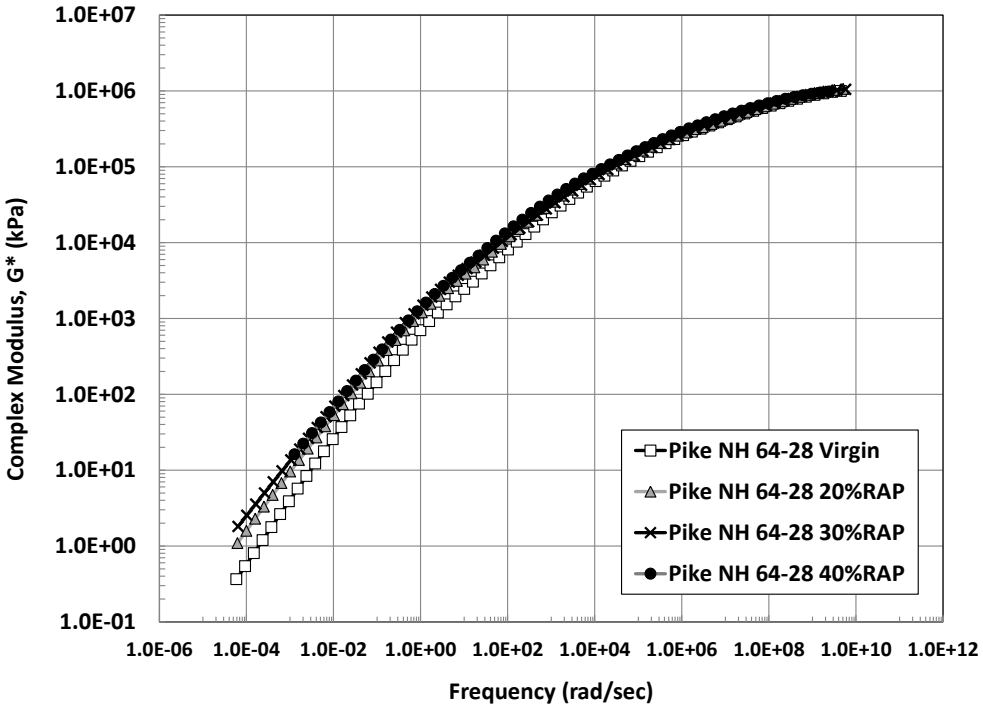

Figure 3-3 Asphalt binder master curves for New Hampshire mixtures

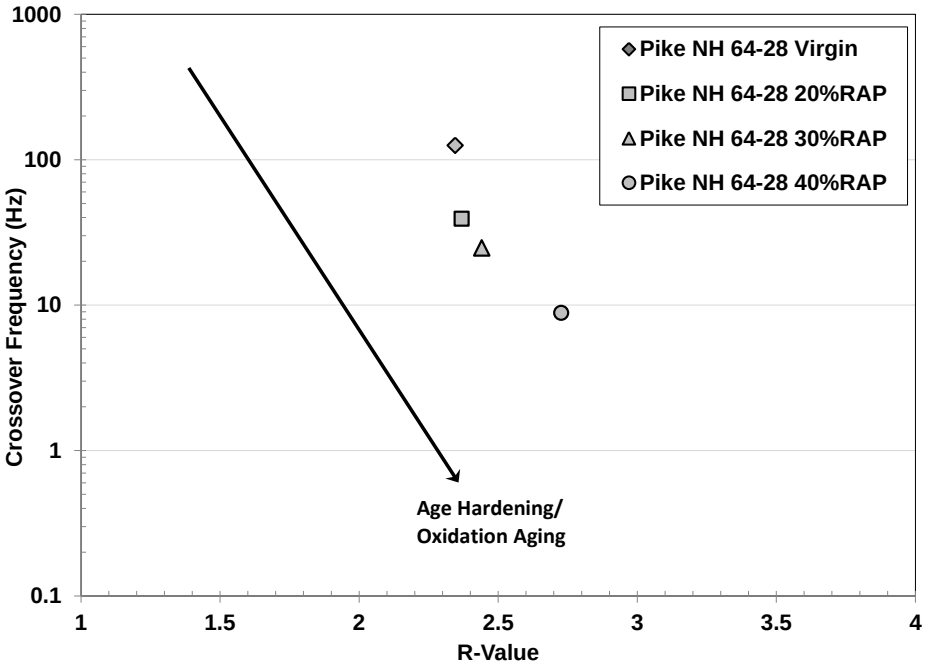

Figure 3-4 Rheological index – crossover frequency space for asphalt binder extracted/recovered from New Hampshire mixtures

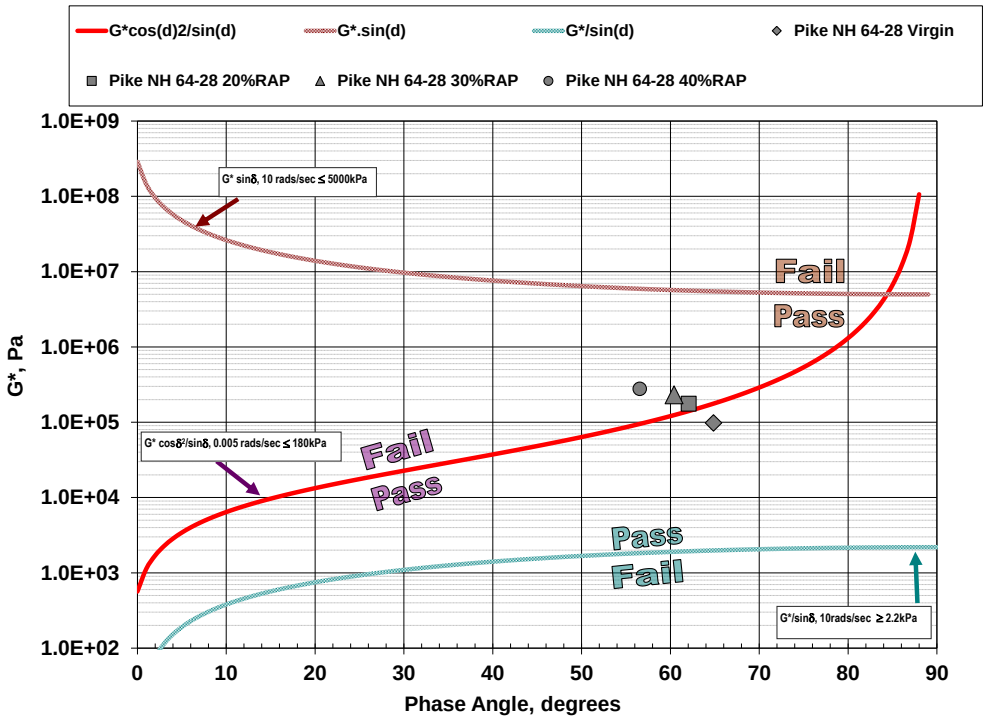

Figure 3-5 Rowe's black space analysis for asphalt binder extracted/recovered from New Hampshire mixtures

3.4 Mixture Testing

3.4.1 *Dynamic Modulus*

The dynamic modulus properties of the asphalt mixtures were determined in accordance to AASHTO TP79. Two sets of test specimens were prepared for evaluation; 1) Test specimens compacted at the asphalt plant and 2) Test specimens produced by reheating loose mix at the laboratory and then compacting the test specimens.

3.4.1.1 Plant Compacted Mixtures

The dynamic modulus (E*) test results for the New Hampshire RAP mixtures compacted at the asphalt plant are shown in Figure 3-6. The results are an average of three test specimens. The stiffness master curves indicate that the 0% RAP mixture generally had the lowest stiffness while the 40% RAP mixture had the highest stiffness values. The trend in test results follows what has been observed by others, which is as the RAP content increases, the mixture stiffness also increases.

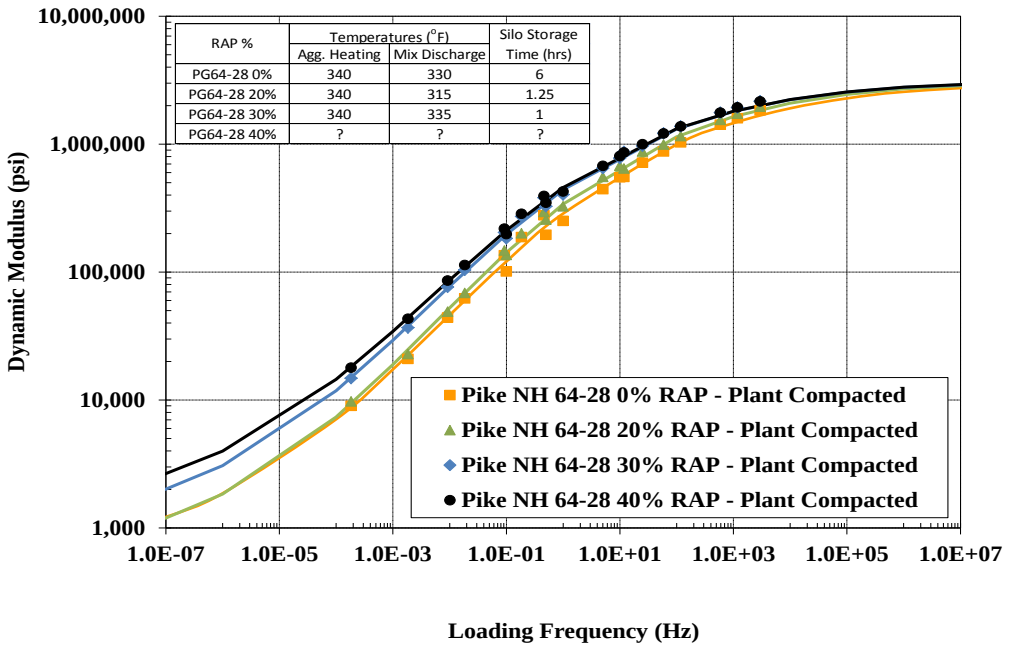

Figure 3-6 Dynamic modulus master curves for New Hampshire mixtures – plant compacted

3.4.1.2 Reheated Loose Mix and Compacted Mixtures

The identical mixtures were tested after the sampled loose mix was reheated and compacted following the test method developed by the Pooled Fund Research Team. The resultant master curves are shown in Figure 3-7. There is a slight change in the test results where the RAP mixtures are all very similar to one another, while the virgin mix does appear to have a lower stiffness at all test temperatures and loading frequencies.

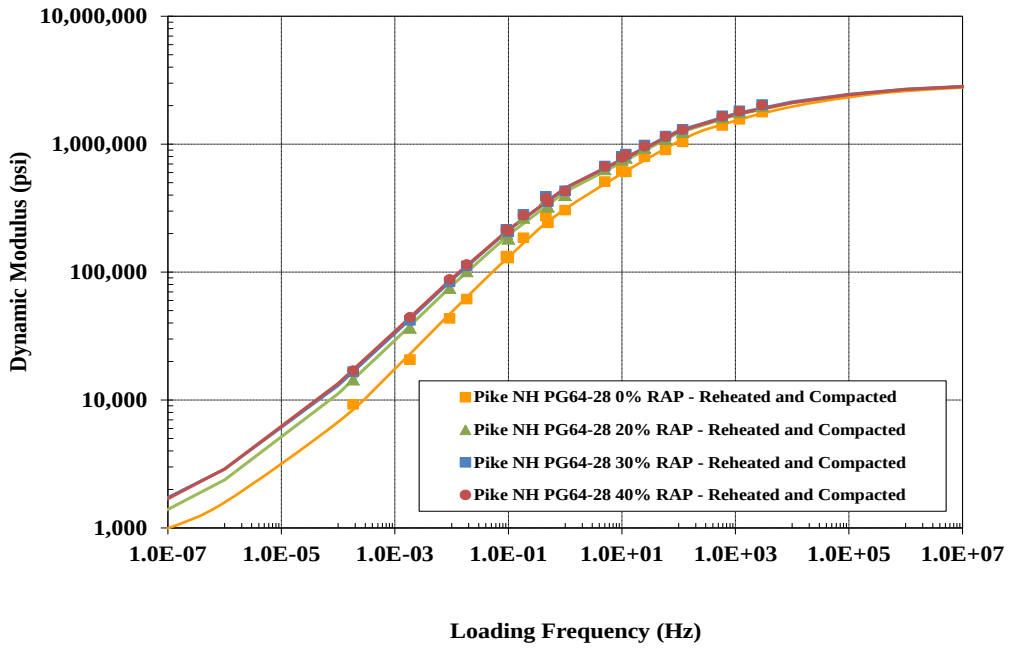

Figure 3-7 Dynamic modulus master curves for New Hampshire mixtures –reheated and compacted loose mix

3.4.1.3 Comparison of Plant Compacted and Reheated Loose Mix Specimens

The testing of the two different specimen types allowed for an evaluation of how the stiffness of the mixtures may change due to the reheating of loose mix in the laboratory. Although reheating loose mix for test specimens is common practice, not much information exists as to how reheating may alter the stiffness of the asphalt mixtures.

Figure 3-8 through Figure 3-10 show the ratio between the reheated/compacted and plant compacted dynamic modulus values at the different test temperatures and loading frequencies. The figures show that slight stiffening is taking place at the lower loading frequencies at the 4 and 20 ºC test temperatures. However, at the 35ºC test temperature, a much larger increase in mixture stiffness is observed for the 20% RAP mixture. The plant production data for the 20% RAP mixture indicated that it has the lowest discharge temperature and that it was only stored in the silo for 1.25 hours. Therefore, due to the lower oxidized RAP content, as well as lower discharge and silo storage time, this mixture may have been more prone to additional stiffening due to reheating than the other mixtures produced.

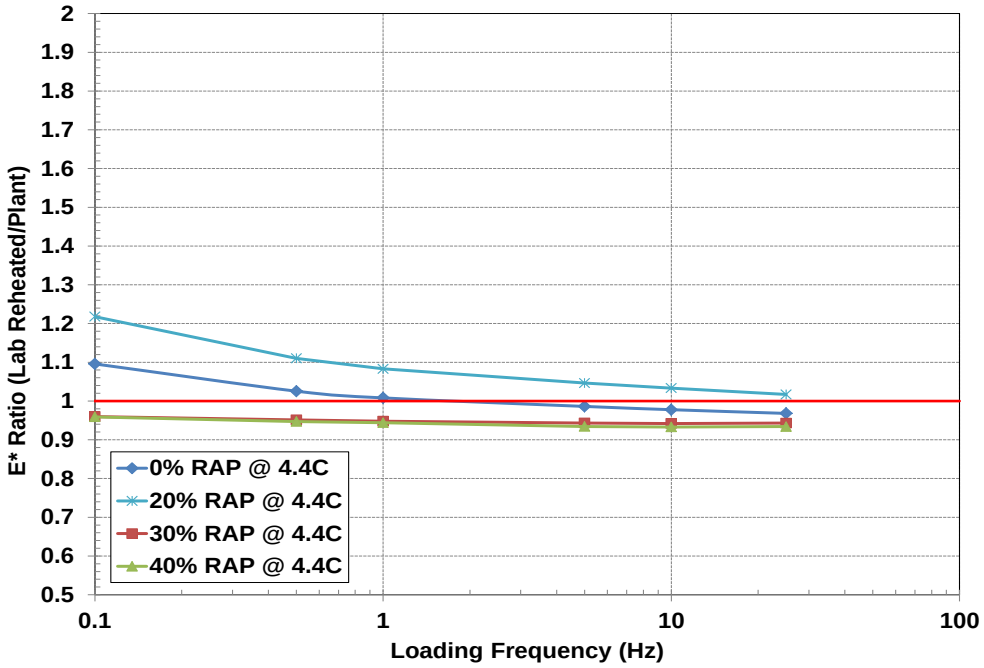

Figure 3-8 Dynamic modulus ratio for 4°C test temperature

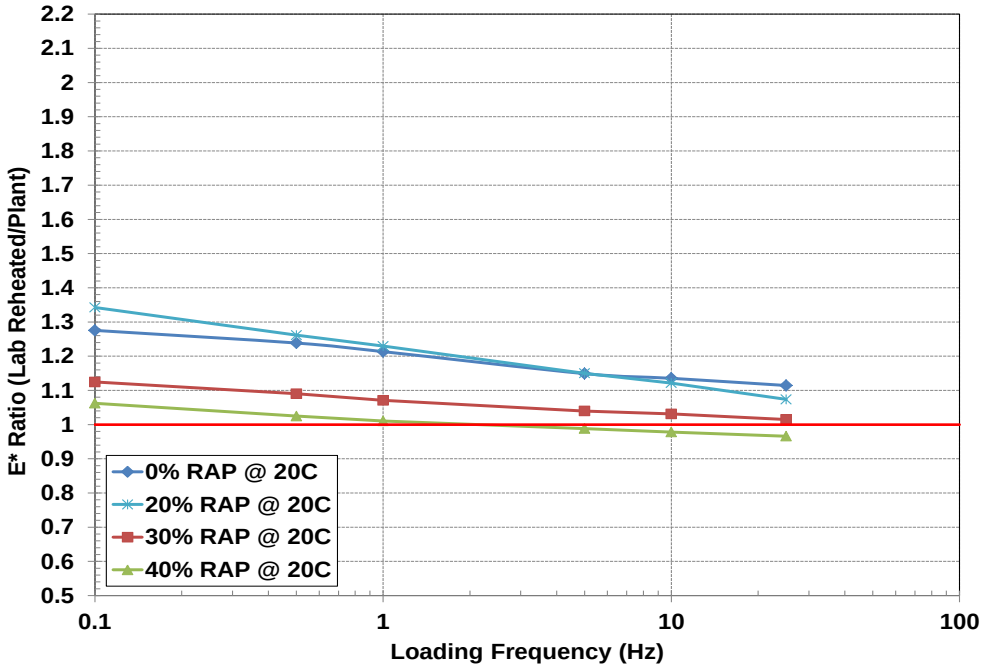

Figure 3-9 Dynamic modulus ratio for 20°C test temperature

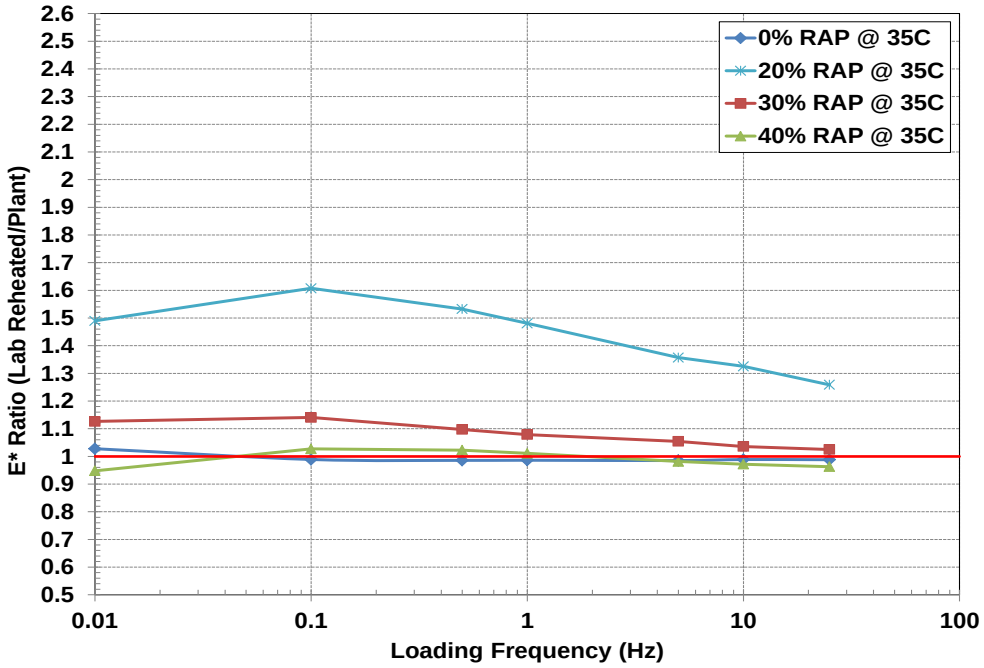

Figure 3-10 Dynamic modulus ratio for 35°C test temperature

3.4.2 *Fatigue*

Fatigue behavior of the mixtures was evaluated using three different tests: S-VECD and beam fatigue to evaluate crack initiation and the overlay tester to evaluate crack propagation.

3.4.2.1 S-VECD

S-VECD testing on the NH PG 64-28 mixtures was conducted in crosshead-controlled (CX) mode of loading at 13°C and 10 Hz. Table 3-9 shows the exponential fit parameters for the S-VECD model for the NH mixtures.

Table 3-9 Exponential Fit Parameters for VECD Model for NH PG 64-28 Mixtures

Mix Type	Alpha	a	b	C_f
NH PG 64-28 0% RAP	4.13	-0.00006653	0.7906	0.31
NH PG 64-28 20% RAP	4.14	-0.00008771	0.7563	0.31
NH PG 64-28 30% RAP	4.19	-0.00013500	0.7113	0.27
NH PG 64-28 40% RAP	4.22	-0.00009147	0.7470	0.30

Figure 3-11 shows the fitted curves for all the NH mixtures on the same graph. As this graph shows, the 0% RAP mix has the lowest position, whereas the three RAP mixtures are similar. This trend is observed in the PMLC (reheated) dynamic modulus test data for these mixtures as well.

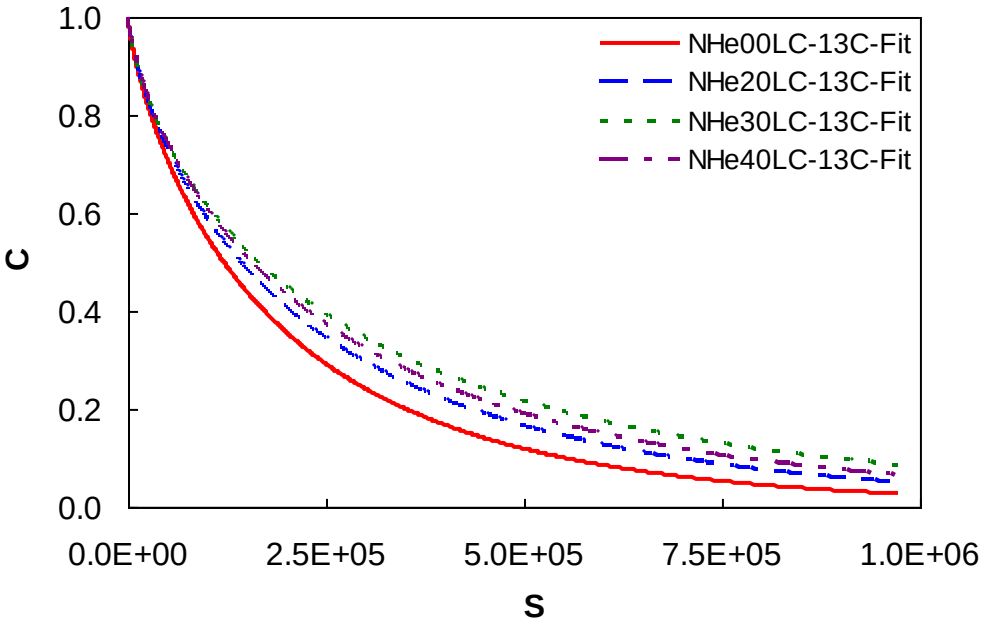

Figure 3-11 Fitted results for CX testing for NH PG 64-28 mixtures at 13°C

The S-VECD proposed failure criterion, which is presented in detail in Appendix, is applied to the NH PG 64-28 mixtures and Figure 3-12 presents results. As this graph shows, for the same level of G^R, the 30% RAP mixture shows the best fatigue resistance, the 0% RAP mix shows the worst fatigue resistance, and the 20% and 40% RAP mixtures are located in between. The differences in silo storage times and production temperatures may explain the differences in fatigue behavior observed between the different RAP contents.

The conventional fatigue relationship (initial on-specimen strain versus N_f) for the fatigue tests that were performed on the NH mixtures is presented in Figure 3-13. This graph shows that the 0% RAP mixture line lies at the bottom (worst performance) and the 30% RAP mixture line is at the top (best performance).

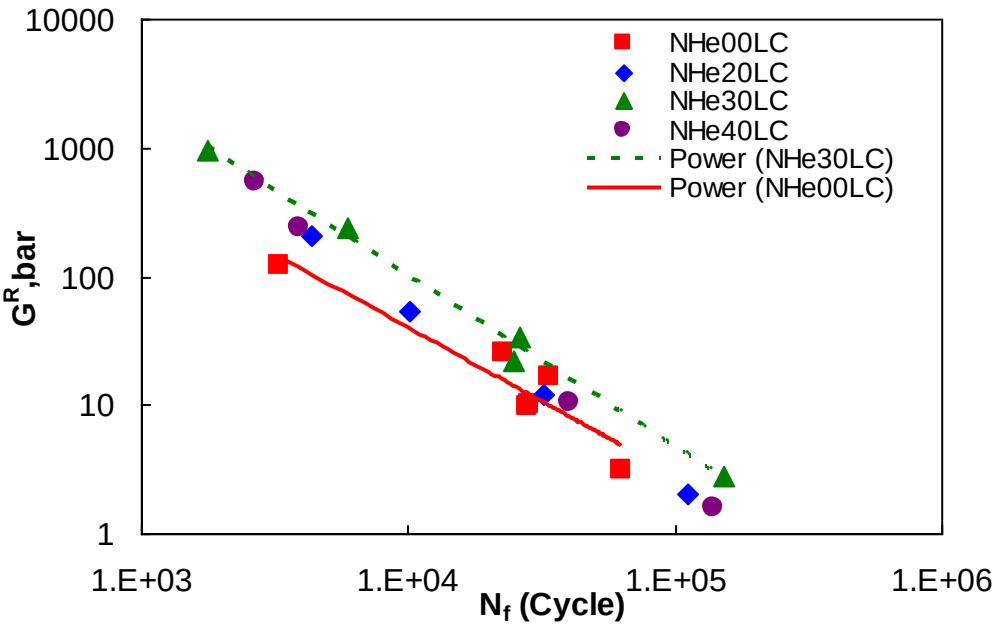

Figure 3-12 Failure criterion for NH PG 64-28 mixtures at 13°C

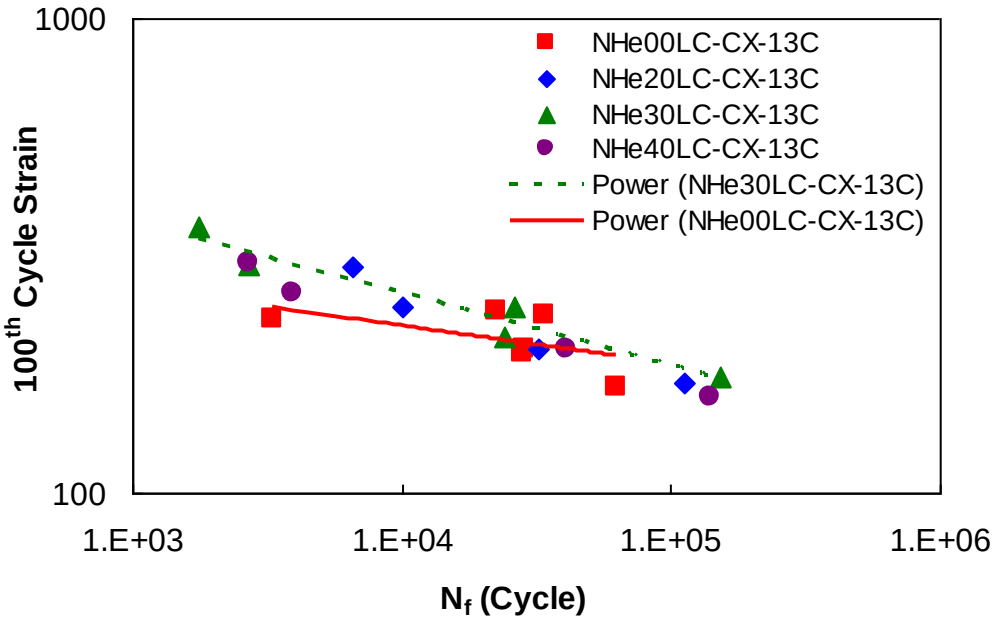

Figure 3-13 Initial strain versus N_f for NH PG 64-28 mixtures at 13°C

Controlled strain simulations were performed at multiple temperatures and strain levels using the S-VECD damage characteristic curve and failure criterion. The simulation results were fitted using the following empirical model, and the coefficients shown in Table 3-10:

$$N_f = k_1 \left(\frac{1}{\varepsilon_0} \right)^{k_2} \left(|E^*| \right)^{k_3} \quad 3.1$$

where

N_f = number of cycles to failure,
ε_0 = applied stain amplitude, and
k_1, k_2, k_3 = material constants.

In the recently developed Mechanistic-Empirical Pavement Design Guide (MEPDG), the mathematical model shown above is used to predict the fatigue performance of hot mix asphalt (HMA), except that a laboratory-to-field adjustment factor is added.

Figure 3-14 shows the results of the 0% RAP mixture simulations at 7°C, 13°C, and 20°C and also the fitting by the empirical model. As this graph shows, the new failure criterion is able to recover the empirical fatigue law-like behavior well. Also, as temperature drops, lower fatigue life is observed, which is expected for controlled-strain behavior. Graphs for the other NH mixes show similar trends.

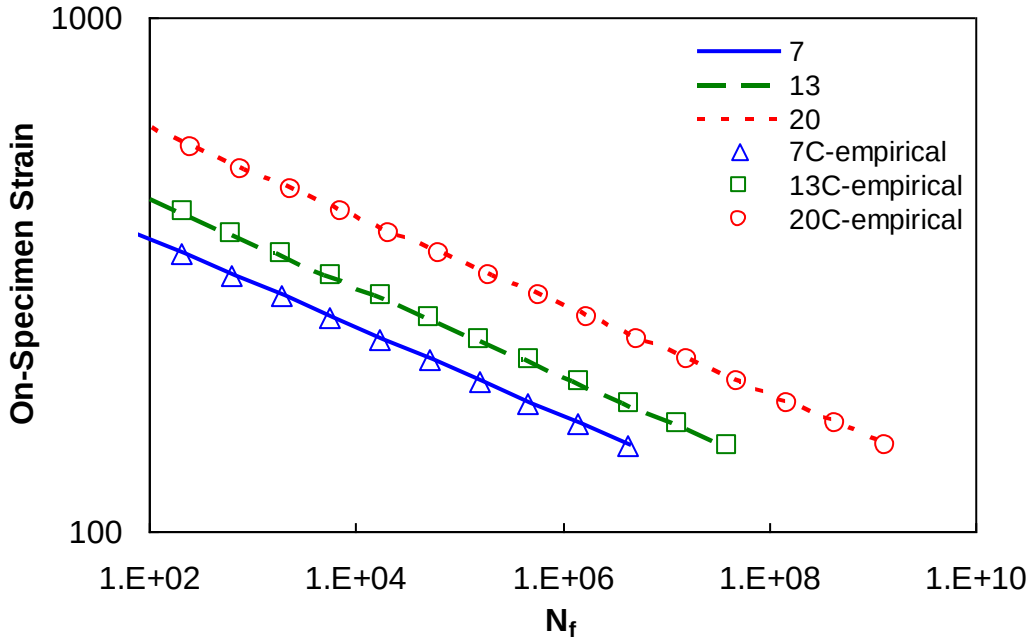

Figure 3-14 Strain-controlled direct tension fatigue test simulations for NH PG 64-28 0% RAP lab fabricated (NCSU) mixture at 7°C, 13°C, and 20°C

Table 3-10 Summary of regression coefficients for empirical model from direct tension fatigue simulations for NH PG 64-28 mixtures

Mixture	K1	K2	K3
NH PG 64-28 0% RAP	2.83E+17	11.590	-7.835
NH PG 64-28 20% RAP	3.75E+10	4.865	-3.353
NH PG 64-28 30% RAP	2.03E+15	7.970	-5.543
NH PG 64-28 40% RAP	6.59E+12	6.269	-4.381

Figure 3-15 shows a comparison of the simulation results at 13°C. As this graph shows, the 0% RAP mixture shows the worst performance at higher strain levels, which is consistent with that seen from actual test data in Figure 3-13. However, at lower strain levels, the 0% and 30% RAP mixtures are similar and have better performance than the 20% and 40% mixtures.

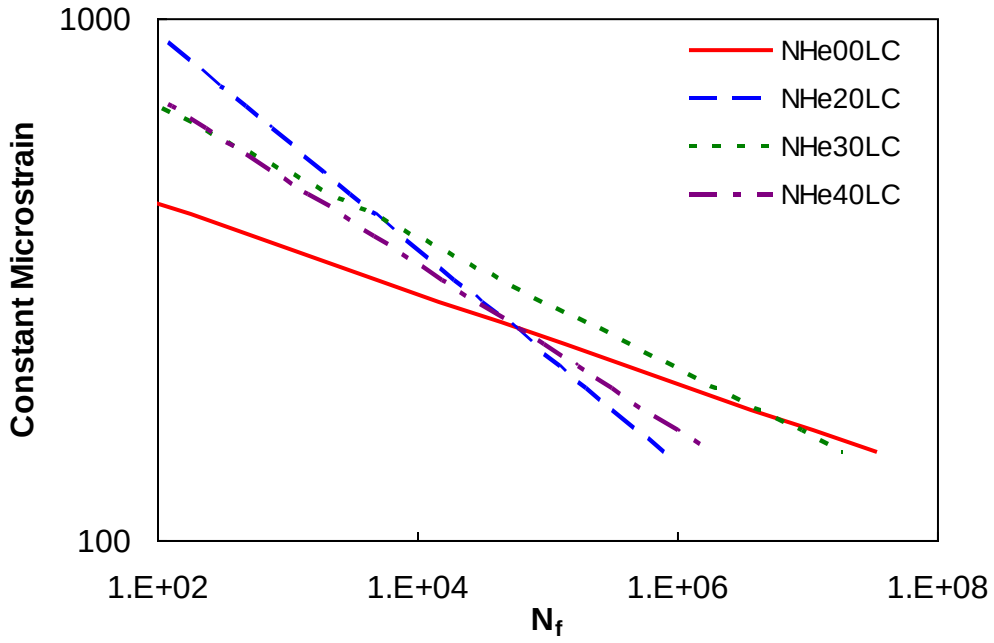

Figure 3-15 Strain-controlled direct tension fatigue test simulations for all NH mixtures at 13°C

It is also interesting to compare the on-specimen strain levels of CX testing at the mid-cycle, i.e., $\frac{N_f}{2}$, with the simulation results at 13°C, as shown in Figure 3-16. This graph shows that the mid-cycle strain points obtained from CX testing almost collapse with the constant strain simulation lines. This observation confirms the hypothesis that a CX test with an average on-specimen strain level of α would result in about the same number of cycles to failure as in a COS test with an on-specimen strain level of α.

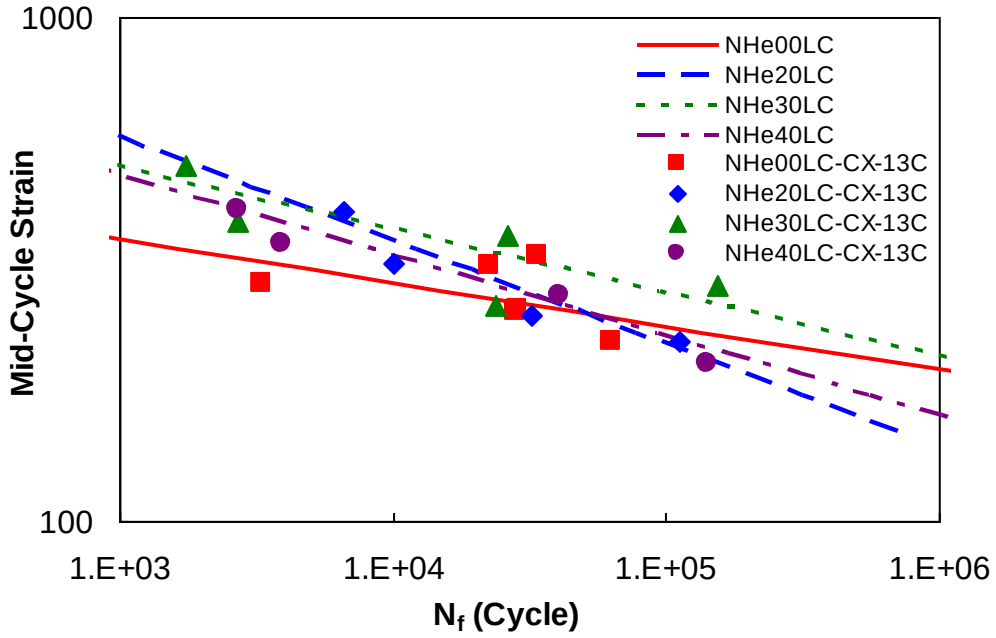

Figure 3-16 Comparison of mid-cycle strain of CX testing with strain-controlled direct tension fatigue test simulations for all NH mixtures at 13°C

3.4.2.2 Beam Fatigue

The beam fatigue testing was done accordance with AASHTO T321 and results are shown in Figure 3-17 for the New Hampshire PG 64-28 mixtures. The test results are scattered due to limited testing (only one replicate per strain level) that was performed, but do show some interesting trends. First, the 0% RAP and 40% RAP mixtures performed very similar to one another and achieved the highest flexural fatigue life among the New Hampshire mixtures. Second, the 20% RAP mixture performed the worst. The 30% RAP mixture results were somewhat inconclusive as it performed poorly at the low tensile strain, but its performance improved significantly at the higher tensile strains. The differences in the beam fatigue rankings are likely influenced by the difference in asphalt content; the 0% and 40% RAP mixtures had the highest actual asphalt contents while the 20% and 30% mixtures had the lowest.

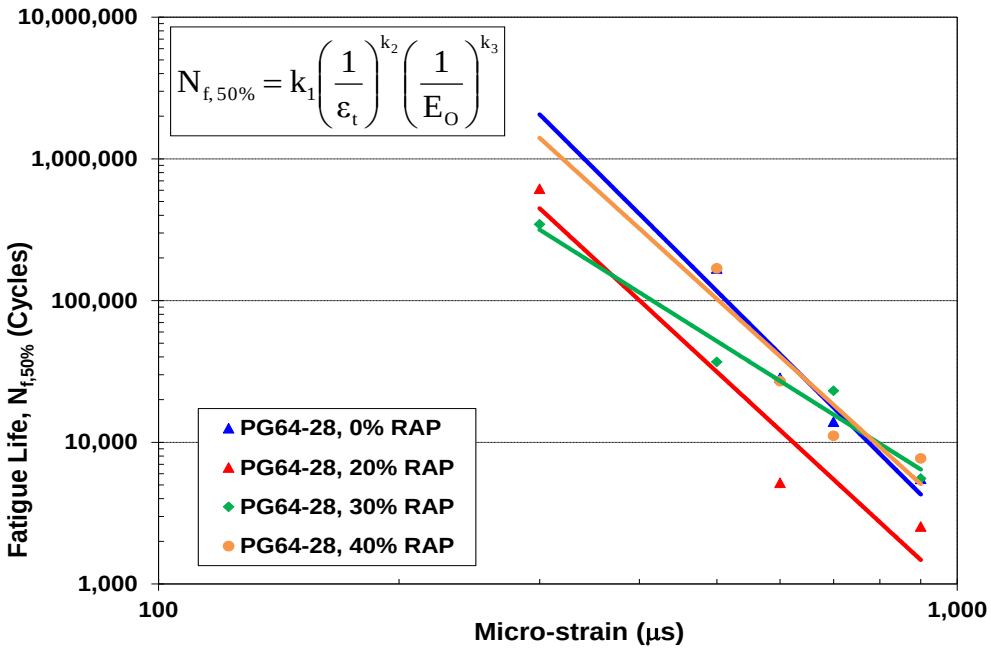

Figure 3-17 Flexural fatigue life for New Hampshire mixtures

3.4.2.3 Overlay Tester

The resistance to propagation of fatigue cracking was evaluated using the Overlay Tester. Sample preparation and test parameters used in this study followed that of TxDOT Tex-248-F testing specifications. The test results for the New Hampshire mixtures are shown in Figure 3-18. The test results clearly indicate that as the RAP content increases, the asphalt mixture's ability to resist crack propagation drastically decreases.

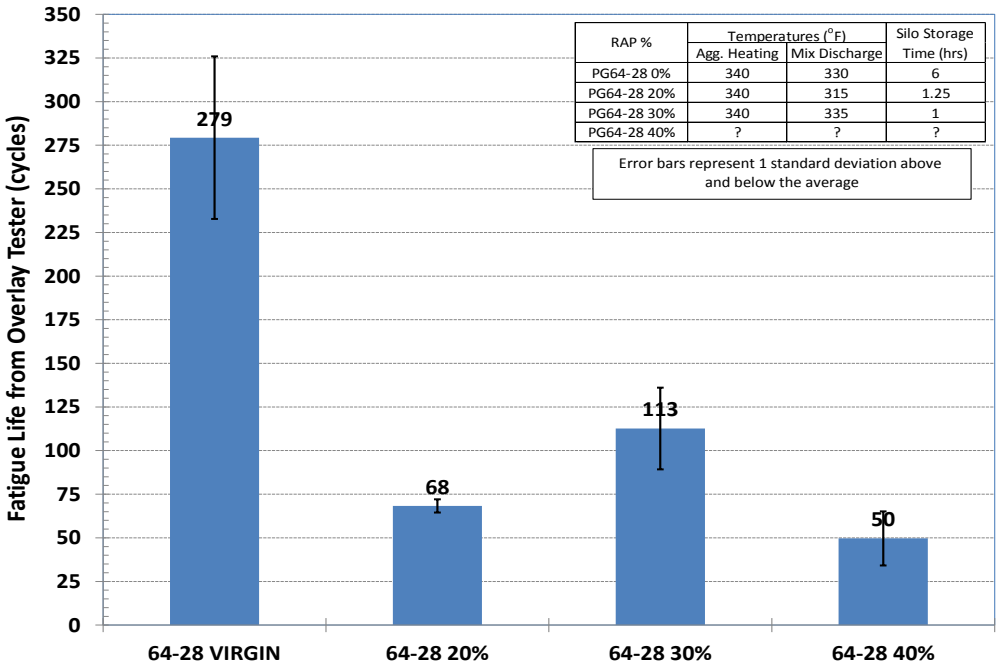

Figure 3-18 Overlay tester results for New Hampshire mixtures

3.4.3 *Low Temperature*

3.4.3.1 TSRST

The asphalt mixtures were evaluated for their respective mixture low cracking temperature in accordance with AASHTO TP10. The TSRST tests started at an initial temperature of 4°C and specimens were cooled at a rate of 10°C hr. The failure temperature and stress were recorded and are shown in Table 3.13. The addition of RAP to the New Hampshire mixtures had a marginal effect on the mixture low temperature cracking resistance as measured in the TSRST. At RAP contents of 20% and 30%, the mixtures had an average low cracking temperature within ±1°C of the control mixture. At the higher 40% RAP content, the effect was more pronounced with the mixture low cracking temperature being approximately 2°C warmer than the control mixture.

Table 3-11 TSRST results for all NH PG 64-28 mixtures

Mixture	Air Voids %	Temp at Failure °C	Load at Failure N	Low Continuous PG Grade °C	Binder Critical Cracking Temp. °C
NH PG 64-28 0%	6.93	-22.88	5183	-28.4	-25.7
NH PG 64-28 20%	7.01	-23.63	5609	-24.1	-25.9
NH PG 64-28 30%	7.51	-22.52	5277	-26.5	-27.6
NH PG 64-28 40%	7.14	-20.64	4627	-23.7	-25.7

3.4.3.2 Low Temperature Creep and IDT Strength

The average low temperature creep compliance master curves at -10°C for the NH mixtures are shown in Figure 3-19. The virgin mixture shows the softest, most compliant response; the response gets stiffer or less compliant as RAP content increases. The strengths of each mixture measured at -10°C are shown in Figure 3-20. The virgin mixture had the lowest strength and the 20% and 40% RAP mixtures had similar strength. The cracking temperature for each of the mixtures determined using the TCModel spreadsheet is shown in Table 3-12. The virgin mixture has the coldest cracking temperature and the addition of RAP results in warmer cracking temperatures. The 30% and 40% RAP mixtures have the warmest cracking temperatures.

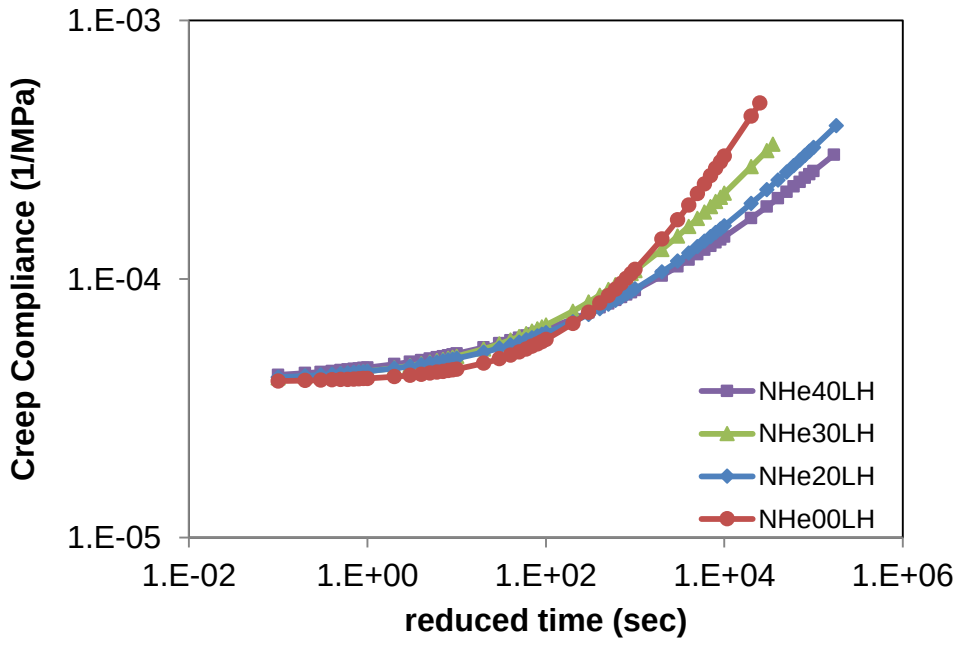

Figure 3-19 Average Creep Compliance Master Curves at -10°C for all NH mixtures

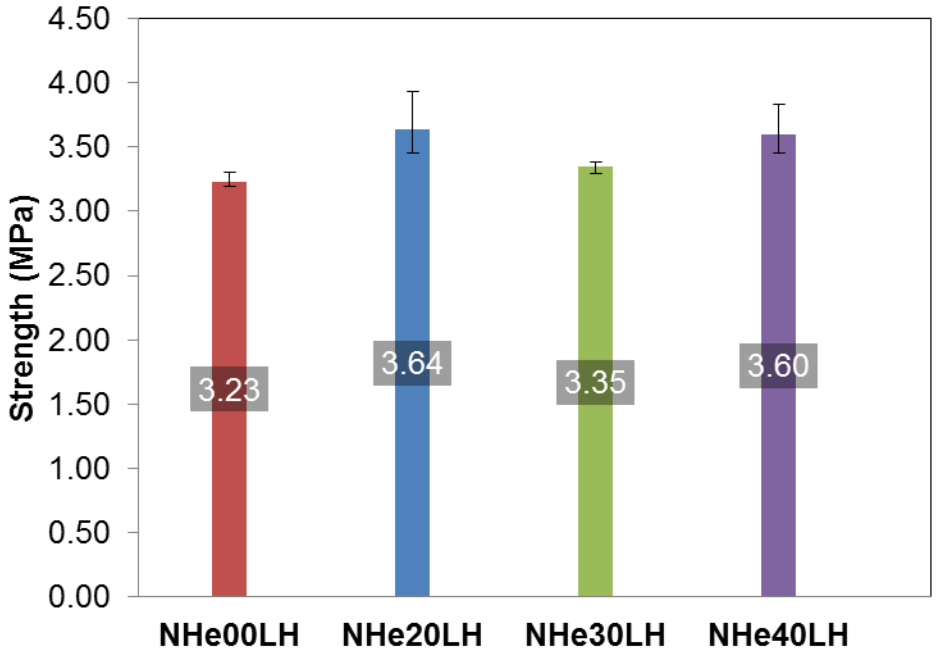

Figure 3-20 Low temperature IDT strength (-10°C) for NH mixtures

3.4.3.3 Comparison with Binder Data

The NH mixture and extracted binder low temperatures are shown together in Table 3-12 for comparison. The rankings of the mixtures for each test are also shown in the table. The extracted binder testing results consistently indicated a colder low temperature than the mixture results. This difference was up to 5.5°C colder than the TSRST temperatures and 11°C colder than the IDT determined temperatures. The low PG grade indicated a more pronounced decrease in low temperature capabilities as the amount of RAP in the mixture is increased. Both mixture tests and the low PG grade indicate that the 40% RAP has the warmest cracking temperature; the rankings of the other mixtures vary by test type.

Table 3-12 Critical cracking temperatures comparisons - NH mixtures

Mix	Mixture				Binder			
	TCMODEL		TSRST		Critical Cracking Temperature		Low Temperature Continuous PG-grade	
	°C	Rank	°C	Rank	°C	Rank	°C	Rank
NH PG 64-28 0 % RAP	-17	1	-22.88	2	-25.7	2	-28.4	1
NH PG 64-28 20 % RAP	-15	2	-23.63	1	-25.9	3	-24.1	3
NH PG 64-28 30 % RAP	-14	3	-22.52	3	-27.6	1	-26.5	2
NH PG 64-28 40 % RAP	-14	3	-20.64	4	-25.7	2	-23.7	4

3.4.4 *Moisture*

3.4.4.1 Hamburg Wheel Tracking Device

The results of the Hamburg testing for the NH mixture are shown in Table 3-13. All of the mixtures passed the moisture susceptibility (no stripping apparent up to 20,000 cycles) and rutting test, thereby indicating that the production parameters utilized were adequate in producing a moisture and rut resistant mixture. The mixtures incorporating RAP showed decreased rutting potential as compared to the virgin mixture; the 30% RAP mixture showed the best rutting performance.

Table 3-13 Hamburg wheel tracking test results for all NH mixtures

State	NMAS	% RAP	Binder Grade	Average Stripping Inflection Point	Avg. Rut Depth at 10,000 Cycles (mm)	Avg. Rut Depth at 20,000 Cycles (mm)
NH	12.5 mm	0	PG64-28	NONE	2.15	3.61
		20	PG64-28	NONE	1.70	2.21
		30	PG64-28	NONE	0.49	0.61
		40	PG64-28	NONE	0.93	1.30

NONE = Mixture passed 20,000 cycle test with no SIP.

3.4.4.2 IDT Tensile Strength Ratio

The results of the TSR testing of the NH Mixtures is shown in Figure 3-21 and the dry strength values for each mixture are shown in Figure 3-22. The bars in Figure 3-22 indicate the range of the results. The TSR values for all of the NH mixtures are close to 1.0, indicating these mixtures should not be susceptible to moisture damage; this agrees with the results of the Hamburg testing. The 30% RAP mixture has the highest average dry strength, but is not statistically different from the 20% RAP mixture.

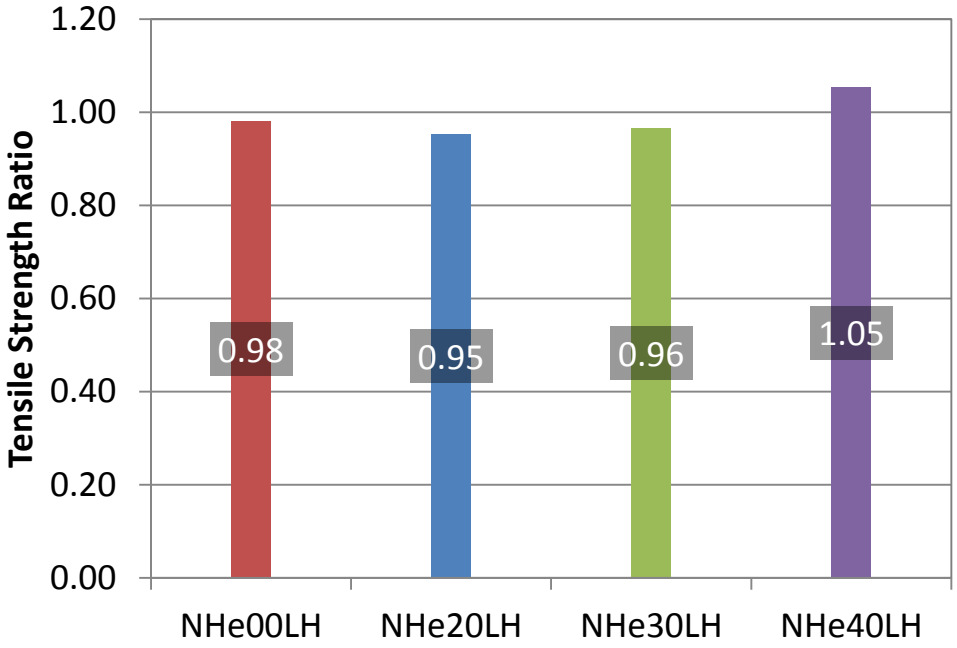

Figure 3-21 Tensile strength ratio - all NH mixtures

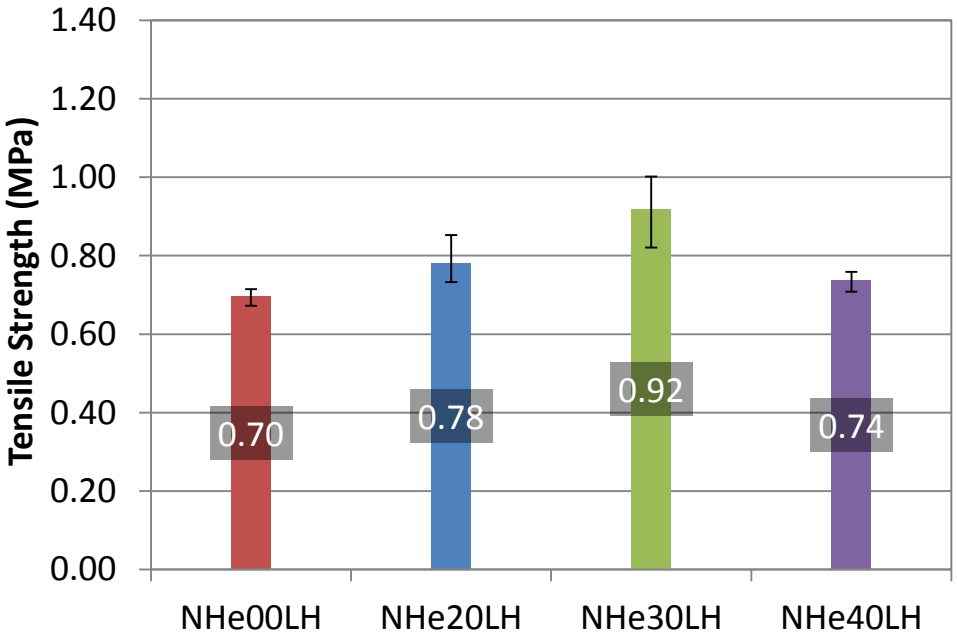

Figure 3-22. Average tensile strength of dry set - all NH mixtures

3.4.5 *Workability Device*

The workability data shown in Figure 3-23 for the New Hampshire mixtures indicates that the addition of RAP to the mixtures decreases the mixture workability as compared to the respective control mixture without RAP. The workability reductions were generally larger as the amount of RAP increased.

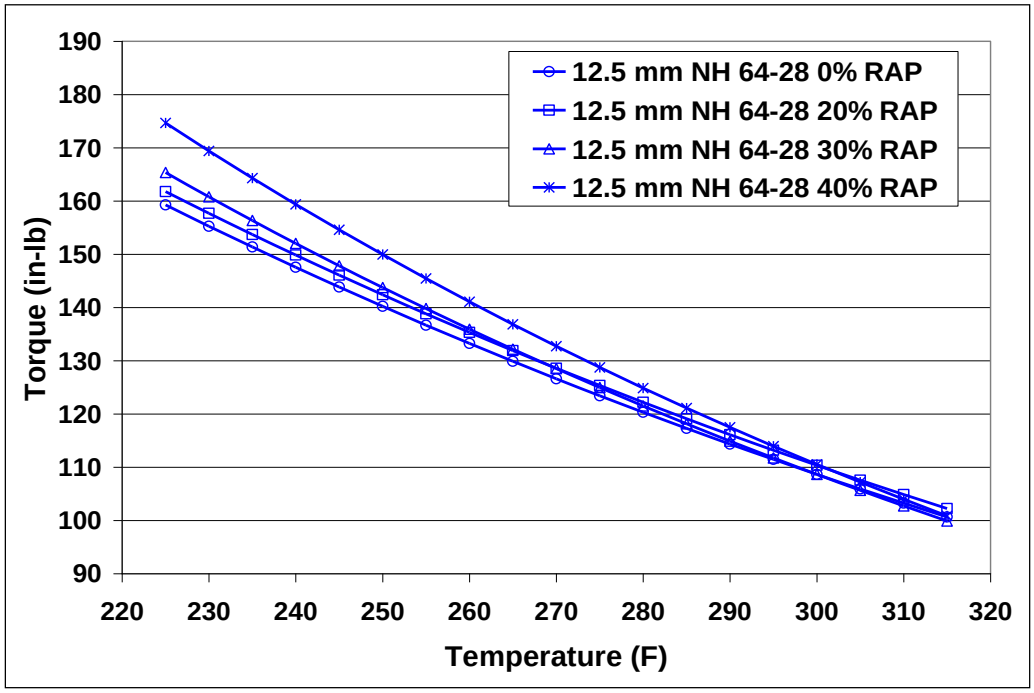

Figure 3-23 Workability test results for all NH mixtures

CHAPTER 4 NEW YORK MIXTURES

4.1 Mixture Design Information

The New York mixtures were produced by Callanan Industries using a Cedar Rapids counter flow drum plant. Production rates during the project were approximately 250 tons per hour for the 30 and 40% RAP mixtures, while the production rate for the Virgin and 20% RAP mixtures was 300 tons per hour. After production, the mixtures were stored in a silo until discharged into delivery trucks.

The general mixture design information for the NY mixtures is shown in Table 4-1 and Table 4-2. The mixtures produced had a nominal maximum aggregate size (NMAS) of 12.5 mm with an optimum asphalt content of 5.2%. The RAP used in the NY mixtures had a continuous grade of PG 87.2-19.9. With the exception of the 30% RAP PG58-28 mixture, the extracted and recovered asphalt content from the produced mixtures was lower than the design optimum. A significant variation in the aggregate gradation for the virgin mixture, compared to the RAP mixtures, is shown in Table 4-2. The virgin mixture is much finer on the #4 to #30 sieves when compared to the RAP mixtures. In fact, as high as 15% difference was found on the #4 sieve between the virgin and 40% RAP mixture.

4.2 Plant Production Information

The plant production information for the NY mixtures is shown in Table 4-3. The asphalt mixtures were produced between 305^{o}F to 330^{o}F, with the 40% RAP mixtures being produced at the higher production temperatures. All mixtures were stored in the silo prior to discharging into the delivery trucks, but for different amounts of time. The PG 64-22 20% RAP mixture was only stored 45 minutes prior to being discharged, while the other mixtures were stored 2 to 3 hours longer.

4.3 Binder Testing

4.3.1 *PG Grading*

The asphalt binder was sampled from the storage tanks, as well as extracted and recovered from the mixtures. The results of the PG grading are shown in Table 4-4, as well as Figure 4-1 and Figure 4-2. The test results indicate that as the RAP content increases, the PG grade gets warmer at both the low and high PG temperatures. The PG 64-22 binder shows a significant increase (8^{o}C) in the high PG temperature just from plant production. By comparison, the addition of the 40% RAP increases the high PG temperature another 5^{o}C for this binder. The PG 58-28 mixtures show close to a 10^{o}C increase in the high PG temperature from 30% to 40% RAP. Although there is not a comparison virgin PG 58-28

mixture, this indicates that the PG 58-28 binder may be more susceptible to stiffening due to the addition of the RAP rather than aging through the plant. The low PG temperature for the PG 58-28 tank binder is S-controlled, but shifts to m-controlled with the addition of the RAP, and becomes more m-controlled at the higher RAP contents. The two tank samples for the PG 58-28 binder show 4-5^{o}C differences at the low PG temperature; the 30% RAP mixtures were produced on 9/7/10 while the 40% RAP mixtures were produced on 7/30/10. This is likely part of the reason why there is a larger (4^{o}C) difference in the m-values from 30% to 40% RAP that is not observed with other mixtures. The low PG temperature for the PG 64-22 binder is m-controlled and becomes more m-controlled with the addition of higher levels of RAP.

Table 4-1 Mix design information – all NY mixtures

Mix	PG Grade	NMAS (mm)	Design Asphalt Content (%)	% RAP	RAP Binder Content (%)	VMA	VFA	Extracted/ Recovered Asphalt Content (%)	% Binder Replacement
NY PG 58-28 30 % RAP	58-28	12.5	5.2	30	4.93	13.7	81.12	4.96	29.8
NY PG 58-28 40 % RAP	58-28	12.5	5.2	40	4.90	12.7	88.36	4.93	39.8
NY PG 64-22 0 % RAP	64-22	12.5	5.2	0	--	12.6	89.32	5.04	0.0
NY PG 64-22 20 % RAP	64-22	12.5	5.2	20	4.95	14.1	79.86	5.15	19.2
NY PG 64-22 30 % RAP	64-22	12.5	5.2	30	4.93	13.0	85.08	5.46	27.1
NY PG 64-22 40 % RAP	64-22	12.5	5.2	40	4.90	12.5	87.9	5.05	38.8

Table 4-2 Mixture gradations - all NY mixtures

Mix	**PG**	**Mixture Gradation**								
		12.5	**9.5**	**#4**	**#8**	**#16**	**#30**	**#50**	**#100**	**#200**
NY PG 58-28 30 % RAP	58-28	97.5	91.2	59.5	33.3	21	14.7	9.7	5.8	5.3
NY PG 58-28 40 % RAP	58-28	98.1	89.3	53.7	32	18	12.5	8.5	5.1	3.2
NY PG 64-22 0 % RAP	64-22	99.8	90.8	68.3	42.3	27	18.9	13.2	5.2	3.8
NY PG 64-22 20 % RAP	64-22	99.1	90.8	59	30.9	19	11.8	8.3	6.7	3.8
NY PG 64-22 30 % RAP	64-22	95	85.8	54.4	30.2	23	16.5	11.6	7.8	6
NY PG 64-22 40 % RAP	64-22	97.6	88.7	53	30.9	19	14.3	10.1	6.1	4.3

Table 4-3 Plant production information - all NY mixtures

Mix	PG Grade	Plant Type	Aggregate Temp. (ºC/ºF)	Discharge Temp. (ºC/ºF)	Compaction Temp. (ºC/ºF)	Silo Storage time (hrs)
NY PG 58-28 30 % RAP	58-28	Drum	n/a	151.7/305	135/275	2.75
NY PG 58-28 40 % RAP	58-28	Drum	n/a	165.6/330	135/275	3.0
NY PG 64-22 0 % RAP	64-22	Drum	n/a	154.4/310	143.3/290	2.75
NY PG 64-22 20 % RAP	64-22	Drum	n/a	160/320	143.3/290	0.75
NY PG 64-22 30 % RAP	64-22	Drum	n/a	151.7/305	143.3/290	3.5
NY PG 64-22 40 % RAP	64-22	Drum	n/a	165.6/330	143.3/290	4.0

Table 4-4 Summary of asphalt binder performance grading (Callanan, NY)

Production Location	Base PG Grade Binder	Tank or Extracted with RAP Content	Continuous PG Grade (°C)				PG Grade (°C), AASHTO R29 & M320	Critical Cracking Temperature (°C), AASHTO R49
			High Temp (RTFO)	Low Temp		Intermediate Temp (PAV)		
				Stiffness (MPa)	m-slope			
Callanan (NY)	58-28	Tank 7/30/10	60.3	-30.8	-31.7	17.2	58-28	-27
		Tank 9/7/10	61	-34.6	-36.7	18.5	58-34	-30.2
		Extracted - 30% RAP	72.1	-27.6	-26.5	21.7	70-22	-26.1
		Extracted - 40% RAP	81.7	-26.3	-22	22.9	76-22	-20.6
	64-22	Tank 7/30/10	67.3	-26.1	-26	22.1	64-22	-25.2
		Tank 9/7/10	67	-26.3	-25.5	21.9	64-22	-23.1
		Extracted - 0% RAP	75.5	-26.3	-22.2	24.7	70-22	-22.2
		Extracted - 20% RAP	78.3	-25.3	-21.8	25.3	76-16	-22.1
		Extracted - 30% RAP	78.4	-25.3	-19.9	26.4	76-16	-21.1
		Extracted - 40% RAP	80.9	-24.2	-17.6	27.2	76-16	-19.3

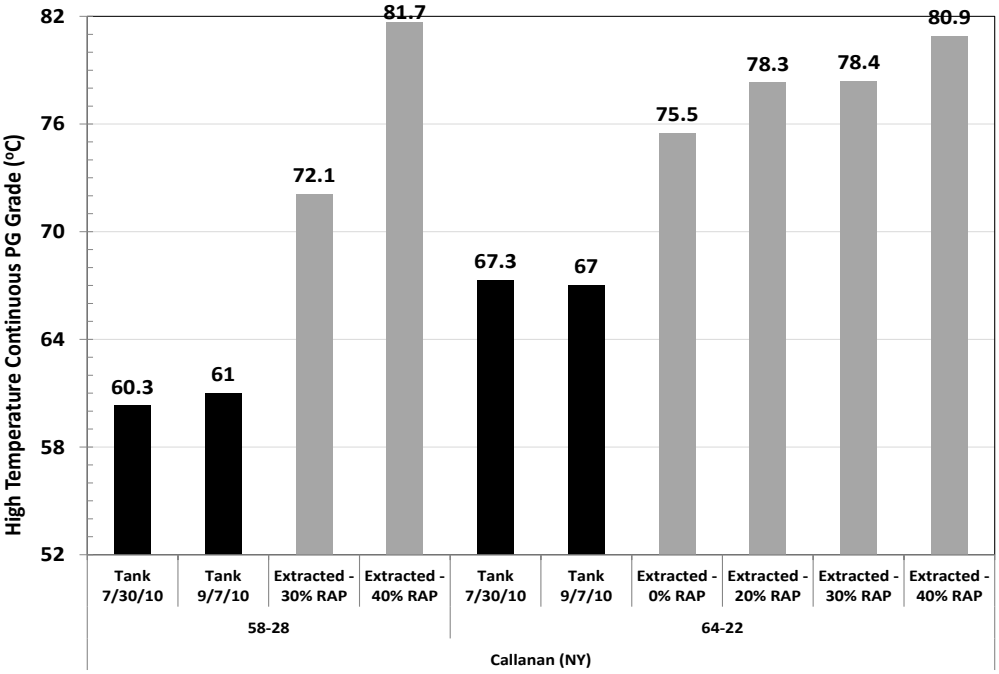

Figure 4-1 High temperature PG grade (Callanan, NY)

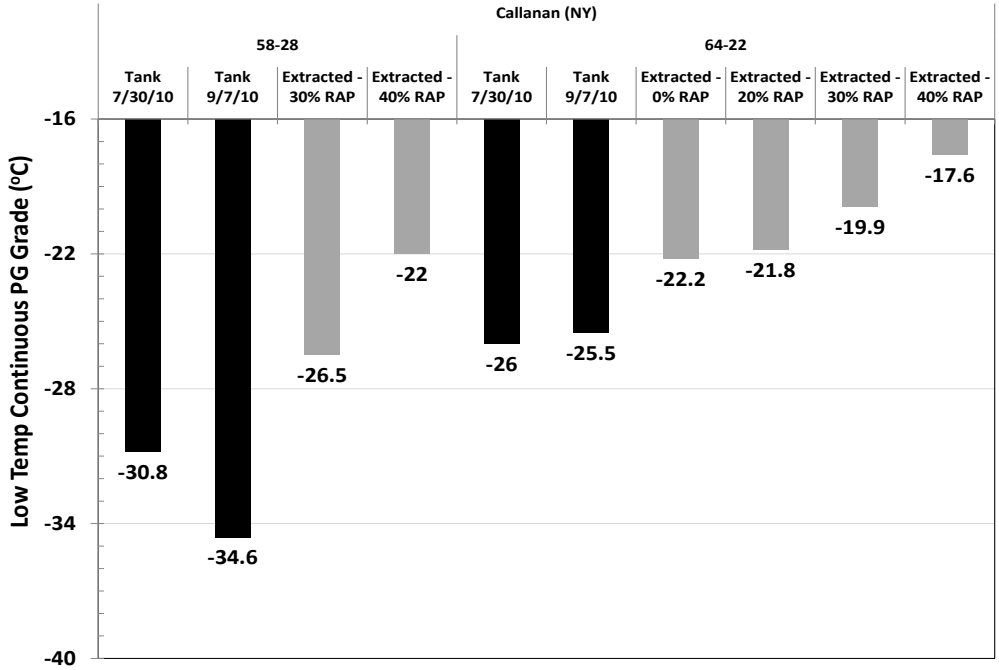

Figure 4-2 Low temperature PG grade (Callanan, NY)

4.3.2 *CCT*

The low temperature critical cracking temperature was measured in accordance with AASHTO R49. The material test properties were used to evaluate different starting temperatures and cooling rates that could occur in the Northeast. It should be noted that the Critical Cracking Temperature (CCT) shown earlier in Table 4-4 is for the standard starting temperature and cooling rate recommended in AASHTO R49 for reporting purposes.

The results of the CCT analysis are shown in Table 4-5 through Table 4-10. The tables indicate that starting temperature has little influence on the CCT of the asphalt binder. Meanwhile, the cooling rate is shown to have a significant impact on the CCT, changing it by almost a full PG grade when increasing the cooling rate from 1 ^{o}C/hr to 10 ^{o}C/hr.

The test results also show that both RAP and PG grade of the base asphalt binder have an influence on the CCT. As would be expected, as the RAP content increased, there was a warming in the CCT – indicating that the asphalt mixture would crack under warmer climate conditions. However, the test results did indicate that using a softer PG grade helped to improve the low temperature CCT, but did not result in a full PG grade improvement in the CCT.

Table 4-5 Cooling rate vs. starting temperature – Callanan, NY PG58-28 & 30% RAP

58-28 30% RAP Callanan, NY				
TCMODEL Critical Cracking Temperature (°C)				
Starting Temp of Cooling Event	Cooling Rate C/hr 1	Cooling Rate C/hr 2	Cooling Rate C/hr 5.6	Cooling Rate C/hr 10
10C	-26.0	-23.9	-21.0	-19.7
5C	-26.0	-24.0	-21.0	-19.7
0C	-26.1	-24.0	-21.1	-19.8
-5C	-26.2	-24.2	-21.3	-20.1

Table 4-6 Cooling rate vs. starting temperature – Callanan, NY PG58-28 & 40% RAP

58-28 40% RAP Callahan, NY				
TCMODEL Critical Cracking Temperature (°C)				
Starting Temp of Cooling Event	Cooling Rate C/hr 1	Cooling Rate C/hr 2	Cooling Rate C/hr 5.6	Cooling Rate C/hr 10
10C	-20.4	-18.8	-16.4	-15.0
5C	-20.5	-18.9	-16.5	-15.1
0C	-20.6	-19.1	-16.8	-15.5
-5C	-20.9	-19.5	-17.3	-16.1

Table 4-7 Cooling rate vs. starting temperature – Callanan, NY PG64-22 & 0% RAP

64-22 0% RAP Callanan				
TCMODEL Critical Cracking Temperature (°C)				
Starting Temp of Cooling Event	Cooling Rate C/hr 1	Cooling Rate C/hr 2	Cooling Rate C/hr 5.6	Cooling Rate C/hr 10
10C	-22.0	-20.4	-18.0	-16.6
5C	-22.1	-20.5	-18.1	-16.8
0C	-22.2	-20.6	-18.3	-17.0
-5C	-22.5	-20.9	-18.7	-17.5

Table 4-8 Cooling rate vs. starting temperature – Callanan, NY PG64-22 & 20% RAP

64-22 20% RAP Callanan				
TCMODEL Critical Cracking Temperature (°C)				
Starting Temp of Cooling Event	Cooling Rate C/hr 1	Cooling Rate C/hr 2	Cooling Rate C/hr 5.6	Cooling Rate C/hr 10
10C	-22.0	-20.4	-18.0	-16.6
5C	-22.0	-20.5	-18.1	-16.7
0C	-22.1	-20.7	-18.3	-17.0
-5C	-22.3	-21.0	-18.8	-17.6

Table 4-9 Cooling rate vs. starting temperature – Callanan, NY PG64-22 & 30% RAP

64-22 30% RAP Callanan				
TCMODEL Critical Cracking Temperature (°C)				
Starting Temp of Cooling Event	Cooling Rate C/hr 1	Cooling Rate C/hr 2	Cooling Rate C/hr 5.6	Cooling Rate C/hr 10
10C	-20.8	-19.3	-16.8	-15.4
5C	-20.9	-19.4	-17.0	-15.6
0C	-21.1	-19.6	-17.3	-16.0
-5C	-21.4	-20.0	-17.8	-16.7

Table 4-10 Cooling rate vs. starting temperature – Callanan, NY PG64-22 & 40% RAP

64-22 40% RAP Callanan				
TCMODEL Critical Cracking Temperature (°C)				
Starting Temp of Cooling Event	Cooling Rate C/hr 1	Cooling Rate C/hr 2	Cooling Rate C/hr 5.6	Cooling Rate C/hr 10
10C	-18.9	-17.3	-14.8	-13.4
5C	-19.1	-17.5	-15.0	-13.7
0C	-19.3	-17.8	-15.5	-14.2
-5C	-19.8	-18.3	-16.2	-15.1

4.3.3 *Asphalt Binder Master Stiffness Curves*

The asphalt binder master curves, constructed using the asphalt binder extracted and recovered from the plant-compacted specimens, are shown in Figure 4-3 (PG 58-28 base asphalt binder) and Figure 4-4 (PG 64-22 base asphalt binder). As would be expected, as the RAP content increases, the stiffness of the extracted/recovered asphalt binders increases.

The influence of using a softer asphalt binder grade on the asphalt binder master curves was evaluated and shown in Figure 4-5 and Figure 4-6. The figures indicate that the use of a softer asphalt binder reduces of the overall stiffness properties of the resultant, extracted and recovered asphalt binder. However, it does need to be pointed out that when conducting the extraction and recovery process, the resultant asphalt binder is *completely blended*. This complete blending of RAP and virgin asphalt binders may not actually occur in the mixture itself.

Figure 4-7 shows the Rheological Index (R) – Crossover Frequency (ω_o) Space; the test results indicate that as RAP content increases, the asphalt binder behavior is that of a progressively aging asphalt binder. This is true for both the PG64-22 and PG58-28 asphalt binders. The extracted and recovered asphalt binders were also evaluated using Rowe's Black Space in Figure 4-8. The test results indicate most of the mixtures would be

classified as “prone” to cracking, except the PG 58-28 30% RAP mixture, which plots on the Pass/Fail border. This analysis shows that there is some benefit in terms of cracking performance with using the softer PG grade binder.

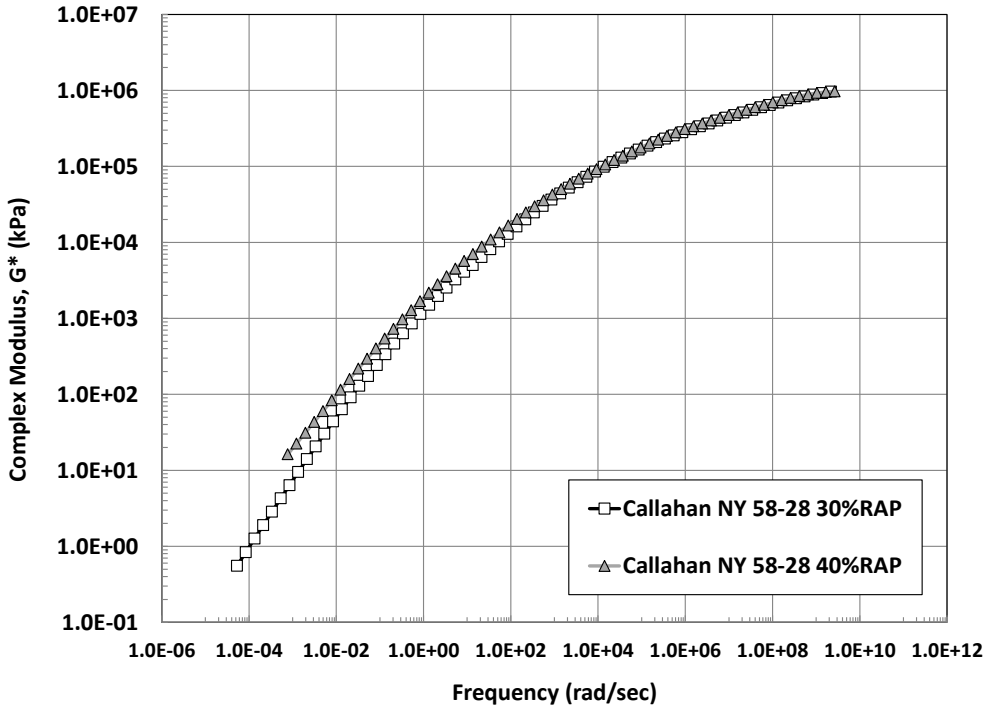

Figure 4-3 Asphalt binder master curves for New York mixtures with PG 58-28 base asphalt binder

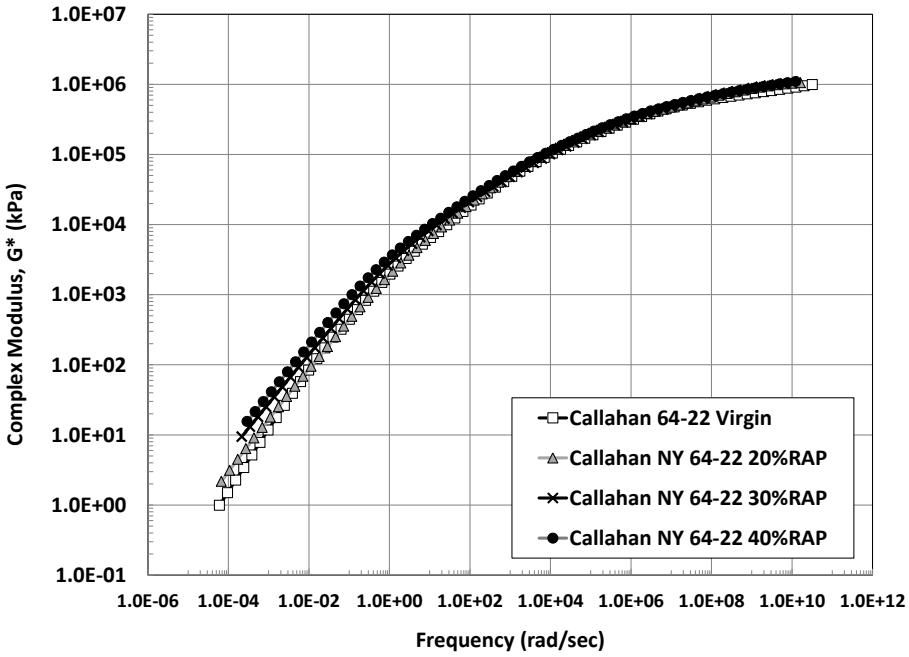

Figure 4-4 Asphalt binder master curves for New York mixtures with PG 64-22 base asphalt binder

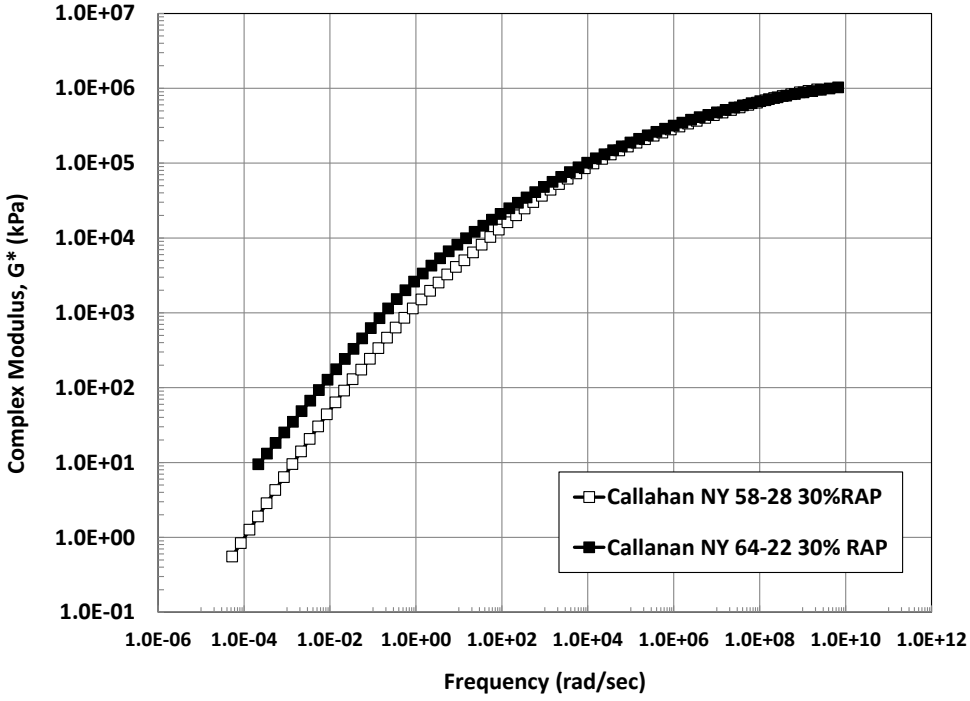

Figure 4-5 Asphalt binder master curves for New York mixtures containing 30% RAP

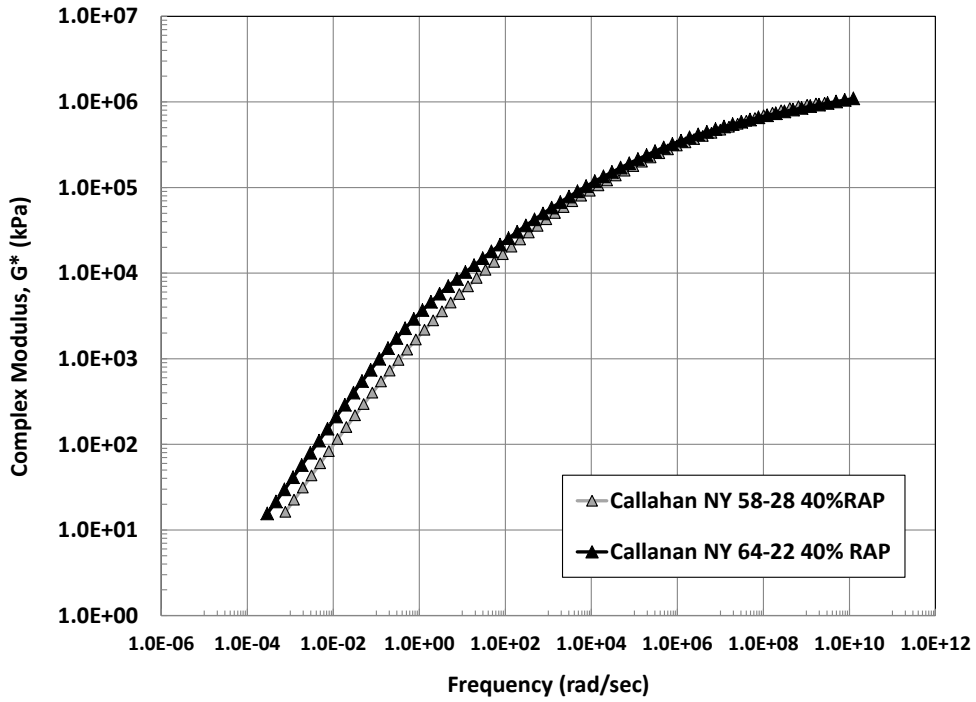

Figure 4-6 Asphalt binder master curves for New York mixtures containing 40% RAP

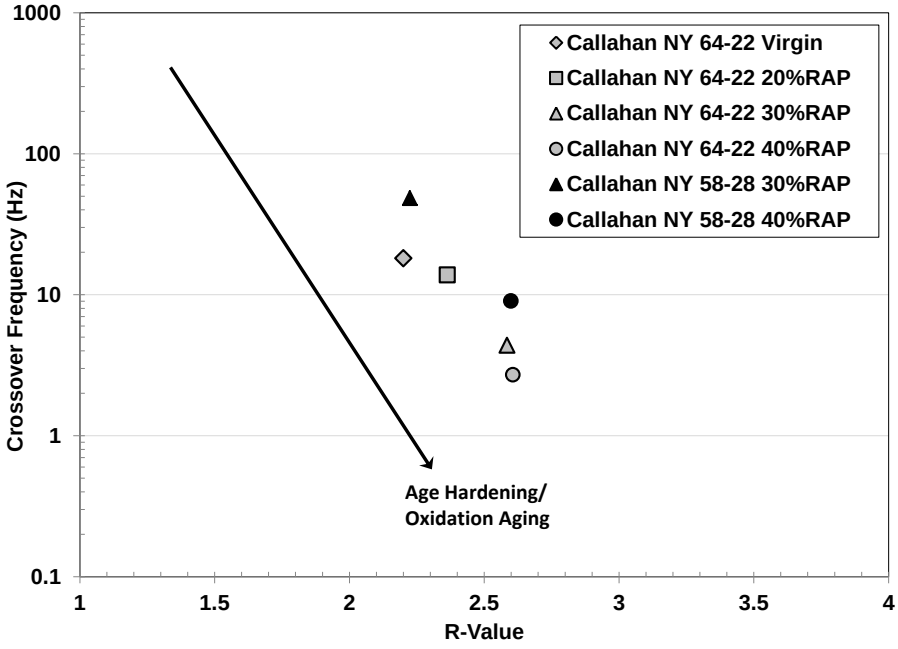

Figure 4-7 Rheological index – crossover frequency space for asphalt binder extracted/recovered from New York mixtures

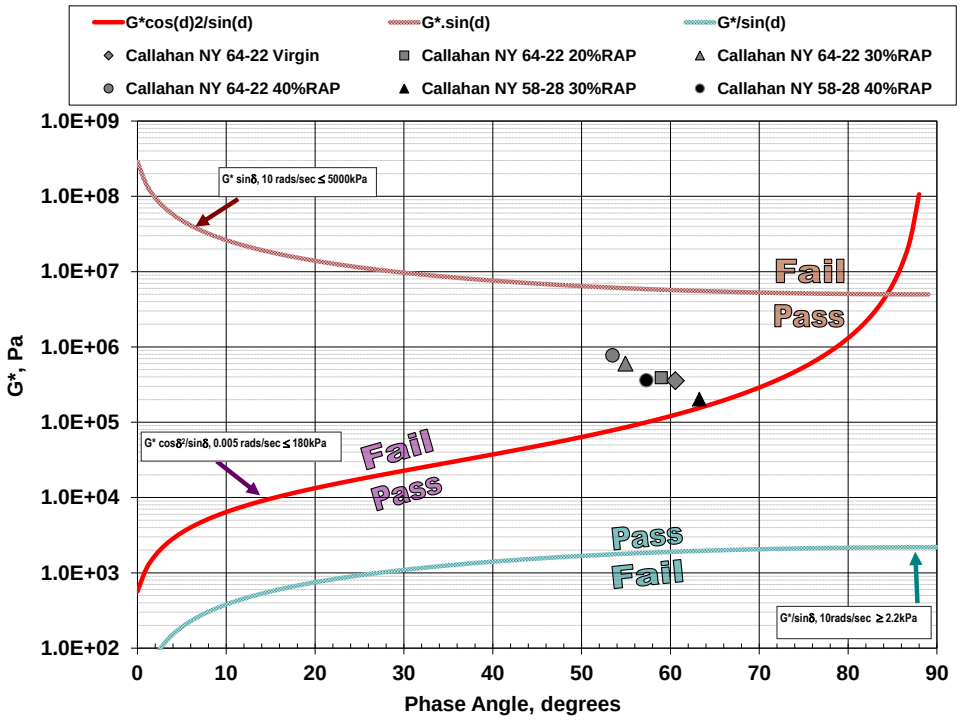

Figure 4-8 Rowe's black space analysis for asphalt binder extracted/recovered from New York mixtures

4.4 Mixture Testing

4.4.1 *Dynamic Modulus*

The dynamic modulus properties of the asphalt mixtures were determined in accordance to AASHTO TP79. Two sets of test specimens were prepared for evaluation; 1) Test specimens compacted at the asphalt plant and 2) Test specimens produced by reheating loose mix at the laboratory and then compacting the test specimens.

4.4.1.1 Plant Compacted Mixtures

The dynamic modulus (E*) test results for the New York RAP mixtures compacted at the asphalt plant are shown in Figure 4-9 and Figure 4-10 for the PG 58-28 and PG 64-22 base PG binders, respectively. The stiffness master curves for the PG 58-28 asphalt binder in Figure 4-9 shows that as RAP content increases, so does the mixture stiffness. Also plotted in Figure 4-9 is the PG 64-22 0% RAP mixture. Since state agencies commonly specify a softer PG grade to help counteract the impacts of RAP, the PG 64-22 0% RAP mixture was included to determine if this approach is effective for the New York mixtures. The test data does indicate that using a softer binder (PG 58-28) helps decrease the stiffness of the 30% RAP mixture. However, as Figure 4-9 indicates, at 40% RAP, the softer binder did

not help to reduce the stiffness of the mixture below that of a virgin PG 64-22 mixture. However, the PG 58-28 40% RAP mixture did have higher production temperatures and longer silo storage time, which may also partially explain the stiffer response.

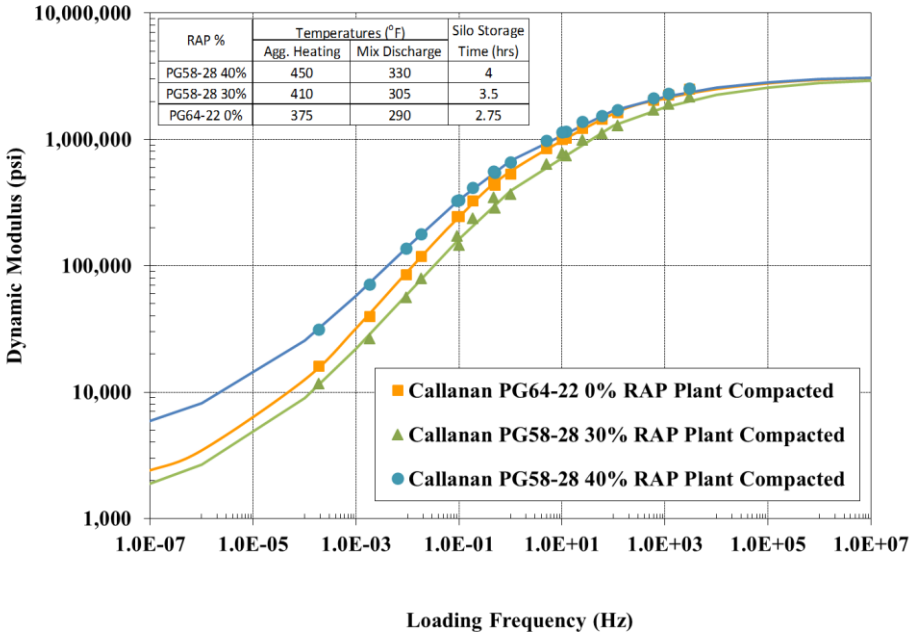

Figure 4-9 Dynamic modulus master curves for New York mixtures (PG 58-28 base PG grade) – plant compacted

Figure 4-10 contains only the PG64-22 base binder mixtures. The trend in mixture stiffness with RAP content is similar to the other mixtures; however, there does appear to be an unexpected trend regarding the behavior of the 20% RAP mixture. For the plant compacted mixtures, the 20% RAP mixture resulted in stiffness values lower than the 0% RAP mixture. Although the exact reason for this is not known, a review of the plant production data does show that the 20% RAP mixture was only silo stored for 45 minutes. This is over 2 hours less than the other mixtures. Therefore, the amount of time under silo storage, as well as the conditions during storage (i.e. – temperature, capacity and amount filled in silo, etc.) may have impacted the mixture stiffness.

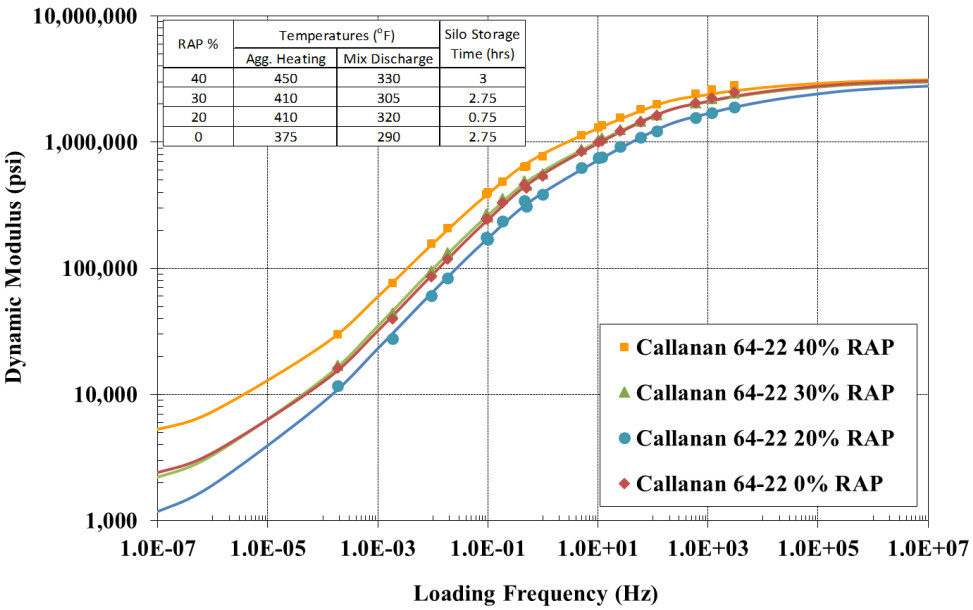

Figure 4-10 Dynamic modulus master curves for New York mixtures (PG64-22 base PG grade) – plant compacted

Figure 4-11 and Figure 4-12 show the comparisons of the 30% RAP and 40% RAP mixtures with the different base binder grades. The PG 58-28 30% RAP mixture has a softer response than the PG 64-22 30% RAP mixture, but there is negligible difference between the two 40% RAP mixtures.

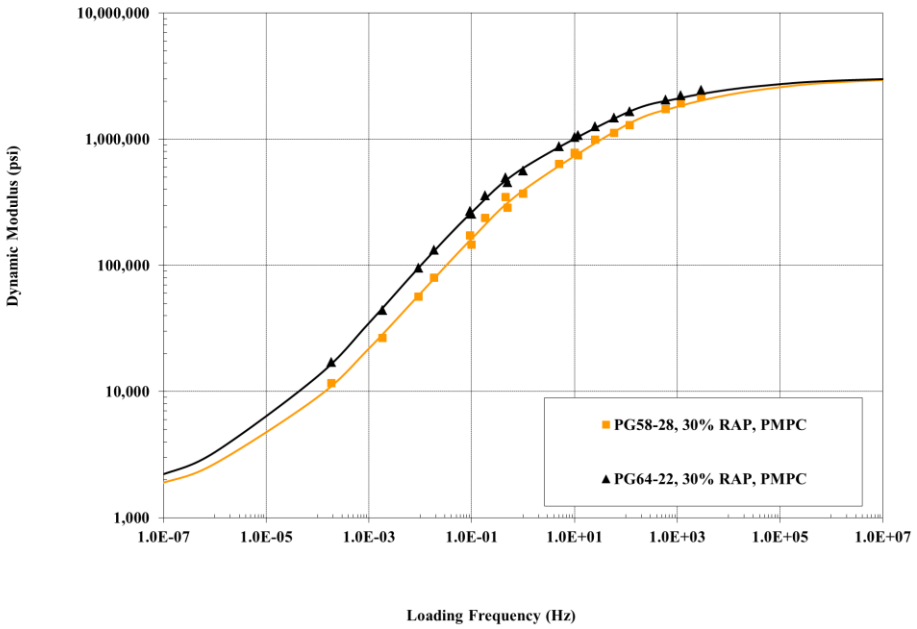

Figure 4-11 Dynamic modulus master curves for NY 30% RAP mixtures – plant compacted

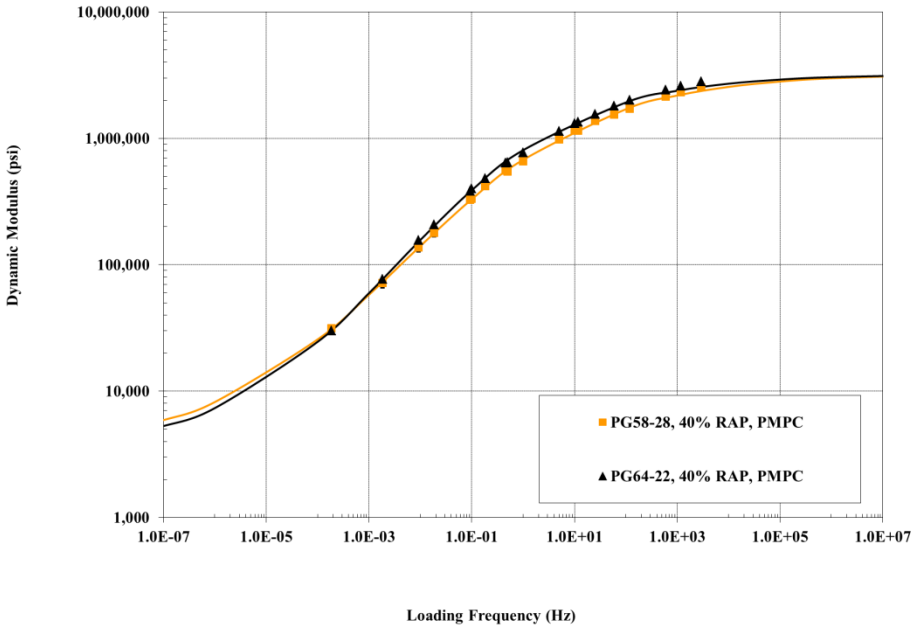

Figure 4-12 Dynamic modulus master curves for NY 40% RAP mixtures– plant compacted

4.4.1.2 Reheated Loose Mix and Compacted Mixtures

The identical mixtures were tested after the sampled loose mix was reheated and compacted following the test method developed by the Pooled Fund Research Team. The resultant master curves are shown in Figure 4-13 and Figure 4-14 for the PG 58-28 and PG 64-22 base PG binders, respectively. For the PG 58-28 mixtures shown in Figure 4-13, the performance trends of the mixtures are almost identical to that of the plant compacted specimens. Again, the use of a softer asphalt binder (PG58-28) did help to keep the stiffness of the 30% RAP mixture similar to the PG 64-22 0% RAP mixture. However, the mixture stiffness of the 40% RAP mixture did exceed that of the PG 64-22 0% RAP mixture. The reheating process for the PG 64-22 base binder mixtures (Figure 4-14) show the 0, 20, and 30% RAP mixtures have almost an identical stiffness, while the 40% RAP mixture has the highest mixture stiffness at all temperatures and loading frequencies. Figure 4-15 and Figure 4-16 show the comparison of the PG binder grades for the reheated and compacted specimens. There is little difference for the two 30% RAP mixtures and the two 40% RAP mixtures are almost identical.

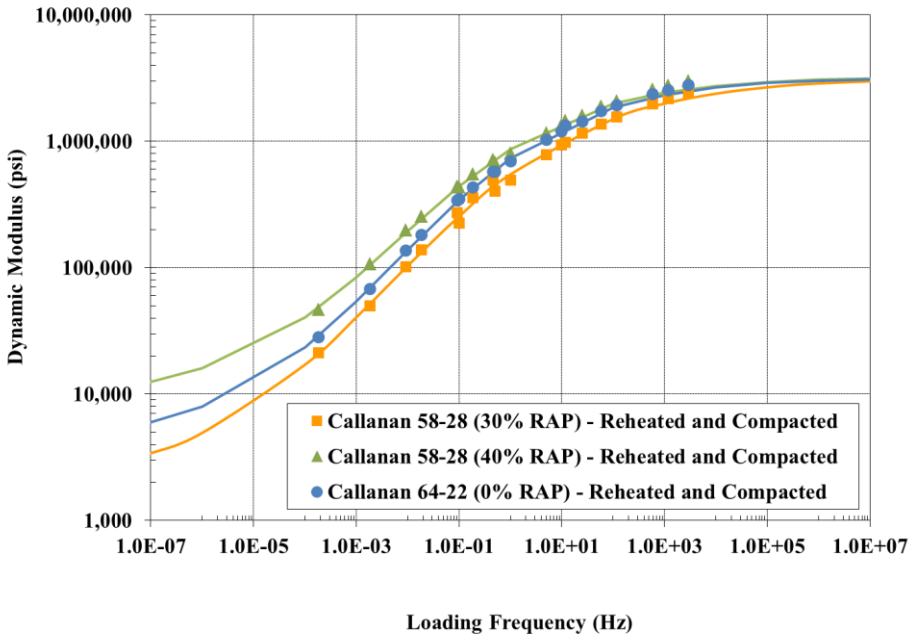

Figure 4-13 Dynamic modulus master curves for New York mixtures (PG58-28 base PG grade) – reheated loose mix

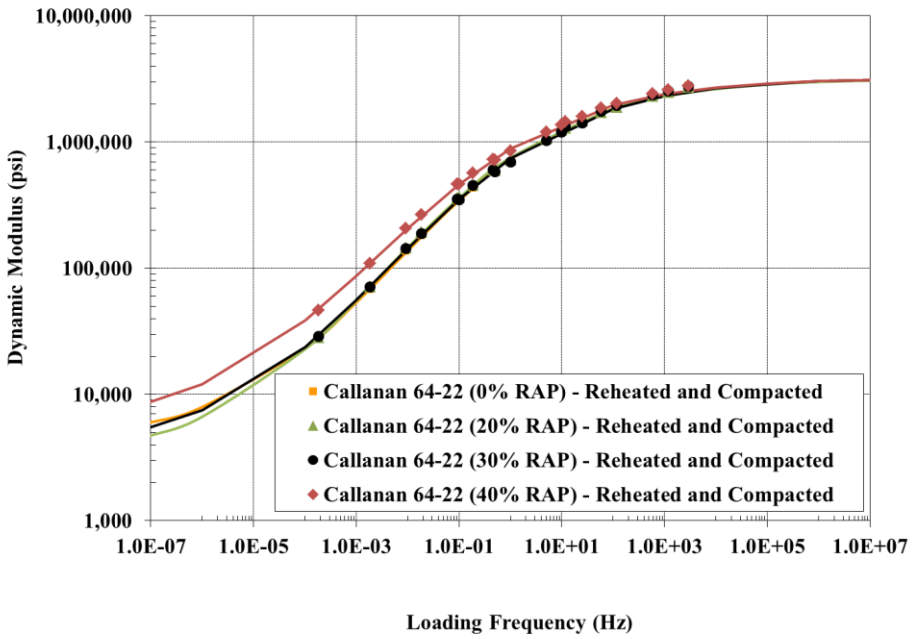

Figure 4-14 Dynamic modulus master curves for New York mixtures (PG64-22 base PG grade) – reheated loose mix

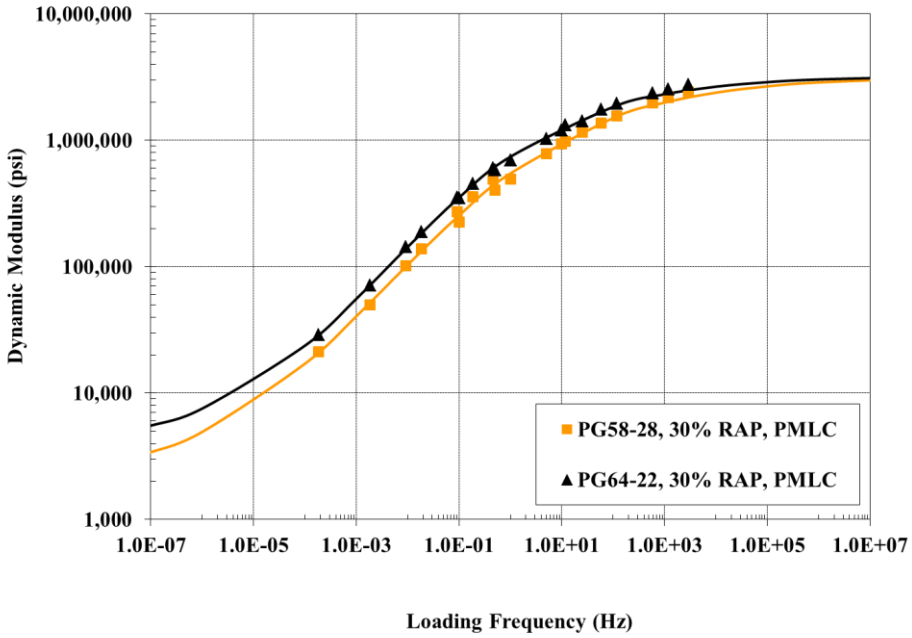

Figure 4-15 Dynamic modulus master curves for NY 30% RAP mixtures – reheated & compacted

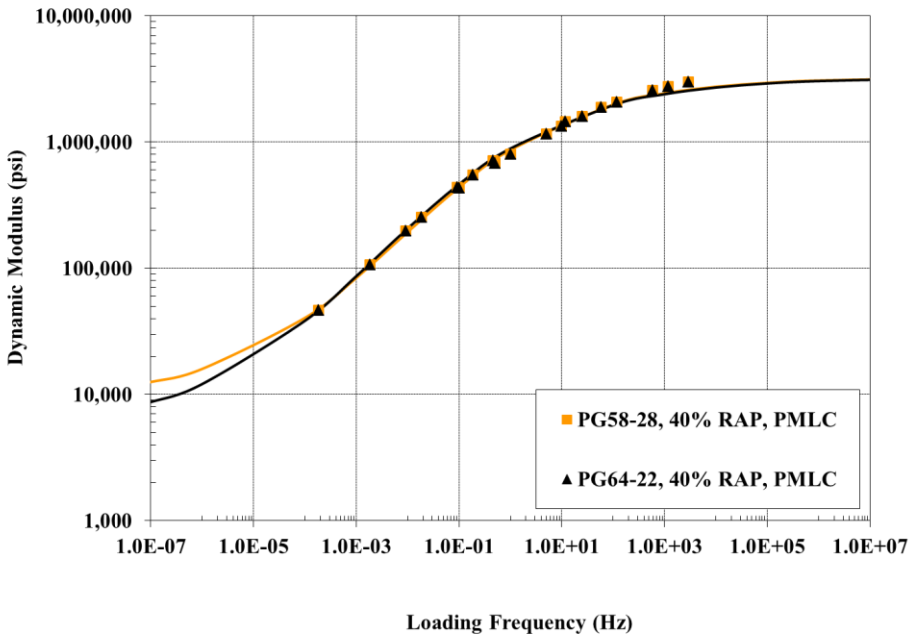

Figure 4-16 Dynamic modulus master curves for NY 40% RAP mixtures – reheated & compacted

4.4.1.3 Comparison of Plant Compacted and Reheated Loose Mix Specimens

The testing of the two different specimen types allowed for an evaluation of how the stiffness of the mixtures may change due to the reheating of loose mix in the laboratory. Figure 4-20 through Figure 4-22 show the ratio between the dynamic modulus of the PG 58-28 mixtures and Figure 4-20 through Figure 4-22 show the ratio between the dynamic modulus of the PG 64-22 mixtures at the two different conditions. A value greater than one indicates that the reheated specimens are stiffer than the plant compacted specimens. The figures show a slight increase in mixture stiffness at the 4.4°C test temperature for most of the mixtures, except the PG 64-22 20% RAP mixture. The 20% RAP mixture showed a much higher increase in mixture stiffness compared to the other RAP contents, possibly due to the shorter silo storage time for this mixture. This trend continues at the 20°C and 35°C test temperature, with the dynamic modulus values doubled at some frequencies simply due to the reheating of the sampled loose mix and in general, more stiffening observed with the mixtures containing lower RAP amounts. This is likely due to the higher amount of virgin binder that could potentially oxidize during additional conditioning.

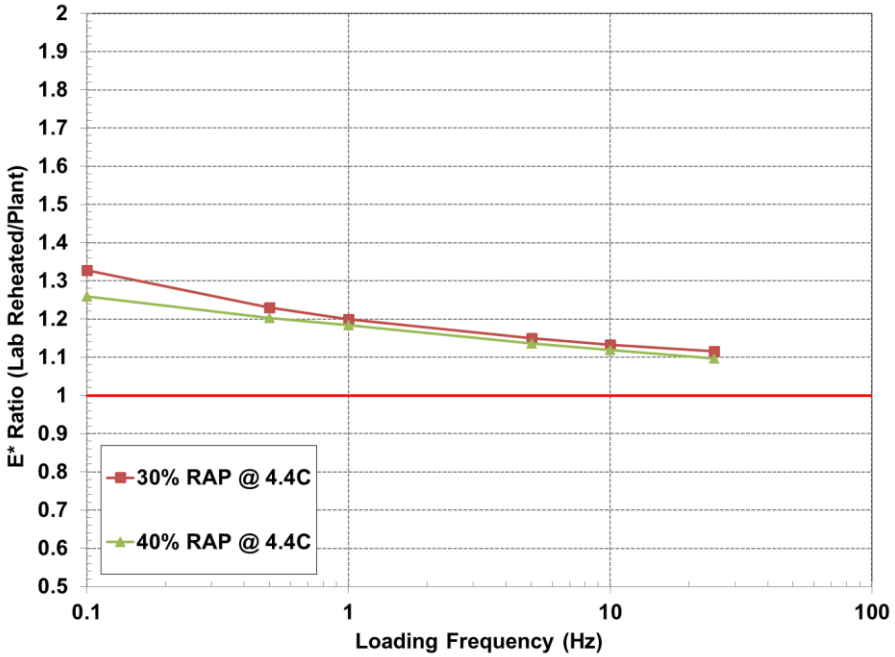

Figure 4-17 E* ratios for NY PG 58-28 mixtures – 4.4°C test temperature

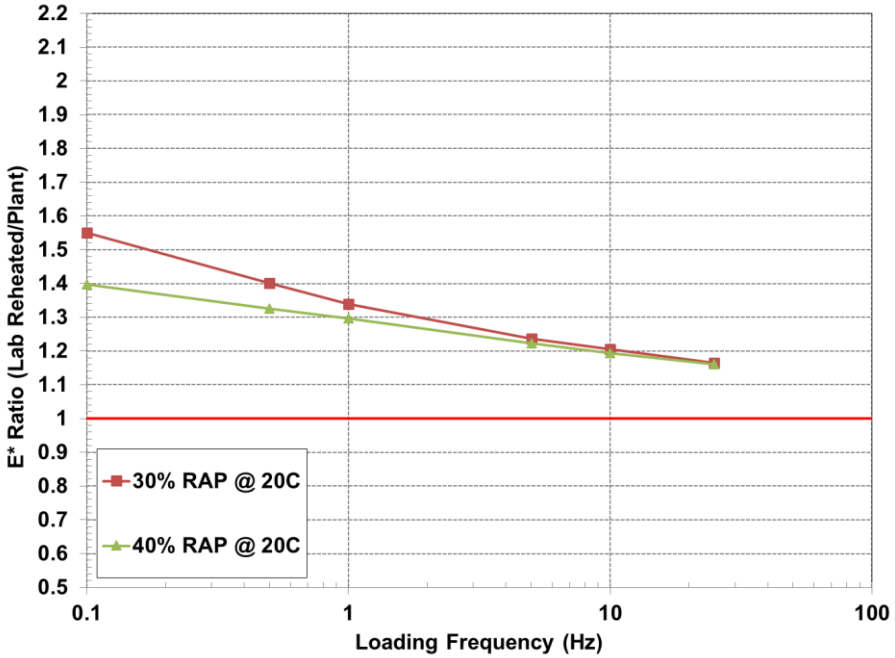

Figure 4-18 E* ratios for NY PG 58-28 mixtures – 20°C test temperature

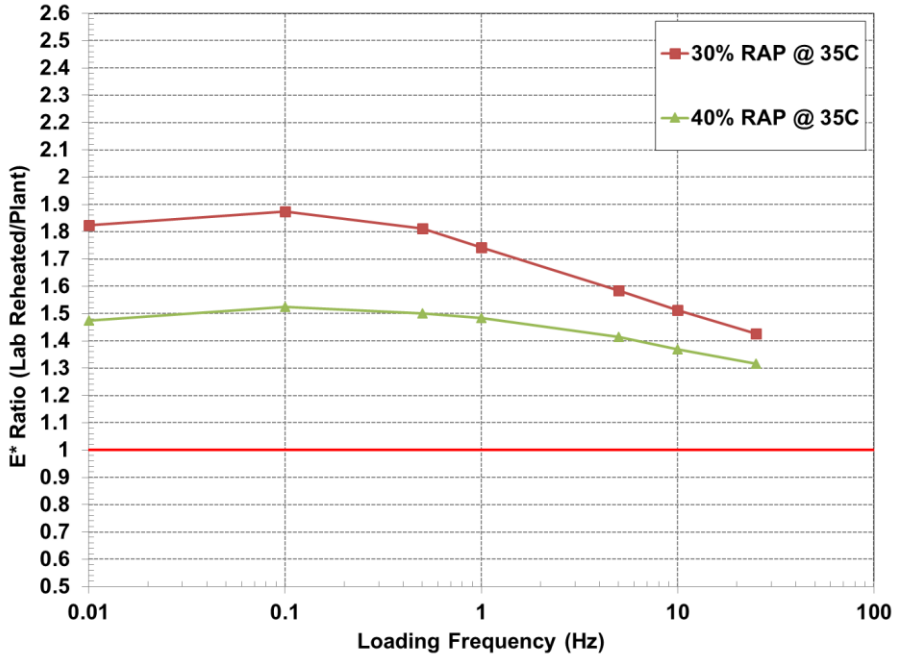

Figure 4-19 E* ratios for NY PG 58-28 mixtures – 35^{o}C test temperature

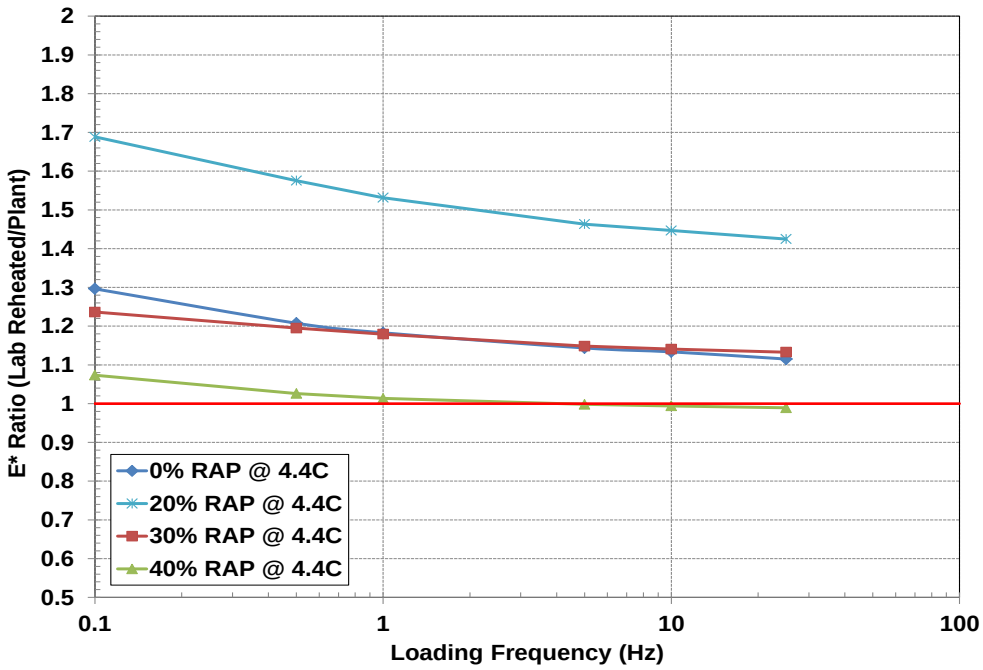

Figure 4-20 E* ratios for NY PG 64-22 mixtures – 4.4^{o}C test temperature

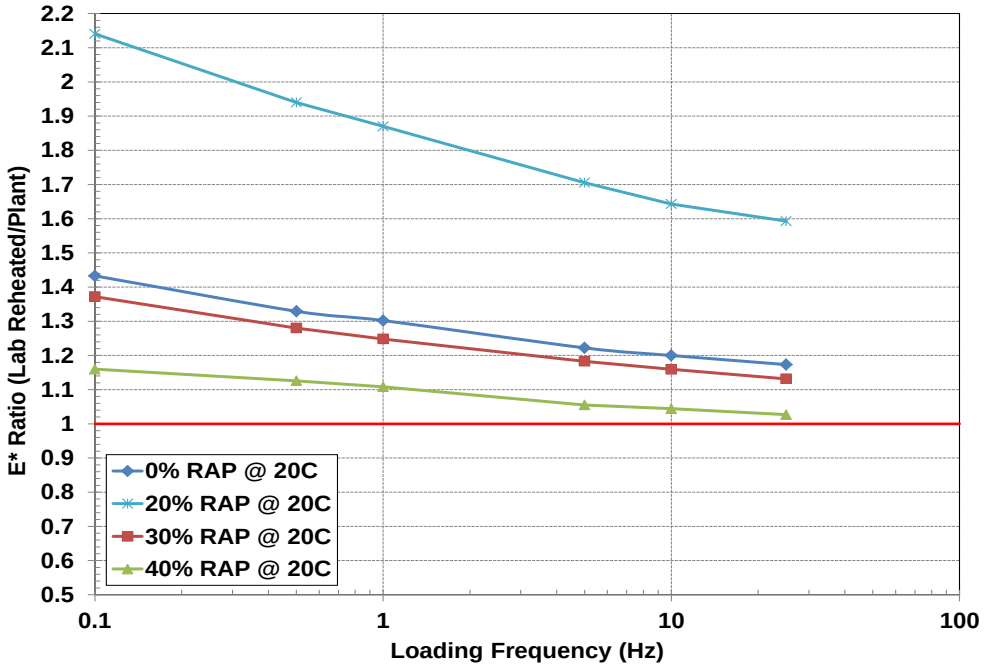

Figure 4-21 E* ratios for NY PG 64-22 mixtures – 20°C test temperature

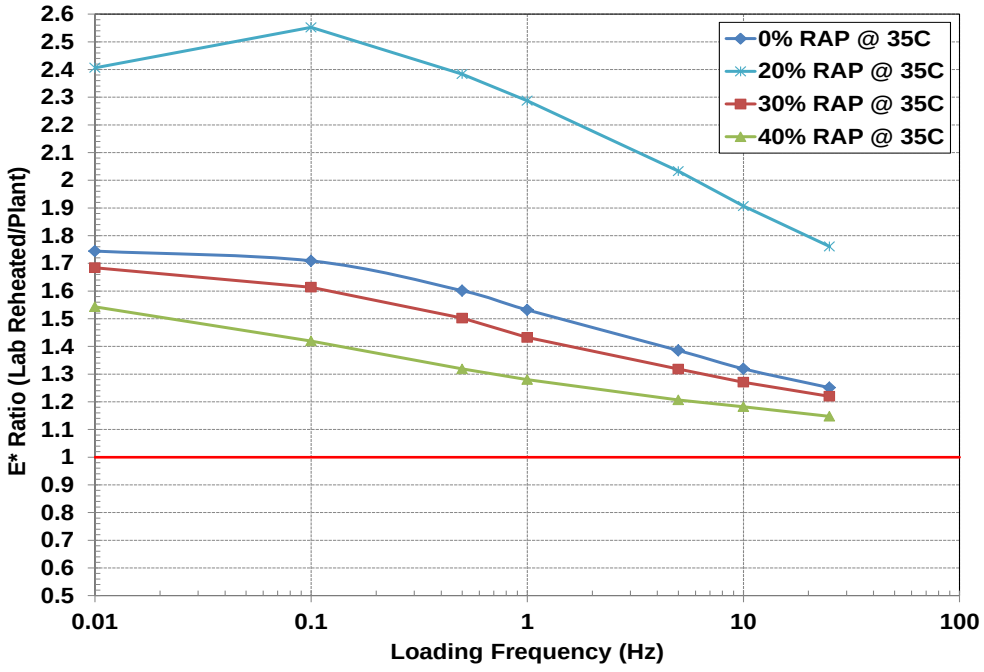

Figure 4-22 E* ratios for NY PG 64-22 mixtures – 35°C test temperature

4.4.2 *Fatigue*

Fatigue behavior of the mixtures was evaluated using three different tests: S-VECD and beam fatigue to evaluate crack initiation and the overlay tester to evaluate crack propagation.

4.4.2.1 S-VECD

S-VECD testing on the NY mixtures was conducted in crosshead-controlled (CX) mode of loading at 19^{o}C and 10 Hz. Figure 4-23 shows the fitted characteristic curves for all of the NY mixtures on one graph and Table 4-11 shows the exponential fit parameters for all the mixtures. The PG 58-28 mixtures are designated with dashed lines and the PG 64-22 mixtures are designated with solid lines. The PG 64-22 mixtures up to 30% RAP all show similar C vs S curves with the 40% RAP curve above the others. The two 40% RAP curves are almost identical, indicating little effect of the PG binder grade for this RAP content. The 30% RAP mixtures show a difference between the two binder grades.

The S-VECD failure criterion for the mixtures is presented in Figure 4-24 through Figure 4-27. There is very little difference among the RAP contents for the PG 64-22 mixtures, with the virgin mixture showing a slightly shallower slope than the other three mixtures. The 40% RAP PG 58-28 mixture shows slightly better fatigue performance than the 30% RAP PG 58-28 mixture. Evaluation of the impact of binder grade shows that there is little difference in performance for the 30% RAP mixtures while the stiffer binder grade at the 40% RAP level actually shows better performance.

Figure 4-28 shows a comparison of the constant strain simulation results at 19^{o}C for all of the NY mixtures. The simulation results indicate that the PG 64-22 0% RAP mixture has the worst performance and the 40% RAP mixtures appear to have the best performance. There is a slight improvement of the fatigue performance with the use of the softer virgin binders.

Table 4-11 Exponential Fit Parameters for VECD Model for NY Mixtures

Mix Type	**Alpha**	**a**	**b**	**C_f**
NY PG 58-28 30% RAP	3.391	-1.79E-03	5.62E-01	0.093
NY PG 58-28 40% RAP	3.391	-1.45E-03	5.57E-01	0.114
NY PG 64-22 0% RAP	3.391	-1.22E-03	5.82E-01	0.155
NY PG 64-22 20% RAP	3.391	-1.88E-03	5.45E-01	0.123
NY PG 64-22 30% RAP	3.391	-1.51E-03	5.60E-01	0.121
NY PG 64-22 40% RAP	3.391	-1.17E-03	5.71E-01	0.123

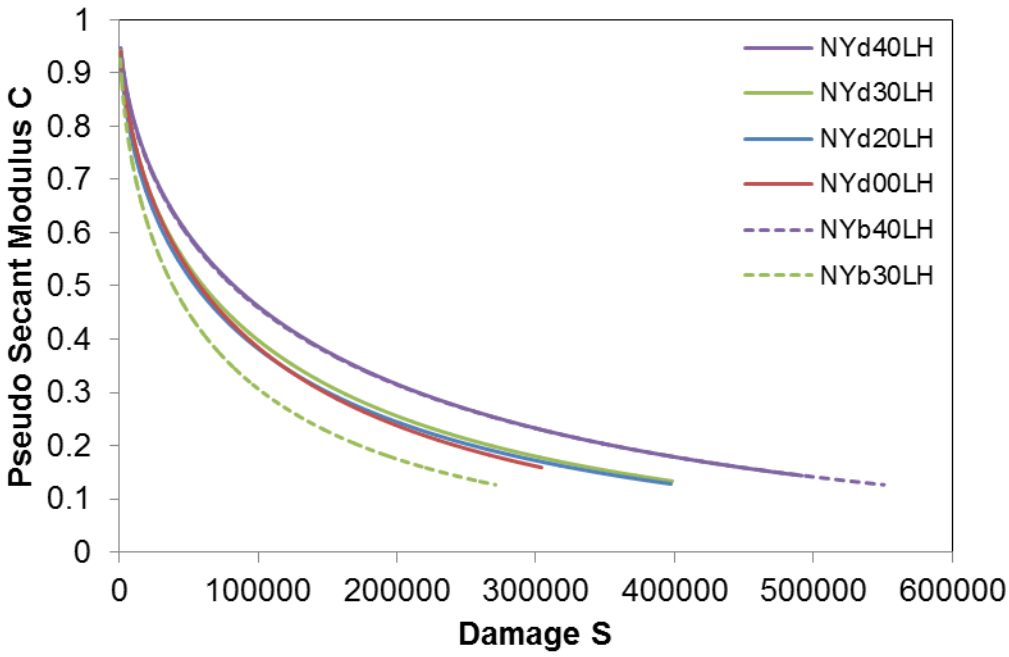

Figure 4-23 Characteristic curve C vs. S - all NY mixtures at 19°C

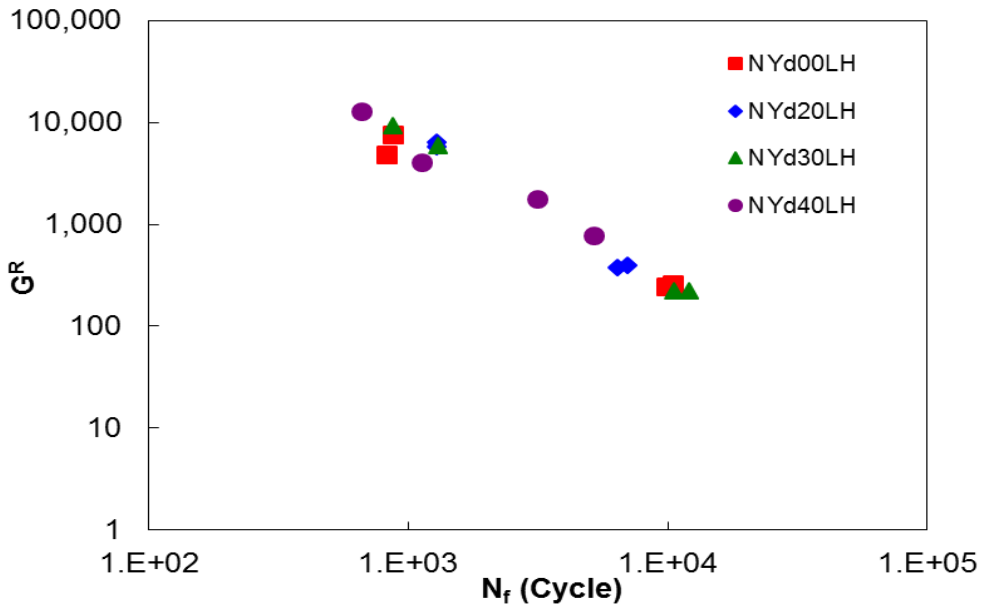

Figure 4-24 Failure Criterion for NY PG 64-22 mixtures at 19°C

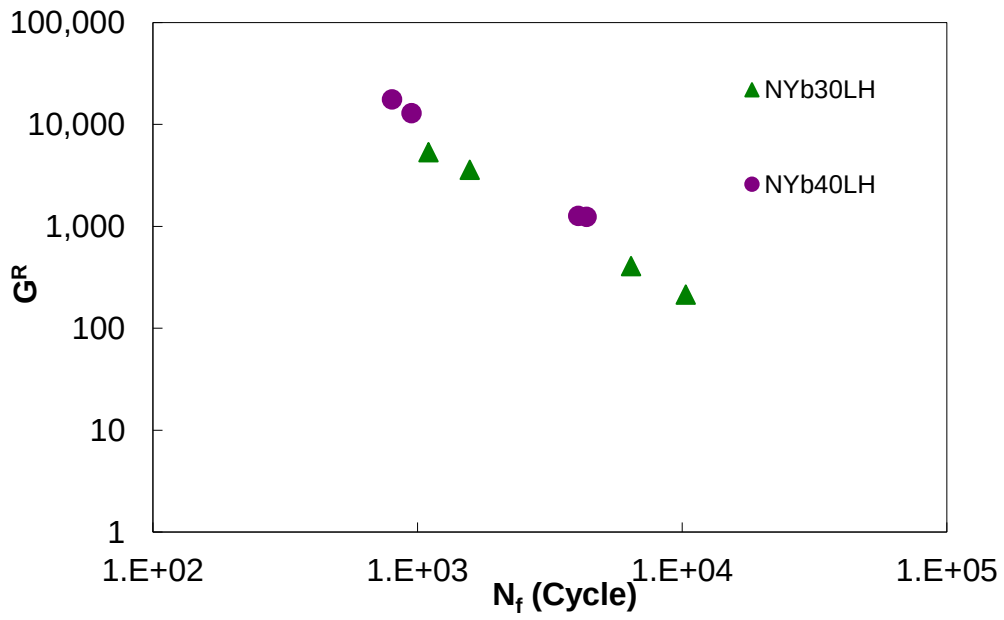

Figure 4-25 Failure Criterion for NY PG 58-28 mixtures at 19ºC

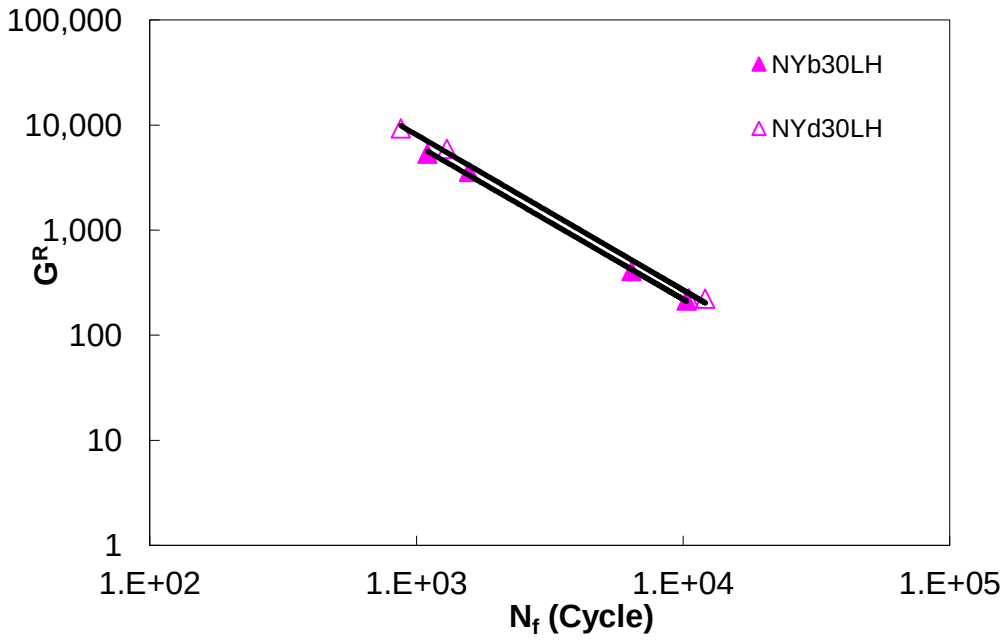

Figure 4-26 Comparison of Failure Criterion for NY 30% RAP mixtures at 19ºC

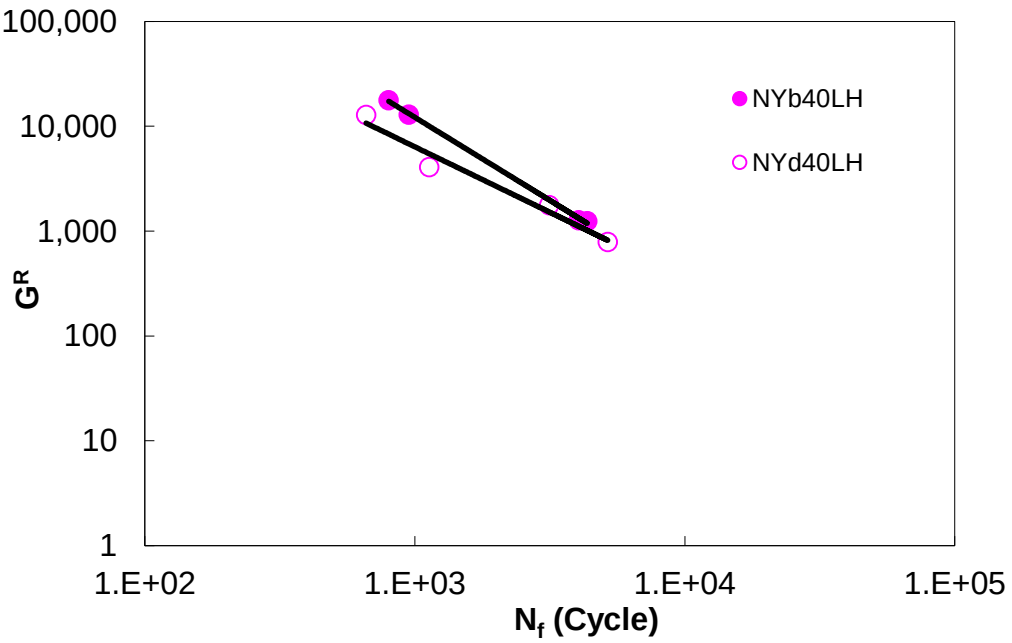

Figure 4-27 Comparison of Failure Criterion for NY 40% RAP Mixtures at 19°C

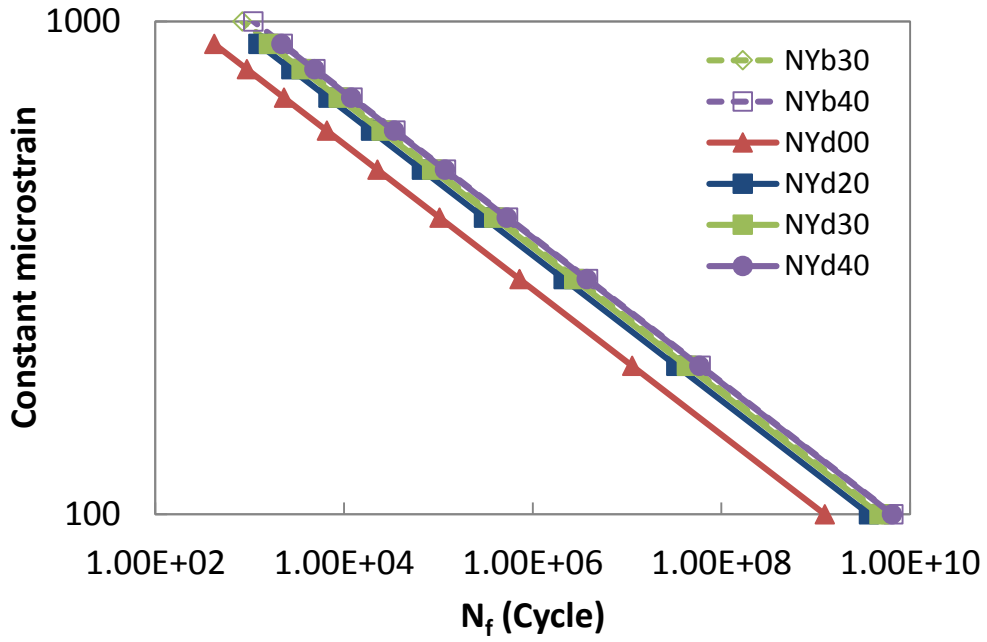

Figure 4-28 Strain-controlled direct tension fatigue test simulations for all NY mixtures

4.4.2.2 Beam

The beam fatigue testing was done according to AASHTO T321, but due to material limitations, only one replicate per strain level was performed. The results for the New York PG 58-28 and PG 64-22 mixtures are shown in Figure 4-29 and Figure 4-30, respectively. The test results shown in Figure 4-29 indicate that the use of a softer asphalt binder at higher RAP contents results in flexural fatigue results similar to a 0% RAP mixture using a PG 64-22 asphalt binder, indicating use of a softer binder helped to improve the fatigue resistance of higher RAP mixtures. Figure 4-30 indicates that all four of the PG 64-22 mixtures performed similarly, with the 40% RAP mixture slightly better than the 0% RAP mixture and the 30% RAP mixture as the worst.

Figure 4-31 and Figure 4-32 shows the comparisons between the 30% and 40% RAP mixtures containing PG 58-28 and PG 64-22 asphalt binders, respectively. The softer binder grade appears to help improve fatigue performance for the 30% RAP mixture, but not for the 40% RAP mixture. However, it is difficult to draw conclusions with the limited testing and the differences in production temperatures and silo storage times that may also be impacting the results.

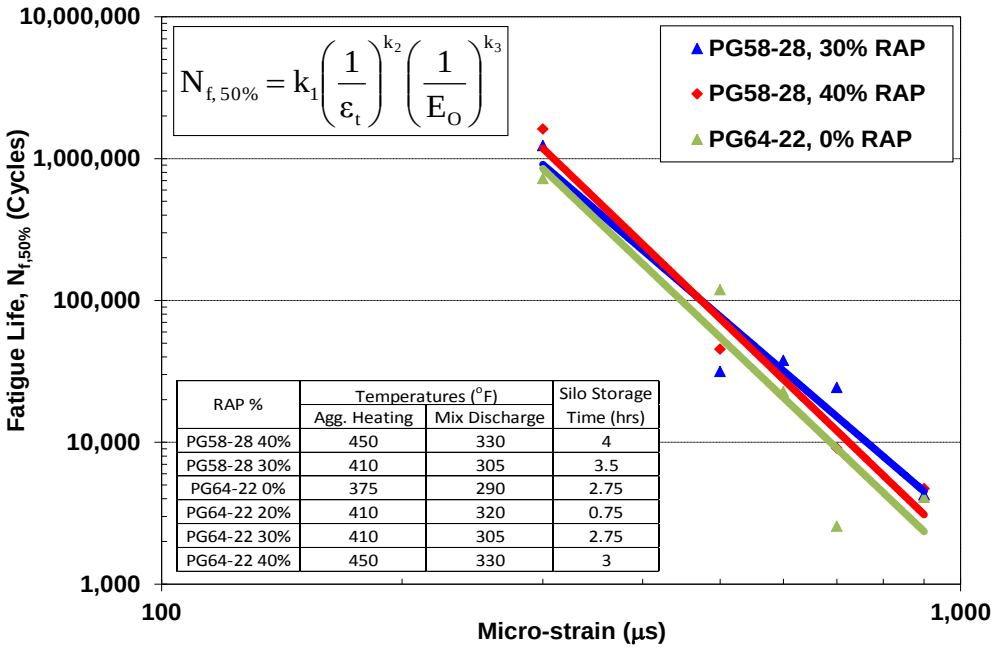

RAP %	Temperatures (°F)		Silo Storage Time (hrs)
	Agg. Heating	Mix Discharge	
PG58-28 40%	450	330	4
PG58-28 30%	410	305	3.5
PG64-22 0%	375	290	2.75
PG64-22 20%	410	320	0.75
PG64-22 30%	410	305	2.75
PG64-22 40%	450	330	3

Figure 4-29 Flexural fatigue life for New York mixtures – PG58-28 asphalt binder

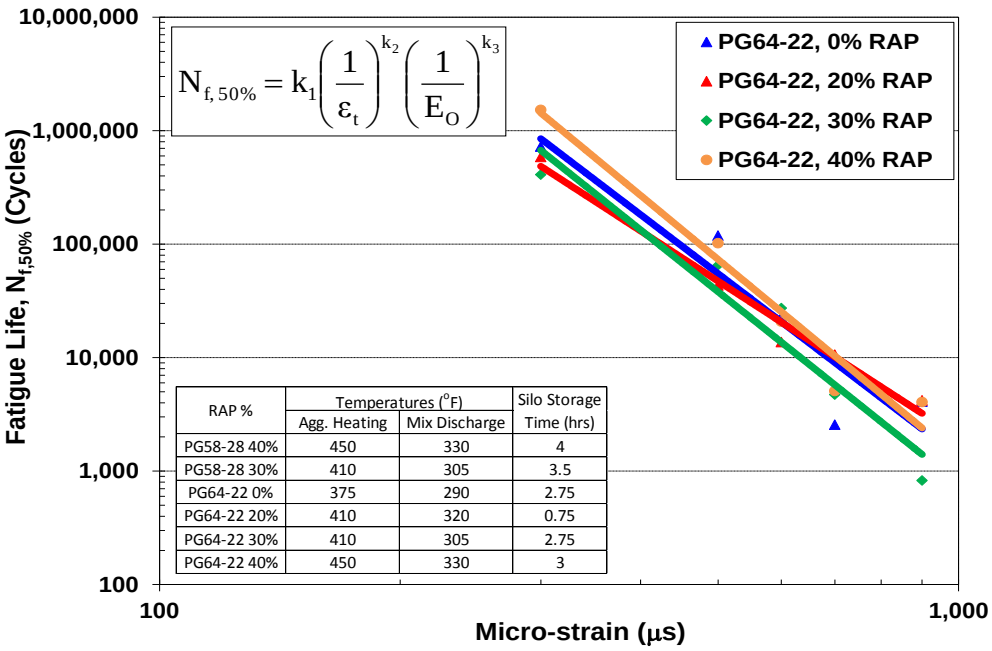

Figure 4-30 Flexural fatigue life for New York mixtures – PG64-22 asphalt binder

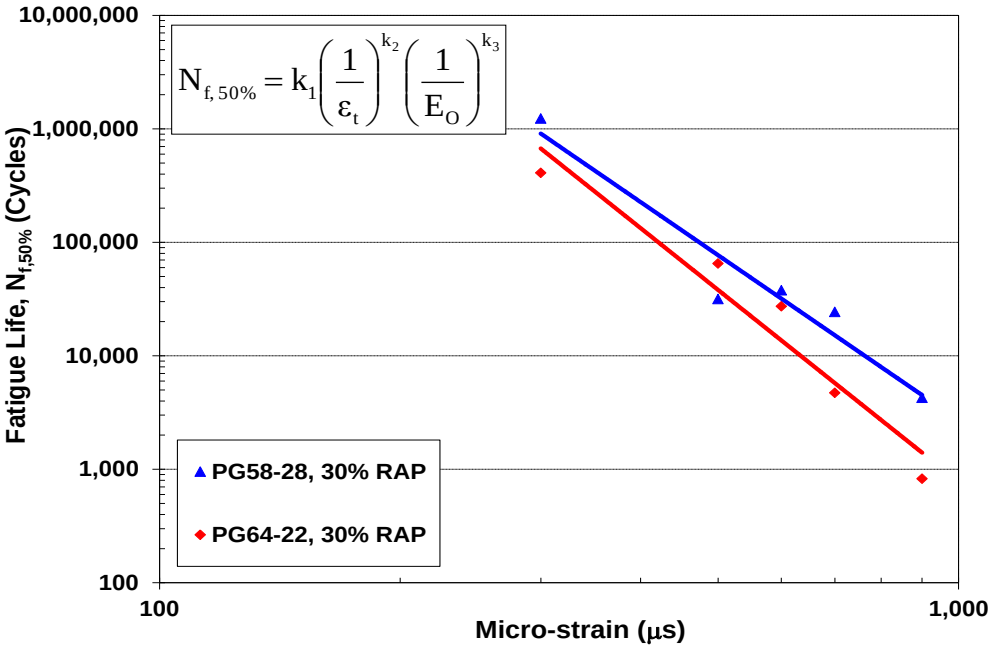

Figure 4-31 Flexural fatigue life results for New York mixtures – 30% RAP

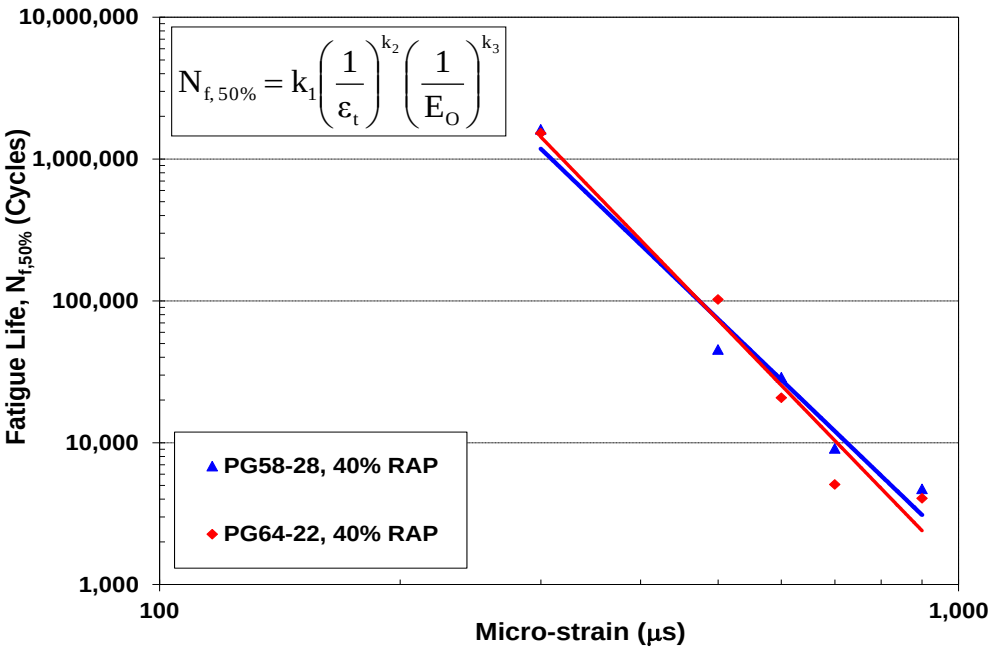

Figure 4-32 Flexural fatigue life results for New York mixtures – 40% RAP

4.4.2.3 Overlay

The resistance to propagation of fatigue cracking was evaluated using the Overlay Tester following sample preparation and test parameters in the TxDOT Tex-248-F testing specifications. The test results for the New York mixtures shown in Figure 4-33 for the PG 64-22 binder indicates that similar fatigue resistance occurs for the 0, 20, and 30% RAP mixtures and a significant drop is observed for the 40% RAP mixture. A similar drop is observed between the 30% RAP and 40% RAP PG 58-28 mixtures. The PG 58-28 binder mixtures show lower fatigue performance than the PG 64-22 mixtures; this could be influenced by the longer silo storage times (approximately one hour) that the PG 58-28 mixtures experienced.

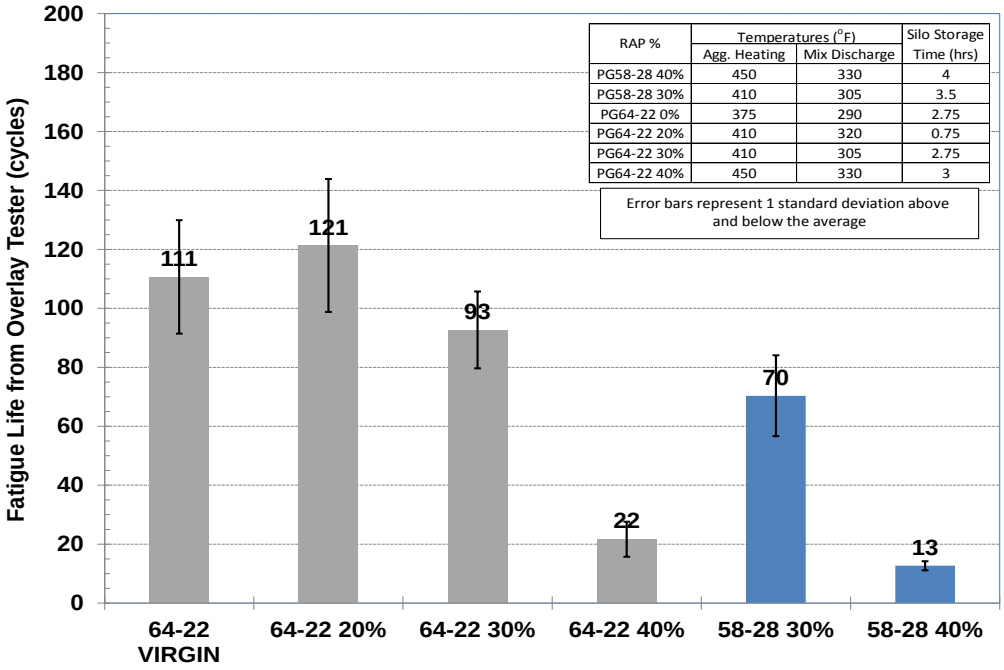

Figure 4-33 Overlay tester results for New York mixtures

4.4.3 *Low Temperature*

4.4.3.1 TSRST

The asphalt mixtures were evaluated for their respective mixture low temperature critical cracking temperature in accordance with AASHTO TP10; tests started at an initial temperature of 4°C and specimens were cooled at a rate of 10°C hr. The failure temperature and stress were recorded and are shown in Table 4-12.

The results in Table 4-12 show that increases in RAP content resulted in warmer cracking temperatures, with changes of approximately 2°C with an increase in RAP content from 30% to 40% for both base PG binders. There is not as much of a change from 20% to 30%

RAP, but the higher air void content of the 20% RAP mixture will cause a warmer cracking temperature than would be expected with specimens at the target 7% air voids. Use of the softer PG grade does improve the cracking temperature, but only by about 3°C.

Table 4-12 TSRST Test Results for New York Mixtures

Mixture	Air Voids %	Temp at Failure °C	Load at Failure N	Low Continuous PG Grade °C	Binder Critical Cracking Temp. °C
NY PG 58-28 30%	7.36	-23.32	7451	-26.5	-26.1
NY PG 58-28 40%	7.12	-21.49	7548	-22.0	-20.6
NY PG 64-22 0%	-[a]	-	-	-22.2	-22.2
NY PG 64-22 20%	9.23	-20.40	5822	-21.8	-22.1
NY PG 64-22 30%	7.57	-19.78	6910	-19.9	-21.1
NY PG 64-22 40%	6.71	-17.88	6997	-17.6	-19.3

[a] No mix available for TSRST testing

4.4.3.2 Low Temperature Creep and IDT Strength

The average low temperature creep compliance master curves at -10°C for the NY mixtures are shown in Figure 4-34 through Figure 4-37. The PG 64-22 base binder mixtures show increasing stiffness with RAP content, except for the virgin mixture, which is the stiffest. The PG 58-28 40% RAP mixture is stiffer than the PG 58-28 30% RAP mixture. Comparing the two base binder grades, the softer binder does make the mixture more compliant for both the 30% and 40% RAP levels.

The low temperature IDT strength measured at -10°C for the NY mixtures is shown in Figure 4-38. There is an increase in the average strength with RAP content for the PG 64-22 mixtures, with the exception of the 20% RAP mixture that has the lowest strength; this could be a result of the shorter silo storage time for this mixture in comparison with the others. The PG 58-28 mixtures also show an increase in strength with RAP content, but are not statistically different than the PG 64-22 mixtures; this indicates that the softer binder grade did not have a significant impact on the low temperature strength.

The cracking temperature for each of the mixtures determined using the TCModel is shown in Table 4-13. The PG 58-28 mixtures have the warmest cracking temperatures (by 2-4°C) and show no difference with RAP content. These mixtures had poor convergence in the TCModel analysis, which could be a reason for the warmer predicted cracking temperatures. For the PG 64-22 mixtures, there is only a 2°C difference between the warmest and coldest temperatures; the 20% RAP mixture has the lowest cracking temperature and no trend with respect to RAP content for the other mixtures.

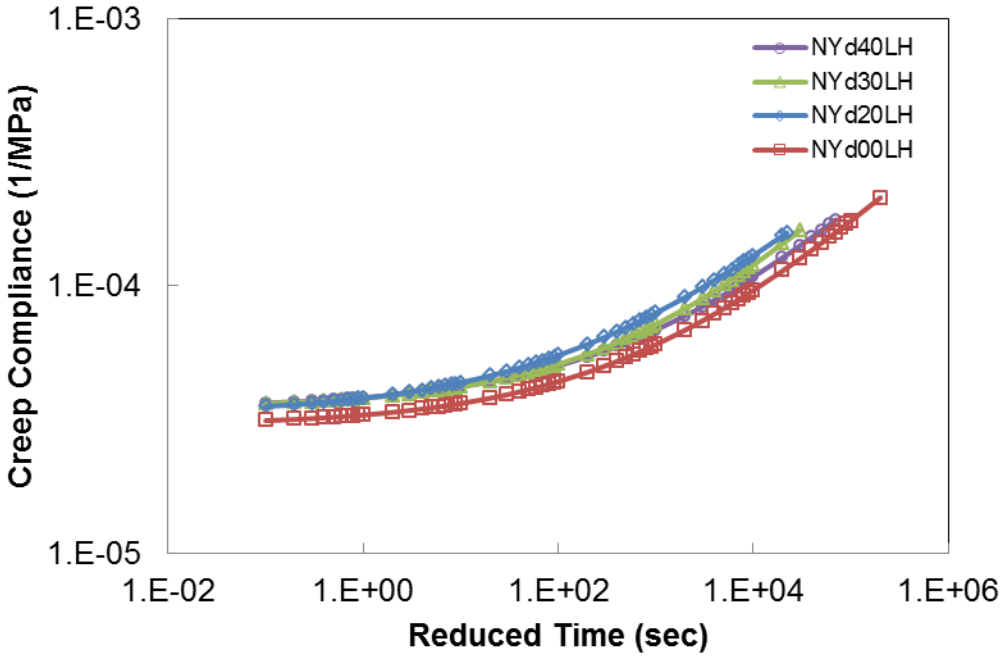

Figure 4-34 Average creep compliance master curves at -10°C for all PG 64-22 NY mixtures

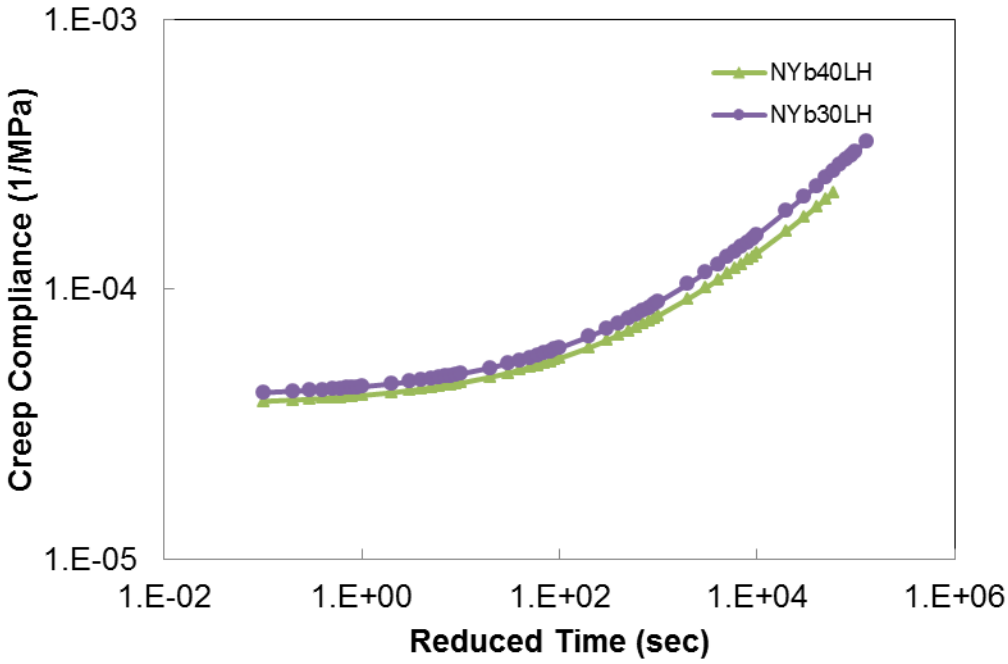

Figure 4-35 Average creep compliance master curves at -10°C for all PG 58-28 NY mixtures

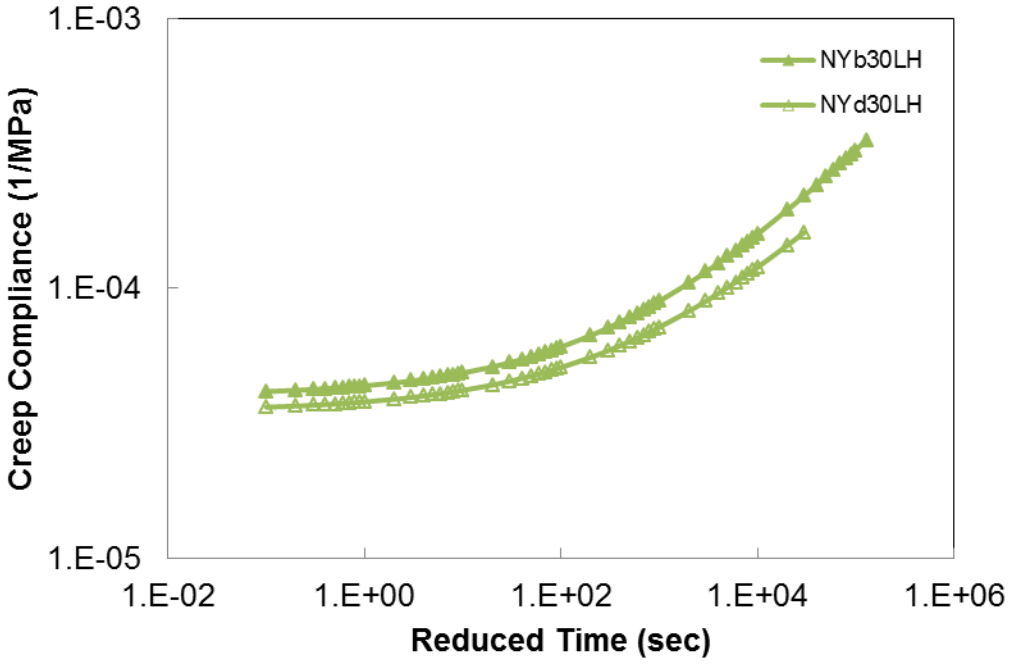

Figure 4-36 Comparison of NY 30% RAP creep compliance curves

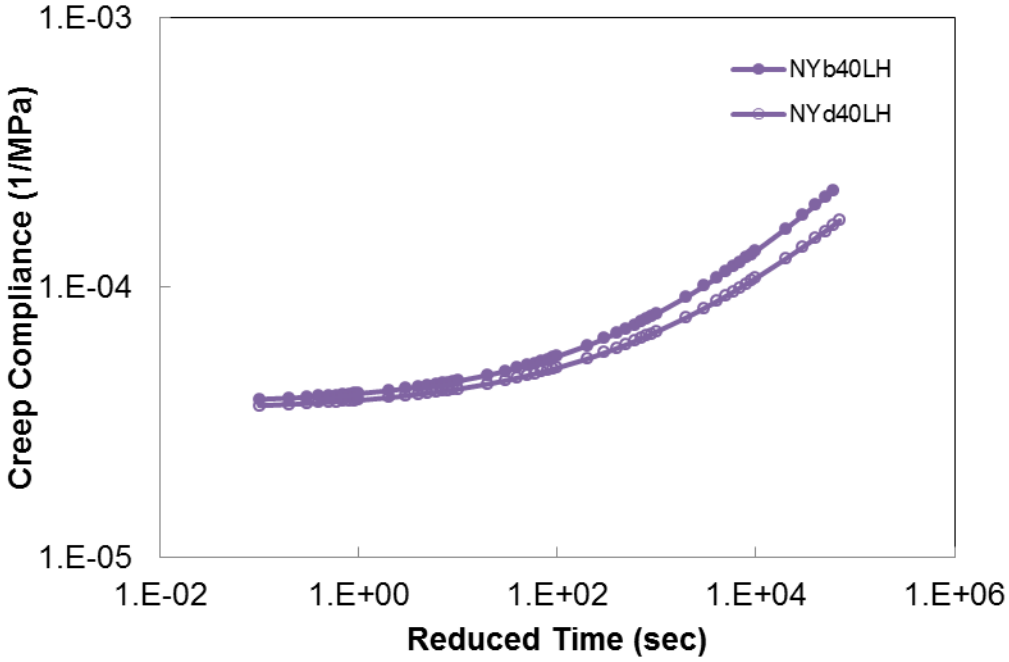

Figure 4-37 Comparison of NY 40% RAP creep compliance curves

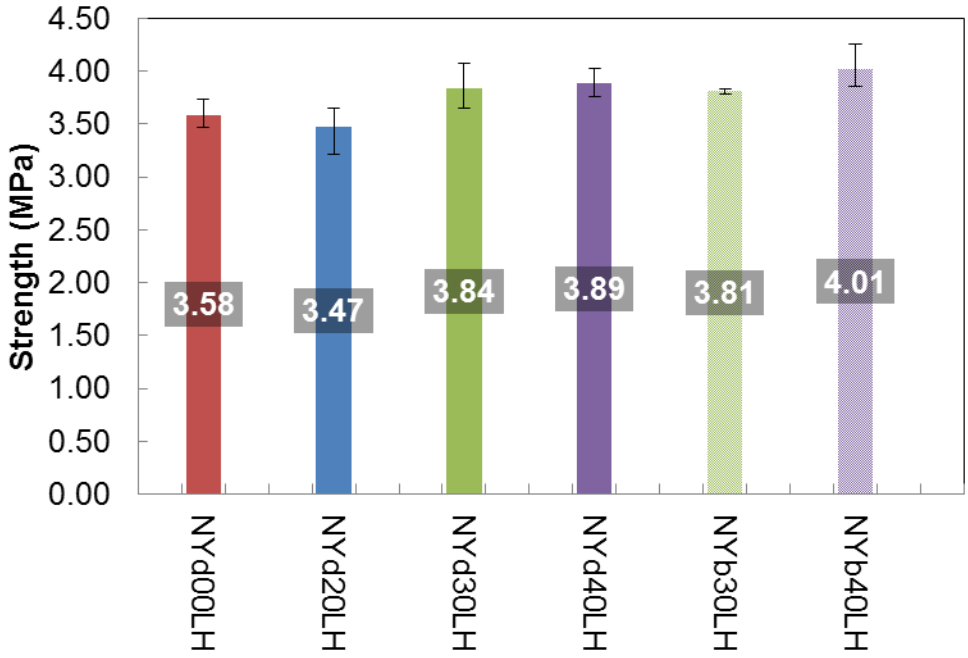

Figure 4-38 Low temperature IDT strength (-10°C) for NY mixtures

4.4.3.3 Comparison

4.4.3.4 Comparison with Binder Data

The NY mixture and extracted binder low temperatures are shown together in Table 4-13 for comparison. The rankings of the mixtures for each test are also shown in the table. Comparing the extracted binder testing results to the TSRST results indicates consistent results with difference less than 2°C between tests for the PG 64-22 mixtures. For the PG 58-28 mixtures, the differences were larger for the 30% RAP mixture (approximately 3°C) and similar for the 40% RAP mixture. Both tests indicated the same trend of a reduction in low temperature capabilities as the amount of RAP in the mixture was increased and an improvement in the low temperature cracking performance with the addition of the softer PG binder. The cracking temperatures determined from the IDT analysis were 10-15°C warmer than the other mixture or binder tests and did not follow expected trends. This is likely due to the difficulty in performing the analysis with the TCModel spreadsheet for these mixtures.

Table 4-13 Critical cracking temperatures comparisons - NY mixtures

Mix	Mixture				Binder			
	TCMODEL		TSRST		Critical Cracking Temperature		Low Temperature Continuous PG-grade	
	°C	Rank	°C	Rank	°C	Rank	°C	Rank
NY PG 58-28 30 % RAP	-7	5	-23.32	1	-26.1	1	-26.5	1
NY PG 58-28 40 % RAP	-7	5	-21.49	2	-20.6	4	-22.0	3
NY PG 64-22 0 % RAP	-10	2	n/a	n/a	-22.2	2	-22.2	2
NY PG 64-22 20 % RAP	-11	1	-20.4	3	-22.1	3	-21.8	4
NY PG 64-22 30 % RAP	-9	4	-19.78	4	-21.1	3	-19.9	5
NY PG 64-22 40 % RAP	-10	2	-17.88	5	-19.3	5	-17.6	6

4.4.4 *Moisture*

4.4.4.1 Hamburg Wheel Tracking Device

The results of the Hamburg testing for the NY mixtures are shown in Table 4-14. The mixtures incorporating RAP performed better than the PG 64-22 control mixture, however there is not a clear trend with increasing RAP content as the 20% RAP mixture performed better than the 30% RAP mixture. The 40% RAP mixtures for both PG binder grades showed the best overall rutting performance, which is expected due to the higher stiffness of these mixtures.

Table 4-14 Hamburg wheel tracking test results for all NY mixtures

State	NMAS	% RAP	Binder Grade	Average Stripping Inflection Point	Avg. Rut Depth at 10,000 Cycles (mm)	Avg. Rut Depth at 20,000 Cycles (mm)
NY	12.5 mm	30	PG58-28	17,400	2.63	6.18
		40	PG58-28	NONE	2.12	3.37
		0	PG64-22	7,200	6.62	n/a
		20	PG64-22	NONE	1.93	3.17
		30	PG64-22	13,370	2.67	8.97
		40	PG64-22	NONE	1.55	2.13

NONE = Mixture passed 20,000 cycle test with no SIP.
n/a = Test terminated prior to reaching specified cycle due to maximum deformation exceeding 20 mm.

4.4.4.2 IDT Tensile Strength Ratio

The results of the TSR testing of the NY mixtures are shown in Figure 4-39 and the dry strength values for each mixture are shown in Figure 4-40. The bars in Figure 4-40 represent the range of the results. The two PG 58-28 mixtures have similar TSR values while the PG 64-22 20% RAP mixture shows the lowest. There is not a trend with the TSR values with respect to RAP content. The relative rankings of the PG 64-22 mixtures differ from those observed from the HWTD test. The dry tensile strengths generally increase with RAP content, with the exception of the PG 64-22 30% RAP mixture; this mixture also had a very high standard deviation, which is likely impacting the results.

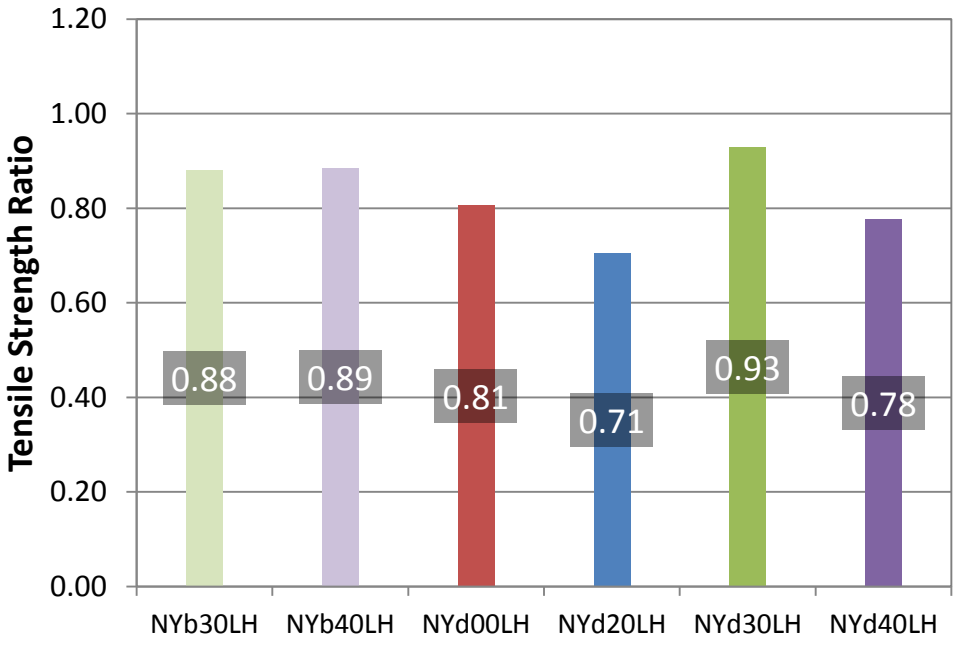

Figure 4-39 Tensile strength ratio - all NY mixtures

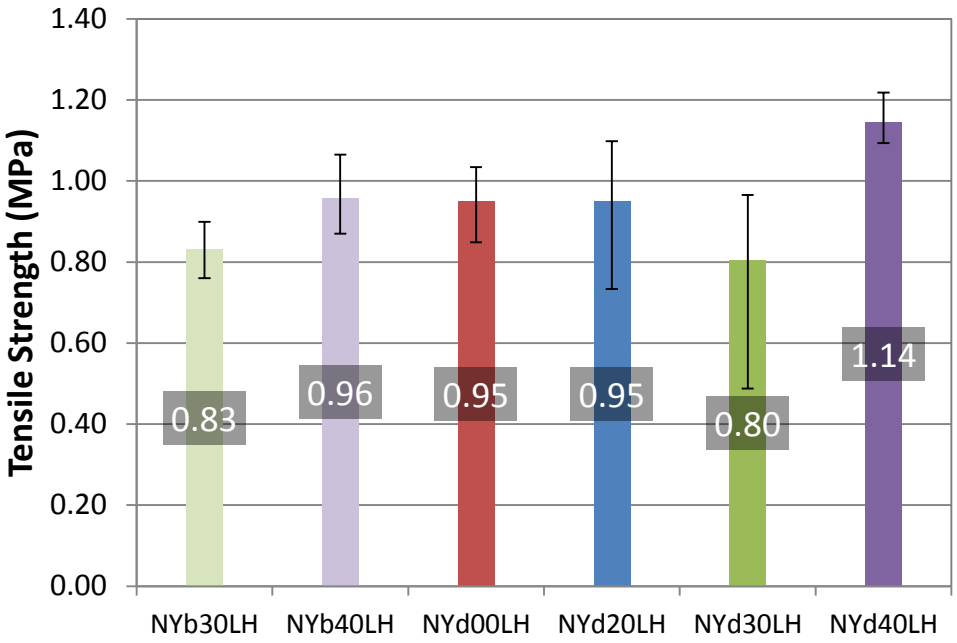

Figure 4-40 Average tensile strength of dry set - all NY mixtures

4.4.5 *Workability Device*

The workability data shown in Figure 4-41 for the New York mixtures indicates that, for the RAP mixtures, the addition of more RAP to the mixture decreased the workability. The workability reductions were larger as the amount of RAP increased in the PG 64-22 mixtures. The data for the PG64-22 control mixture does not fit the trend as it shows the mixture was less workable than some of the RAP mixtures. The reason for this occurrence is not known. The data does suggest that the use of the softer binder could improve the workability of RAP mixtures.

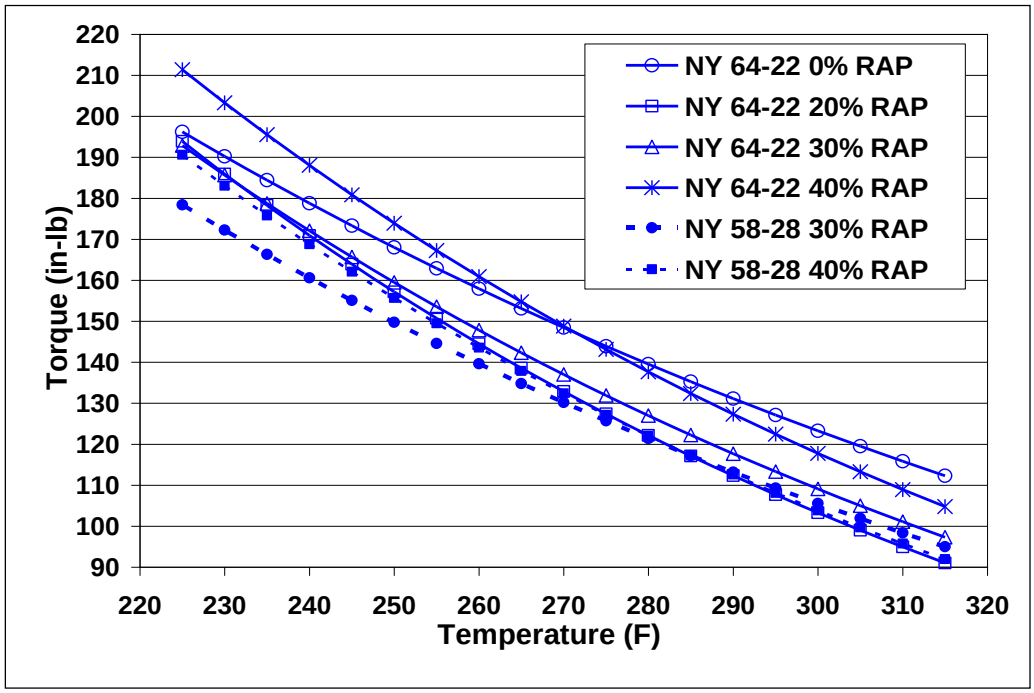

Figure 4-41 Workability test results for all NY mixtures

CHAPTER 5 VERMONT MIXTURES

5.1 Mixture Design Information

The Vermont mixtures were produced by Pike Industries, Inc. using an H&B 5 ton batch plant located in Williston, VT. After production, mixtures were discharged to trucks for sampling; they were not stored in a silo. The general mixture design information for the VT mixtures is shown in Table 5-1 and Table 5-2. The mixtures produced had a nominal maximum aggregate size (NMAS) of 9.5 mm with an optimum asphalt contents ranging from 6.5% to 6.8%. The RAP used in the VT mixtures had a continuous grade of PG 73.8-25.2. The extracted and recovered asphalt contents from the produced mixtures were lower than the design optimum, the PG 64-28 being significantly lower. The aggregate gradations are consistent with the PG 64-28 40% RAP mixture being slightly coarser and the PG 64-28 20% RAP mixture slightly finer than the others.

5.2 Plant Production Information

The plant production information for the VT mixtures is shown in Table 5-3. The mixtures were produced between 295°F to 340°F and discharged for sampling; these mixtures were not placed. The ambient temperatures during production were 40-50 °F with cloudy, wet weather. Moisture was observed in the 30% and 40% RAP mixtures.

5.3 Binder Testing

5.3.1 *PG Grading*

The asphalt binder was sampled from the storage tanks, as well as extracted and recovered from the mixtures. The results of the PG grading are shown in Table 5-4, as well as Figure 5-1 and Figure 5-2. The test results indicate that as the RAP content increases, the PG grade gets warmer at both the low and high PG temperatures, with the exception of the PG 52-34 40% RAP mixture that has a softer binder than the PG 52-34 30% RAP mixture, which may be a result of the difference in production temperatures. The PG 52-34 tank binder had a continuous grade of PG 56.3-32.5, missing the low end by 1.5 degrees. The PG 52-34 binder also shows a significant stiffening (9°C) in the high PG temperature just from plant production, which may be a result of the relatively high production temperature for the virgin mix. By comparison, the addition of the 30% RAP increases the high PG temperature another 6°C for this binder. The PG 64-28 mixtures show a 10°C increase in the high PG temperature from 0% to 40% RAP. The use of the softer binder grade shows an improvement for the high PG temperature at all RAP levels, but minimal impact at the low PG temperature for the 0% and 20% RAP mixtures. The 30% RAP mixtures shows an

improvement of the low PG temperature but the 40% RAP mixtures show a reverse trend. The reason for these trends is unknown.

The low PG temperature for both tank binders is m-controlled; the PG 52-34 binder shows a 4.3 ^{o}C difference in the S and m values while the PG 64-28 only shows a 1.5^{o}C difference. Both binders become more m-controlled at the higher RAP contents.

Table 5-1 Mix design information – all VT mixtures

Mix	PG Grade	NMAS (mm)	Design Asphalt Content (%)	% RAP	RAP Binder Content, %	VMA	VFA	Extracted/ Recovered Asphalt Content (%)	% Binder Replacement
VT PG 52-34 0 % RAP	52-34	9.5	6.7	0	--	20.2	76.3	6.58	0.00
VT PG 52-34 20 % RAP	52-34	9.5	6.8	20	5.41	18.8	81.9	6.27	17.26
VT PG 52-34 30 % RAP	52-34	9.5	6.6	30	5.41	17.7	82.5	6.13	26.48
VT PG 52-34 40 % RAP	52-34	9.5	6.6	40	5.41	18	77.8	6.12	35.36
VT PG 64-28 0 % RAP	64-28	9.5	6.5	0	--	20.3	71.5	5.84	0.00
VT PG 64-28 20 % RAP	64-28	9.5	6.7	20	5.41	18.7	79.7	5.46	19.82
VT PG 64-28 30 % RAP	64-28	9.5	6.6	30	5.41	19.1	75.9	5.31	30.56
VT PG 64-28 40 % RAP	64-28	9.5	6.6	40	5.41	18.2	76.4	6.02	35.95

Table 5-2 Mixture gradations - all VT mixtures

Mix	PG	Mixture Gradation								
		12.5	**9.5**	**#4**	**#8**	**#16**	**#30**	**#50**	**#100**	**#200**
VT PG 52-34 0 % RAP	52-34	100	98.8	78.8	51.1	31.4	19.3	10.7	6.1	3.8
VT PG 52-34 20 % RAP	52-34	100	98.4	79.2	51.1	30.7	19.1	11.8	7.4	4.6
VT PG 52-34 30 % RAP	52-34	100	98.6	75.0	48.1	29.5	18.7	11.7	7.4	4.5
VT PG 52-34 40 % RAP	52-34	100	97.9	76.8	48.8	29.3	18.4	11.8	7.5	4.6
VT PG 64-28 0 % RAP	64-28	100	99.6	76.9	48.8	29.7	18.0	9.9	5.5	3.3
VT PG 64-28 20 % RAP	64-28	100	98.7	81.3	53.5	32.3	19.9	11.9	7.1	4.3
VT PG 64-28 30 % RAP	64-28	100	97.8	77.5	48.9	29.0	17.8	11.0	7.0	4.3
VT PG 64-28 40 % RAP	64-28	100	98.5	75.1	46.6	26.8	15.7	9.0	4.8	4.5

Table 5-3 Plant production information - all VT mixtures

Mix	PG Grade	Binder Temp (ºF)	Burner Set Point (ºF)	Mixing Times Dry/Wet (s)	Discharge Temp. (ºF)	Sampling Temp. (ºF)	Moisture
VT PG 52-34 0 % RAP	52-34	296	452	6/36	340	340	none
VT PG 52-34 20 % RAP	52-34	299	606	10/36	324	324	none
VT PG 52-34 30 % RAP	52-34	-	613	14/36	320	320	mix bubbling
VT PG 52-34 40 % RAP	52-34	-	-	13/36	300	295	water present
VT PG 64-28 0 % RAP	64-28	286	451	6/36	330	300	none
VT PG 64-28 20 % RAP	64-28	286	580	10/36	300	300	none
VT PG 64-28 30 % RAP	64-28	-	667	13/36	322	310	mix bubbling
VT PG 64-28 40 % RAP	64-28	305	635	13/36	295	295	water visible, heavy steam

Table 5-4 Summary of asphalt binder performance grading (Williston, VT)

Production Location	Base PG Grade Binder	Tank or Extracted with RAP Content	Continuous PG Grade (°C)				PG Grade (°C), AASHTO R29 & M320	Critical Cracking Temperature (°C), AASHTO R49
			High Temp (RTFO)	Low Temp		Intermediate Temp (PAV)		
				Stiffness (MPa)	m-slope			
Pike (Williston, VT)	52-34	Tank	56.3	-36.8	-32.5	12.1	52-28	-34.2
		Extracted - 0% RAP	65.4	-36.9	-28.3	10.9	64-28	-33.3
		Extracted - 20% RAP	68.3	-35.3	-28.1	12.5	64-28	-31.9
		Extracted - 30% RAP	71.4	-34.8	-26.3	12.8	70-22	-32.7
		Extracted - 40% RAP	68.6	-33.4	-21	14.1	64-16	-28.4
	64-28	Tank	64.4	-31.7	-30.2	16.6	64-28	-30.6
		Extracted - 0% RAP	67.4	-30.8	-28.1	17.7	64-28	-26.9
		Extracted - 20% RAP	69.6	-30.4	-27	18.9	64-22	-27.2
		Extracted - 30% RAP	74.7	-30	-23	19.9	70-22	-25.2
		Extracted - 40% RAP	78	-30.4	-24.9	18	76-22	-26.5

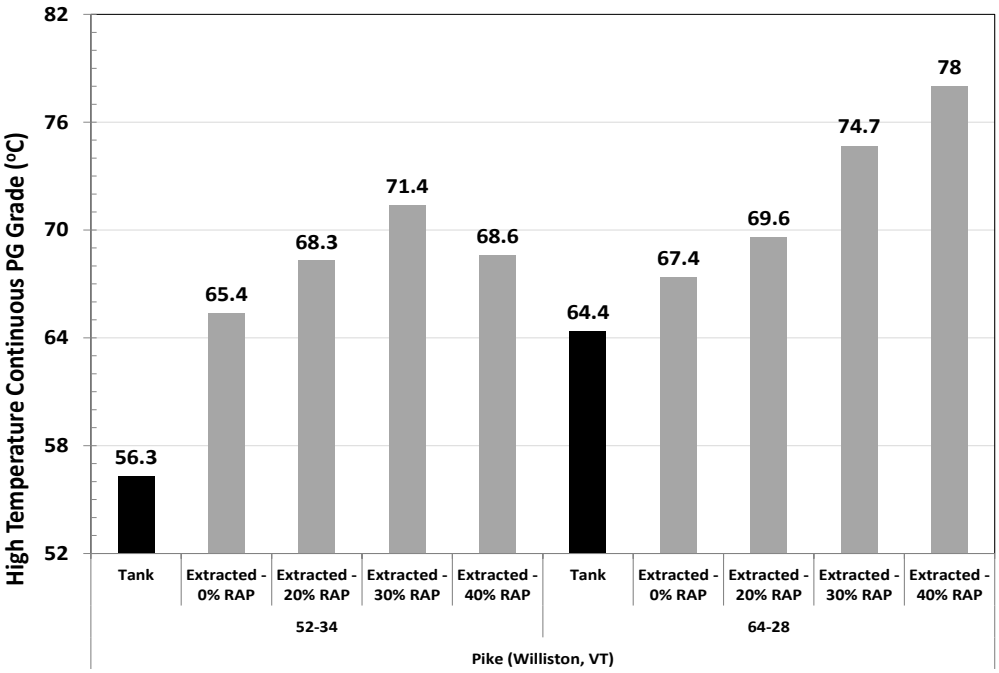

Figure 5-1 High temperature PG grade (Williston, VT)

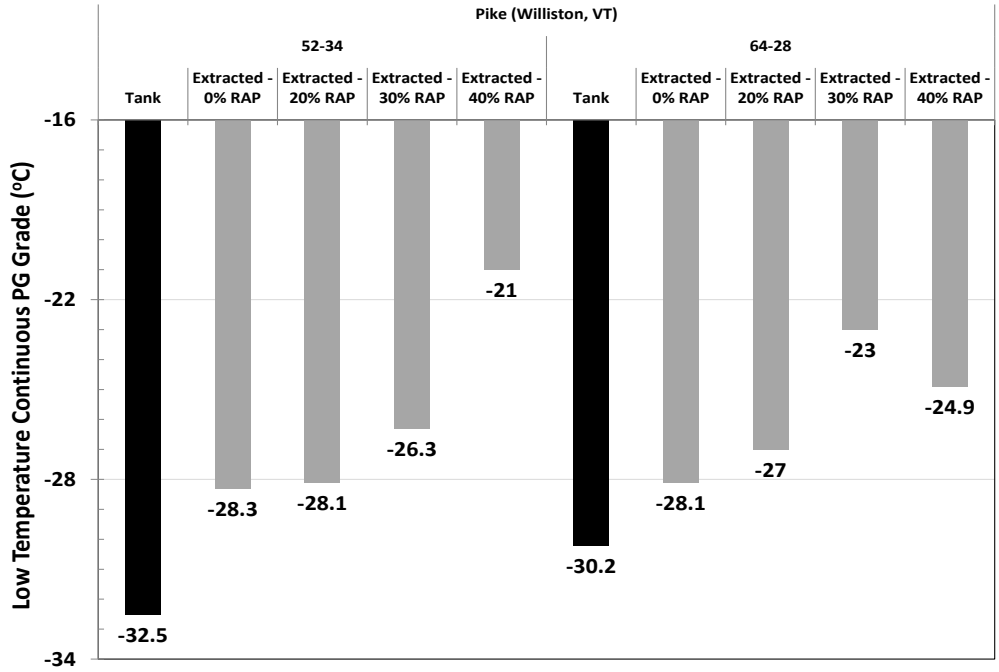

Figure 5-2 Low temperature PG grade (Williston, VT)

5.3.2 *CCT*

The low temperature critical cracking temperature was measured in accordance with AASHTO R49. The material test properties were used to evaluate different starting temperatures and cooling rates that could occur in the Northeast. It should be noted that the Critical Cracking Temperature (CCT) shown earlier in Table 5-4 is for the standard

starting temperature and cooling rate recommended in AASHTO R49 for reporting purposes.

The results of the CCT analysis are shown in Table 5-5 to Table 5-12. The tables indicate that starting temperature has little influence on the CCT of the asphalt binder. Meanwhile, the cooling rate is shown to have a significant impact on the CCT, changing it by almost a full PG grade when increasing the cooling rate from 1 ^{o}C/hr to 10 ^{o}C/hr.

The test results also show that both RAP and PG grade of the base asphalt binder have an influence on the CCT. As would be expected, as the RAP content increased, there was a warming in the CCT – indicating that the asphalt mixture would crack under warmer climate conditions. However, the test results did indicate that using a softer PG grade helped to improve the low temperature CCT, but did not result in a full PG grade improvement in the CCT.

Table 5-5 Cooling rate vs. starting temperature – Pike, VT PG52-34 0% RAP

52-34 Virgin Pike VT				
TCMODEL Critical Cracking Temperature (°C)				
Starting Temp of Cooling Event	Cooling Rate C/hr 1	Cooling Rate C/hr 2	Cooling Rate C/hr 5.6	Cooling Rate C/hr 10
10C	-33.3	-31.7	-29.3	-27.9
5C	-33.3	-31.8	-29.3	-28.0
0C	-33.3	-31.8	-29.4	-28.0
-5C	-33.4	-31.8	-29.5	-28.1

Table 5-6 Cooling rate vs. starting temperature – Pike, VT PG52-34 20% RAP

52-34 20% RAP Pike VT				
TCMODEL Critical Cracking Temperature (°C)				
Starting Temp of Cooling Event	Cooling Rate C/hr 1	Cooling Rate C/hr 2	Cooling Rate C/hr 5.6	Cooling Rate C/hr 10
10C	-31.8	-30.3	-27.9	-26.5
5C	-31.8	-30.3	-28.0	-26.6
0C	-31.9	-30.4	-28.0	-26.7
-5C	-32.0	-30.5	-28.2	-26.9

Table 5-7 Cooling rate vs. starting temperature – Pike, VT PG52-34 30% RAP

52-34 30% RAP Pike VT				
TCMODEL Critical Cracking Temperature (°C)				
Starting Temp of Cooling Event	Cooling Rate C/hr 1	Cooling Rate C/hr 2	Cooling Rate C/hr 5.6	Cooling Rate C/hr 10
10C	-32.6	-30.9	-28.2	-26.6
5C	-32.6	-30.9	-28.2	-26.7
0C	-32.7	-31.0	-28.3	-26.8
-5C	-32.8	-31.1	-28.5	-27.0

Table 5-8 Cooling rate vs. starting temperature – Pike, VT PG52-34 40% RAP

52-34 40% RAP Pike VT				
TCMODEL Critical Cracking Temperature (°C)				
Starting Temp of Cooling Event	Cooling Rate C/hr 1	Cooling Rate C/hr 2	Cooling Rate C/hr 5.6	Cooling Rate C/hr 10
10C	-28.3	-27.0	-25.0	-23.8
5C	-28.4	-27.0	-25.0	-23.8
0C	-28.4	-27.1	-25.1	-23.9
-5C	-28.5	-27.1	-25.2	-24.1

Table 5-9 Cooling rate vs. starting temperature – Pike, VT PG64-28 0% RAP

64-28 0% RAP Pike VT				
TCMODEL Critical Cracking Temperature (°C)				
Starting Temp of Cooling Event	Cooling Rate C/hr 1	Cooling Rate C/hr 2	Cooling Rate C/hr 5.6	Cooling Rate C/hr 10
10C	-26.8	-25.3	-23.0	-22.1
5C	-26.8	-25.3	-23.0	-22.1
0C	-26.9	-25.4	-23.1	-22.2
-5C	-27.0	-25.5	-23.3	-22.4

Table 5-10 Cooling rate vs. starting temperature – Pike, VT PG64-28 20% RAP

64-28 20% RAP Pike VT				
TCMODEL Critical Cracking Temperature (°C)				
Starting Temp of Cooling Event	Cooling Rate C/hr 1	Cooling Rate C/hr 2	Cooling Rate C/hr 5.6	Cooling Rate C/hr 10
10C	-27.1	-25.6	-23.3	-22.0
5C	-27.1	-25.7	-23.4	-22.1
0C	-27.2	-25.7	-23.5	-22.2
-5C	-27.3	-25.8	-23.6	-22.4

Table 5-11 Cooling rate vs. starting temperature – Pike, VT PG64-28 30% RAP

64-28 30% RAP Pike VT				
TCMODEL Critical Cracking Temperature (°C)				
Starting Temp of Cooling Event	Cooling Rate C/hr 1	Cooling Rate C/hr 2	Cooling Rate C/hr 5.6	Cooling Rate C/hr 10
10C	-25.0	-23.5	-21.2	-19.8
5C	-25.1	-23.6	-21.3	-20.0
0C	-25.2	-23.7	-21.4	-20.1
-5C	-25.3	-23.9	-21.7	-20.5

Table 5-12 Cooling rate vs. starting temperature – Pike, VT PG64-28 40% RAP

64-28 40% RAP Pike VT				
TCMODEL Critical Cracking Temperature (°C)				
Starting Temp of Cooling Event	Cooling Rate C/hr 1	Cooling Rate C/hr 2	Cooling Rate C/hr 5.6	Cooling Rate C/hr 10
10C	-26.4	-24.9	-22.6	-21.3
5C	-26.4	-25.0	-22.7	-21.4
0C	-26.5	-25.1	-22.8	-21.6
-5C	-26.6	-25.2	-23.1	-21.9

5.3.3 *Asphalt Binder Master Stiffness Curves*

The asphalt binder master curves, constructed using the asphalt binder extracted and recovered from the plant-compacted specimens, are shown in Figure 5-3 (PG52-34 base asphalt binder) and Figure 5-4 (PG64-28 base asphalt binder). As the RAP content increases, the stiffness of the extracted/recovered asphalt binders increases, especially at the higher test temperatures (lower loading frequencies).

The impact of asphalt binder grade was also compared using the data from the 30 and 40% RAP mixtures. The results are shown in Figure 5-5 and Figure 5-6. There does not appear to be a significant difference between the recovered/extracted binders from the mixtures with the different base binder grades at these RAP contents. The exact reason for this behavior is unknown, but may be due to a combination of production factors such as temperatures and moisture, the relatively soft RAP that was used for these mixtures, and the higher asphalt contents overall.

Figure 5-3 shows the Rheological Index (R) – Crossover Frequency (ω_o) Space for the asphalt binders; the test results indicate that as RAP content increases, the asphalt binder behavior is that of a progressively aging asphalt binder. This is true for both the PG 64-28 and PG 52-34 asphalt binders. The extracted and recovered asphalt binders were also evaluated using Rowe's Black Space analysis and are shown in Figure 5-4. The test results indicate that asphalt mixtures containing more than 20% RAP would be prone to cracking and that the softer PG binder has a larger effect at the lower RAP contents.

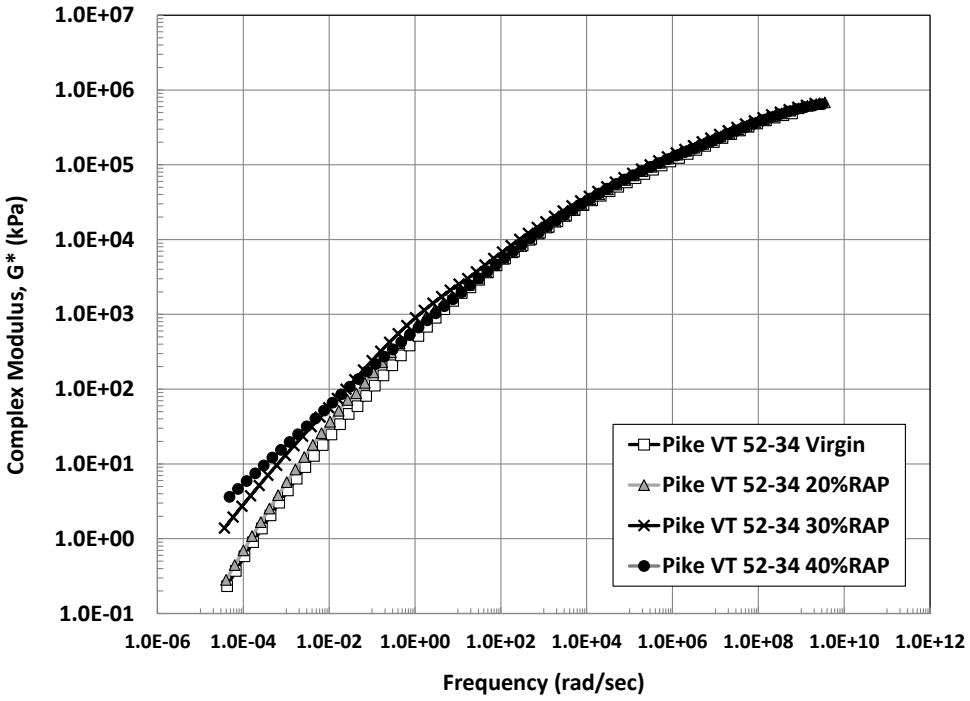

Figure 5-3 Asphalt binder master curves for Vermont mixtures with PG 52-34 base asphalt binder

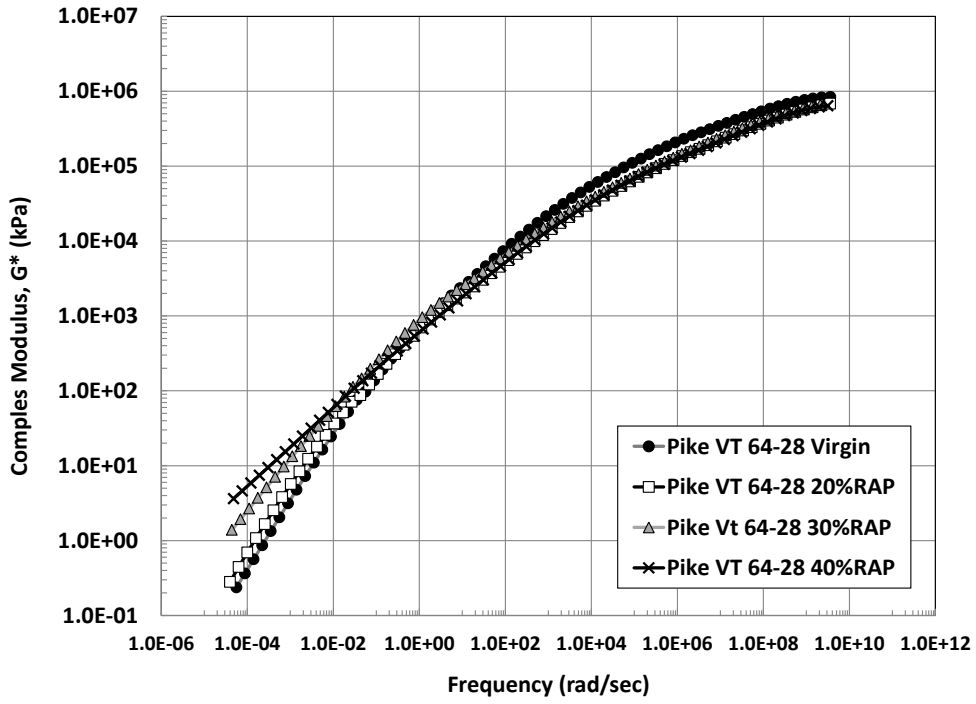

Figure 5-4 Asphalt binder master curves for Vermont mixtures with PG 64-28 base asphalt binder

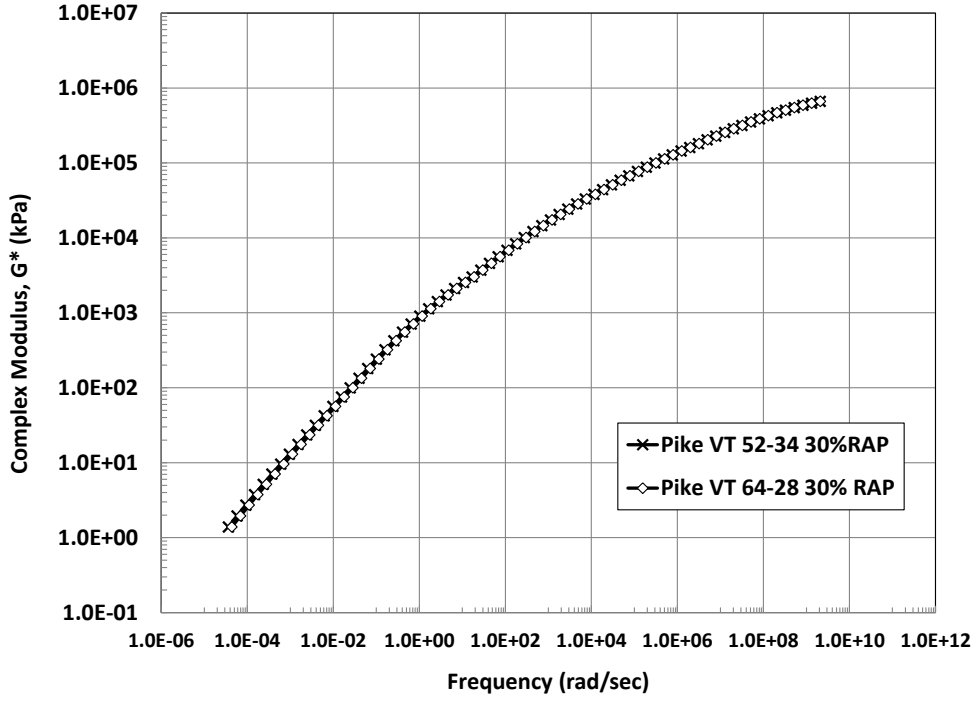

Figure 5-5 Asphalt binder master curves for Vermont mixtures with 30% RAP

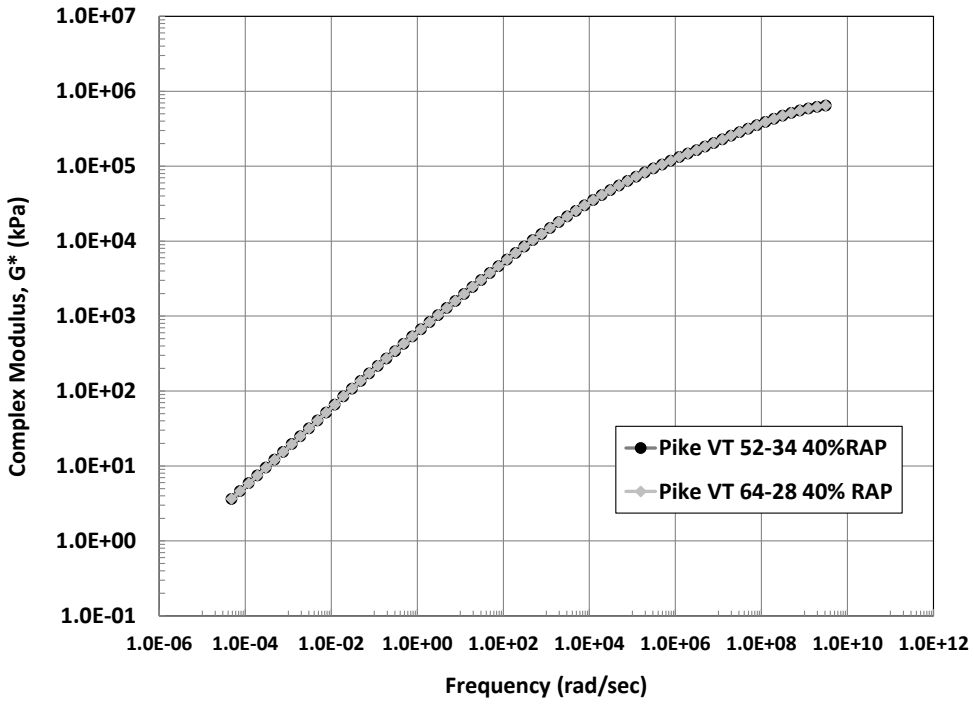

Figure 5-6 Asphalt binder master curves for Vermont mixtures with 40% RAP

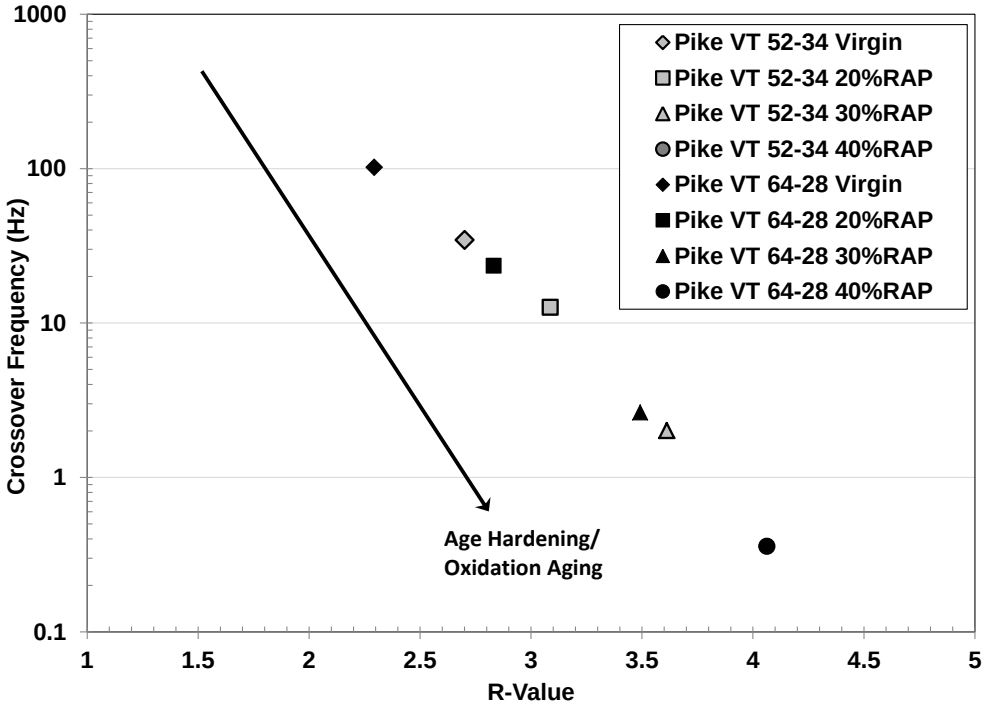

Figure 5-7 Rheological index – crossover frequency space for asphalt binder extracted/recovered from Vermont mixtures

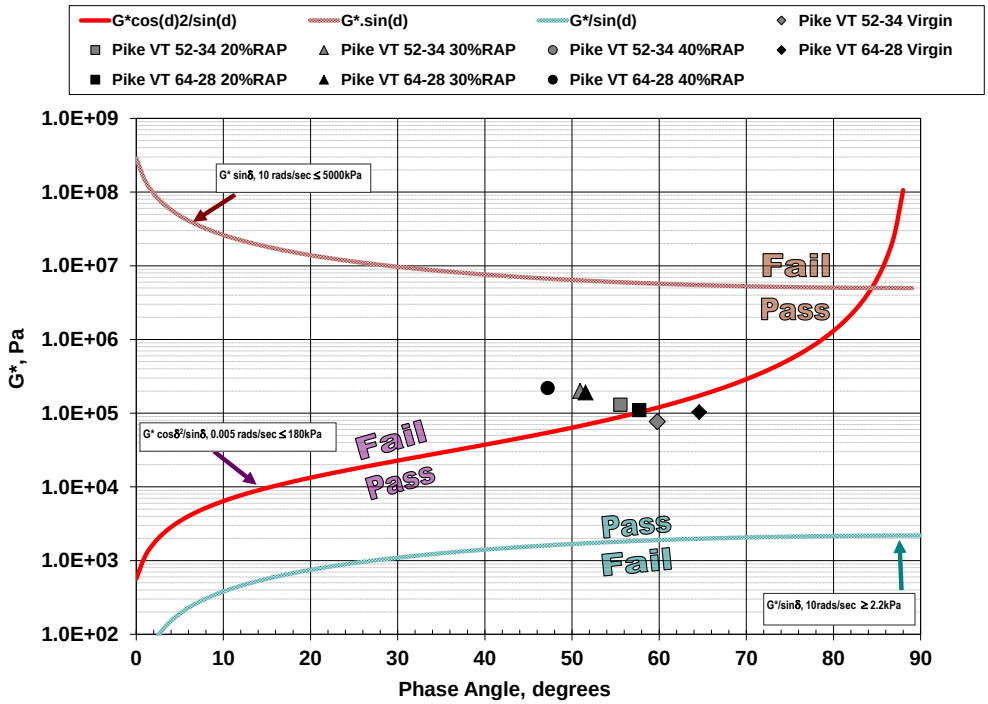

Figure 5-8 Rowe's black space analysis for asphalt binder extracted/recovered from Vermont mixtures

5.4 Mixture Testing

5.4.1 *Dynamic Modulus*

The dynamic modulus properties of the asphalt mixtures were determined in accordance to AASHTO TP79. Two sets of test specimens were prepared for evaluation; 1) Test specimens compacted at the asphalt plant and 2) Test specimens produced by reheating loose mix at the laboratory and then compacting the test specimens.

5.4.1.1 Plant Compacted Mixtures

The dynamic modulus (E*) test results for the Vermont RAP mixtures, compacted at the asphalt plant, are shown in Figure 1 and Figure 2 for the PG 52-34 and PG 64-28 base PG binders, respectively. The master stiffness curves for both mixtures show that as RAP content increases, the mixture stiffness increases. However, the PG 64-28 VT mixtures show very little increase in stiffness with RAP content, especially at higher frequencies, as compared to the other sets of mixtures (NH and NY) evaluated in this project. This may be due to a combination of mixture properties (finer gradation, higher asphalt content, softer RAP) and production parameters (batch plant, moisture in mix). Figure 5-11 through Figure 5-14 show a comparison of the different PG base binder grades for each RAP

content. The softer binder grade produces a lower dynamic modulus, but the difference decreases with increasing RAP contents.

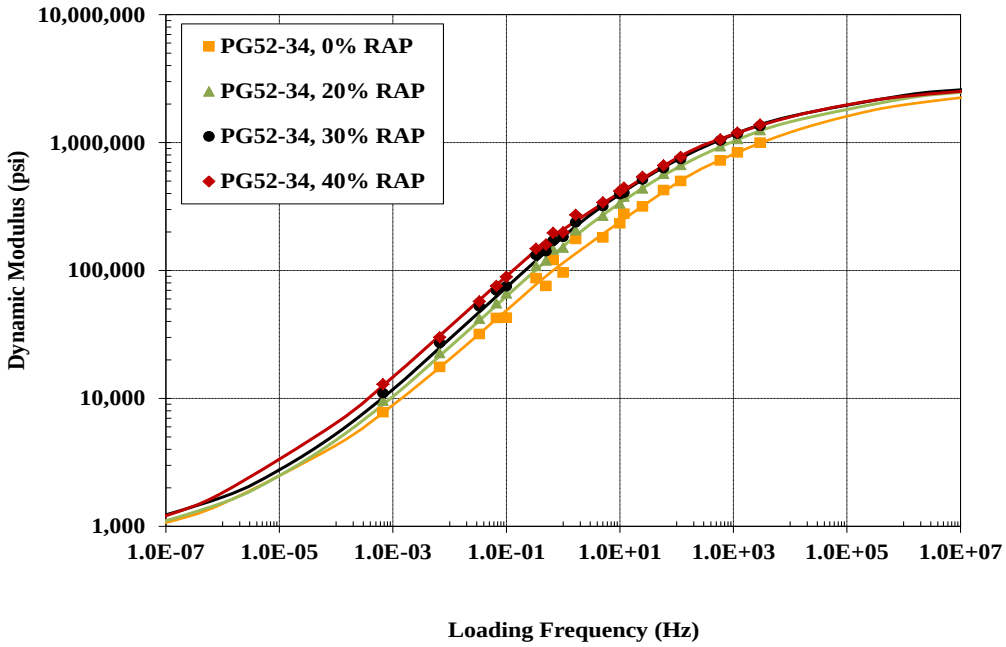

Figure 5-9 Dynamic modulus master curves for Vermont mixtures (PG52-34 base PG grade) – plant compacted

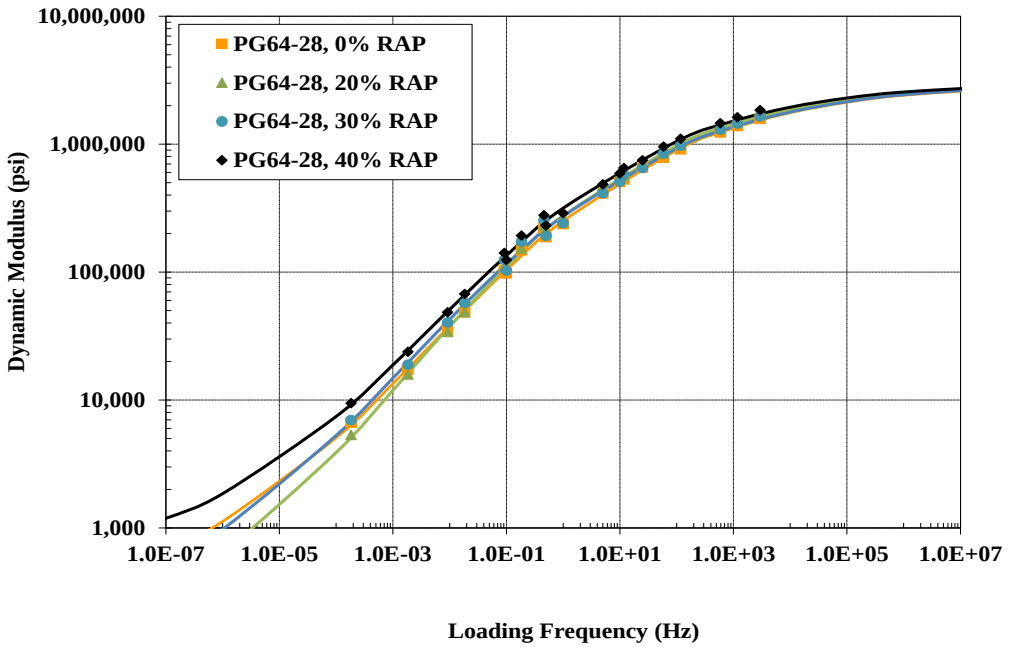

Figure 5-10 Dynamic modulus master curves for Vermont mixtures (PG64-28 base PG grade) – plant compacted

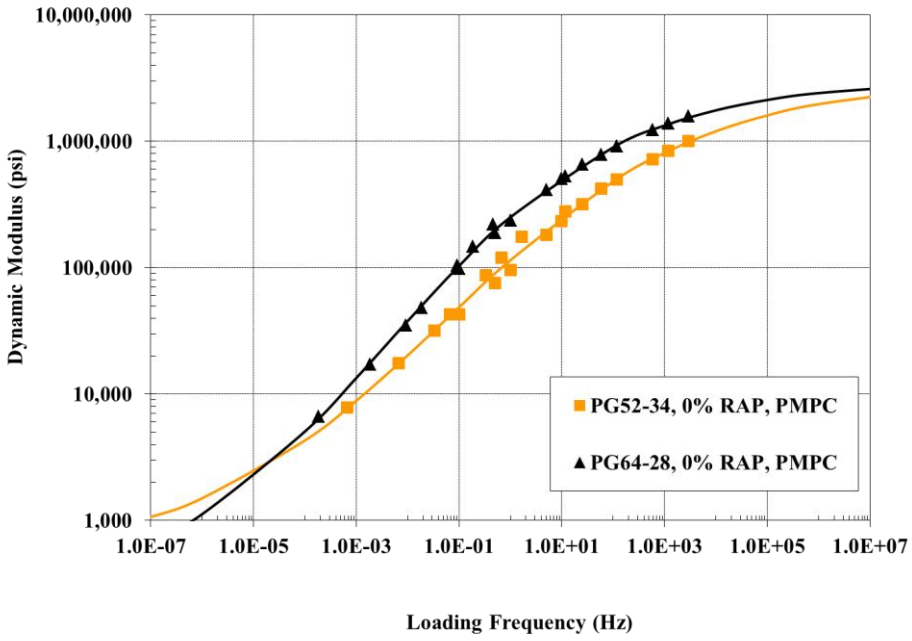

Figure 5-11 Dynamic modulus master curves for Vermont 0% RAP mixtures – plant compacted

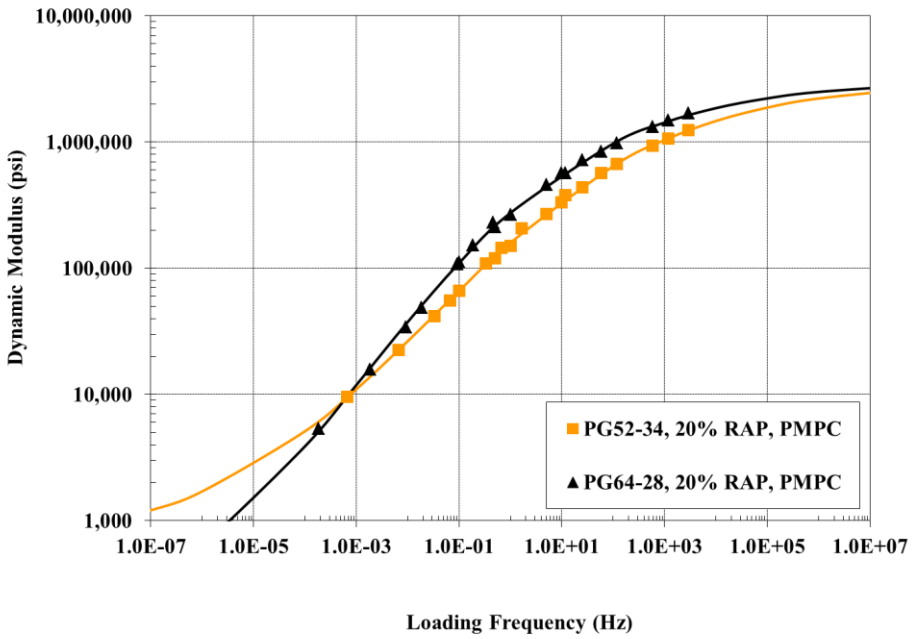

Figure 5-12 Dynamic modulus master curves for Vermont 20% RAP mixtures – plant compacted

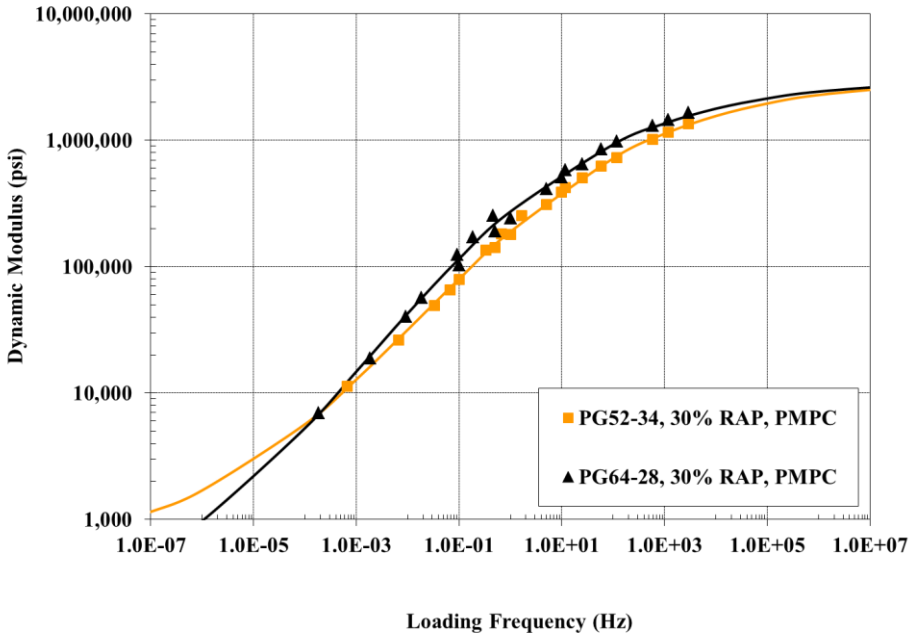

Figure 5-13 Dynamic modulus master curves for Vermont 30% RAP mixtures – plant compacted

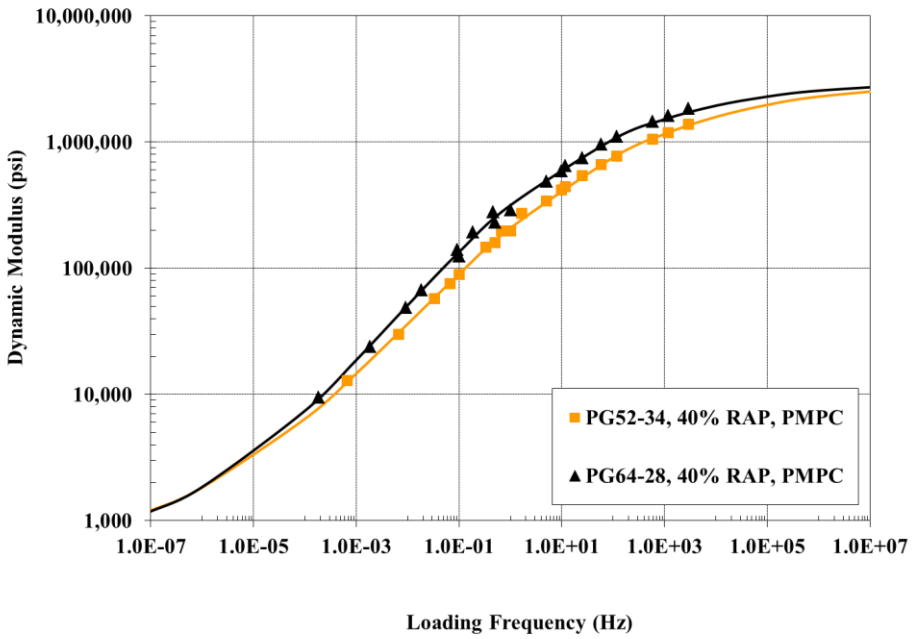

Figure 5-14 Dynamic modulus master curves for Vermont 40% RAP mixtures – plant compacted

5.4.1.2 Reheated Loose Mix and Compacted Mixtures

The identical mixtures were tested after the sampled loose mix was reheated and compacted following the test method developed by the Pooled Fund Research Team. The resultant master curves are shown in Figure 5-15 and Figure 5-16 for the PG 52-34 and PG 64-28 base PG binders, respectively. The PG 52-34 RAP mixtures were all very similar in stiffness, with the virgin mix showing a softer response. The PG 64-28 mixtures show very little difference at all among the virgin and RAP mixtures. Figure 5-17 through Figure 5-20 show the comparison of the two PG grades for the various RAP contents. Larger differences are observed with lower RAP content.

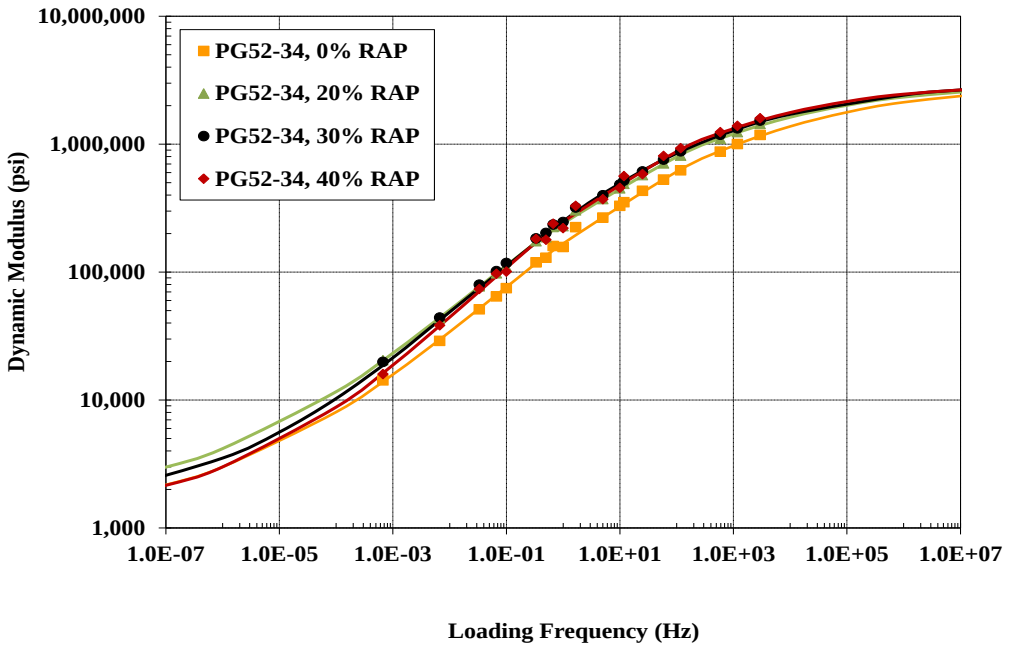

Figure 5-15 Dynamic modulus master curves for Vermont mixtures (PG52-34 base PG grade) – reheated loose mix

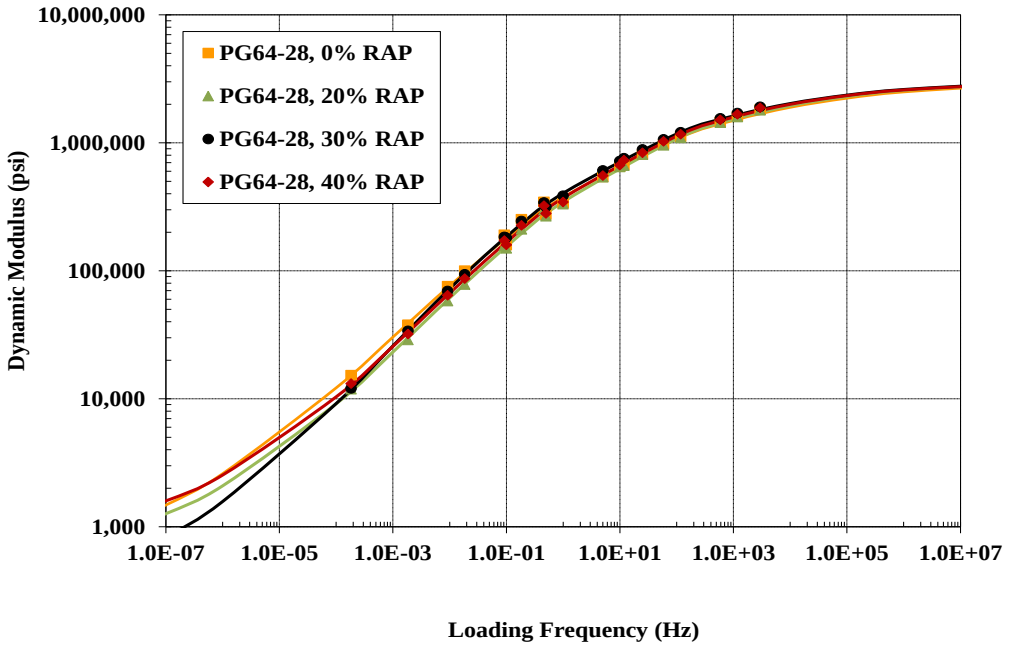

Figure 5-16 Dynamic modulus master curves for Vermont mixtures (PG64-28 base PG grade) – reheated loose mix

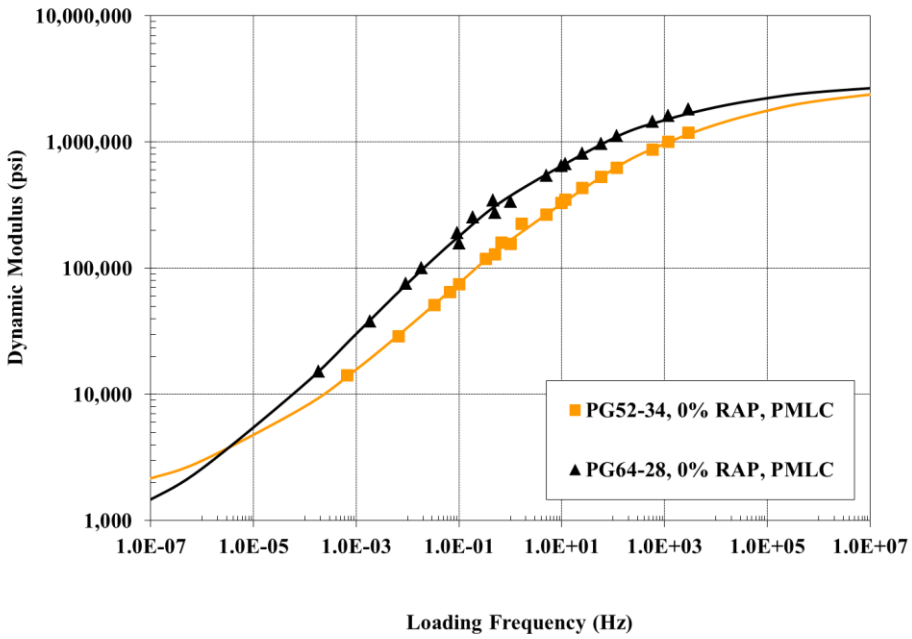

Figure 5-17 Dynamic modulus master curves for Vermont 0% RAP mixtures – reheated loose mix

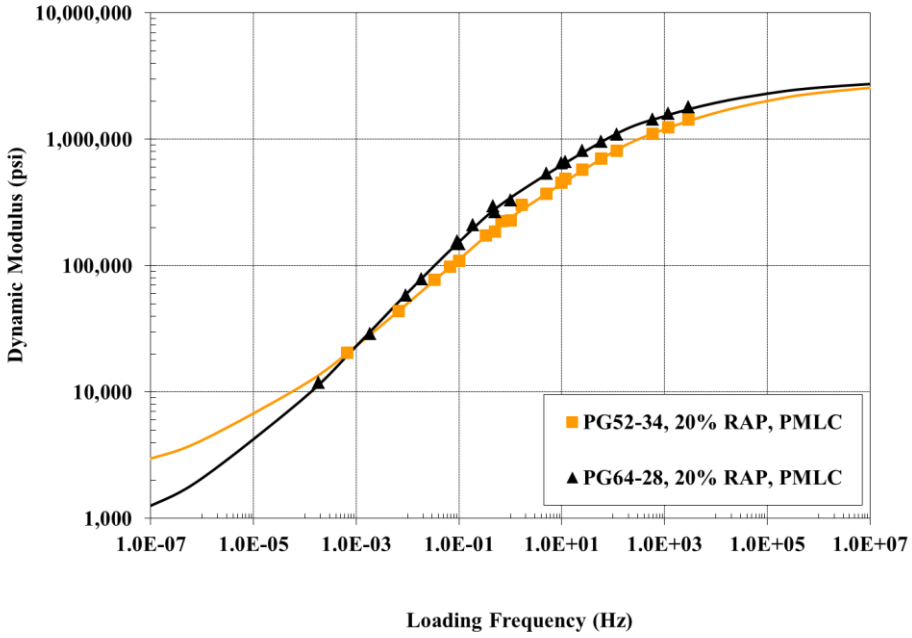

Figure 5-18 Dynamic modulus master curves for Vermont 20% RAP mixtures – reheated loose mix

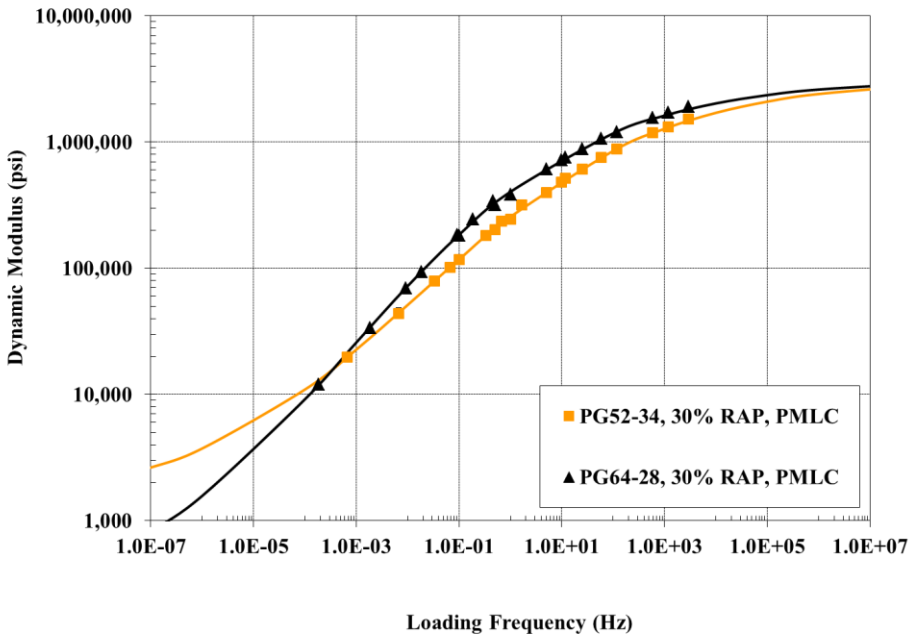

Figure 5-19 Dynamic modulus master curves for Vermont 30% RAP mixtures – reheated loose mix

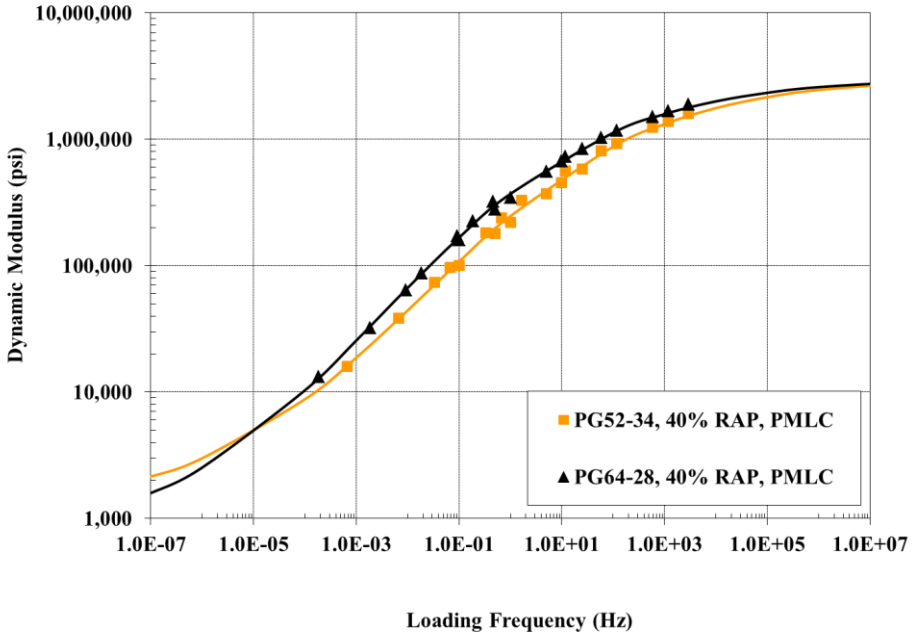

Figure 5-20 Dynamic modulus master curves for Vermont 40% RAP mixtures – reheated loose mix

5.4.1.3 Comparison of Plant Compacted and Reheated Loose Mix Specimens

The testing of the two different specimen types allowed for an evaluation of how the stiffness of the mixtures may change due to the reheating of loose mix in the laboratory. Figure 5-21 through Figure 5-23 show the relative change in stiffness using the ratio (E* Ratio) between the reheated loose mix and the plant compacted specimens for the PG 52-34 asphalt binder mixtures. The E* ratio indicates that little to no change occurs at the 4.4°C test temperature. However, as the test temperature increases, a clear increase in the stiffness occurs in the reheated loose mix specimens. An approximate 50% increase occurs at the 20°C test temperature while the stiffness of the reheated loose mix samples doubles at the 35°C test temperature. The increase in the E* ratio is also more prevalent in the 0% and 20% RAP mixtures, which is an indication that the mixtures with the greater amounts of virgin liquid binder are undergoing more oxidative aging during the reheating process than the mixtures with a greater amount of RAP – which already contains oxidized asphalt binder.

Figure 5-24 through Figure 5-26 show the E* ratio analysis for the PG 64-28 mixtures. A very similar trend occurs with the different RAP contents, although for the PG 64-28 asphalt binder mixtures, the 30% RAP mixture also is showing a relatively high amount of aging during the reheating process, which may be due to the lower asphalt content in the mixture.

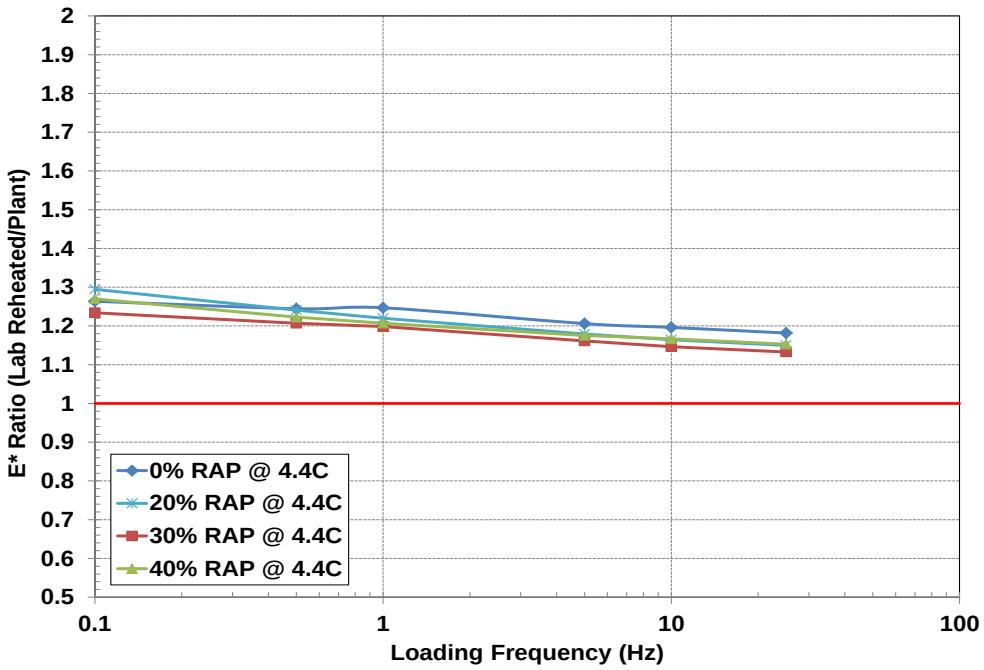

Figure 5-21 Dynamic modulus ratio (E* ratio) at 4.4°C – PG52-34 mixtures

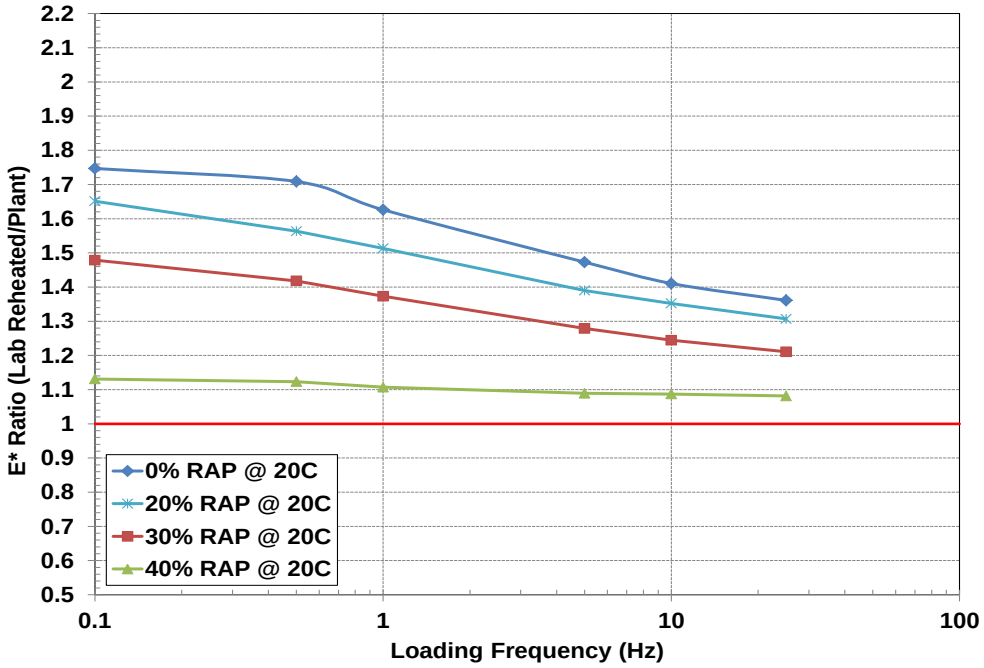

Figure 5-22 Dynamic modulus ratio (E* ratio) at 20ºC – PG52-34 mixtures

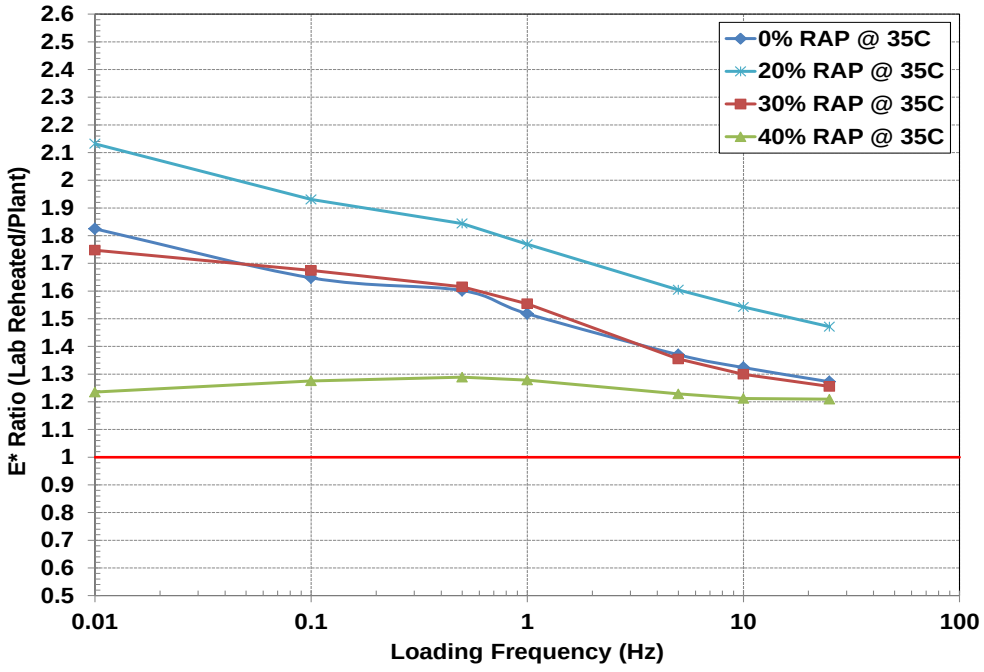

Figure 5-23 Dynamic modulus ratio (E* ratio) at 35ºC – PG52-34 mixtures

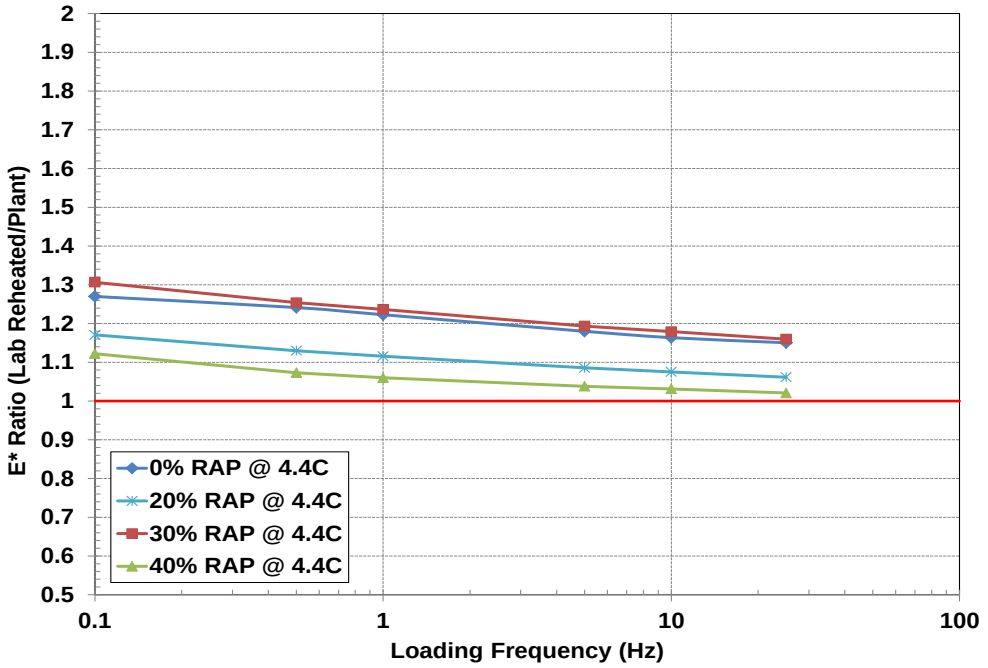

Figure 5-24 Dynamic modulus ratio (E* ratio) at 4.4ºC – PG64-28 mixtures

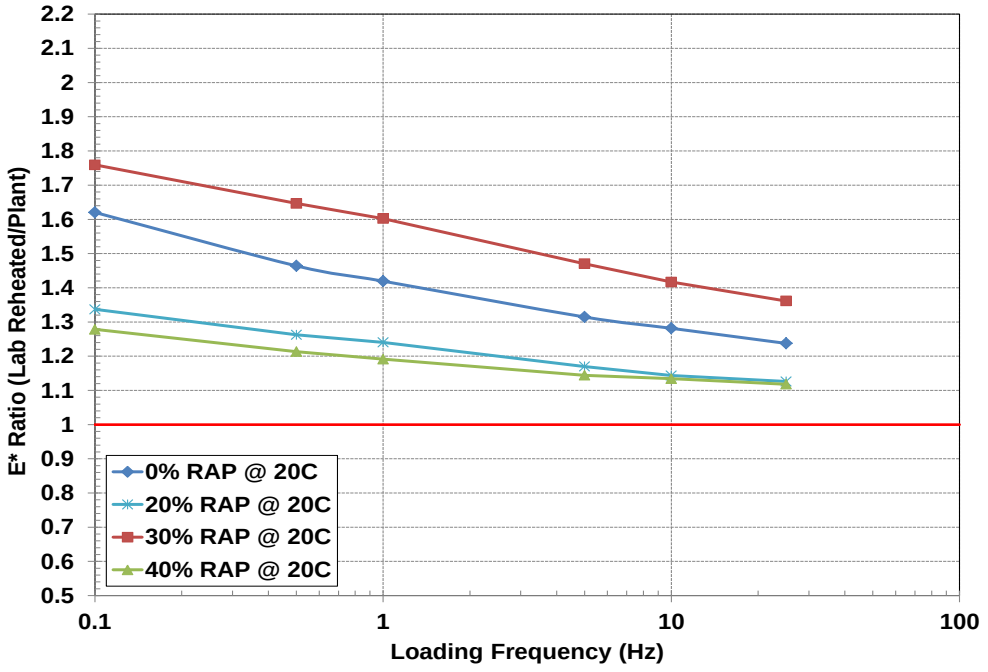

Figure 5-25 Dynamic modulus ratio (E* ratio) at 20ºC – PG64-28 mixtures

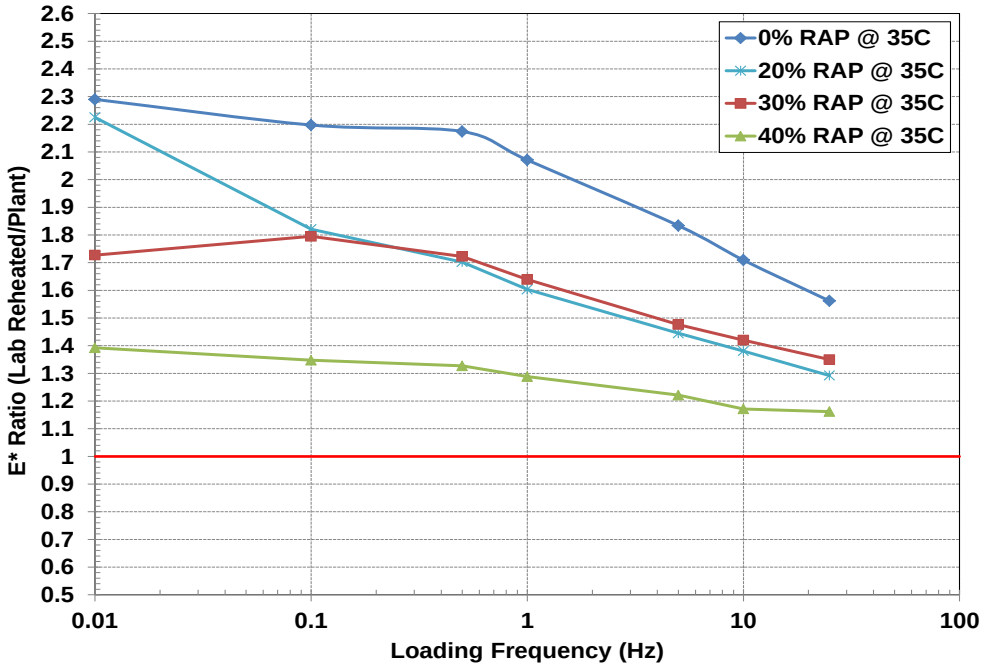

Figure 5-26 Dynamic modulus ratio (E* ratio) at 35ºC – PG64-28 mixtures

5.4.2 *Fatigue*

Fatigue behavior of the mixtures was evaluated using three different tests: S-VECD and beam fatigue to evaluate crack initiation and the overlay tester to evaluate crack propagation.

5.4.2.1 SVECD

S-VECD testing of the VT PG 64-28 mixtures was conducted under multiple modes of loading and multiple temperatures. All the PG 64-28 mixtures were tested in CX mode at 7°C, 13°C and 20°C and 10 Hz. Also, the PG 64-28 0% and 30% RAP mixtures were tested in on-specimen strain-controlled mode at 13°C and 10 Hz. Finally, the PG 64-28 30% RAP mixture was tested in stress-controlled mode at 13°C and 10 Hz.

Table 5-13 presents the VECD model parameters at different temperatures using the exponential form (Equation 2.2). This table shows that, for all the PG 64-28 mixtures, pseudo stiffness at failure, C_F, is around 0.25 at 7°C and 13°C. This value drops to around 0.15 once the temperature increases to 20°C. This drop is due to the material being more ductile at higher temperatures, so the failure happens at a lower C_F value.

Table 5-13 Parameters for VECD model for VT PG 64-28 mixtures

Mix Type	Alpha	Temp (°C)	a	b	C_F
VT PG 52-34 0% RAP	4.64	13	-0.00040878	0.6374	0.16
VT PG 52-34 20% RAP	4.05	13	-0.00057296	0.6152	0.17
VT PG 52-34 30% RAP	4.19	13	-0.00036720	0.6437	0.21
VT PG 52-34 40% RAP	4.25	13	-0.00076187	0.5809	0.20
VT PG 64-28 0% RAP	4.31	7	-0.00004677	0.7903	0.24
		13	-0.00021314	0.6768	0.24
		20	-0.00072424	0.5981	0.15
VT PG 64-28 20% RAP	4.06	7	-0.00004677	0.7903	0.24
		13	-0.00017425	0.6921	0.23
		20	-0.00072424	0.5981	0.17
VT PG 64-28 30% RAP	4.08	7	-0.00008036	0.7513	0.22
		13	-0.00054682	0.5951	0.25
		20	-0.00094639	0.5657	0.16
VT PG 64-28 40% RAP	4.00	7	-0.00010437	0.7273	0.27
		13	-0.00022793	0.6691	0.24
		20	-0.00052863	0.6206	0.13

Figure 5-27 shows the fitted curves at 7C for all of the VT mixtures on the same graph. The mixtures with the same virgin binder grade are clustered together with similar damage characteristic curves. The curves for the PG 64-28 mixtures (VTe) are above those for the PG 52-34 (VTa) mixtures.

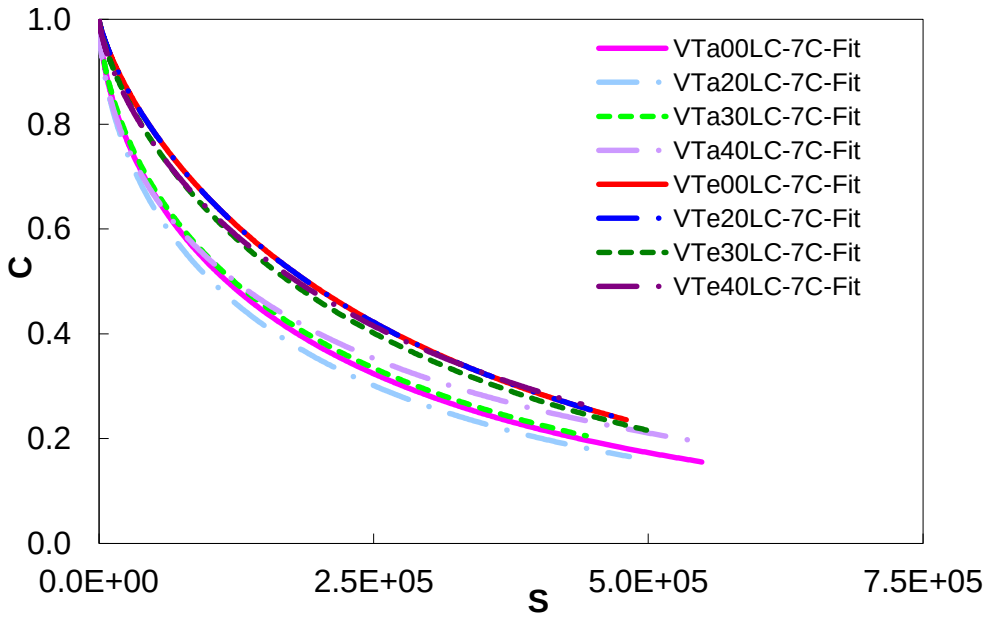

Figure 5-27 Fitted results for CX testing for all VT mixtures at 7°C

Figure 5-28 shows the fitted curves for the VT PG 64-28 20% RAP mixture at different temperatures on the same graph. This graph shows that, as the temperature increases, the C versus S fitted curve position lowers slightly; this observation may be due to the effect of higher viscoplasticity at higher temperatures. This trend is observed with the other VT mixtures as well.

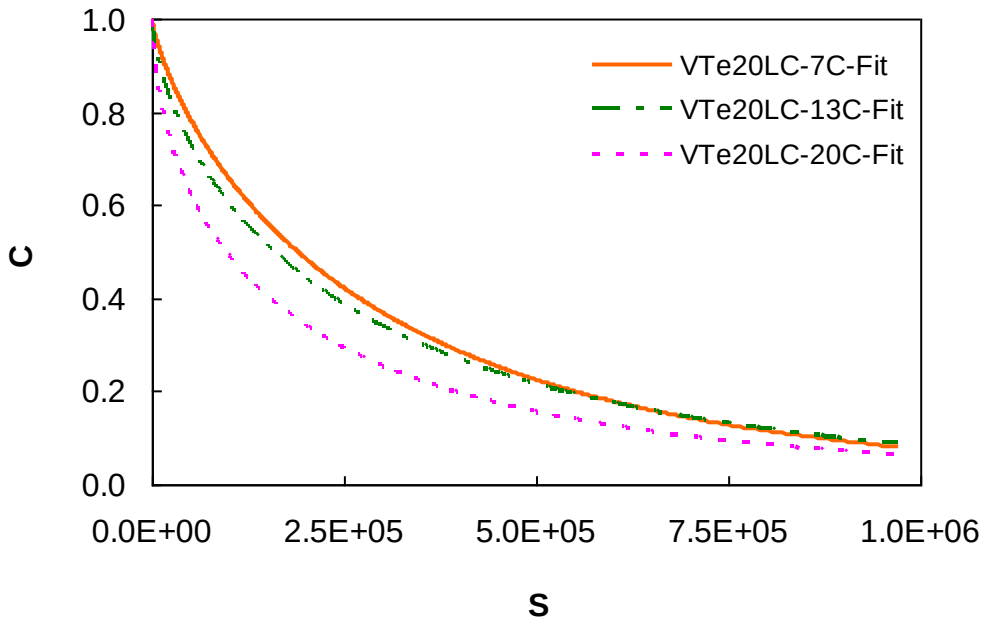

Figure 5-28 Fitted results for CX testing for VT PG 64-28 20% RAP mixture at different temperatures

Figure 5-29 and Figure 5-30 show the individual results for fatigue testing on the VT PG 64-28 0% RAP and VT PG 64-28 30% RAP mixtures in the COS mode of loading at 13°C, respectively, and Figure 5-31 shows the individual results for fatigue testing on the VT PG 64-28 30% RAP mixture in CS mode of loading at 13°C. These graphs demonstrate that the C vs S curves for the different modes of loading show good repeatability, indicating that the SVECD methodology is appropriate for the RAP mixtures. The CX mode of loading will be the primary mode used for further analysis.

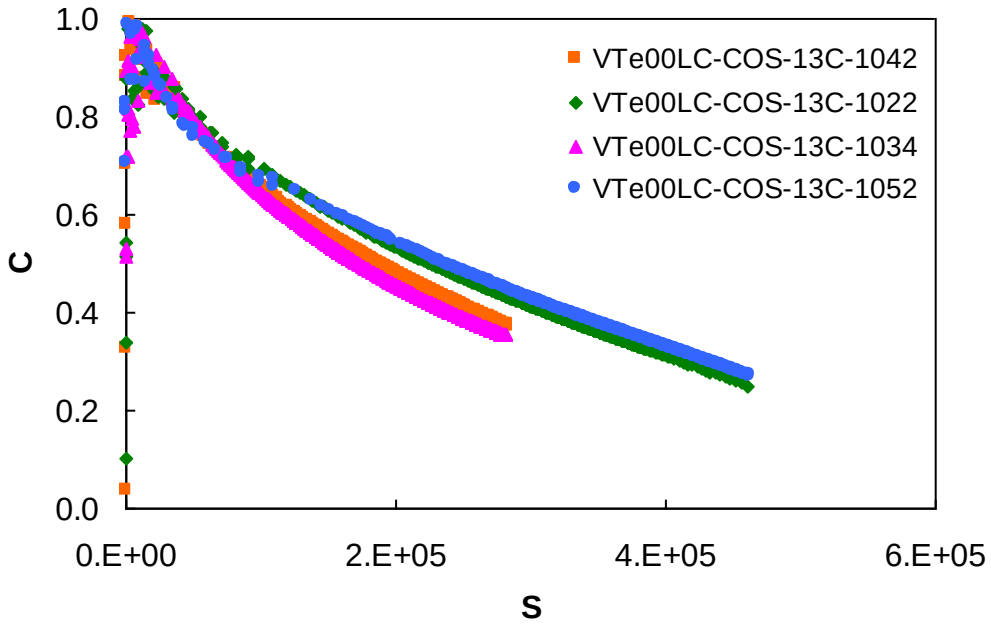

Figure 5-29 Individual results for COS testing for VT PG 64-28 0% RAP mixture at 13°C

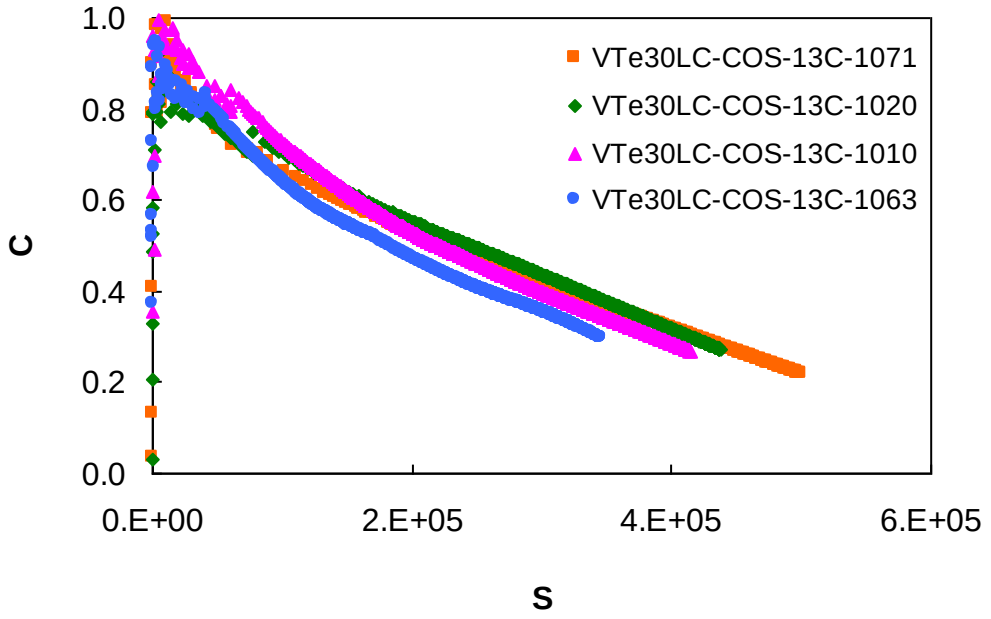

Figure 5-30 Individual results for COS testing for VT PG 64-28 30% RAP mixture at 13°C

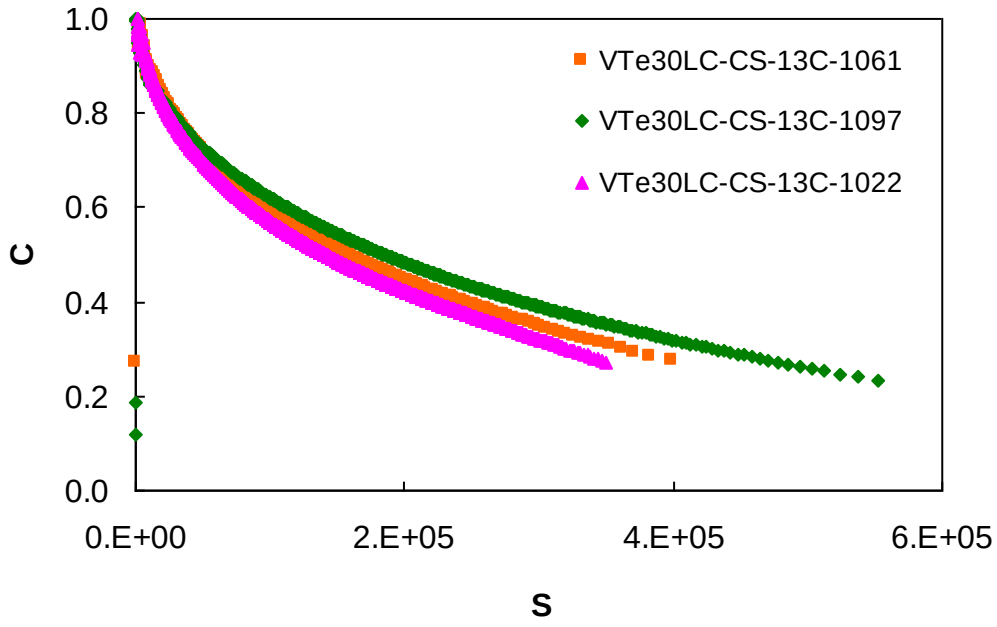

Figure 5-31 Individual results for CS testing for VT PG 64-28 30% mixture at 13°C

Figure 5-32 through Figure 5-34 show the fitted curves for the different VT PG 64-28 mixtures at 7°C, 13°C, and 20°C, respectively. The performance of all the RAP mixtures is very similar, with the 30% RAP mixture showing a slightly higher curve at the warmer temperatures.

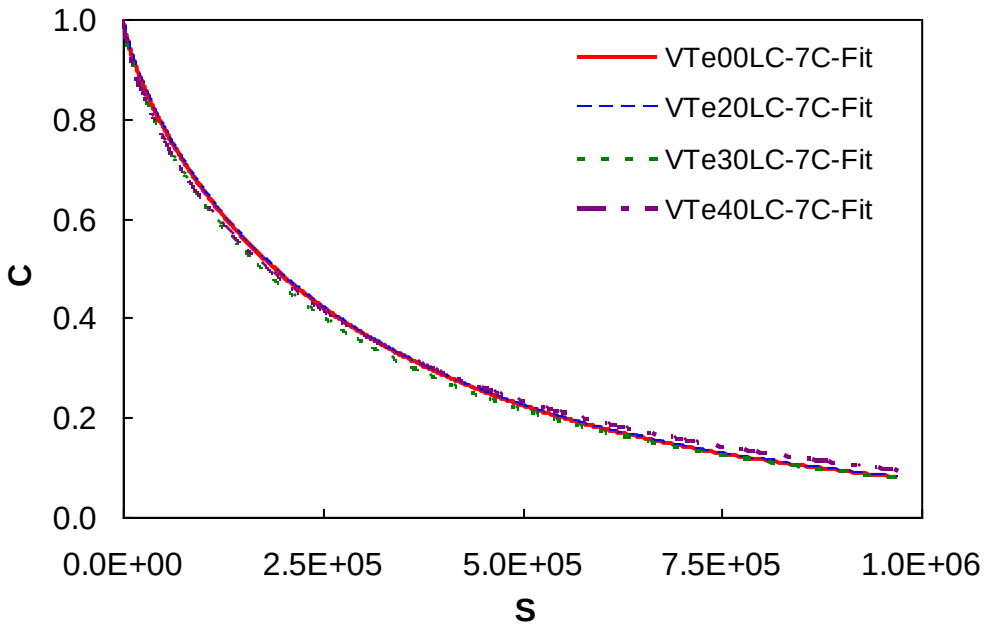

Figure 5-32 Fitted results for CX testing for VT PG 64-28 mixtures at 7°C

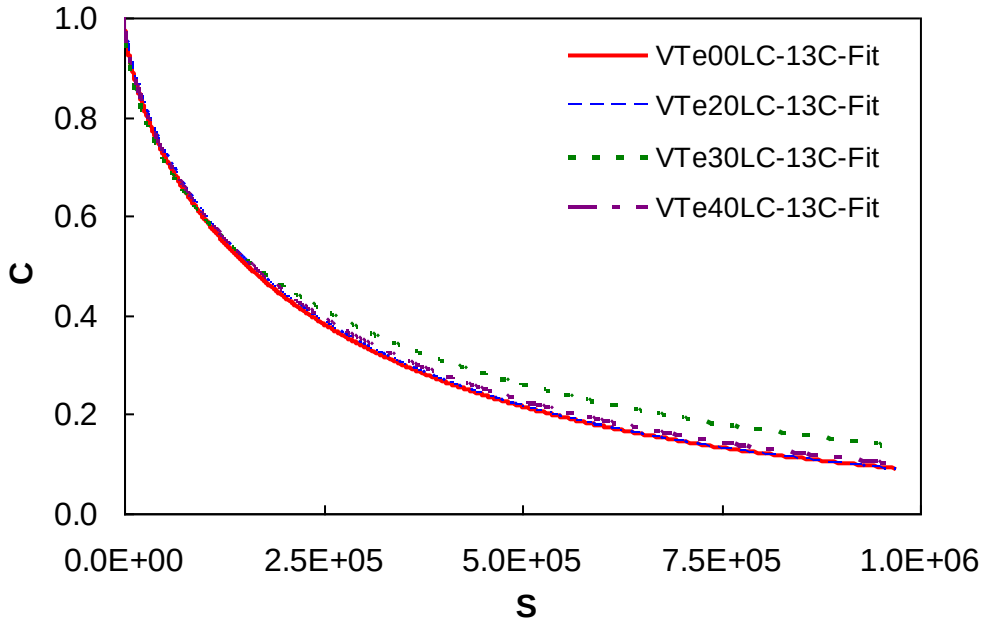

Figure 5-33 Fitted results for CX testing for VT PG 64-28 mixtures at 13°C

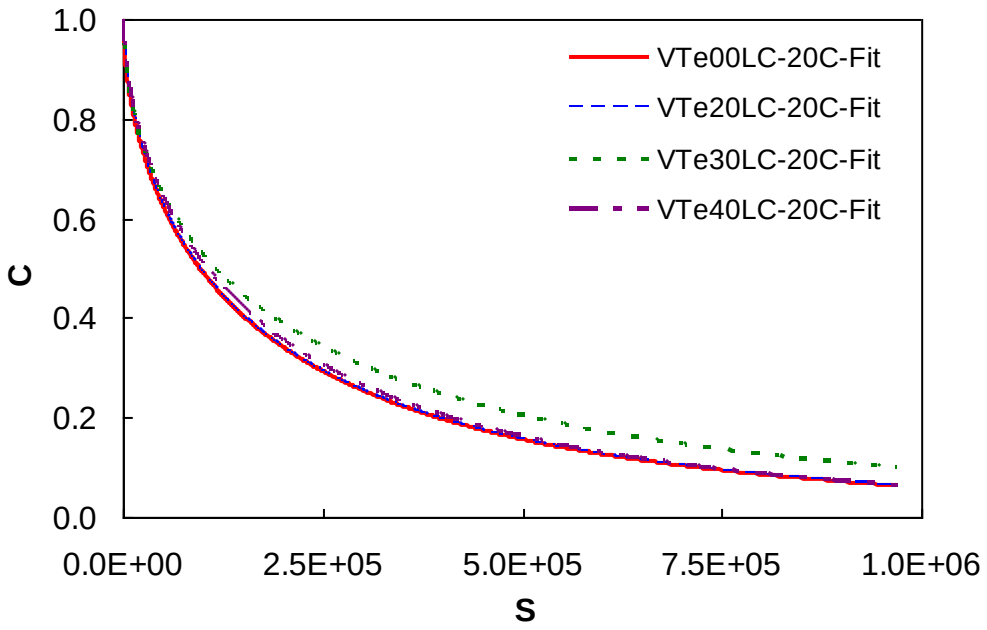

Figure 5-34 Fitted results for CX testing for VT PG 64-28 mixtures at 20°C

The S-VECD failure criterion applied to the VT PG 52-34 and VT PG 64-28 mixtures is shown in Figure 5-35 and Figure 5-36, respectively. The VT PG 52-34 virgin mixture shows the best performance, followed by the 20% PG 52-34 mixture. The 30% RAP and 40% RAP VT PG 52-34 mixtures are very similar. The characteristic relationships for the four VT PG 64-28 mixtures do not seem to have any significant differences, which suggest that incorporating RAP into the VT PG 64-28 mixtures does not affect their fatigue resistance. Figure 5-37 through Figure 5-40 show the impact of the different PG binder grade at the different RAP contents. As the RAP content increases, the impact of the PG grade binder decreases and the performance of the mixtures with the different binders become more similar, likely due to the increased amount of recycled material.

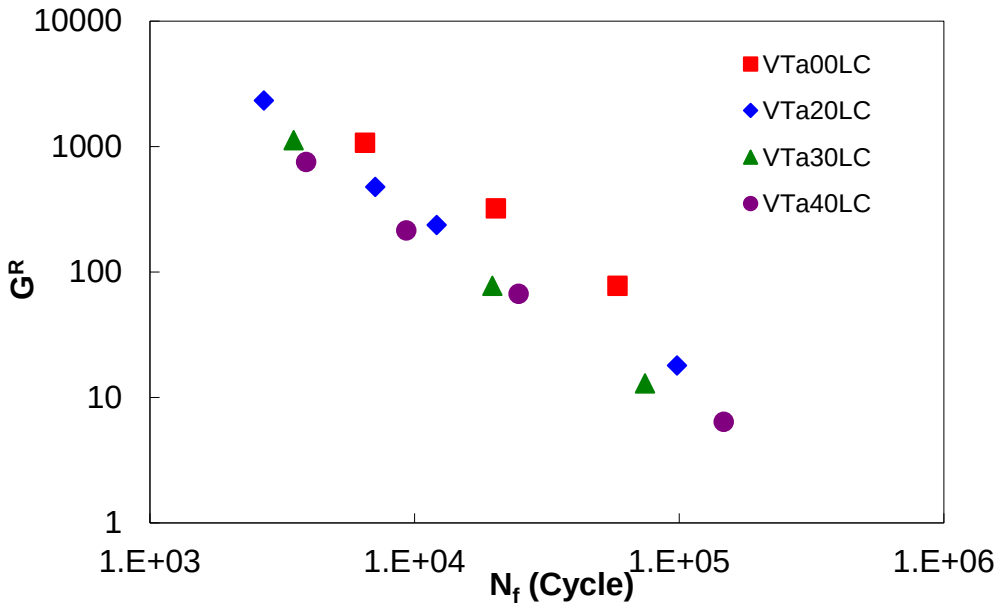

Figure 5-35 Fatigue Failure Criterion for VT PG 58-34 mixtures at 13ºC

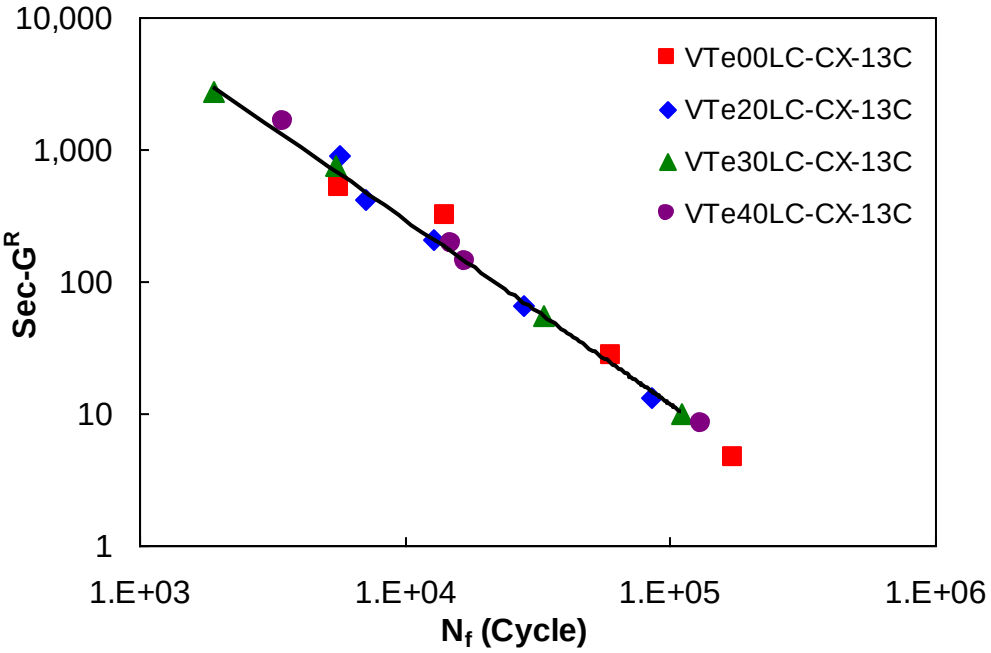

Figure 5-36 Fatigue failure criterion for VT PG 64-28 mixtures at 13°C

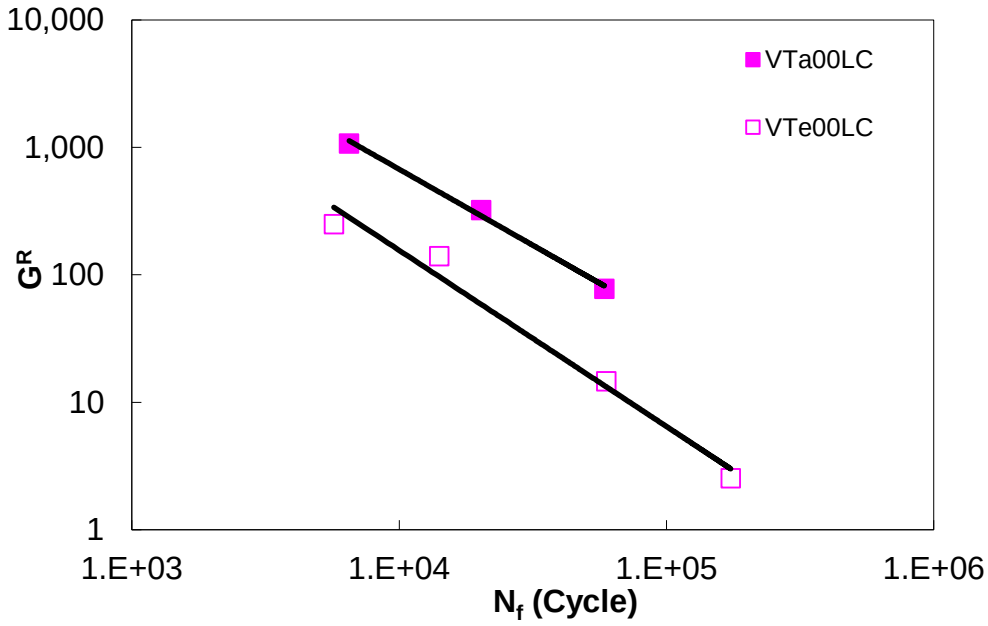

Figure 5-37 Fatigue failure criterion for VT virgin mixtures

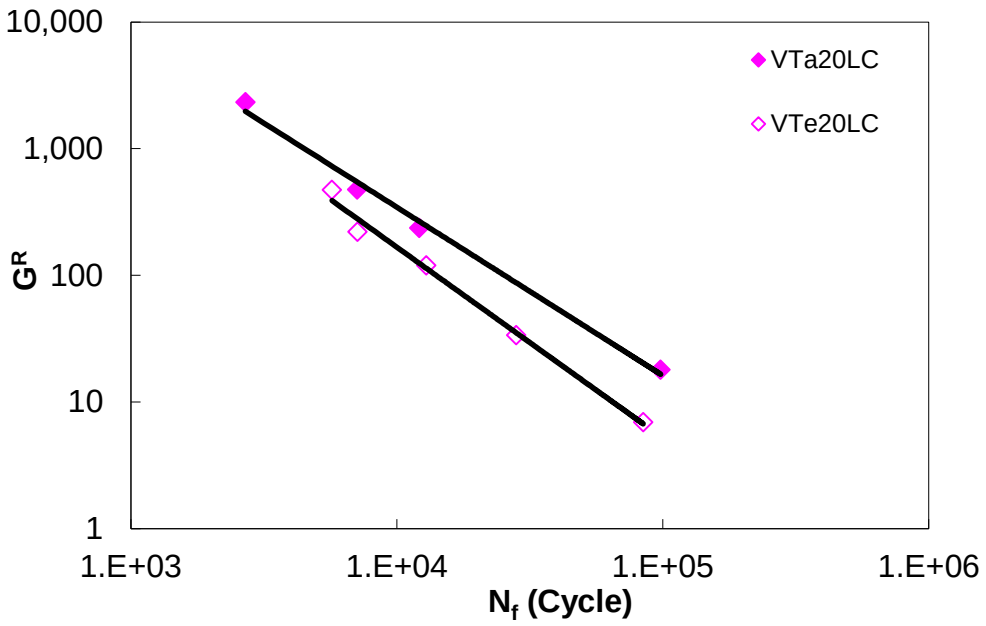

Figure 5-38 Fatigue failure criterion for VT 20% RAP Mixtures

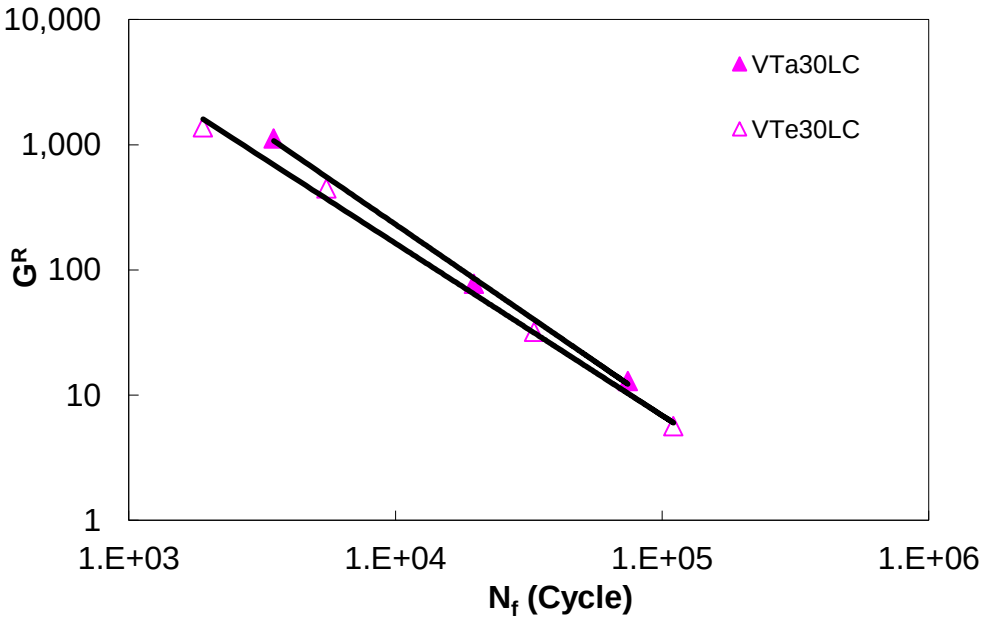

Figure 5-39 Fatigue failure criterion for VT 30% RAP mixtures

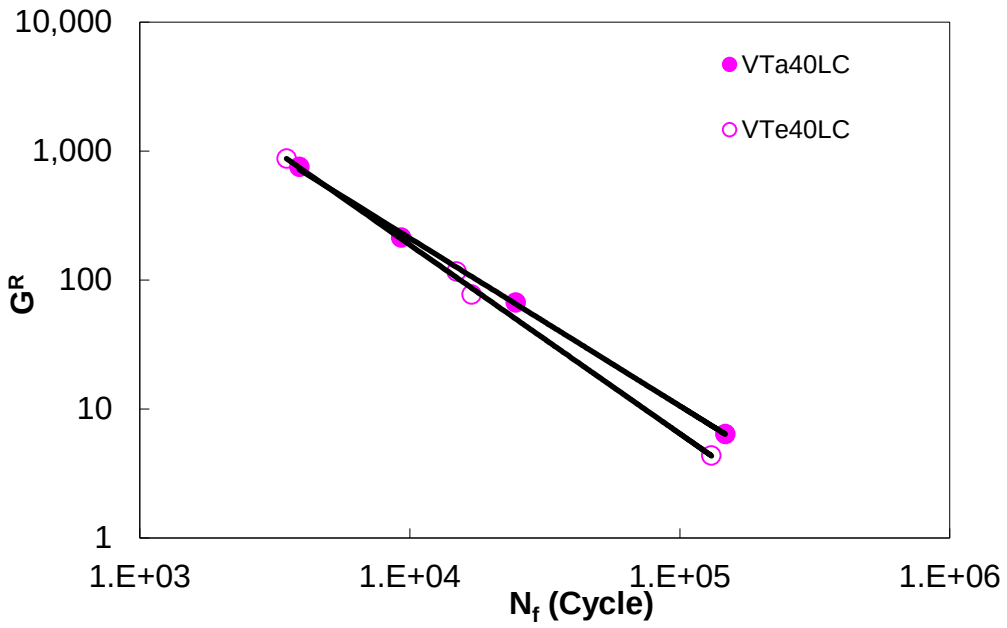

Figure 5-40 Fatigue failure criterion for VT 40% RAP mixtures

Figure 5-41 shows the results of the constant strain fatigue simulations for all of the VT mixtures. The virgin PG 52-34 mixture shows the best performance and the addition of RAP decreases the fatigue resistance of the PG 52-34 mixtures, with the 30% RAP and 40% RAP mixtures having similar performance. The PG 64-28 mixtures have lower fatigue resistance, with the virgin mixture showing the worst performance. However, there are significant differences in the binder contents of these mixtures that partially explains the difference in the results.

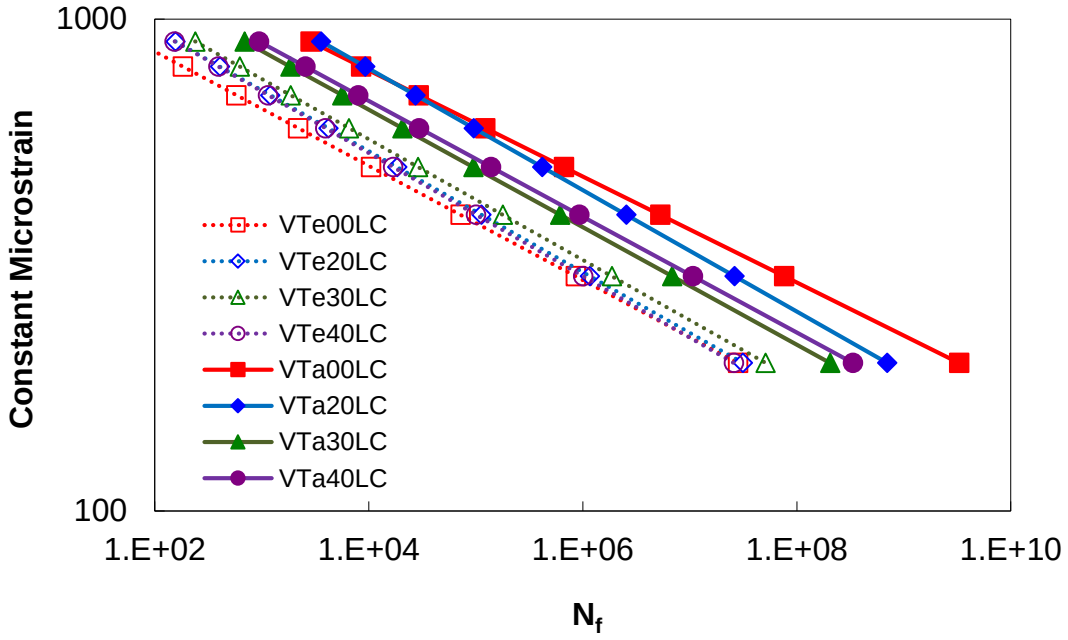

Figure 5-41 Strain-controlled direct tension fatigue simulation results for all VT mixtures

5.4.2.2 Beam

The beam fatigue testing was done according to AASHTO T321, but due to material limitations, only one replicate per strain level was performed. The test results for the VT PG 52-34 and PG 64-28 mixtures are shown in Figure 5-42 and Figure 5-43, respectively. The flexural fatigue results in Figure 5-42 indicate that the PG 52-34 20% RAP mixture performed the worst out of the three mixtures evaluated, while the PG 52-34 0% RAP and 30% RAP mixtures performed similarly. It should be noted that there was not enough material for evaluation of the PG 52-34 40% RAP mixture. The test results for the PG 64-28 mixtures shown in Figure 5-43 indicate all four of the mixtures resulted in almost identical flexural fatigue performance and no conclusion can be drawn as to which mixture performed the best.

Comparisons were made for each of the different RAP contents to determine if the use of a softer asphalt binder improved the crack initiation properties of the asphalt mixtures. Figure 5-44 through Figure 5-46 show the flexural fatigue results for the 0, 20, and 30% RAP mixtures. In all cases, the use of a softer asphalt binder resulted in an improvement in flexural fatigue performance at the identical RAP content. However, the asphalt contents for the PG 52-34 mixtures were 0.1-0.8% higher than the PG 64-28 mixtures, which will also improve the fatigue performance of the PG 52-34 mixtures.

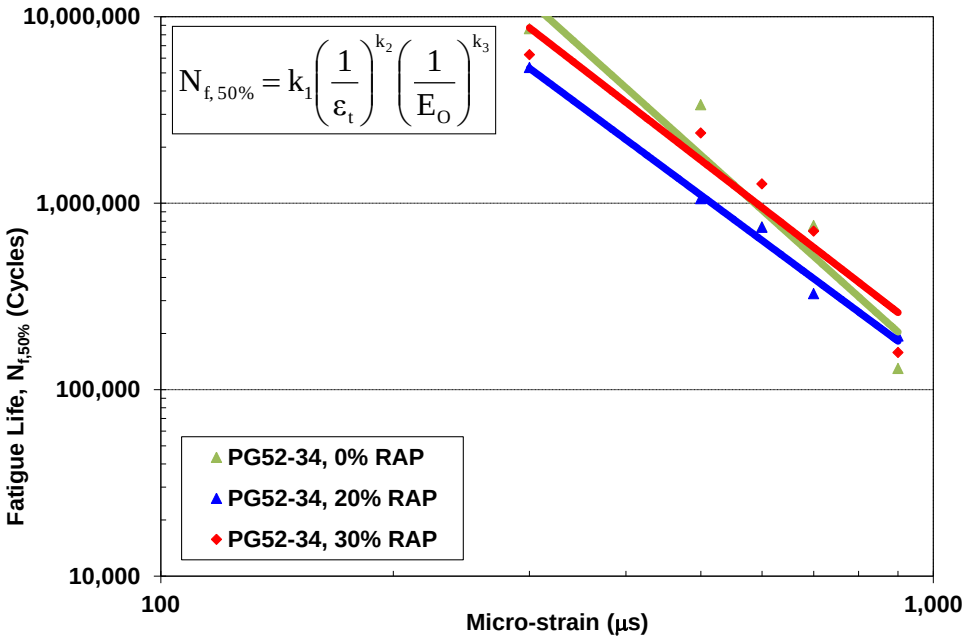

Figure 5-42 Flexural fatigue life for Vermont mixtures – PG 52-34 asphalt binder

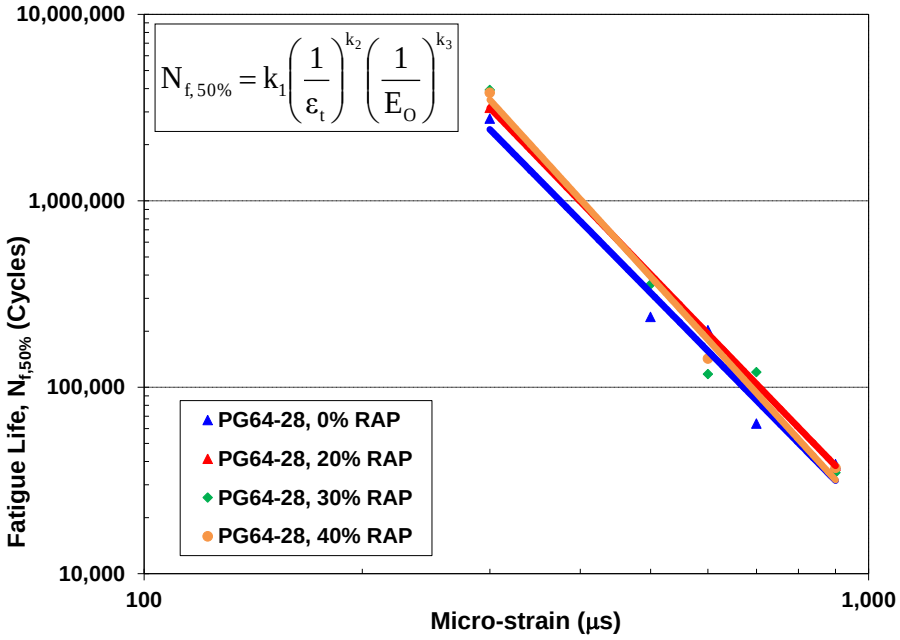

Figure 5-43 Flexural fatigue life for Vermont mixtures – PG 64-28 asphalt binder

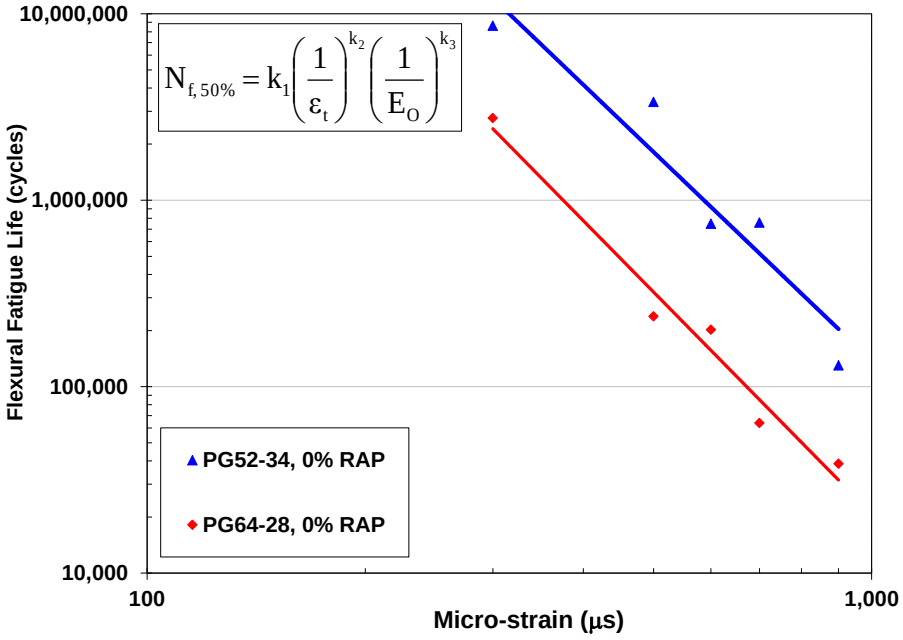

Figure 5-44 Flexural fatigue life results for Vermont mixtures – 0% RAP

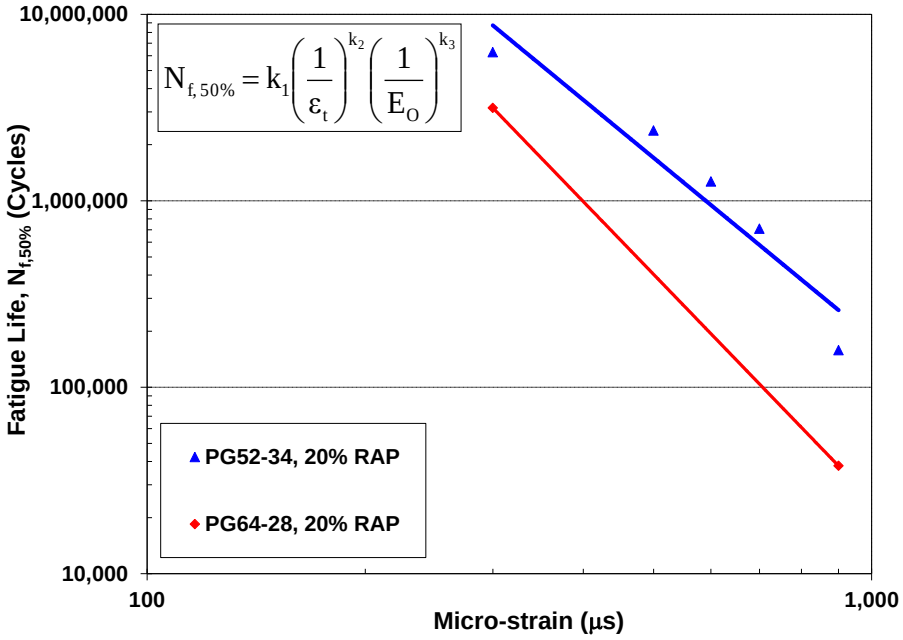

Figure 5-45 Flexural fatigue life results for Vermont mixtures – 20% RAP

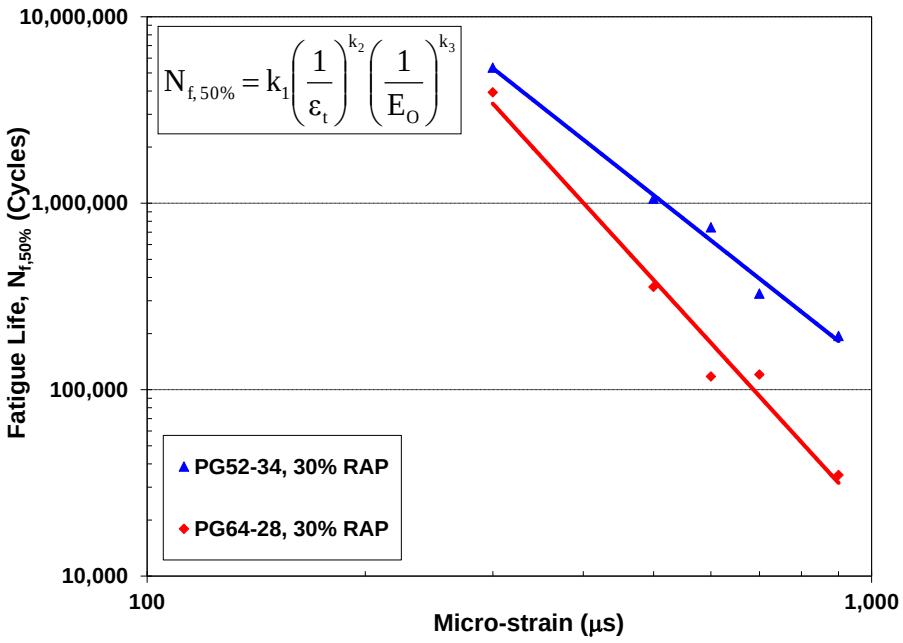

Figure 5-46 Flexural fatigue life results for Vermont mixtures – 30% RAP

5.4.2.3 Overlay

The resistance to propagation of fatigue cracking was evaluated using the Overlay Tester following sample preparation and test parameters in the TxDOT Tex-248-F testing specifications. The test results for the Vermont mixtures are shown in Figure 5-47. The test results for the PG 52-34 asphalt binders show that the 0 and 20% RAP mixtures did not fail at the maximum number of cycles set in the machine (1,200 cycles). However, the fatigue life dropped significantly at the 30% RAP level and further dropped at the 40% RAP level. The PG 64-28 0% RAP mixture showed good performance in the overlay tester, but all RAP levels showed a significant drop in the overlay tester results with 20% and 30% RAP mixtures performing similarly and the 40% RAP mixture performing the worst. The softer binder grade does appear to show a benefit in performance in the overlay tester, however the PG 52-34 mixtures also had higher asphalt contents (some by up to 0.8 %), which could also explain the difference in fatigue performance observed.

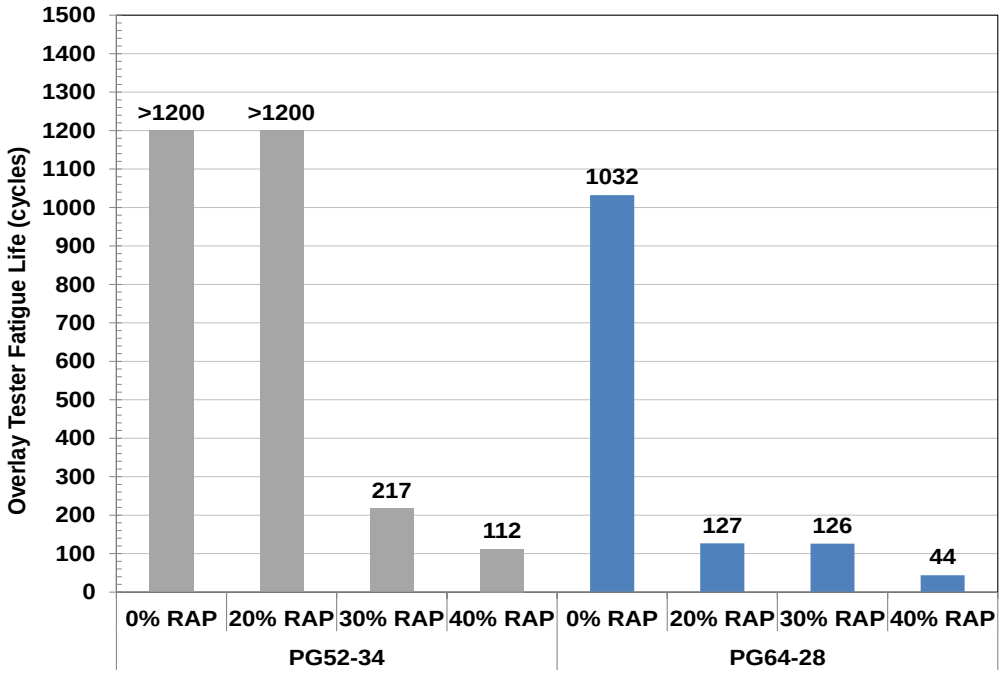

Figure 5-47 Overlay Tester Results for Vermont Mixtures

5.4.3 *Low Temperature*

5.4.3.1 TSRST

The asphalt mixtures were evaluated for their respective mixture low temperature critical cracking temperature in accordance with AASHTO TP10; tests started at an initial temperature of 4°C and specimens were cooled at a rate of 10°C hr. The failure temperature and stress were recorded and are shown in Table 5-14.

The results show that the cracking temperatures do not change much with the addition of RAP for either base binder grade. The mixtures with the PG 52-34 binder do show cracking temperatures that are approximately 4°C colder than the PG 64-28 mixtures, however there is also the difference in asphalt content between the two sets of mixtures that is likely contributing to the observed performance differences as well.

Table 5-14 TSRST Test Results for Vermont Mixtures

Mixture	Air Voids %	Temp at Failure °C	Load at Failure N	Low Continuous PG Grade °C	Binder Critical Cracking Temp. °C
VT PG 52-34 0%	7.44	-29.47	6088	-36.9	-33.3
VT PG 52-34 20%	6.92	-30.66	6938	-35.3	-31.9
VT PG 52-34 30%	6.69	-28.64	6721	-34.8	-32.7
VT PG 52-34 40%	7.45	-28.21	6438	-33.4	-28.4
VT PG 64-28 0%	7.70	-24.82	5707	-30.8	-26.9
VT PG 64-28 20%	6.45	-25.02	7095	-30.4	-27.2
VT PG 64-28 30%	6.97	-24.77	6705	-30	-25.2
VT PG 64-28 40%	7.03	-23.99	6985	-30.4	-26.5

5.4.3.2 Low Temperature Creep and IDT Strength

The average low temperature creep compliance master curves at -10°C for the VT mixtures are shown in Figure 5-48 through Figure 5-53. The virgin and 30% RAP mixtures for the PG 52-34 base binder have similar performance at longer times while the 20% and 40% RAP show a less compliant response. The higher production temperatures for the 0% and 20% PG 52-34 mixtures may be contributing to this response. The 30% RAP mixture has the softest response of the PG 64-28 base binder mixtures; the reason for this is unknown, although the presence of moisture may have an impact. Comparison of the base binder grades shows that the softer binder grade results in a more compliant mixture for all RAP contents; this is expected due to the softer binder and the lower asphalt contents in the PG 64-28 mixtures.

The low temperature IDT strength measured at -10°C for the VT mixtures is shown in Figure 5-54. There is an increase in the average strength with RAP content for the PG 52-34 and PG 64-28 mixtures, with the exception of the PG 64-28 40% RAP mixture. The PG 52-34 base binder mixtures have lower strengths than the PG 64-28 mixtures due to a combination of the softer binder grade and higher asphalt contents.

The cracking temperature for each of the mixtures determined using the TCModel spreadsheet is shown in Table 5-15. There is not a distinct trend with respect to RAP content for either base binder grade other than the 40% RAP mixtures showing the warmest cracking temperatures. The PG 52-34 base binder mixtures have colder cracking temperatures, but only by a small amount.

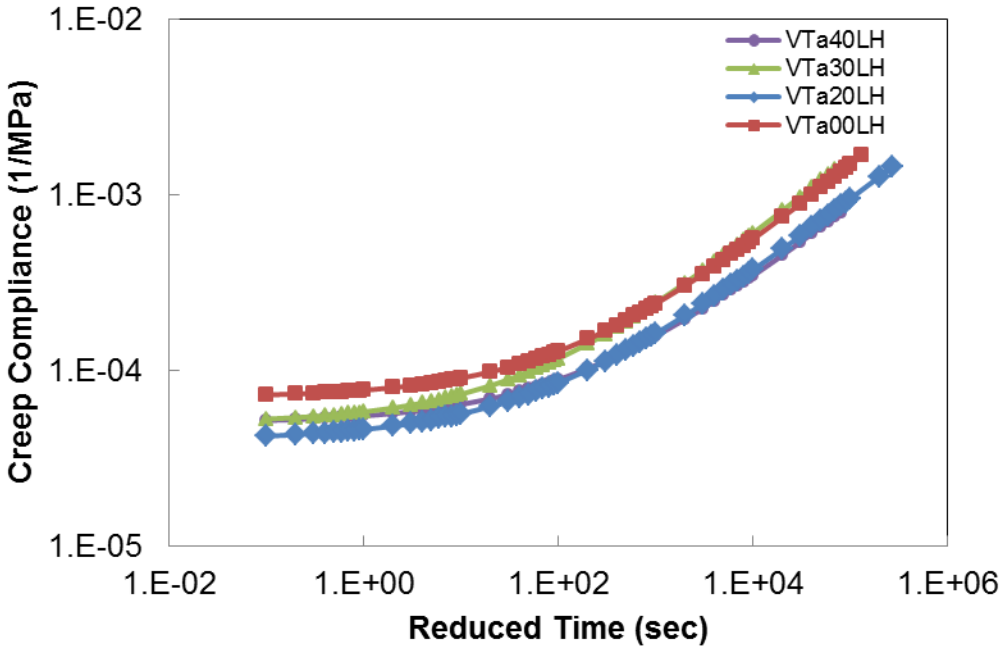

Figure 5-48 Creep compliance - VT mixtures PG 52-34

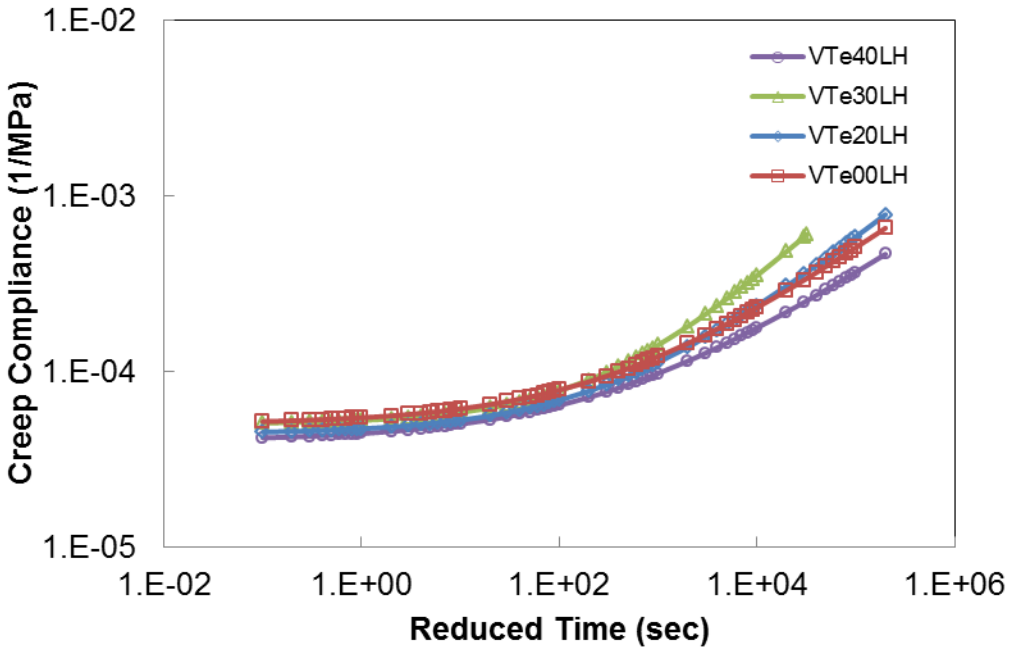

Figure 5-49 Creep compliance - VT mixtures PG 64-28

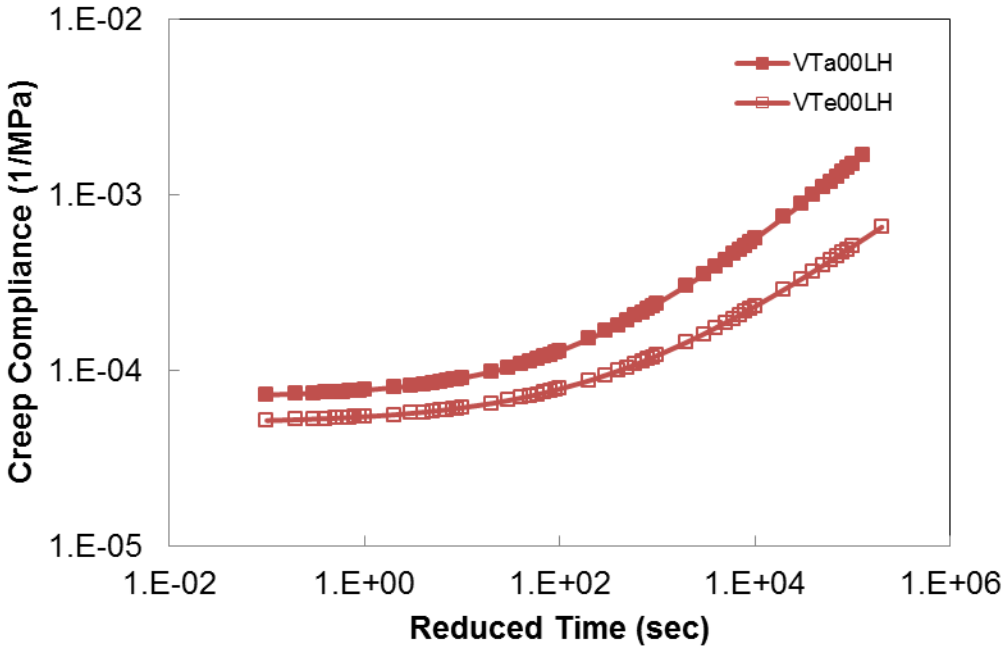

Figure 5-50 Creep compliance - VT mixtures 0% RAP

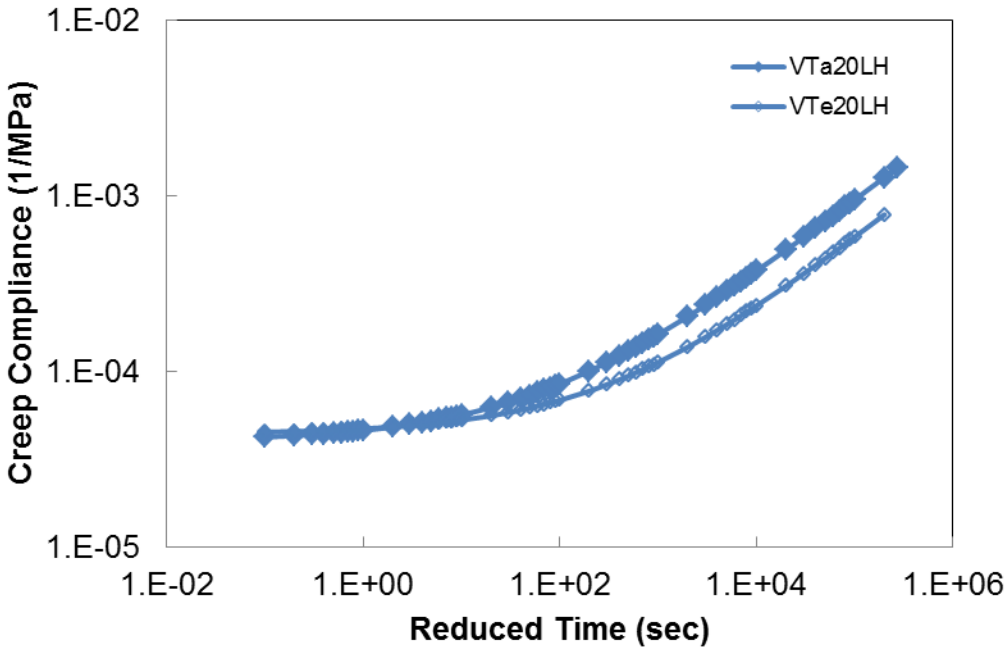

Figure 5-51 Creep compliance - VT mixtures 20% RAP

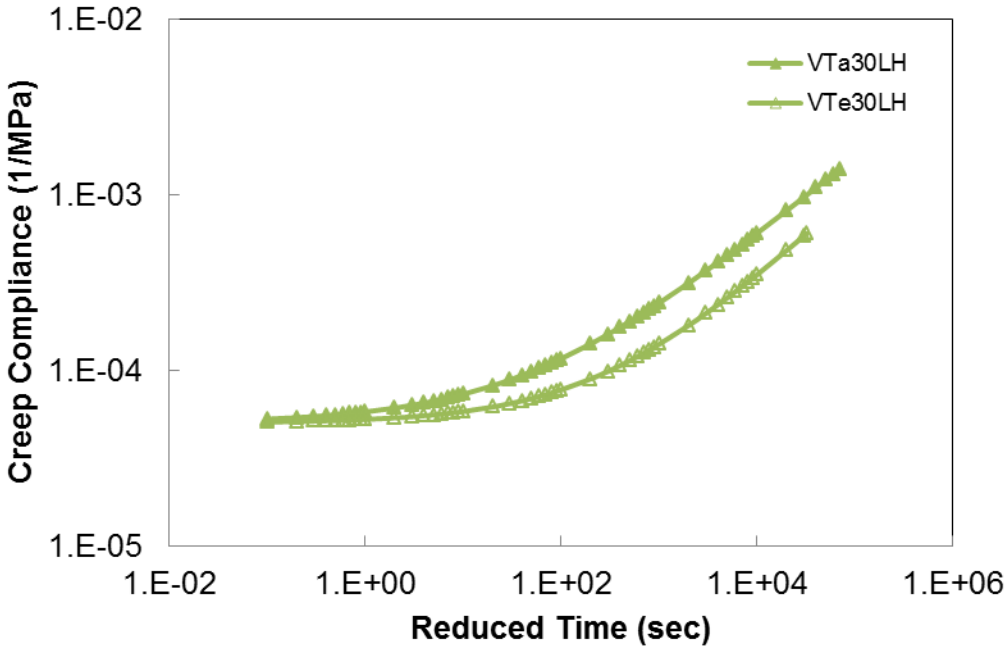

Figure 5-52 Creep compliance - VT mixtures 30% RAP

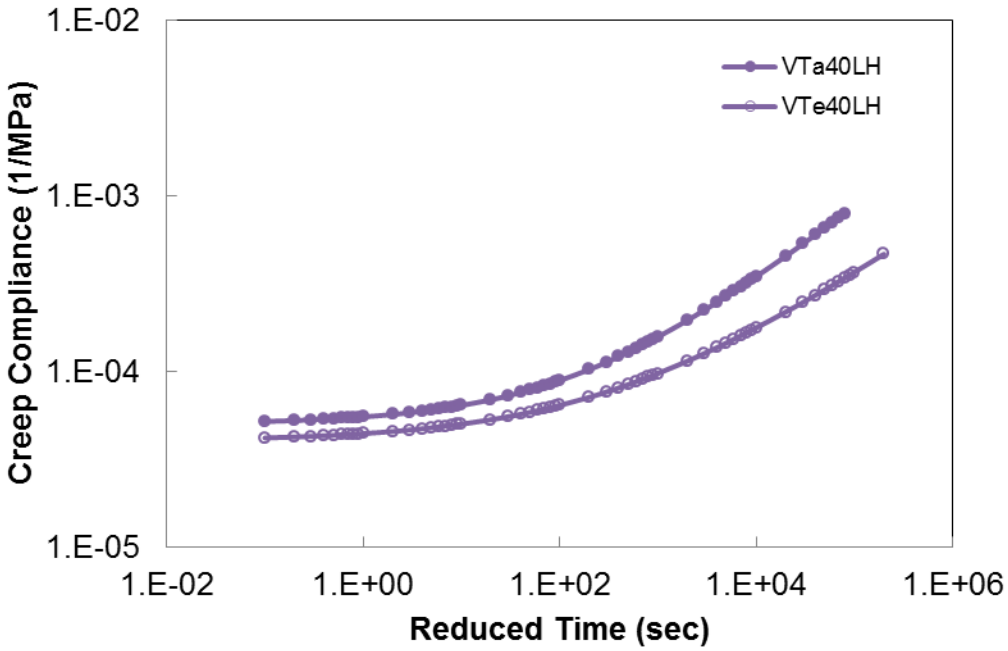

Figure 5-53 Creep compliance - VT mixtures 40% RAP

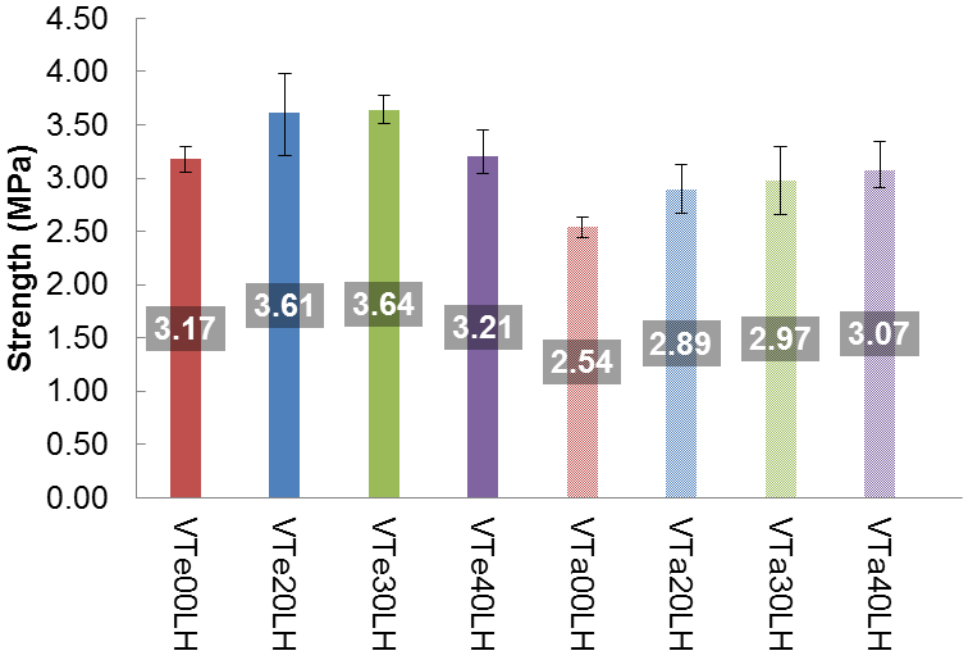

Figure 5-54 Low temperature strength (-10°C) - VT mixtures

5.4.3.3 Comparison with Binder Data

The VT mixture and extracted binder low temperatures are shown together in Table 5-15 for comparison. The rankings of the mixtures for each test are also shown in the table. The TSRST temperatures are between the two extracted and recovered binder results for most of the mixtures. The temperatures determined from the TCModel are consistently at least 10°C warmer than the other tests. All of the tests generally show that the addition of RAP results in warmer cracking temperatures and that a softer PG binder does help improve the low temperature cracking performance, but not by a full binder grade. The exact ranking of the mixtures does vary from test to test however, with production and other mix parameters also influencing the results.

Table 5-15. Critical cracking temperatures comparisons - VT mixtures

Mix	Mixture				Binder			
	TCMODEL		TSRST		Critical Cracking Temperature		Low Temperature Continuous PG-grade	
	°C	Rank	°C	Rank	°C	Rank	°C	Rank
VT PG 52-34 0 % RAP	-17	4	-29.5	2	-33.3	1	-28.3	1
VT PG 52-34 20 % RAP	-18	2	-30.7	1	-31.9	3	-28.1	2
VT PG 52-34 30 % RAP	-18	2	-28.6	3	-32.7	2	-26.3	4
VT PG 52-34 40 % RAP	-14	6	-28.2	4	-28.4	4	-21.0	7
VT PG 64-28 0 % RAP	-16	5	-24.8	6	-26.9	6	-28.1	2
VT PG 64-28 20 % RAP	-13	7	-25.0	5	-27.2	5	-27.0	3
VT PG 64-28 30 % RAP	-19	1	-24.8	7	-25.2	8	-23.0	6
VT PG 64-28 40 % RAP	-12	8	-24.0	8	-26.5	7	-24.9	5

5.4.4 *Moisture*

5.4.4.1 Hamburg Wheel Tracking Device

The results of the Hamburg testing for the VT mixtures are shown in Table 5-16. The moisture susceptibility and rutting data indicate that all the VT mixtures performed poorly regardless of the binder utilized, amount of RAP, or production parameters. This might be the result of poor quality fine materials as uncoated fine materials were observed coming out of the specimens during testing. The mixtures generally show an improvement in performance with the higher RAP content, stiffer binder grade, and lower asphalt contents.

Table 5-16. Hamburg Wheel Tracking Test Results for All VT Mixtures

State	NMAS	% RAP	Binder Grade	Average Stripping Inflection Point	Avg. Rut Depth at 10,000 Cycles (mm)	Avg. Rut Depth at 20,000 Cycles (mm)
VT	9.5 mm	0	PG52-34	850	n/a	n/a
		20	PG52-34	1,600	n/a	n/a
		30	PG52-34	2,050	n/a	n/a
		40	PG52-34	1,450	n/a	n/a
	9.5 mm	0	PG64-28	1,350	n/a	n/a
		20	PG64-28	2,100	n/a	n/a
		30	PG64-28	2,650	n/a	n/a
		40	PG64-28	2,900	n/a	n/a

n/a = Test terminated prior to reaching specified cycle due to maximum deformation exceeding 20 mm

5.4.4.2 TSR

The results of the TSR testing of the VT mixtures are shown in Figure 5-55and the dry strength values for each mixture are shown in Figure 5-56. The bars in Figure 5-56 represent the range of the results. The TSR values for the PG 52-34 mixtures are marginal, with the PG 64-28 mixture results indicating better performance. There is not a consistent trend with respect to RAP content for either base binder grade. The dry tensile strengths of these mixtures are low, which may help explain the poor performance under the HWTD as well.

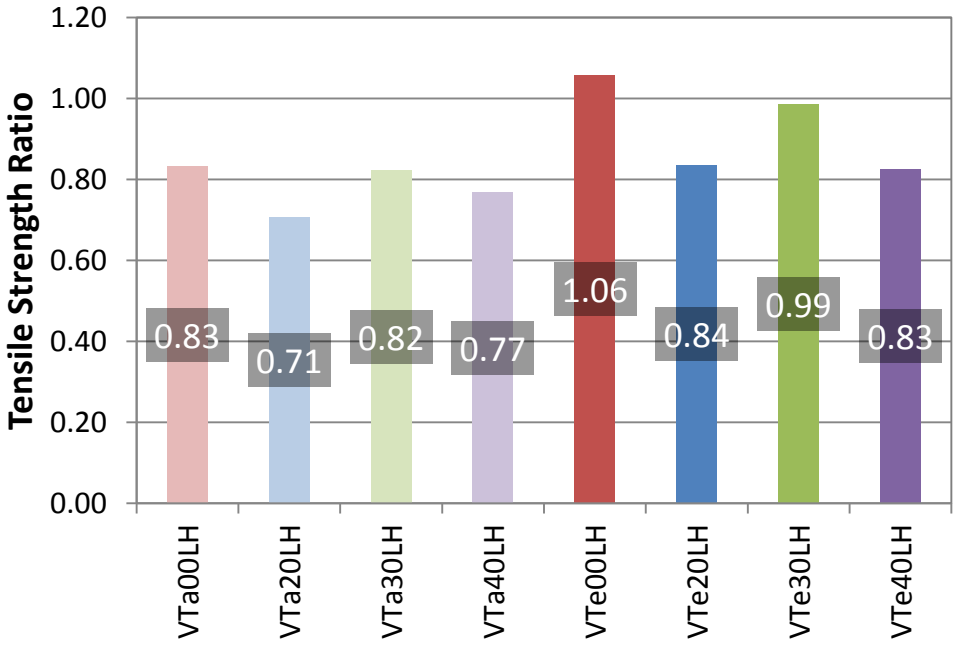

Figure 5-55 Tensile strength ratio - all VT mixtures

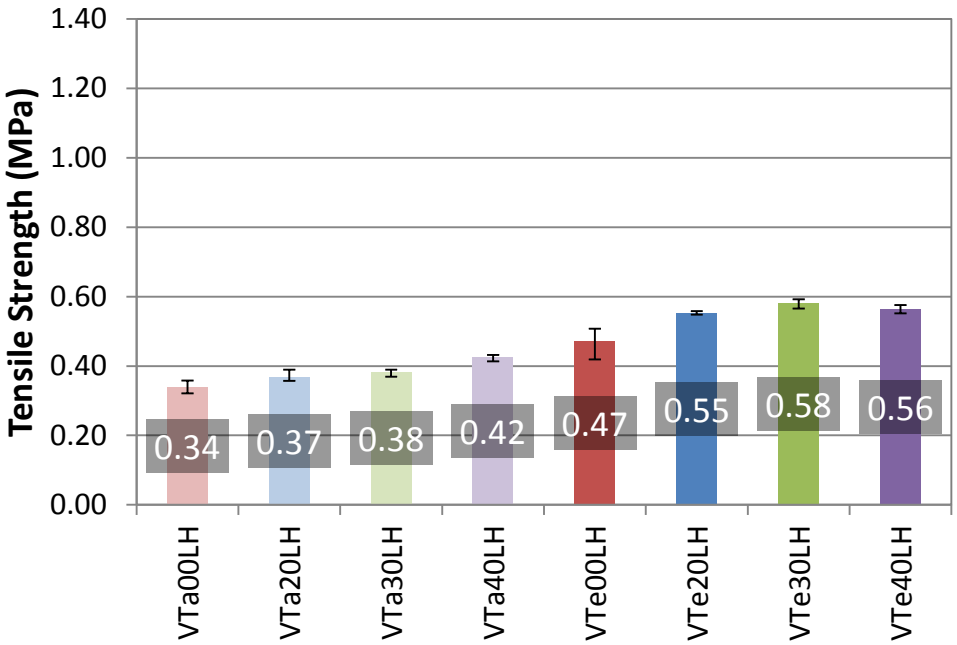

Figure 5-56 Average tensile strength of dry set - all VT mixtures

5.4.5 *Workability Device*

The workability data for the Vermont mixtures is shown in Figure 5-57. The results do not follow any defined trends with respect to RAP content or PG binder grade. This may be attributed to overall lower mixture modulus coupled with the effect of softer asphalt binders and higher asphalt binder contents.

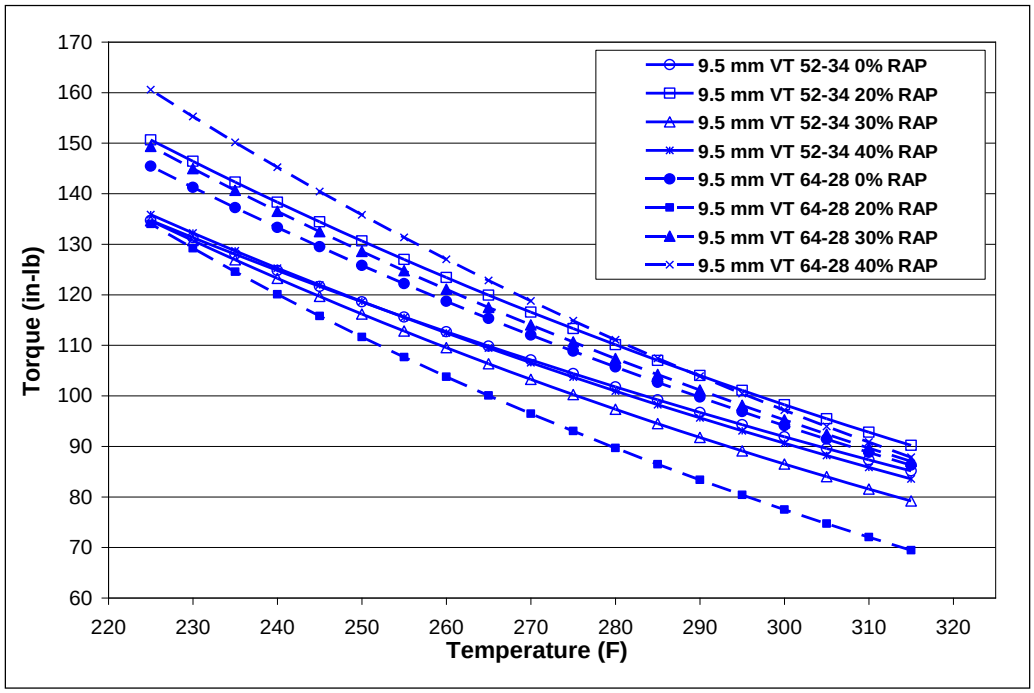

Figure 5-57 Workability Test Results for All VT Mixtures

CHAPTER 6 OVERALL CONCLUSIONS FROM PHASE I

In this chapter the overall conclusions from the 18 mixtures that have been tested as part of Phase I are presented.

6.1 Impact of RAP Percentage

In general, the addition of RAP stiffens the mixture as expected; however, the magnitude of the impact of higher RAP percentages varies with each set of mixtures and the test used to evaluate stiffness. The results from PG grading of the extracted and recovered binders is summarized in Figure 6-1 and Figure 6-2 below. The high PG grade increases 1-3°C with each 10% increase in recycled binder content and the low PG grade increases about 1-2°C with each 10% increase in recycled binder content. These results agree with results reported by other researchers as well (Bonnaquist).

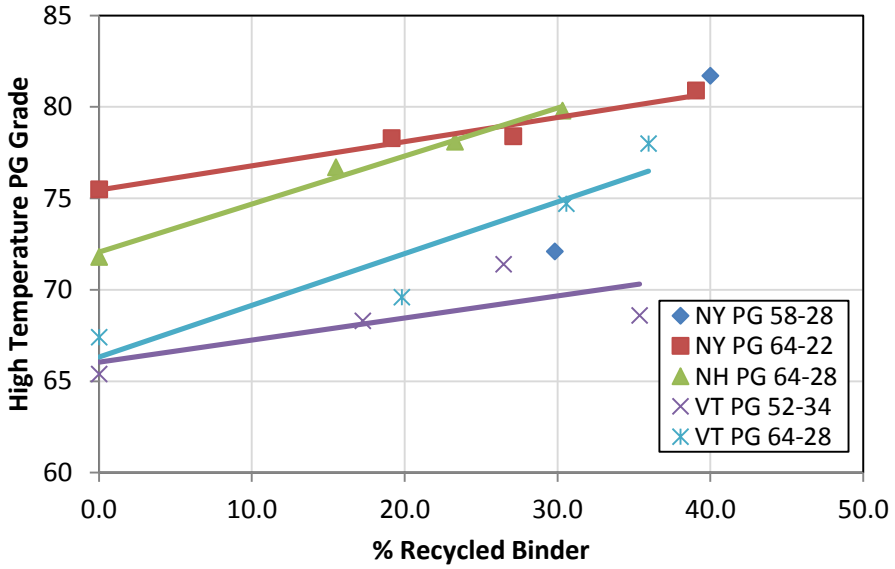

Figure 6-1 Extracted and recovered high temperature PG grade as a function of RAP content

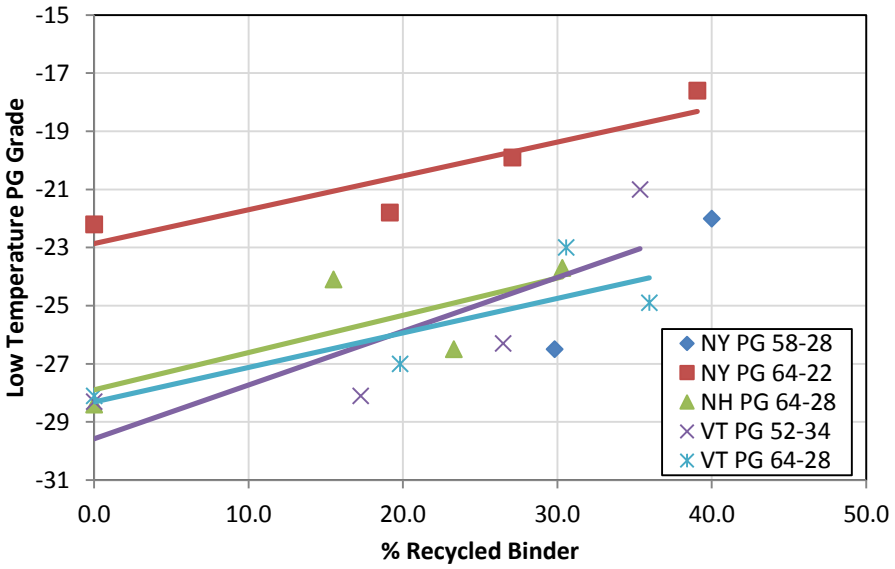

Figure 6-2 Extracted and recovered low temperature PG grade as a function of RAP content

The addition of RAP results in stiffer dynamic modulus values; the amount of increase in stiffness with RAP appears to be impacted by several factors:

- Specimen preparation method: specimens compacted at the plant (PMPC) show larger differences with increases in RAP content than specimens reheated and compacted in the lab (PMLC). This may be due to the additional aging that occurs when mixture is reheated in the lab; the mixtures with more virgin binder are susceptible to more aging during this process and will stiffen more than the higher RAP mixtures.
- Mix design and materials: the VT specimens used a softer RAP and also had a higher virgin asphalt content; these mixtures showed very little impact of RAP on the dynamic modulus master curves
- Production parameters: the results indicate apparent effects of mix temperatures and silo storage time on the measured dynamic modulus values. Lower mix temperatures may result in softer mixtures as less aging happens during the mixing process and longer storage times may result in stiffer mixtures as additional aging occurs as the material is stored for longer times at high temperature. Water was also observed with all the VT 30% and 40% RAP mixtures, which may have impacted the measured stiffness of these mixtures.

The low temperature creep compliance testing shows similar trends as were observed with the dynamic modulus testing. The TSRST tests on the mixtures showed that slightly warmer cracking temperatures occurred with increases in RAP content, with some apparent effects of mixture and production parameters.

Fatigue cracking was evaluated using several test methods: S-VECD, beam fatigue, and overlay tester. The beam fatigue test is a measure of crack initiation while the overlay tester is a measure of crack propagation. The S-VECD test yields the cracking resistance in both initiation and propagation stages. Proper evaluation of asphalt mixture's cracking resistance by the S-VECD model requires the analysis of pavement structures using the LVECD (*L*ayered *V*isco*E*lastic pavement analysis for *C*ritical *D*istresses) program. Without the pavement analysis, the energy-based failure criteria from the S-VECD results are found to be sensitive to mixture parameters. The comparison of the failure criteria show poorer fatigue performance for higher RAP content using the same binder in general, and this decrease in the cracking resistance depends on virgin binder grade and content, RAP binder grade, and other production parameters. Flexural fatigue results showed that the higher RAP contents for all mixtures performed similarly to the comparison virgin mixtures; intermediate RAP contents had mixed results with some performing similar to the other mixtures and others performing worse. The overlay test results show that the addition of any amount of RAP significantly decreases the mixture resistance to crack propagation for the NH and VT PG 64-22 mixtures, the VT PG 52-34 mixture does not show a drop until RAP contents go above 20% while the NY mixtures do not show a drop until RAP contents go above 30%.

Workability tests showed that an increase in RAP content decreases the workability of the mixture, except for the VT mixtures that did not follow any trends. This may be a result of the higher asphalt contents and softer asphalts used in the VT mixtures. Hamburg testing showed that the higher RAP contents resulted in more rut resistant mixtures, which is expected based on the stiffness increases with RAP.

6.2 Impact of PG Grade

The impact of dropping the PG grade of the virgin binder to compensate for the addition of higher levels of RAP shows varied results based on the mixtures tested in Phase I of this study. The extracted binder results show that a softer virgin binder grade improves both the high and low PG grades, but the magnitude of the improvement varies with RAP content and mixture, as seen in Figures 8.1 and 8.2 above.

The use of a softer virgin PG grade did decrease the dynamic modulus for both the VT and NY mixtures and improved the workability. However, there was also a significant difference in binder contents for the VT mixtures that would also contribute to the difference in stiffness. There was no trend observed with the drop in PG grade for the Hamburg testing. The softer virgin grade did result in an improvement in low temperature cracking by several degrees, as measured by the TSRST test.

Fatigue testing showed that the softer virgin binder helped the flexural performance of all the VT mixtures and helped the NY 30% mixture some, but had negligible effect with the 40% RAP mixture. The S-VECD analysis showed better fatigue performance for the stiffer virgin binders. The NY mixtures showed worse overlay test results with the softer virgin binder, while the VT mixtures showed a benefit, especially with the 20% RAP mixture. The higher asphalt contents in the softer VT mixtures likely also contributed to the better performance observed.

From the mixtures tested in this study, the impact of using a softer virgin binder grade varies from mix to mix and for different mixture properties. It appears to help improve some properties, has negligible effect on others, and may make others worse.

6.3 Impact of Plant Production

Plant production parameters such as mixture temperature and silo storage time show apparent impacts on mixture properties measured in this project. Specifically, lower initial stiffness and more stiffening upon reheating were observed with the NH and NY 20% mixtures that were stored in the silo for shorter periods than the companion virgin mixtures. The NH 20% mixture also had a lower discharge temperature. Because neither mix temperature nor storage time was controlled for these mixtures, it is difficult to separate out the effects as they may cancel out for some mixtures that had lower mix temperatures but longer storage times, or vice versa. Moisture was also observed in all the VT 30% and 40% mixtures, which may have had an impact on the mixture properties measured, particularly those from the plant compacted (not reheated) specimens.

CHAPTER 7 ONGOING AND FUTURE WORK

This section presents a summary of the Phase II and Phase III work that is currently being conducted in this project as well as recommendations for future additional work.

7.1 Phase II summary

The mixtures being evaluated in Phase II of the project were produced during the 2011 construction season. They include mixtures with higher PG grades from Virginia, additional mixtures from New Hampshire that have field sections, and a set of silo storage study mixtures from New York. The Phase II mixtures are summarized in Table 7-1.

Testing and analysis of the Phase II mixtures is ongoing and should be completed in 2014. The virgin silo storage study mixtures were found to be contaminated with a modified binder, and so a new silo storage study is recommended under future work.

Table 7-1. Phase II Mixtures

Plant	NMAS (mm)	Virgin PG Grade	RAP Content (%) by total wt. of mix				
			0	15	25	30	40
Pike NH (drum)	12.5	58-28	x	x	x	-	-
		52-34	-	-	x	x	x
Superior VA (drum)	12.5	76-22	x	-	-	-	-
		70-22	-	x	-	-	-
		64-22	-	-	-	x	x
Callanan NY (drum)	12.5	64-28	0, 2.5, 5.0, 7.5 hrs silo storage time	-	0, 2.5, 5.0, 7.5, 10.0 hrs silo storage time	-	-

7.2 Phase III summary

The testing plan proposed for Phase III consists of a laboratory study of 8-10 mixtures to evaluate the impacts of asphalt binder grade and asphalt content on the mixture properties. The laboratory study is proposed to allow for better control of production variables (temperature, gradation, short term aging). NH Phase I mixtures were selected for comparison with plant produced mixtures tested previously. The conditions to be tested are shown in Table 7-2. The impact of a combination of changing binder grade and adding additional asphalt cement (conditions in parenthesis) will only be evaluated after examining the results of changing binder grade and increasing asphalt content

independently. The percent binder replacement and RAP credit values for the two RAP contents being evaluated in Phase III are shown in Table 7-3.

The testing plan for the Phase III laboratory mixtures consists of both binder testing and mixture testing as summarized in Table 7-4 and Table 7-5 below. It is expected that the Phase III testing will be completed in 2014.

Table 7-2. Phase III laboratory test mixtures

Mixture	**Asphalt content**	**RAP Content (total weight)**		
		0	**20**	**40**
NH Pike Mixture from Phase I, 12.5 mm	optimum	PG 64-28	PG 64-28 PG58-28	PG 64-28 PG 58-28
	+0.5%	-	PG 64-28	PG 64-28 (PG 58-28)
	+1.0%	-	-	PG 64-28 (PG 58-28)

Table 7-3. Phase III binder replacement and RAP credit values

		Optimum	+0.5%	+1.0%
% binder replacement	20% RAP	16.8	15.5	-
	40% RAP	33.7	31.0	28.7
RAP credit	20% RAP	100	47.9	-
	40% RAP	100	74.0	47.9

Table 7-4. Phase III binder testing (virgin & extracted)

Test/Test Parameter	Test Method/Reference	Title	Lab
Extraction and Recovery			Rutgers
Performance Grade	AASHTO R29 & AASHTO M320	Grading or Verifying the Performance Grade of an Asphalt Binder & Performance-Graded Asphalt Binder	Rutgers
Binder Modulus (G*) & Binder Master Curve			Rutgers
Critical Cracking Temperature	AASHTO R49-09	Determination of Low-Temperature Performance Grade (PG) of Asphalt Binders	Rutgers

Table 7-5. Phase III mixture testing

Test/Test Parameter	Test Method/Reference	Title	Lab
Dynamic Modulus	AASHTO TP 62	Determining Dynamic Modulus of Hot Mix Asphalt Concrete Specimens	NCSU
Fatigue Test	Push-Pull Fatigue (S-VECD)	Proposed Standard Method of Test for Determining the Damage Characteristic Curve of Asphalt Concrete from Direct Tension Cyclic Fatigue Tests	NCSU
Permanent Deformation		Triaxial Stress Sweep	NCSU
Low Temperature Cracking		Thermal Stress Restrained Specimen Test (TSRST)	UMass

7.3 Recommendations for Future Work

Based on the results of the work completed thus far in the project, the research team anticipates that the results of the Phase III laboratory study will suggest additional laboratory studies on other mixtures and also testing on plant produced mixtures where there is more control over some of the production variables. Also, a new silo storage study

phase is currently being developed to fill gaps from the initial silo storage study conducted in Phase II of this project. The research team also suggests that the research should move towards evaluating a combination of warm mix technologies and high RAP mixtures. The research team will be working with the technical committee on developing appropriate scopes of work and funding for these suggested studies.

CHAPTER 8 REFERENCES

AASHTO (2011). *Developing Dynamic Modulus Master Curves for Hot Mix Asphalt (HMA) Using the Asphalt Mixture Performance Tester (AMPT)* (2011). AASHTO, Washington, D.C.

AASHTO. (T283-03). *Resistance of Compacted Asphalt Mixtures to Moisture-Induced Damage.*

AASHTO. (T322-03). *Determining the Creep Compliance and Strength of Hot-Mix Asphalt (HMA) Using the Indirect Tensile Test Device.*

AASHTO. (T324). *Hamburg Wheel-Track Testing of Compacted Hot-Mix Asphalt (HMA).*

ASTM. (D3549). *Thickness or Height of Compacted Bituminous Paving Mixture Specimens.*

Austerman A.J., Mogawer W.S., Bonaquist R., "Investigation of the Influence of Warm Mix Asphalt Additive Dose on the Workability, Cracking Susceptibility, and Moisture Susceptibility of Asphalt Mixtures Containing Reclaimed Asphalt Pavement", In *Canadian Technical Asphalt Association (CTAA) Proceedings*, Moncton - New Brunswick, November 2009, pg. 51-71.

Bahia, H. (1991). *A Dissertation in Partial Fulfillment of the Requirements of the Degree of Doctor of Philosophy. Submitted to the Graduate Faculty of Pennsylvania State University.*

Bennert, T. and A. Maher, 2013, "Forensic Study on the Cracking of New Jersey's LTPP Specific Pavement Study (SPS-5) Sections", *Transportation Research Record: Journal of the Transportation Research Board, No. 2371*, Transportation Research Board of the National Academies, Washington, D.C., pp. 74 - 86. (In Press)

Bennert, T., W. Worden, and M. Turo, 2009, "Field and Laboratory Forensic Analysis of Reflective Cracking on Massachusetts Interstate 495", *Transportation Research Record: Journal of the Transportation Research Board, No. 2126,* Transportation Research Board of the National Academies, Washington, D.C., pp. 27 – 38.

Bhasin A., V. T. F. Castelo Branco, E. Masad, and D. N. Little (2009) . Quantitative Comparison of Energy Methods to Characterize Fatigue in Asphalt Materials. *Journal of Materials in Civil Engineering*, JMCE, Vol. 21, No. 2.

Castelo Branco, V. T. F., E. Masad, A. Bhasin, and D. N. Little (2008). "Fatigue Analysis of Asphalt Mixtures Independent of Mode of Loading." *Proceedings, 87th Annual Transportation Research Board Meeting*, TRB, Transportation Research Board of the National Academiecs, Washington, D.C.

Chehab, G. (2002). *Characterization of Asphalt Concrete in Tension Using a ViscoElastoPlastic Model*. Ph.D. dissertation,, North Carolina State University. Raleigh, NC.

Chehab, G. R., Y. R. Kim, R. A. Schapery, M. Witczack, and R. Bonaquist (2003). Characterization of Asphalt Concrete in Uniaxial Tension Using a Viscoelastoplastic Model. *Asphalt Paving Technology*, AAPT, Vol. 72, pp. 315-355.

Christensen, D. (1998). Analysis of Creep Data from Indirect Tension Test on Asphalt Concrete. *The Association of Asphalt Paving Technologists*, (pp. 458-492).

Daniel J. S. (2001). *Development of a Simplified Fatigue Test and Analysis Procedure Using a Viscoelastic, Continuum Damage Model and Its Implementation to WesTrack Mixtures*. Ph.D. dissertation, North Carolina State University, Raleigh, NC.

Daniel, J. S. and Y. R. Kim (2002). Development of a Simplified Fatigue Test and Analysis Procedure Using a Viscoelastic Continuum Damage Model. *Journal of the Association of Asphalt Paving Technologists*, AAPT, Vol. 71, pp. 619-650.

Gudimettla, J., L. Cooley, and E. Brown. "Workability of Hot Mix Asphalt", Report #03-03, National Center for Asphalt Technology (NCAT), Auburn, AL, 2003.

Ghuzlan, K. A. and S. H. Carpenter (2000). Energy-Derived, Damage-Based Failure Criterion for Fatigue Testing. *Transportation Research Record*, No. 1723, pp. 141-149.

Hou, T. (2009). *Fatigue Performance Prediction of North Carolina Mixtures Using Simplified Viscoelastic Continuum Damage Model*. Master of Sscience dissertation, North Carolina State University, Raleigh, NC.

Hou, T., B. S. Underwood, and Y. R. Kim (2010). Fatigue Performance Prediction of North Carolina Mixtures Using Simplified Viscoelastic Continuum Damage Model. *Journal of the Association of Asphalt Paving Technologists*, AAPT, Vol. 79, pp. 35-80.

Kim, Y., Daniel, J. S., & Wen, H. (2000). *Fatigue Performance Evaluation of WesTrack and Arizona SPS-9 Asphalt Mixtures Using Viscoelastic Continuum Damage Approach Final Report to Federal Highway Adminstration / North Carolina Department of Transportation.*

Kim, Y. R. and D. N. Little (1990). One-Dimensional Constitutive Modeling of Asphalt Concrete. *ASCE Journal of Engineering Mechanics*, Vol. 116, No. 4, pp. 751-772.

Kim, Y. R., D. N. Little, and R. L. Lytton (2003). Fatigue and Healing Characterization of Asphalt Mixtures. *Journal of Materials in Civil Engineering*, JMCE, Vol. 15, No. 1, pp. 75-83.

Kim, Y. R., M. N. Guddati, B. S. Underwood, T. Y. Yun, V. Subramanian, S. Savadatti, and S. Thirunavukkarasu (2008). *Development of a Multiaxial VEPCD-FEP++.*

Publication FHWA-HRT-08-073, U.S. Department of Transportation, Federal Highway Administration.

Kim, Y., Seo, Y., & Momen, M. (2009). Chapter5: Complex Modulus from the Indirect Tension Test. In Y. R. Kim, *Modeling of Asphalt Concrete.*

Lee, H. J. and Y. R. Kim (1998a). A Uniaxial Viscoelastic Constitutive Model for Asphalt Concrete under Cyclic Loading. *ASCE Journal of Engineering Mechanics*, Vol. 124, No. 1, pp. 32-40.

Lee, H. J. and Y. R. Kim (1998b). A Viscoelastic Continuum Damage Model of Asphalt Concrete with Healing. *ASCE Journal of Engineering Mechanics*, Vol. 124, No. 11, pp. 1224-1232.

Maggoiore, C., J. Grenfell, G. Airey, and C. Collop (2012). Evaluation of Fatigue Life Under Dissipated Energy Methods. *7th RILEM International Conference on Cracking in Pavements*, pp. 643-652.

Masad, E., V. T. F. Castelo Branco, D. N. Little, and R. L. Lytton (2008). A Unified Method for Analysis of Controlled-Strain and Controlled-Stress Fatigue Testing. *International Journal of Pavement Engineering*, Vol. 9, No. 4, pp. 233-246.

NCAT. (1996). *Hot Mix Asphalt Materials, Mixture Design and Construction.* National Asphalt Pavement Association Research and Education Foundation.

Reese, R. (1997). Properties of Aged Asphalt Binder Related to Asphalt Concrete Fatigue Life. *Journal of the Association of Asphalt Paving Technologists*, AAPT, Vol. 66, pp. 604-632.

Roque, R., & Buttlar, W. G. (1992). The Development of a Measurement and Analysis System to Accurately Determine Asphalt Concrete Properties Using the Indirect Tensile Mode. *The Association of Asphalt Paving Technologists*, (pp. 304-333).

Schapery, R. A. (1984). Correspondence Principles and a Generalized J-integral for Large Deformation and Fracture Analysis of Viscoelastic Media. *International Journal of Fracture*, Vol. 25, pp. 195-223.

Shen, S. and S. H. Carpenter (2005). Application of Dissipated Energy Concept in Fatigue Endurance Limit Testing. *Transportation Research Record*, TRB, No. 1929, pp. 165-173.

Si, Z., D. N. Little, and R. L. Lytton (2002). Characterization of Microdamage and Healing of Asphalt Concrete Mixtures. *Journal of Materials in Civil Engineering*, JMCE, Vol. 14, No. 6, pp. 461-470.

Underwood, B. S. and, Y. R. Kim (2009). Analytical Techniques for Determining the Endurance Limit of Hot Mix Asphalt Concrete. *International Conference on Perpetual Pavement.*

Underwood, B. S., C. M. Baek, and Y. R. Kim (2012). Use of Simplified Viscoelastic Continuum Damage Model as an Asphalt Concrete Fatigue Analysis Platform. *Transportation Research Record: Journal of the Transportation Research Board*, TRB, No. 2296, pp. 36-45.

Underwood, B. S., Y. R. Kim, and M. N. Guddati (2006). Characterization and Performance Prediction of ALF Mixtures Using a Viscoelastoplastic Continuum Damage Model. *Journal of the Association of Asphalt Paving Technologists*, AAPT, Vol. 75, pp. 577-636.

Underwood, B. S., Y. R. Kim, and M. N. Guddati (2010). Improved Calculation Method of Damage Parameter in Viscoelastic Continuum Damage Model. *International Journal of Pavement Engineering*, IJPE, Vol. 11, pp. 459-476.

Van Dijk, W. and W. Visser (1977). The Energy Approach to Fatigue for Pavement Design. *Asphalt Paving Technology*, AAPT, Vol. 46, pp.: 1-40.

Van Dijk, W., H. Moreaud, A. Quedeville, and P. Uge (1972). "The Fatigue of Bitumen and Bituminous Mixes." *Proceedings, 3rd International Conference on the Structural Design of Asphalt Pavements*, Vol. 1, London, pp.: 354-366.

Wen, H. (2001). *A Dissertation in Partial Fulfillment of the Requirements of the Degree of Doctor of Philosophy. Submitted to the Graduate Faculty of North Carolina State University.*

Zhang, J. (2012). *Development of Failure Criteria for Asphalt Concrete Mixtures under Fatigue Loading.* Master of Sscience dissertation,. North Carolina State University, Raleigh, NC.

Zhang, J., M. Sabouri, Y. R. Kim, and M. N. Guddati (2013). Development of a Failure Criterion for Asphalt Mixtures under Fatigue Loading. *Journal of the Association of Asphalt Paving Technologists*, AAPT, In press.

Zhou, F., S. Hu, and T. Scullion, 2007, *Development and Verification of the Overlay Tester Based Fatigue Cracking Prediction Approach*, FHWA/TX-07/9-1502-01-8, 90 pp

Zhou, F. and Tom Scullion, 2005, "Overlay Tester: A Simple Performance Test for Thermal Reflective Cracking", Journal of the Association of Asphalt Paving Technologists, Vol. 74, pp. 443 – 484.